ANNUAL REPORT 2017-18

Institute of Seismological Research

Department of Science and Technology
Government of Gujarat

Contributors

Group& PI	Scientist/ Researcher
Near Real Time Seismology PI: Dr. Santosh Kumar, Scientist-D	Dr. P. Mahesh, Scientist-B Dr. A. P. Singh, Scientist-B Dr. Pavan Kumar Gayatri, Scientist-B Mr. Ketan Singha Roy, Scientist-B Ms.Vishwa Joshi, Scientist-B Ms. Vandana Patel, Sr Geophysicist Mr. Alla Sateesh, Sr Geophysicist Mr. Arpan Shastri, Geophysicist Ms. Monika Bhatia, JRF
Seismic Hazard Assessment and Microzonation PI: Dr. Sumer Chopra, Scientist-G	Dr. Kapil Mohan, Scientist-C Dr. Pallabee Choudhury, Scientist-C Dr. Madan Mohan Rout, Scientist-C Dr. B. Sairam, Scientist-B Dr. Pavan Kumar Gayatri, Scientist-B Mr. Vasu Pancholi, Scientist-B Ms. Archana Das, Scientist-B Ms. Vandana Patel, Sr Geophysicist Mr. Naveen Kumar, Sr Geophysicist Mr. Vinay Kumar Dwivedi, Sr Geophysicist Mr. Tarun Solanki, Sr Geophysicist Ms. Sarda Maibam, Geologist Mr. Peush Chaudary, Geophysicist Mr. D. M. Tripathi, Geophysicist Mr. Pruthul Patel, Geophysicist Mr. Dilip Singh, Geophysicist Mr. Mehul Nagar, Geophysicist Ms. Charu Kamra, JRF Mr. Kunal Rathod, JRF
Solid Earth Geophysics PI: Dr.M.Ravi Kumar, Distinguished Scientist	Dr. A. P. Singh, Scientist-B Ms. Jyoti Sharma, Scientist-B Dr. Pavan Kumar Gayatri, Scientist-B Dr. Chinmay Halder, Scientist-B Mr. Avinash Chauhan, Sr. Geophysicist Mr. Mayank Dikshit, Geophysicist Mr. Arjav Shukla, Geophysicist Mr. Mehul Nagar, Geophysicist Mr. Dilip Singh, Geophysicist Mr. Virender Kumar Singh, JRF Mr. Nawneet Kumar, JRF Ms. Indu Chaudhary, JRF Ms. Smita Mishra, JRF Ms. Monika Bhatia, JRF
Earthquake Precursory Research PI: Dr. K.M. Rao, Scientist-D	Mr. M. S. B. S. Prasad, Scientist-B Mr. C. P. Simha , Geophysicist Mr. Sushant Sahoo, Geophysicist Mr. Shivam Joshi, JRF

Active Tectonics PI: Dr. Pallabee Choudhury, Scientist-C	Dr. Girish Kothyari, Scientist-B Dr. Falguni Bhattacharya, Scientist-B Dr. Siddharth Prizomwala, Scientist-B Dr. Rakesh Dumka, Scientist-B Ms. Archana Das, Scientist-B Mr. Tarun Solanki, Sr.Geologist Mr. Nisarg Makwana, Geophysicist Ms. Drasti Gandhi, SRF Mr. Durga Prasad, JRF Mr. Raj Sunil Kandergula, JRF Ms. Sneha Mishra, JRF Ms. Riyanka Talukdar, JRF Ms. Neha Joshi, JRF
Commercial Research and Development PI: Dr.Kapil Mohan, Scientist-C	Dr. Siddharth Prizomwala, Scientist-B Mr. Vasu Pancholi, Scientist-B Ms. Smita Mishra, JRF

Contents

		Page No.
RESEARCH HIGHLIGHTS		**1**
RESEARCH CONTRIBUTIONS		**4**
1. NEAR REAL TIME SEISMOLOGY		**4**
1.1	Earthquake Monitoring and Seismicity Patterns in Gujarat	4
1.2	Description of Recorded Earthquakes in Different Parts of Gujarat during 2017	5
1.3	Description of Recorded Earthquakes in Different Parts of Gujarat since inception of the network till 2017	7
1.4	MEQ data processing and interpretation collected during Jan-Dec 2016 for the study of seismogenic sources around the Subansiri Lower Hydro Electric (H.E) Project, Arunachal Pradesh	9
1.5	Micro-earthquake (MEQ) studies at Bursar Hydro Electric (H.E) Project, Jammu and Kashmir	10
1.6	Local earthquake tomography (LET) studies around the dam site of Bursar project, Jammu & Kashmir	11
1.7	Upper Mantle structure of the North-west Deccan Volcanic Province from Teleseismic Tomography	13
1.8	Reservoir Induced seismicity studies for SSNNL	15
1.9	Local Magnitude scale for Saurashtra region	16
1.10	Estimation of source parameters for North Gujarat	16
1.11	Seasonal variations of secondary microseism sources	17
1.12	Active Tectonics in Lower Narmada basin	19
1.13	Identification of the traces of neotectonic activity in the vicinity of Sardar Sarovar reservoir	20
2. SEISMIC HAZARD ASSESSMENT AND MICROZONATION		**23**
2.1	Estimation of PGA and causes of building collapse during 2001 Bhuj Earthquake	23
2.2	Generation of Site specific Response Spectra at surface of IOCL Bongaigaon Refinery, Assam State, India using Probabilistic Seismic Hazard Assessment	24
2.3	Seismic Hazard Assessment of Devni Mori site, Sabarkantha, Gujarat	25
2.4	Assessment of Seismic Hazard in Ahmedabad City incorporating parametric uncertainties	27
2.5	Assessment of Seismic Hazard in Gandhinagar City incorporating parametric uncertainties	30
2.6	Geological Map of the Dadra and Nagar Haveli (U.T)	32
2.7	Delineation of Palaeochannels in Dadra and Nagar haveli (U.T.)	34
2.8	Study of Deformation in Quaternary sediments in Dadra and Nagar Haveli (U.T.)	35
2.9	Vulnerability Assessment in the Rambaug area of Ahmedabad	37
2.10	Rapid Visual Screening of Sector 2 and 23, Gandhinagar City	38

		Page No.
2.11	Seismic Risk assessment in Bhachau city	40
2.12	Scenario based seismic risk assessment in northern part of Gandhinagar City	41
2.13	Rapid Visual Screening of RC frame buildings in Vasna area of Ahmedabad, Gujarat.	43
2.14	Estimation of Source parameters of Mw 7.1 Central Mexico City Earthquake	43
2.15	Simulation of strong ground motion of Mw 7.1 Central Mexico City Earthquake	44
2.16	Probabilistic seismic hazard assessment of Bongaigaon, Assam, Northeast India	45
2.17	A review of Seismic hazard assessment of Gujarat, a highly active intra-plate region of the world	46
2.18	Characterization of Kachchh Mainland Fault and Katrol Hill Fault in the western central part of Kachchh	46
2.19	Magnetotelluric Study in the western part of Kachchh, Gujarat	48
2.20	2-D subsurface model of little Rann area, Kachchh using Magnetotellurics	50
3.	**SOLID EARTH GEOPHYSICS**	**51**
3.1	Geological and seismological field investigations at Navsari, Valsad and Silvas areas of South Gujarat	51
3.2	Local site effects estimated from Ambient Vibration measurements at Mehsana City, Western India	52
3.3	Microtremor survey along the borehole sites located in Gandhinagar and Ahmedabad cities	52
3.4	Site response study in and around the Bhuj City	52
3.5	Subsurface structure in the Eastern Indian Shield region using ambient vibration	53
3.6	Shallow Subsurface Imaging of Eastern Kachchh using Transient electromagnetic studies	54
3.7	Shallow subsurface Imaging of Kachchh Mainland Fault (KMF)	55
3.8	Magnetotelluric investigations in Eastern part of the Kachchh rift basin	56
3.9	Assessment of base metal mineralization in Banaskantha Distrist, within Aravalli's using Joint geological and geophysical Investigations (AMBAJI)	58
3.10	Delineation of structural features over Ambaji mineralization zone, Gujarat, NW India using gravity and magnetic data	59
3.11	Crustal studies over the northern Cambay basin using high resolution gravity measurements	60
3.12	Astronomical and Meteorological Earthquake precursors in the Kachchh Rift Basin, Northwestern India	60
3.13	Discrimination of quarry blasts from micro earthquakes in the Surendranagar region of Saurashtra province, Northwestern India	61
3.14	Remotely triggered tremors in Kachchh region, Northwestern India following large teleseismic earthquakes	61
3.15	Source characteristics for the Gujarat region	62
3.16	Seismic evidence for décollement plane beneath the Arunachal Himalaya	64

		Page No.
3.17	3-D seismic structure beneath the Shillong Plateau area of Northeast India	65
3.18	Estimation of shear wave velocity contrast (δβM) across the Moho in Gujarat Region	66
3.19	Seismic evidence for secular evolution and alteration of Archaean crust in Indian shield	67
3.20	Estimating the thickness of the crust of Gujarat using PmP phases	68
3.21	A review on role of mantle convection in geoid anomalies	68
4.	**EARTHQUAKE PRECURSORY RESEARCH**	**69**
4.1	Preliminary results of magnetic pulsations during the storm occurred on 8th Jan 2015	69
4.2	Empirical Mode Decomposition based Hilbert Huang Transform on Soil Radon (Rn^{222}) data of Kutch, Gujarat, India: Identification of Daily quasi-periodic oscillations and Earthquake precursors	69
4.3	Application of the Artificial Neural Network (ANN) on the Soil Radon (Rn^{222}) time series for identifying Earthquake Precursors in Kutch, Gujarat	74
4.4	Spatial and temporal behaviour of Ionospheric VTEC during the shallow earthquake of Newzealand (M 7.8) occurred on 13th November 2016	75
4.5	The effect of geomagnetic storms on the magnetic field observed at four Indian stations	78
4.6	ULF magnetic field variations before a moderate Earthquake (M 4.0) in Kachchh, Gujarat, India	78
4.7	Geomagnetic anomalies possibly linked with 2001 Bhuj, Gujarat earthquake (Mw 7.7): a study on earthquake precursors	79
4.8	Empirical Mode Decomposition based Hilbert Huang Transform to the Soil Radon (Rn^{222}) time series during Jan-Dec 2017	81
4.9	Geomagnetic and Geochemical anomalies before a moderate earthquake of M 4.8 on March 29 2018 at Kachchh, Gujarat, India	83
4.10	Observation of Magnetic pulsations during quiet and disturbed times	85
5.	**ACTIVE TECTONICS**	**87**
5.1	Defining the geometrical characteristics of the fault scarp from topographic profiles and fault bedding	87
5.2	Satellite data analysis to delineate Geomorphology of the KMF	87
5.3	Neotectonics and Paleoseismic Investigations along the Kachchh Mainland Fault Zone, Western India: Implications for Seismic Hazard Assessment	88
5.4	Gradient anomaly for rivers of Kachchh (for ~100 river channels) to determine the tectonic subsidence and uplift associated with the major active faults	89
5.5	Evolution of drainage in response to brittle-ductile dynamics and surfaces processes in Kachchh Rift Basin, Western India	90
5.6	Palaeoseismological Investigation along the Back thrust of HFT, Soan Dun, Northwest Himachal Himalaya, India	91
5.7	Evaluation of Neotectonic variability along major Himalayan thrusts within the Kali River Basin using the geomorphic markers, Central Kumaun Himalaya	92

		Page No.
5.8	Quaternary landform developments and climatic variability in tectonically active region of Central Kumaun Himalaya, India	93
5.9	Morpho-structural evidence of neotectonic movement along Vigogi fault: Kachchh Rift Basin	94
5.10	GPS measurements of deformation caused by the seasonal filling and emptying cycles of four hydroelectric reservoirs in India	95
5.11	Reconstructing climate-tectonic signatures from terraces of central and eastern Northern Hill Range (NHR)	95
5.12	Geomorphic Expressions of Active Strike-slip faulting (Girnar Fault), Saurashtra, Western India	95
5.13	Signatures of middle to late Holocene high sea level/paleo environmental/paleoclimatic changes from the Banni plain, Rann and its linkage with the declination of past civilization	96
5.14	Geological evidence for AD 1008 tsunami along the Kachchh coast, Western India: Implications for recurrence along the Makran Subduction Zone	97
5.15	Sedimentological, geochemical and chronological constraints from a palaeochannel near Lothal ~ a Harappan dockyard: Implications for palaeoenvironmental changes during the Middle to Late Holocene period.	97
6.	**COMMERCIAL RESEARCH AND DEVELOPMENT**	**99**
6.1	Estimation of strong ground motion at surface level and design spectra in the coastal region of Odisha near Dhamra.	99
6.2	Seismic Hazard Assessment at LPG treatment facility Bongaigaon	101
6.3	Seismic hazard assessment of mounded LPG bullet plant at Bongaigaon Refinery, IOCL, Assam.	104
6.4	Estimation of Mesozoic sediment thickness in the eastern part of Kachchh, Little Rann region	106
6.5	Possible Geothermal process in the Tuwa Godhra region	107
PUBLICATIONS		**110**
NOTABLE EVENTS		**117**
SOCIETAL OUTREACH		**123**
CAMPUS NEWS AND EVENTS		**126**

RESEARCH HIGHLIGHTS

- A total of 1814 local earthquakes were recorded by the broadband seismic network of ISR during the year 2017. Out of these, 839 shocks of M0.5 - 4.9 lie in the Kachchh region, 887 shocks of M0.5 – 3.9 in the Saurashtra region and 88 shocks of M0.5 - 4.9 in the Mainland region.
- Spectrogram analysis of 1100 ground motions (M≥1.1) recorded at different regions in Saurashtra enabled distinction between quarry blasts and earthquakes in terms of their varying frequency content. A detailed investigation brought forward an intriguing observation about mining-induced seismicity.
- The Dholavira earthquake (2012) of magnitude 5.0 was analyzed for identifying the variations in the land surface thermal anomalies. It is interpreted that the land surface temperature shows an increase seven days prior to this earthquake.
- Local earthquake tomography (LET) studies conducted around the dam site of Bursar project, Jammu & Kashmir, reveal that the smaller magnitude earthquakes are mainly occurring in the zone of moderately low *Vp,* low *Vs* and high *Vp/Vs*, between the Main Central Thrust and the Kishtwar Thrust (KT). The KT is imaged as a transition between low and high velocity zones. The velocity images obtained in the LET study are well correlated with the geology of the area.
- A review and synthesis of the seismic hazard assessment of Gujrat indicates that the PGAs vary from 0.05 to 0.36g and 0.07 to 0.80g for 10% and 2% PE in 50 years at Vs=760 m/s. The deterministic values of PGA range from 0.02 to 0.90g at surface.
- Seismic hazard maps of the 33 districts of Gujarat state have been prepared in the form of a booklet. The booklet contains PGA and SA maps of all the districts at 10% and 2% P.E in 50 years.
- The soil study in the vicinity of collapsed buildings (near to Ahmedabad passport office) during the 2001 Bhuj earthquake reveals that the possible reason for their destruction is the presence of clay with medium plasticity.
- Microtremor analysis in the Mehsana district yields thickness of the upper soft soils in the range of 270 and 345 m.
- Local site effects in and around the Bhuj City determined using microtremor data reveal that the predominant frequency varies between 0.4 and 2.0 Hz. The sites associated with low amplitude values at the predominant frequencies suggest their siting on a compact platform of Cretaceous sandstone of Bhuj formation, with no other soft rock deposits lying over or in contact with it.
- A 2D Geoelectric section of the Magnetotelluric (MT) data collected in the central part of Kachchh suggests a maximum sediment thickness of 2.3 km in the region. The thickness is estimated as 2.2 km in the northern part near KMF and ~ 2.0 km between the Kutch Mainland Fault(KMF) and Katrol Hill Fault(KHF). The KMF is found to be almost vertical up to 7-8 km and dipping northward afterwards, at an angle of about 45^{o}.
- Shallow geophysical imaging using transient electromagnetic technique delineated splays of the primary KMF. Some of the *en echelon* splays form a flower structure, suggesting localized transtension in this regional compressive regime. Presence of

buried colluvial wedges seen as high conductive zones in the hanging wall side of the fault, could indicate the record of palaeo-earthquakes, suggesting neotectonic activity in the region.

- A study involving Geological and Geophysical field investigations conducted at Navsari, Valsad and Silvas areas of South Gujarat infers that the recent heavy rainfall during the Indian summer monsoon might be a possible cause for the swarm activities in these areas.
- Relationship between age and bulk crustal thicknesses of the Indian shield derived from receiver function studies is anti-correlated. This observation reveals that most of the crust is formed in the early Archean and subsequently altered, making it more evolved in composition.
- The decollement plane beneath the Arunachal Himalaya was imaged by the Seismic tomography method.
- 3-D seismic velocity structure of the Shillong Plateau mapped by Seismic tomography method provides further evidence for pop-up tectonics.
- The shear-wave velocity contrast across the Moho in the Gujarat region was estimated using the transmitted P- to -s wave amplitude variations with ray-parameter. It is noticed that the Moho in Gujarat region is not uniform in terms of the transmission of seismic waves as the shear wave velocity contrast ($\delta\beta$) is highly variable all throughout the region.
- Derivative analysis of gravity and magnetic data delineated major NE-SW trending lineaments like, Chambal-Jamnagar Lineament (CJL), Pisangan-Vadnagar Lineament (PVL) and the NW-SE oriented Jaisalmer-Barvani Lineament (JBL) in the Ambaji region, Banaskantha district, Gujarat. The high gravity anomalies in the western part indicate that the basement is shallow in the region. The Magnetic high at the south-western part correlating with the JBL possibly indicates the deep rooted nature of the lineament.
- The Empirical Mode Decomposition based Hilbert Huang Transform was applied to the Soil Radon (Rn^{222}) data of Desalpar and Badargadh stations in Kutch, Gujarat, The daily quasi-periodic oscillations and earthquake precursors of two moderate earthquakes of magnitudes 5.5 and 4.0 on 20th October and 10th November 2011 respectively, are identified.
- Spatial and temporal variation of the Ionospheric VTEC during the shallow earthquake of New Zealand (M 7.8), that occured on 13th November 2016, was observed. The TEC is found to reach the maximum value around 08:30 UT onwards till earthquake time (11:03 UT) in Newzealand area.
- The influence of solar wind parameters (density and pressure) on the magnetic field measurements at low latitude magnetic stations of India during two severe geomagnetic storms in 2015 was examined. The first storm was on March 17-18, 2015 (Dst= -223nT), the most intense geomagnetic storm (G4) of the current solar cycle and another storm was on June 22-23, 2015 (Dst= -204 nT).
- ULF magnetic field variations are observed as precursory signals to a moderate earthquake of M 4.0, which occurred in Kachchh region on 13th June 2017.
- Pre-seismic signatures of five local earthquakes are observed in Soil Radon (Rn^{222}) data of Badargadh recorded during Jan-Dec 2017.

- A study on GPS measurements of crustal deformation caused by seasonal filling and emptying of four surface reservoirs of varying dimensions, located in various geological domains of India suggests that there appears to be no lower threshold on the size of reservoir to cause deformation in the surrounding medium and to trigger earthquakes, as long as the faults are critically stressed.
- The palaeo-environmental studies in Banni Plains using a host of multiproxy techniques inferred that the Plains evolved owing to the Middle Holocene high sea stand and subsequent fall during the last 2 ka period. The extent of high sea stands up to 2m above MSL corroborated well with ancient port settlements of Late Harappan period.
- Based on the OSL and geochemical studies, it is suggested that the landscape around Lothal seems to have been uplifted by 3m during the last 4 ka period, hinting at a long-term uplift rate around 0.75 mm/a.
- A study reported the first geological evidence of 1008 AD tsunami from the Indian coastline.
- Gradient Anomaly for rivers of Kachchh (for ~100 river channels) was analysed to determine the tectonic subsidence and uplift associated with major active faults
- Geomorphic signature of the Girnar fault was identified using remote sensing data.
- Results of Magnetotelluric studies revealed that the Mesozoic sediment thickness in the little Rann of Kachchh is ~1km.
- Strong ground motion and design spectra at surface level are estimated in the coastal region of Odisha near Dhamra. The soil liquefaction is observed in the coastal Odisha, Dhamra at a depth of about 13.5m.

RESEARCH CONTRIBUTIONS

1. Near Real Time Seismology

1.1 Earthquake Monitoring and Seismicity Patterns in Gujarat

(Santosh Kumar, P Mahesh, A P Singh, Ketan Singha Roy, Vandna Patel)

The Gujarat State Seismic Network comprising 60 Broadband Seismograph Stations (BBS) and 54 Strong Motion Accelerographs (SMA) spread throughout the state and neighbouring areas is in operation since July 2006 (Fig.1.1). 45 of these BBS are connected via VSAT to ISR. The network has a detectability of M2.0 in the Kachchh region and M2.5 in the other areas of Gujarat.

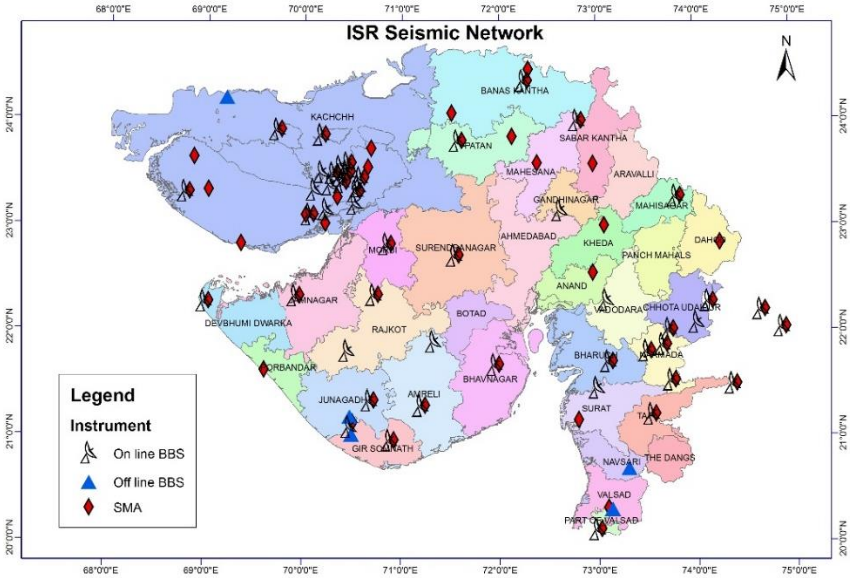

Figure 1.1: Gujarat network of 60 Seismograph stations and 54 Accelerographs.

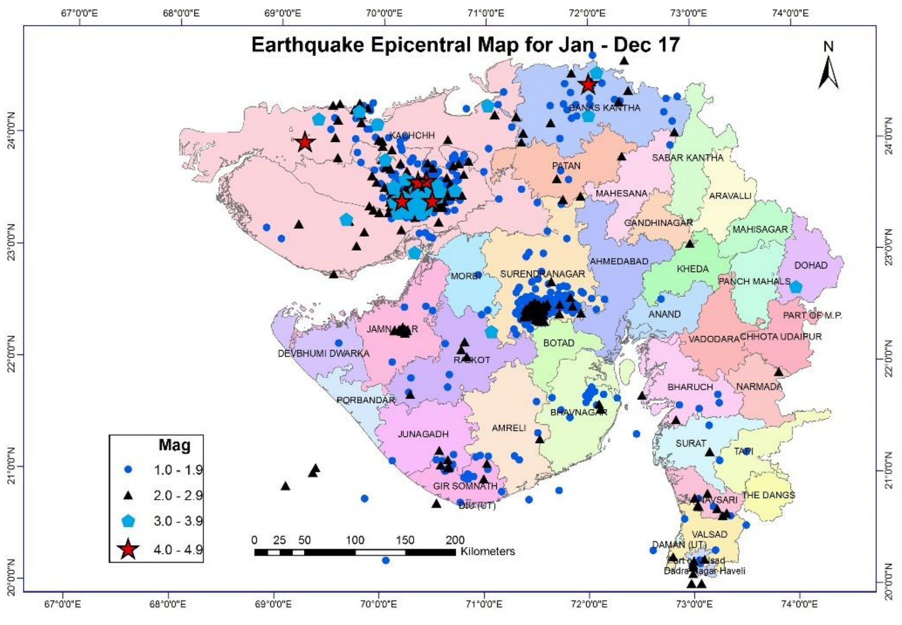

Fig. 1.2: Epicenters of earthquakes of M≥1 in Gujarat located during 2017

During 2016, the network recorded nearly 2062 shocks, out of which the hypocentral parameters of 1814 local shocks were determined. Additionally, 76 regional earthquakes were recorded from other states. Nearly 168 distant earthquakes of M5.0 or greater were recorded including the M8.2, Mexico earthquake on 8th Sept. 2017.

1.2 Distribution of Earthquakes in Different Parts of Gujarat

(Santosh Kumar, P Mahesh, A P Singh, Ketan Singha Roy, Vandna Patel)

The magnitude-wise distribution of earthquakes in the three regions of Gujarat, during 2017, is given in Table 1.1. A total of 839 shocks between M1.0 - 4.7 in Kachchh, 887 shocks between M1.0 – 3.1 in Saurashtra and 88 shocks between M1.0-4.4 in the mainland, were located(Fig. 1.2).

Table 1.1: Regional Distribution of Earthquakes Located in Gujarat during 2017

Region	0.5 – 1.9	2.0 – 2.9	3.0 – 3.9	4.0 – 4.9	Total
Kachchh	516	271	47	5	839
Saurashtra	773	113	1	0	887
Mainland	47	35	5	1	88
Total:	**1336**	**419**	**53**	**6**	**1814**

Seismicity in Kachchh

This year, in Kachchh, there were 839 shocks out of which 516 are of M1.0-1.9, 271 shocks are of M2.0-2.9, 47 shocks are of M3.0-3.9, and 5 shocks are of M4.0-4.2. A shock of M4.7 occurred on 9th January 2017, 49 km ENE from Lakhpat, Kachchh

Seismicity in Saurashtra

This year, in Saurashtra, there were 773 shocks of M<2.0, 113 shocks of 2.0-2.9, and 1 shock of M3.1. The maximum magnitude in this region was 3.1, that occurred on 12-06-2017, 27 Km from Rajkot (Table 1.2).

Earthquakes in Mainland Gujarat

In the Mainland, 47 shocks of M<2.0, 35 shocks of M2.0-2.9, 5 shocks of M3.0 – 3.9 and 1 shock of M4.0-4.9, were located. The maximum magnitude in this region was 4.4 that occurred on 13-03-2017, 32 km NNW from Deesa, Banaskantha. (Table 1.3).

Table 1.2: List of Earthquakes with magnitude M≥ 3.0 in the Saurashtra region, during 2017

No.	Date	Lat	Long	M	Location
1	06-12-2017	22.279	71.064	3.1	27 Km ESE from Rajkot, Saurashtra

Table 1.3: List of earthquakes with Magnitude 1.0 – 4.4 in the Mainland region during 2017

Sr. No.	Date	Time (IST)	Lat.	Long	M
1	05-01-2017	06:26 AM	23.651	71.698	2.2
2	06-01-2017	03:46 AM	24.322	71.764	1.5
3	07-01-2017	06:12 PM	23.723	71.734	1.7
4	14-01-2017	01:47 AM	23.851	72.332	2.4
5	21-01-2017	05:21 PM	24.162	72.826	1.1
6	14-02-2017	03:44 PM	25.166	73.435	2.1
7	16-02-2017	06:40 PM	24.347	72.317	1.3
8	16-02-2017	02:16 PM	24.245	72.746	1

9	07-03-2017	01:24 PM	24.506	72.141	1.3
10	12-03-2017	04:39 AM	24.757	72.05	1.1
11	13-03-2017	09:37 PM	24.478	72.035	1.3
12	13-03-2017	09:15 PM	24.52	72.037	2.1
13	13-03-2017	07:44 PM	24.602	72.088	3.4
14	13-03-2017	04:00 PM	24.373	72.018	1.7
15	13-03-2017	03:52 PM	24.504	72.007	4.4
16	24-03-2017	02:30 AM	23.496	71.927	2.3
17	24-03-2017	02:06 AM	23.643	71.812	1.7
18	11-04-2017	10:32 AM	23.948	72.803	1.4
19	17-04-2017	01:03 PM	24.383	72.878	1.3
20	08-05-2017	09:31 PM	24.01	71.728	1.7
21	11-05-2017	10:27 PM	24.061	71.367	2.8
22	11-05-2017	02:06 PM	24.314	72.023	1.7
23	16-05-2017	03:33 PM	24.341	72.305	2.3
24	17-05-2017	06:48 PM	23.977	71.351	2.1
25	20-05-2017	04:35 PM	24.226	71.089	2.7
26	20-05-2017	07:33 AM	24.422	71.831	1.8
27	31-05-2017	03:15 AM	24.366	72.769	1.7
28	01-06-2017	05:12 PM	24.307	71.021	3.2
29	02-06-2017	09:35 AM	24.503	71.775	1.8
30	13-06-2017	08:39 AM	24.71	72.362	2.1
31	25-06-2017	11:15 AM	23.42	71.74	1.9
32	29-06-2017	12:38 AM	24.441	72.398	2.8
33	13-07-2017	11:35 AM	24.113	71.256	1.6
34	02-08-2017	08:54 PM	24.153	71.639	2.2
35	06-09-2017	12:59 AM	24.209	71.301	2.7
36	07-09-2017	12.46 AM	23.064	72.989	2
37	14-09-2017	01:00 AM	24.064	72.847	2.2
38	18-10-2017	04:10 AM	24.428	71.177	1.7
39	19-10-2017	12:10 AM	24.217	72.005	3
40	30-10-2017	7:32am	24.599	71.842	2.1
41	03-11-2017	1:02pm	24.36	72.263	1.4
42	04-11-2017	12:02pm	23.556	71.351	1.5
43	15-11-2017	2:26pm	24.213	71.892	1.3
44	15-11-2017	2:15pm	24.268	71.8	1.4
45	15-11-2017	2:13pm	24.194	71.842	1.4
46	15-11-2017	2:06pm	24.315	71.884	1.9
47	03-12-2017	4:35am	24.305	71.633	1.8

Strong Motion Accelerograph data

During the year 2017, 47 shocks of M1.7-4.4 were recorded on strong motion accelerographs (Fig. 1.3), out of which 25 shocks were recorded at two or more stations. The remaining shocks were recorded on only one SMA station. In Kachchh, tremors of M4.0-4.4 were recorded by 3 to 8 SMA stations. In the Mainland Gujarat, there was one earthquake of M4.4 that occurred 32 km NNW from Deesa in Banaskantha, which was recorded by 3 SMA Stations (Table 1.4).

Table 1.4: List of earthquakes of M4 or more and no. of SMA station triggered

M	Date	Time	Lat	Long	NST	Location
4.7	09-01-17	3:48 PM	23.969	69.237	4	49 km ENE from Lakhpat, Kachchh
4.0	05-03-17	2:45 PM	23.45	70.484	5	17 km WSW from Rapar Kachchh
4.4	13-03-17	3:52 PM	24.504	72.007	3	32 km NNW from Deesa, Banaskantha
4.0	13-06-17	7:48 PM	23.616	70.345	7	31 km WNW from Rapar, Kachchh
4.1	23-08-17	3:12 PM	23.447	70.189	8	16 km NNE From Dudhai, Kachchh
4.1	11-12-17	4:47 PM	23.63	70.425	5	23 Km WNW from Rapar, Kachchh

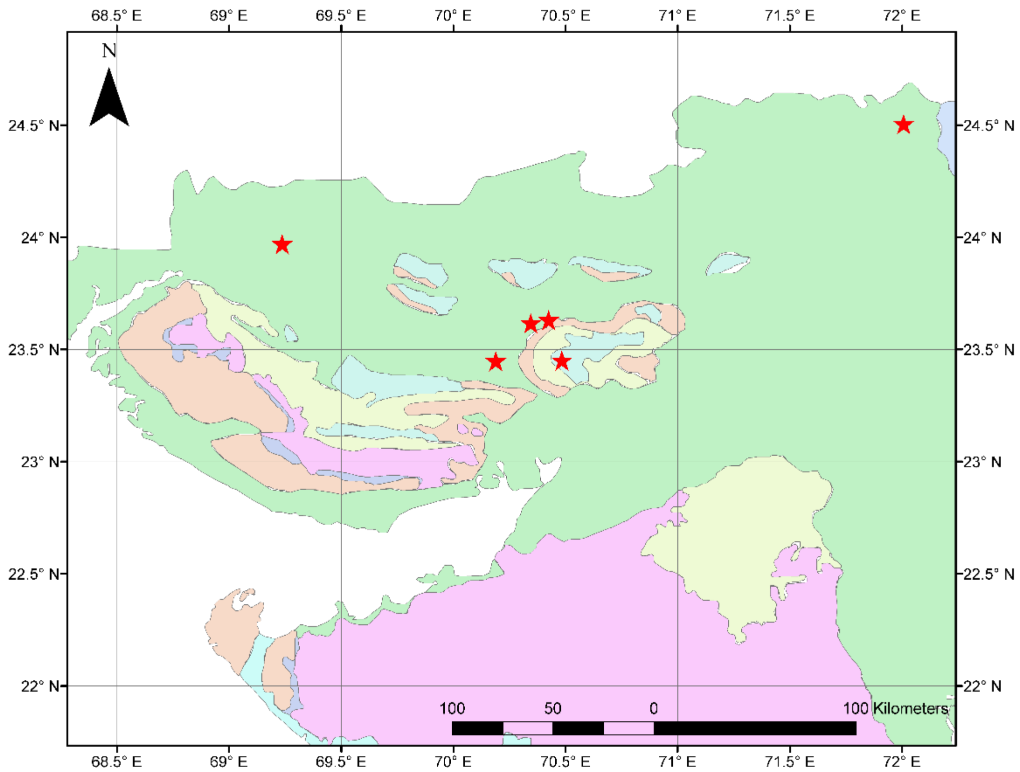

Fig 1.3: Earthquakes (M≥4.0) that occurred in 2017 recorded by ISR SMA network

1.3 Description of Recorded Earthquakes in Different Parts of Gujarat since inception of the network till 2017

(Santosh Kumar, P Mahesh, A P Singh, Ketan Singha Roy, Vandna Patel)

Seismicity in Kachchh has consistently been lower since 2008 (Fig. 1.5 and Table 1.5) with about 60 shocks of M≥3/y. The seismicity is comparable to that occurred in year 2016, as there are 47 shocks of M3.0 – 3.9 in 2017 and 49 shocks of M 3.0 – 3.9 in the year 2016. There are five shocks of M4-4.9 in Kachchh, in 2017.

Table 1.5: Showing the no. Of earthquakes of M≥3.0 which occurred in Kachchh between 2001 and 2017

Year	2006	2007	2008	2009	2010	2011	2012	2013	2014	2015	2016	2017
3.0 – 3.9	405	143	66	73	52	62	56	59	45	70	49	47
4.0 – 4.9	20	6	5	4	1	3	2	3	1	1	2	5
≥5.0	4	0	0	0	0	0	1	0	0	0	0	0

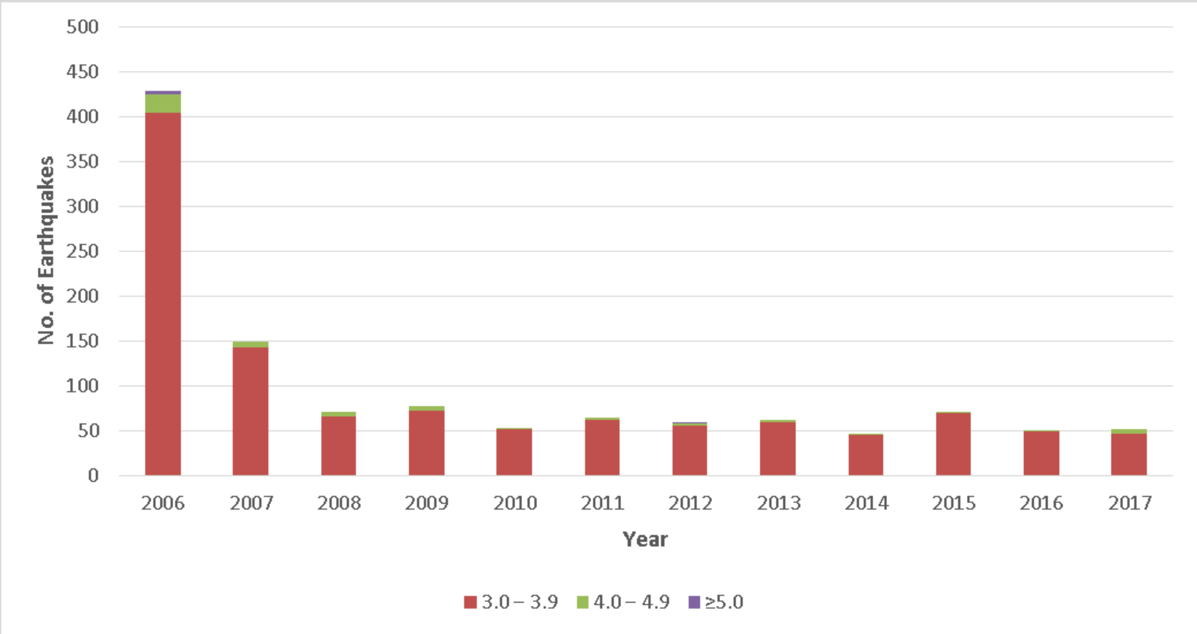

Fig. 1.4: Annual number of shocks in Kachchh during 2001-2017.

During August 2006 to December 2016, 137 earthquakes M3-3.9, 8 earthquakes of M4-4.9, and 2 earthquakes of M5.0 & M5.1 were recorded from Saurashtra (Tables 1.6, 1.7 & Fig. 1.5).

Table 1.6: Seismicity of M≥3.0 from Aug 2006 to Dec 2017 in the Saurashtra region

M	No. of earthquakes
3.0 – 3.9	137
4.0 – 4.9	8
≥5.0	2

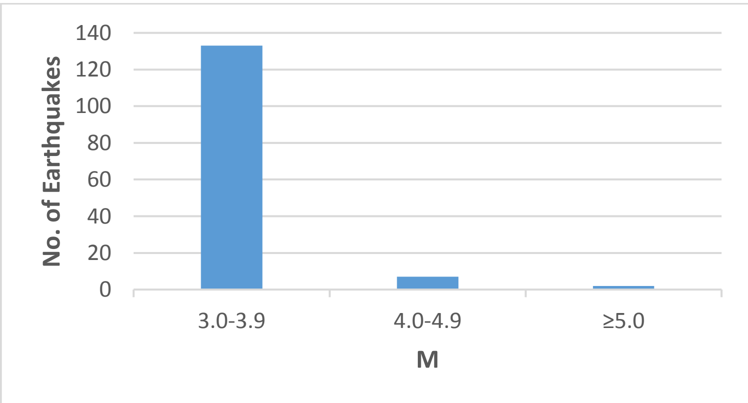

Fig. 1.5: Number of earthquakes in Saurashtra during Aug. 2006 to Dec. 2017, in three magnitude categories.

Table 1.7: Annual number of earthquakes of M 0.5 to 5.1 in the Saurashtra region from 2007 to 2017

Year	2007	2008	2009	2010	2011	2012	2013	2014	2015	2016	2017
3.0 – 3.9	30	12	6	12	18	6	3	5	7	3	1
4.0 – 4.9	1	2	0	0	4	0	0	0	0	1	0
5≥	1	0	0	0	1	0	0	0	0	0	0
Total:	**32**	**14**	**6**	**12**	**23**	**6**	**3**	**5**	**7**	**4**	**1**

1.4 Processing and interpretation of MEQ data collected during Jan-Dec 2016 for the study of seismogenic sources around the Subansiri Lower Hydro Electric (H.E) Project, Arunachal Pradesh

(P. Mahesh, A. Satish and Satosh Kumar)

NHPC Limited is carrying out microearthquake (MEQ) studies in the Subansiri Lower HE Project, Arunachal Pradesh, since May 2006. The earthquake data has been acquired by NHPC by operating a network of 6 seismograph observatories. The work of analysis and interpretation of the data is entrusted to the Institute of Seismological Research (ISR). The data are of 12 months period, from January to December 2016. In total, within the periphery of about 300km from the Subansiri Lower project site, 158 earthquakes were located in the magnitude range of M1.0-4.9, during 2016. There are 7 earthquakes between magnitude 1.0 and 3.8, within 50 km radius of the dam site (Fig. 1.6) and most of these are in the depth range of 10-30 km. Within 50 km radius of the dam site, all the shocks are micro earthquakes (M<4.0), and the largest is M3.8, located around 49 km from the dam site. Epicenters of shocks of M≥4.0 are at distance of 108 km or more from the dam site. The pattern of seismicity revealed that earthquakes are associated with the known tectonic features in the region.

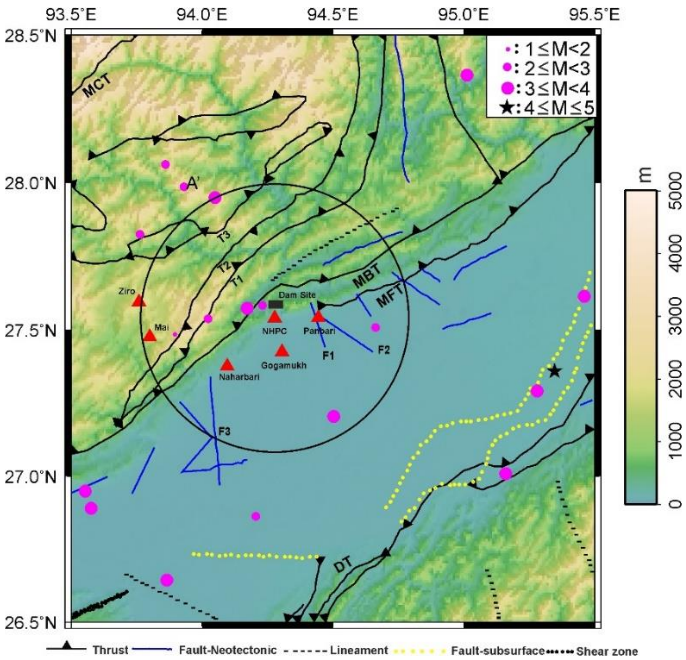

Figure 1.6: Distribution of epicenters of the earthquakes (S-P <15 sec) recorded during the period Jan-Dec. 2016. MCT: Main Central Thrust, MBT: Main Boundary Thrust, MFT: Main Frontal Thrust, DT: Dauki Thrust. The small black rectangle represents the dam location. The black circle is drawn with a radius of 50 km around the dam site.

1.5 Micro-earthquake (MEQ) studies at Bursar Hydro Electric (H.E) Project, Jammu and Kashmir

(P. Mahesh, A. Satish and Santosh Kumar)

NHPC Limited is planning to construct a HE project at Bursar, Jammu & Kashmir. As a part of the initial investigations, the work of MEQ studies is entrusted to ISR. ISR has installed 6 seismic stations around 50 km radius of the dam, in May 2016.The network was uninstalled in March 2017. We have collected 10 months (May-March) data from the network and data of 4 months are processed and analysed. We have located a total of 630 earthquakes of magnitude between 1.4 and 5.1 during 26 August to 23 Nov., 2016. There are 120 earthquakes of magnitude between 1.4 and 4.2 within 50 km radius of the NHPC proposed dam site. In total, 1444 earthquakes of magnitude M1.2- 5.4 have been located in 10 months during 18th May 2016 to 18th March 2017. Out of these, there are 251 earthquakes of magnitude M1.2-4.2 within 50 km radius of the Bursar dam site (Fig. 1.7). Within this radius, all the shocks are small (M<5.0) and the largest earthquake of magnitude 4.2 is located at a distance of around 21 km from the Bursar dam site. The pattern of seismicity during May 2016 to March 2017, reveals that the majority of the earthquakes are associated with the known features in the region like the Main Central Thrust (MCT) and Kishtwar Thrust (KT). We have also determined focal mechanism solutions of the significant earthquakes of M≥4 within 50 km radius of the dam site (Fig. 1.7.) The obtained focal mechanism solutions are in conformity with the thrust environment in the region.

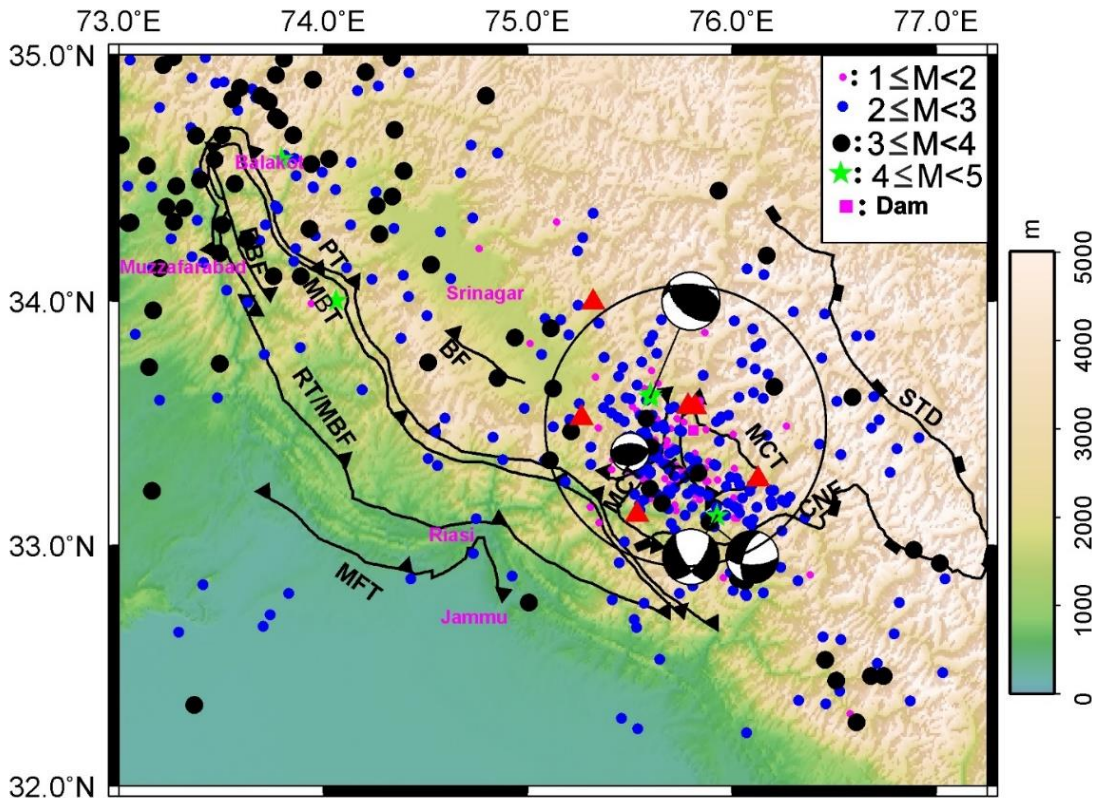

Figure 1.7: Distribution of epicenters of the earthquakes recorded by 3 or more stations during 18th May 2016- 18th March 2017. MCT: Main Central Thrust, MBT: Main Boundary Thrust, MFT: Main Frontal Thrust, KT: Kishtwar Thrust, MBF: Main Boundary Fault, RT: Riasi Thrust, BBF: Balakot Bagh Fault, BF: Balapur Fault, CNF: Chenab Normal Fault, STD: Southern Tibet Detachment, LH: Lesser Himalaya. Square (magenta colour) represents the dam location. The black circle is drawn with a radius of 50 km around the dam site.

1.6 Local earthquake tomography (LET) studies around the dam site of Bursar project, Jammu & Kashmir

(P. Mahesh, A. Satish and Santosh Kumar)

To understand the possible linkage between seismicity, existing faults and crustal structure, we determine 3-D seismic P- wave velocity (*Vp*), S-wave velocity (*Vs*) and *Vp/Vs* perturbations using seismic tomography. We used 209 well located local earthquakes recorded by 6 broadband seismographs operated during May 2016-March 2017, with at least four P and three S arrivals (Fig. 1.8). The earthquake magnitudes vary between 1.2 and 4.2. We inverted 1035 P and 1020 S-wave arrivals using the LOTOS code developed by Koulakov (2009a,b) and Koulakov et al. (2010), that performs iterative simultaneous inversions for the P and S wave velocities (*Vp* and *Vs*) and the earthquake source locations. The study region was parameterized in terms of velocities at the nodes of a 3-D grid and linear velocity gradients between the nodes. The velocity at any arbitrary point in the 3-D grid was calculated by linear interpolation of the values at the surrounding nodes. The reliability of the inversion results depends on the initial reference model. We used the 1-D velocity model of Kumar et al. (2009) as the initial reference model and used an initial *Vp/Vs* value of 1.73. With 33.5˚N, 75.5˚E as the centre of the grid, the model space was defined by 32.9˚-34.1˚N, 74.9˚-76.5˚E and 0-25 km in latitude, longitude and depth ranges, respectively. The seismic ray path distribution is shown in Figure 1.9. To suppress large perturbations in the calculated parameters, we used damping. The optimal damping parameters for the Vp and Vs were selected based on the empirical approach of Eberhart-Phillips (1986). The damping parameters for the P and S arrival times were set to be 12 and 15, respectively. We conducted tomographic inversion with a horizontal and vertical grid spacing of 10 km and 5 km, respectively. Final residuals after three iterations for Vp and Vs are 0.213 and 0.321, respectively.

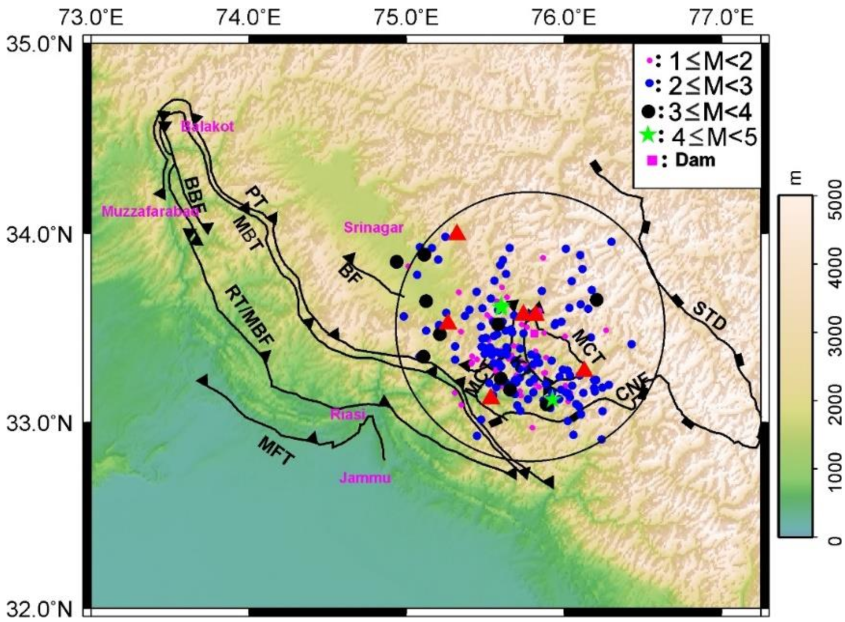

Figure 1.8: Distribution of epicenters of the 209 earthquakes recorded during 18th May 2016 to 18th March 2017 used for LET study. MCT - Main Central Thrust, MBT - Main Boundary Thrust, MFT-Main Frontal Thrust, KT- Kishtwar Thrust, MBF- Main Boundary Fault, RT- Riasi Thrust, BBF-Balakot Bagh Fault, BF- Balapur Fault, CNF-Chenab Normal Fault, STD- Southern Tibet Detachment), LH-Lesser Himalaya. Square (magenta colour) represents the dam location. Circle shows 50 km distance from the dam site.

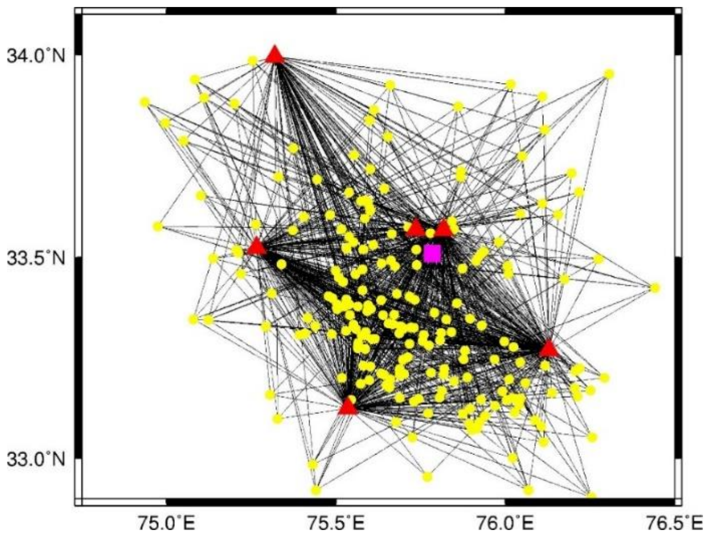

Figure 1.9: The distribution of seismic ray paths, in plain view. The seismic stations and events are represented by red triangles and yellow dots, respectively. Pink square shows the dam location.

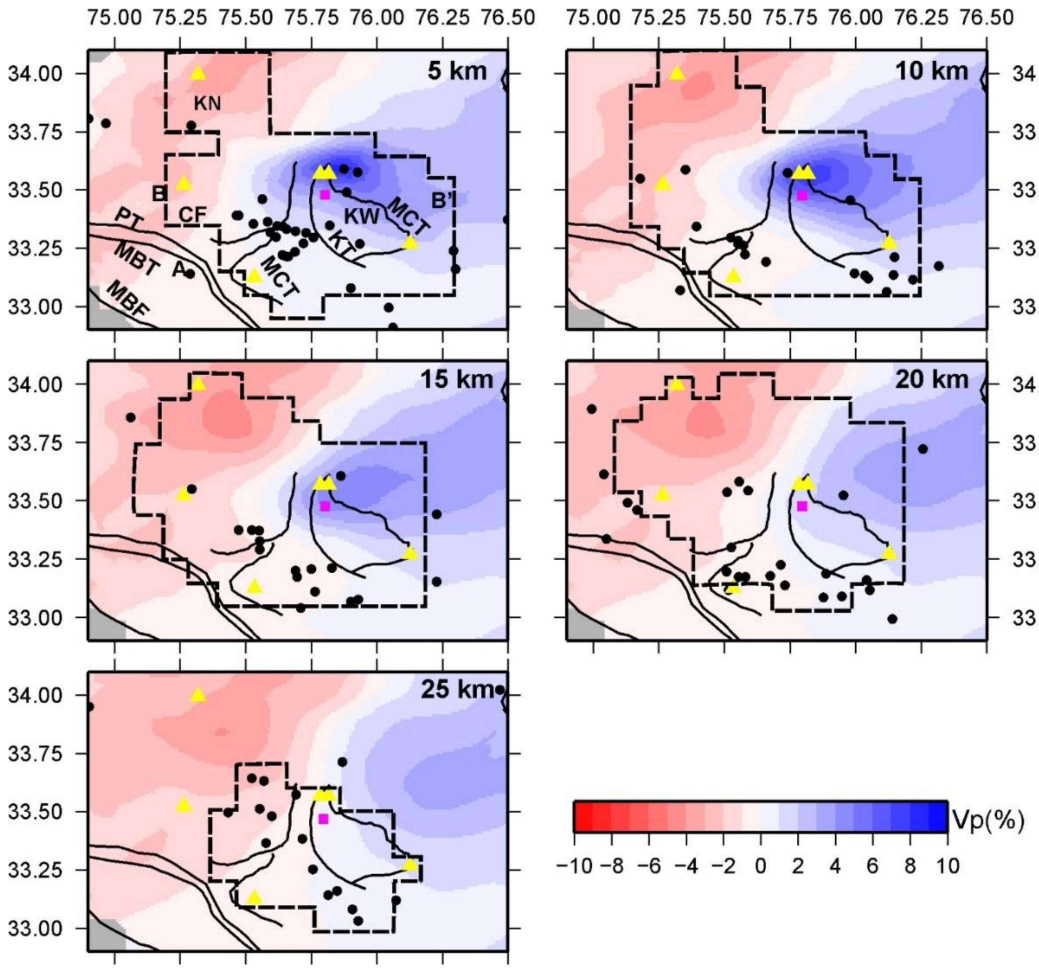

Figure 1.10: The plan view of *P*- wave velocity (*Vp*) perturbations. The black dotted lines enclose the better resolved regions. The layer depths are shown on the upper-right corner of each map. Red and blue colours indicate low and high *Vp* perturbations, respectively. The *P*- velocity perturbation scale (in %) is shown at the bottom. The yellow triangles represent the station locations. Black dots show the earthquakes that occurred within 2.5 km on either side of each depth slice. The pink square shows the location of Bursar project.

Figure 1.10 show *P* wave velocity (V_P) perturbations in plain view, and the seismicity within 2.5 km of either side of each depth layer. The smaller magnitude earthquakes are mainly falling in the zone of moderately low *Vp,* low *Vs* and high *Vp/Vs* between the Main Central Thrust (MCT) and Kishtwar Thrust (KT). The KT is imaged as a transition between low and high velocity zones. We observed that the velocity images obtained in the LET study are well correlated with the geology of the study area.

1.7 Upper Mantle structure of the North-west Deccan Volcanic Province from Teleseismic Tomography

(A Satish and P. Mahesh)

Teleseismic events (in the distance range 30°-90° from the center of the Gujarat State Seismic Network) of Mw>5.5 recorded during 2007-2016 are considered for the study. A band pass filter (frequency range 0.2 Hz-2 Hz) is applied to each trace to optimize the signal-to-noise ratio. To sort according to the distance, all the sesismograms were visually inspected. The earthquakes, which had good signal-to-noise ratio and recorded at 6 or more stations were selected for further analysis. The final dataset contains 745 earthquakes recorded at different 92 seismic stations (Fig. 1.11).

The travel time residual was calculated by subtracting the observed P arrival time from the theoretical P arrival time with respect to IASP91 global reference model and then the residuals at each station were plotted according to the back azimuth. Almost all the stations exhibited positive residual values. Most of the positive raw residuals indicate that the observed travel times are greater than the predicted travel times. The positive raw residual values vary from 0 to 5 seconds, while the negative values vary from 0 to -2 seconds.

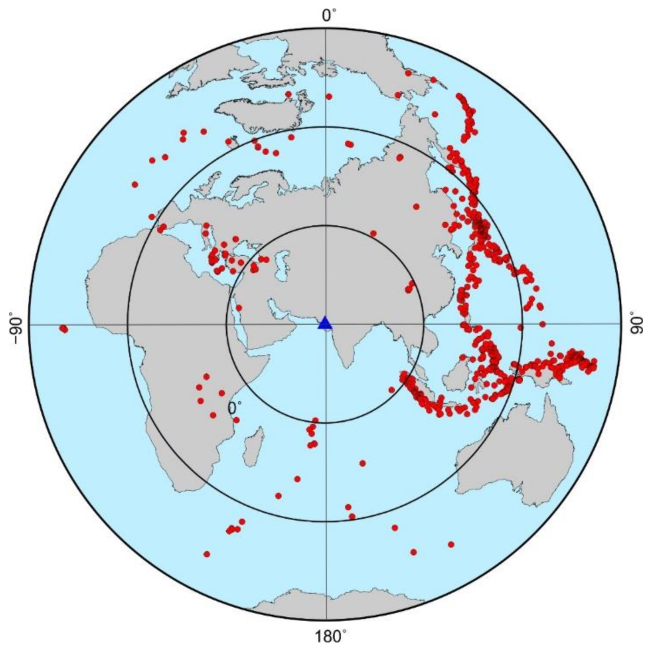

Figure 1.11: Map of epicenters of earthquakes (red circles) used in this study. Blue triangle indicates the center of Gujarat State Seismic Network.

The relative residual distribution versus azimuth and angle of incidence (or distance) of teleseismic rays, can be used to qualitatively delineate anomalous regions at depth (Steepsles and Iyer, 1976). We use the relative rather than absolute arrival-time residuals to reduce source errors and the effects of mantle heterogeneity outside the model volume. The relative arrival-time residual for each station (t_{res}) is given by the difference between the arrival time at each station (t_i) and the theoretical IASP91 arrival times, t_{iasp} with the mean residual for each event (t_{mean}) removed

$$t_{res} = (t_i - t_{iasp}) - t_{mean}$$

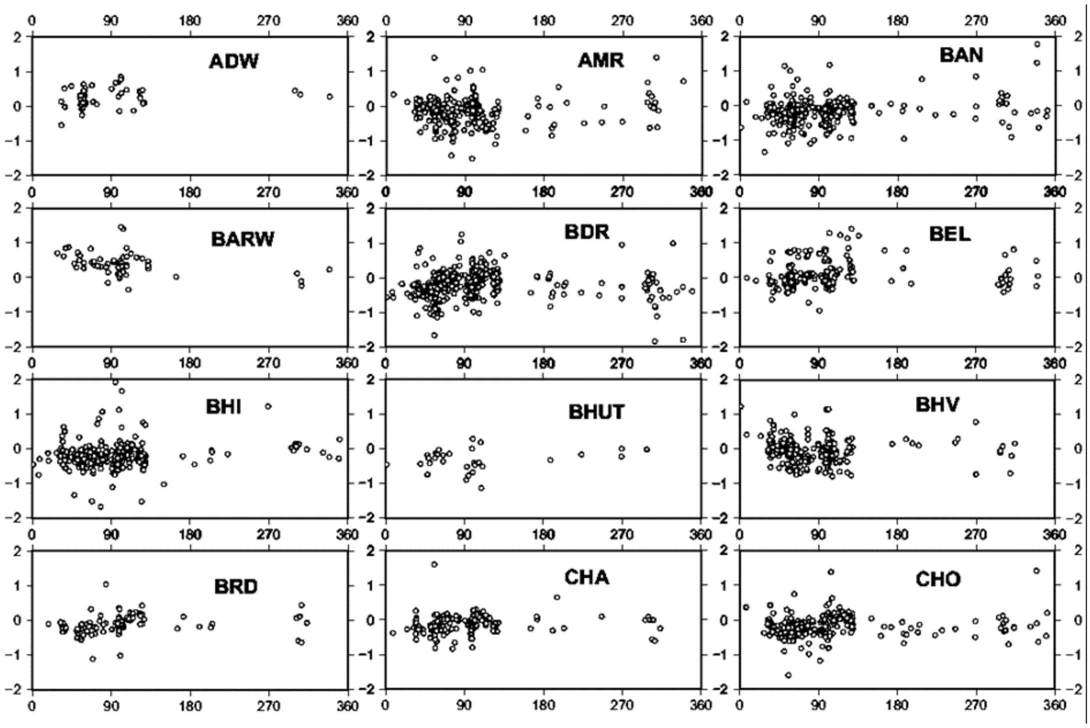

Figure 1.12: Relative travel time residuals with respect to azimuth

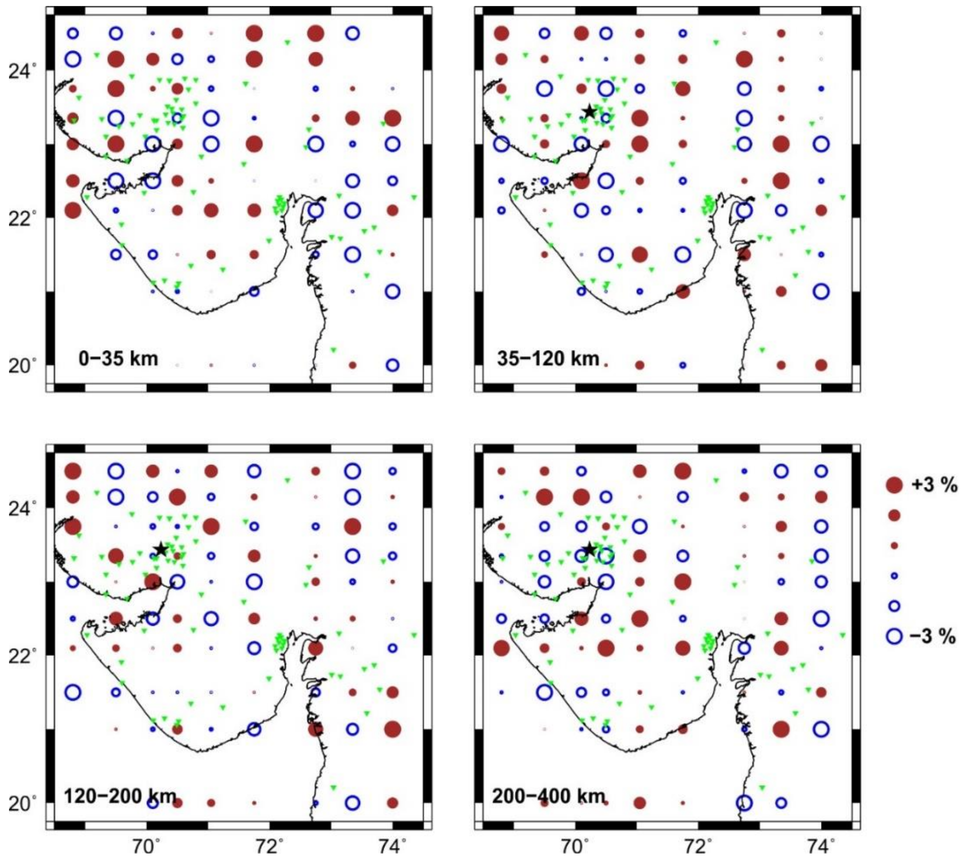

Figure 1.13: Checkerboard Resolution Test

The checkerboard synthetic resolution was performed with grid node spacing interval varies from 0.1 to 1 degrees. Overall the checkerboard synthetic test suggests good resolution. For comparing the tomographic results with the checkerboard test we used identical sources and phases from the raw dataset. The travel time residuals were calculated from the checkerboard model with maximum +/-3% of velocity perturbation. Figure 1.13 shows the horizontal slices ranging from 35 km to 400 km. The resolution pattern is good at the area close to the closed seismic stations which is due to the dense ray coverage.

The relative residuals are inverted to obtain the velocity structure using teleseismic tomography method of Zhao et al., 1994. At present, the inversion is performed with 12×11×6 grids in horizontal and vertical directions. It is observed that some areas are not well resolved due to poor ray coverage. It is intended to add the 2016 data for better ray coverage. Conclusive results with optimum grid nodes will be presented after including the 2016 data.

1.8 Reservoir Induced seismicity studies for SSNNL

(Vishwa Joshi and Santosh Kumar)

A multipurpose concrete gravity dam of 1210 m length with a maximum height of 146.5 m is being constructed across the river Narmada, near Navagam village of Nandod taluka in Gujarat state, by the Sardar Sarovar Narmada Nigam Limited (SSNNL). Now 18.3m high gates are being installed. In the absence of the gates, the maximum height is EL 121.92m. The Sardar Sarovar Narmada Project region falls in the zone III of the seismic zoning map of India (IS: 1893 - "Criteria for Earthquake Resistant Design of Structures ", Bureau of Indian Standards, New Delhi).

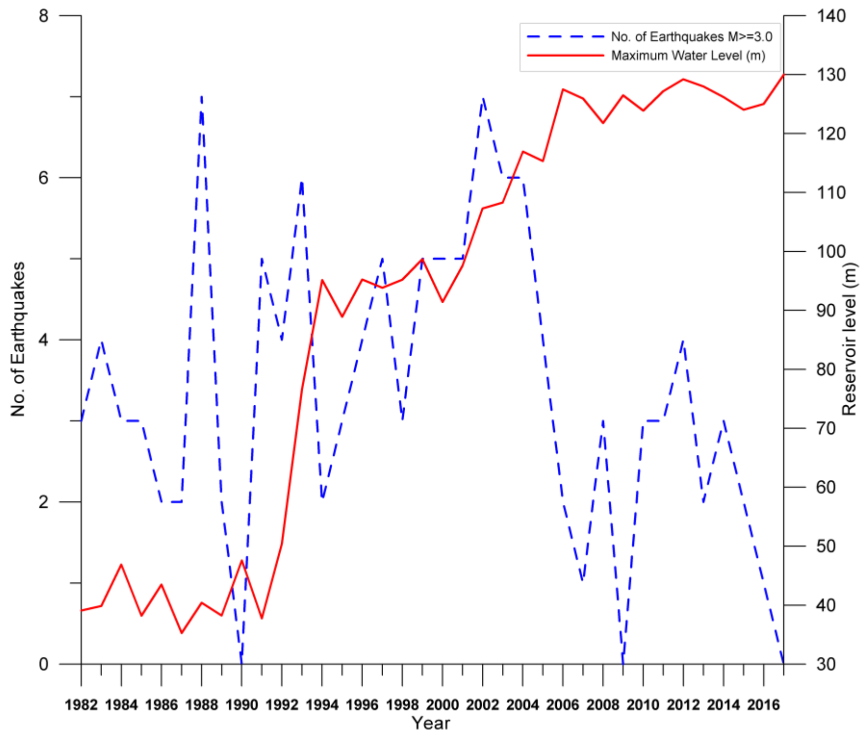

Figure 1.14: Year wise plot between no. of earthquakes and reservoir level of SSNNL

To monitor the seismic activity, ISR is running a seismic network of 9 stations in and around the SSP area. In order to study the reservoir induced seismicity, the number of earthquakes (of M≥3.0) along with the maximum reservoir level are plotted for the period 1982-2017 (Fig. 1.14). It is observed that till now, there is no correlation between the reservoir filling and increase in the number of earthquakes. No significant activity or cluster has been noticed due to the reservoir filling. Increase in number of micro-earthquakes (M<=3.0) is observed year wise, which may be due to the increase in the detectability level. Low level seismicity is noticed along Barwani-Sukta, Rajpardi and Piplod faults

1.9 Local Magnitude scale for Saurashtra region

(Vishwa Joshi, Sumer Chopra and Santhosh Kumar)

Local magnitude is an important parameter in earthquake hazard assessment, both in quantifying the rate and amount of seismicity and also in understanding the attenuation of ground motion with distance. We obtain the station corrections, which represent deviation in the average velocity model in the vicinity of the station and depend strongly on the topography and lateral velocity variations associated with heterogeneous near-surface structures. A negative (or positive) station correction means the true velocities are higher (or lower) than the predicted ones at the recording station. The station corrections for the seismic stations used in the present study were determined by inversion. A total of 548 earthquakes were used to determine local magnitude scale for Saurashtra region. Amplitudes measured on the waveforms were inverted to obtain two attenuation parameters, i.e., geometrical spreading and anelastic attenuation. Local magnitude scale for Saurashtra region for 17 km and 100 km normalisation has been prepared.

1.10 Estimation of source parameters for North Gujarat

(*Arpan Shatri and Santosh Kumar)*

We have estimated the source parameters for the North Gujarat (NG) region using 302 velocity time histories of 92 shocks recorded during 2010–2016. The Static Brune stress drop is found to vary between .04 bar and 104 bars with most of the values around 10-15 bars for NG. The corner frequency varies between 1.16 and 9.15 Hz and source radius between 60.8 and 648 m.

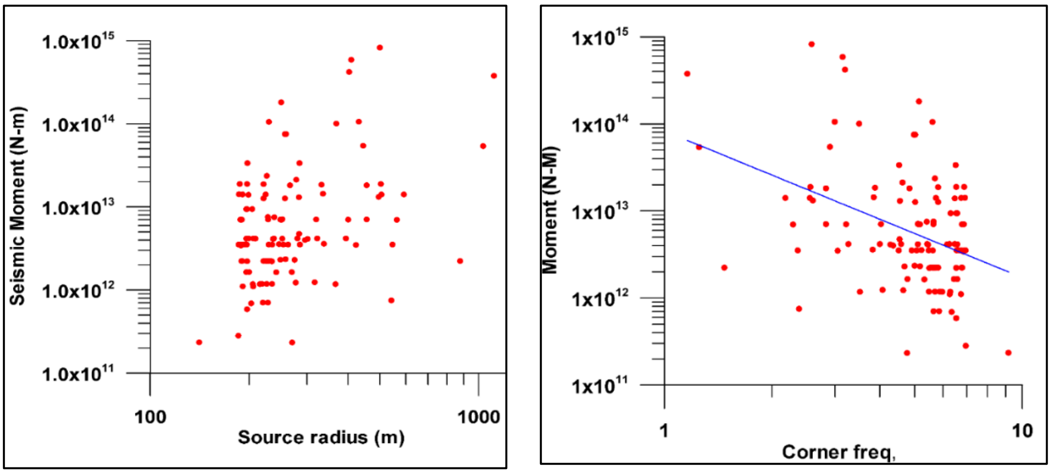

Figure 1.15: Plot showing the relation between the seismic moment and source radius (left) and corner frequency (right).

1.11 Seasonal variations of secondary microseism sources

(Ketan Singha Roy)

We have computed frequency dependent amplitude spectra and degree of polarization (DOP) of the seismic signals recorded at 10 seismic stations of the Institute of Seismological Research (ISR), recorded during 2016 (Fig. 1.16). Daily probabilistic power spectral density (ppsd) has been calculated for 4hr time window length with 50% overlapping. Time series and ppsd curves of vertical component at station JUN for day 2016-06-05 is shown in figure 1.17.

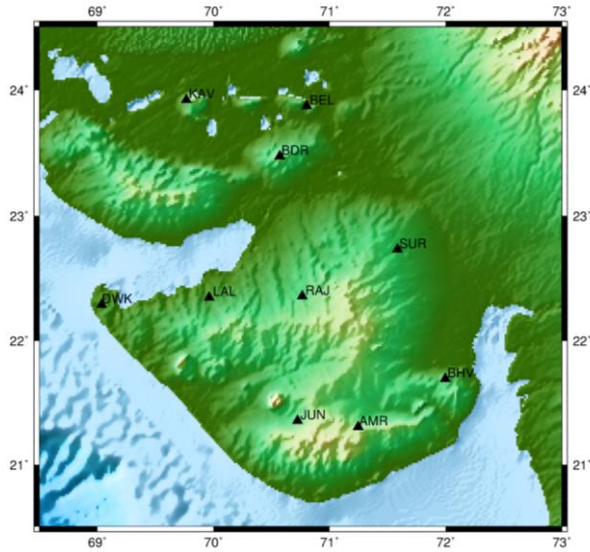

Figure 1.16: Location of seismic stations.

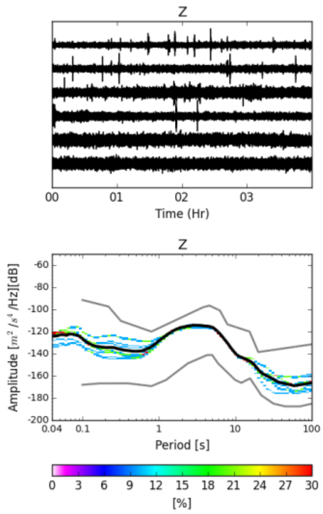

Figure 1.17: Time series (top) and amplitude spectrum (bottom) of vertical component at seismic station JUN for a particular day (2016-06-05).

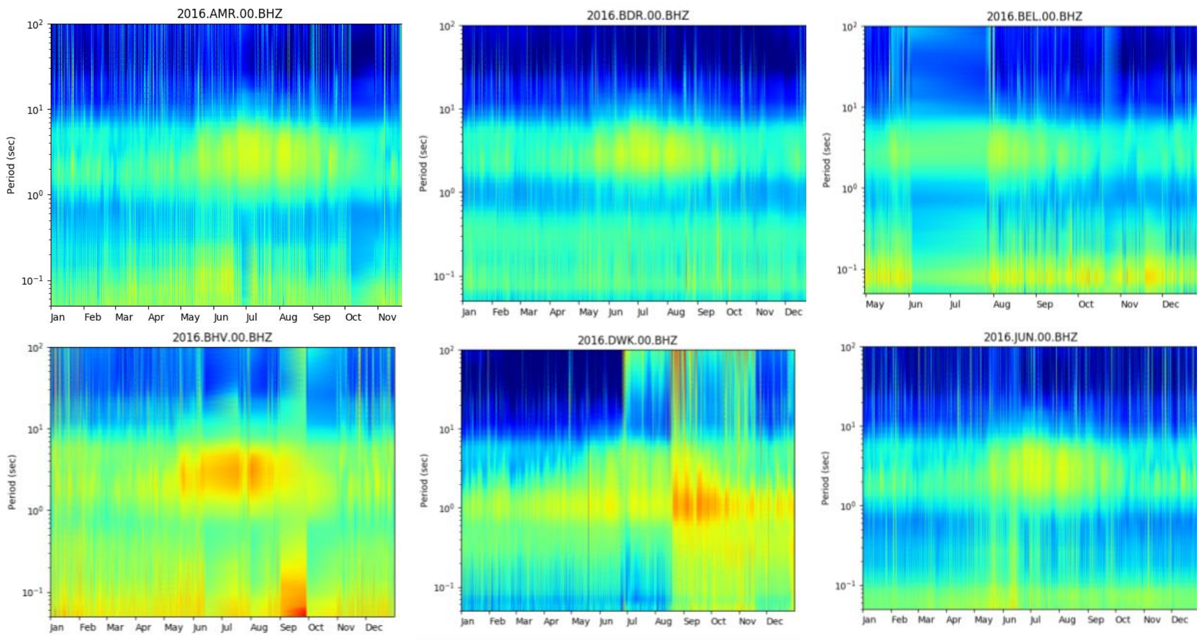

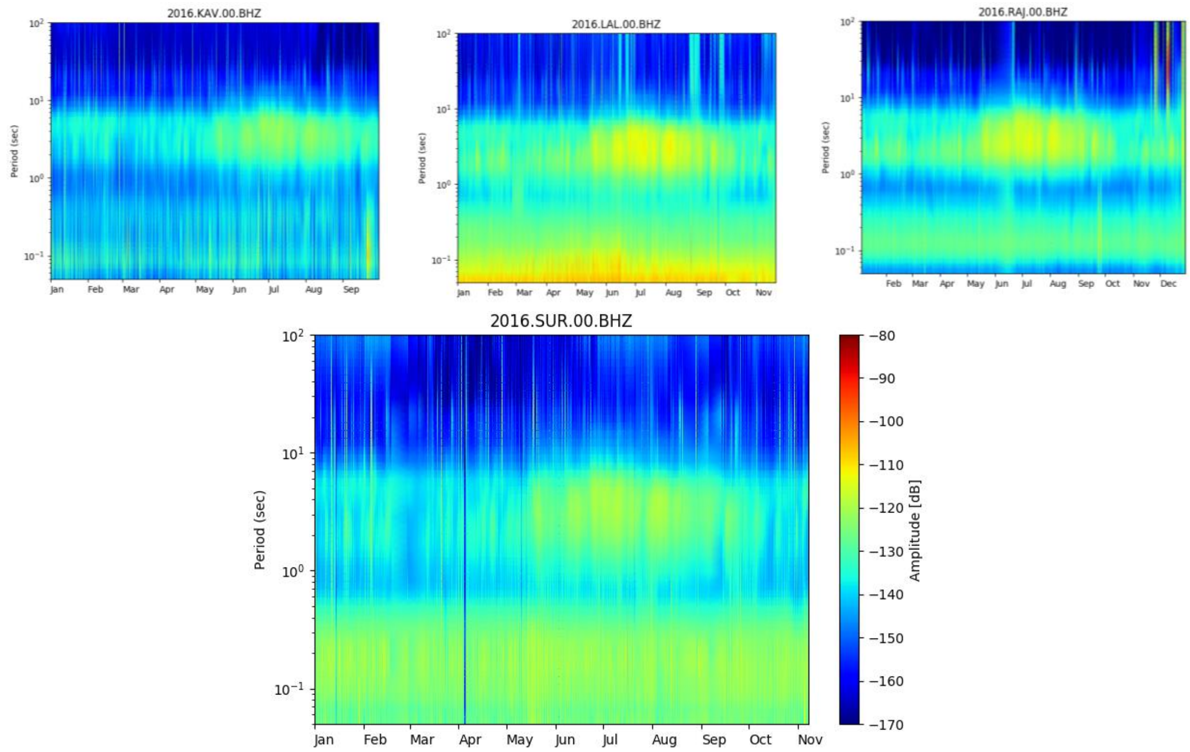

Figure 1.18: Seismic noise amplitude variations over 1 year in dB in the period range 0.05-100 s.

Figure 1.18 shows the noise level variation over one year in the period band 0.05–100s for the 10 stations of the ISR network. The noise level is maximum during the period May to October, in the period range 1.0-10.0s. This may be due to secondary microseism generated by the interaction of ocean gravity waves of similar periods that travel in opposite directions (Fig. 1.19). We computed the degree of polarization of the secondary microseisms during the period May to October for 3 stations namely Amreli (AMR), Junagarh (JUN), and Bhavnagar (BHV).

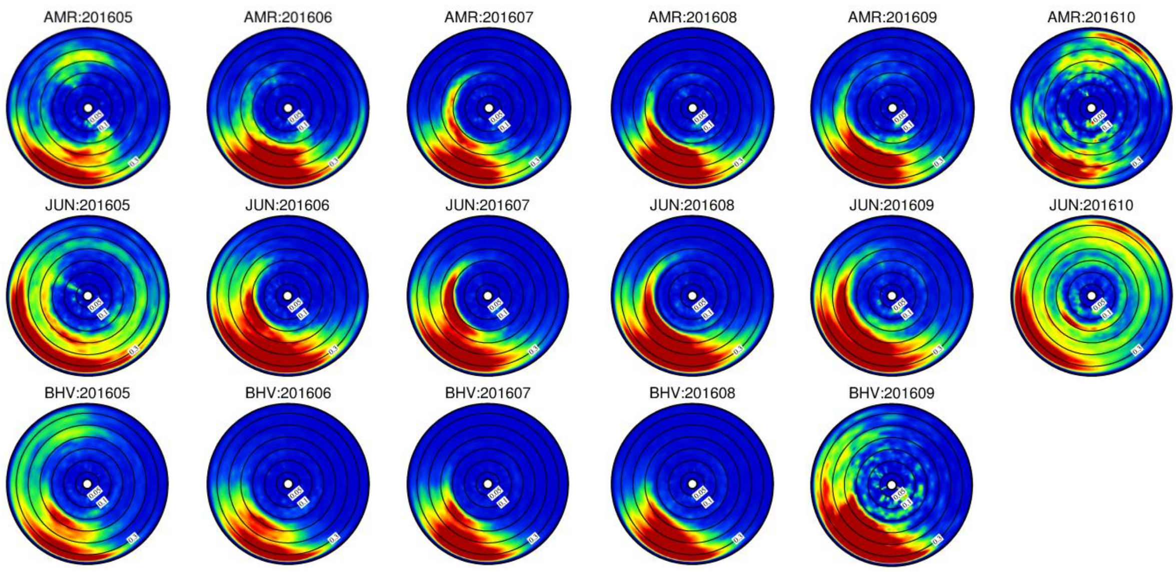

Figure 1.19: Frequency dependant back-azimuth

1.12 Active Tectonics in Lower Narmada basin

(Poorti Gosain and Suraj Balan)

The study area involves the lower Narmada Basin in which the Narmada River flows along the Narmada Son Fault, that trends ENE-WSW. The area has a deposition of a huge thickness of Tertiary and Quaternary sediments (Chamyal, 2001). The main objective of this study is to identify the tectonic activity by mapping the active fault(s) in the area. Seven river basins, namely, Karjan, Madhumati, Hakran, Kaveri, Amravati, Nandikhadi and Chandras Khadi have been studied in order to map the geomorphologic features. SRTM DEM (one arc second) and Cartosat DEM satellite data have been used for the study.

Different morphometric parameters such as Asymmetry Factor (AF), Tilting, Hypsometric Curve (HC) and Hypsometric Integral (HI), Bifurcation Ratio (Rb) have been calculated to discern the tectonics of the study area.

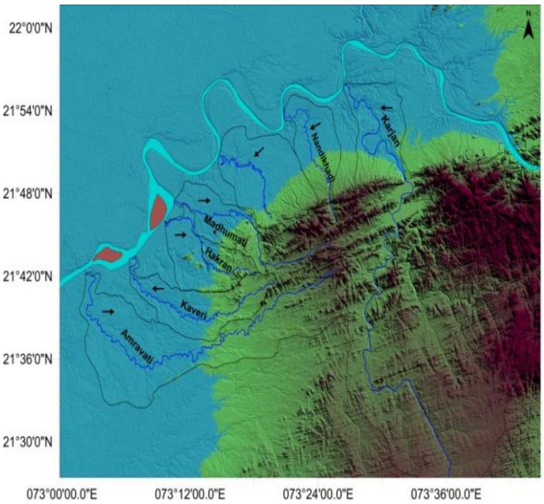

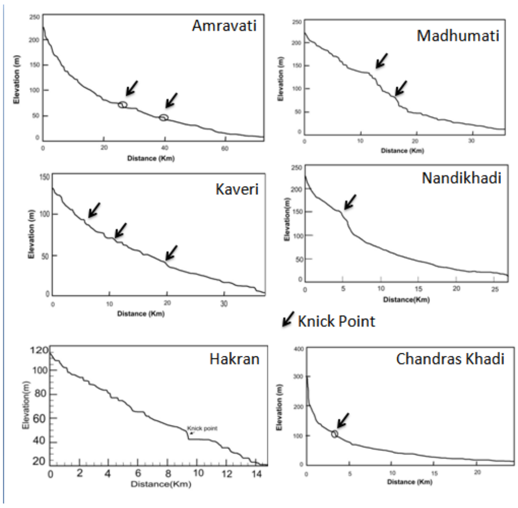

Asymmetry factor gives information regarding the tilt in the study area, based on which a Tilt map has been made. This indicates that the basin is tectonically active and still uplifting.

Bifurcation Ratio indicates that the Nandikhadi and Chandras khadi basins have experienced less tectonic activities than the other basins of the study area. Hypsometric curve and hypsometric integral gives information about the different stages of the river, at present. The values of HI and longitudinal profiles across different basins in our study area reveal that the watershed is highly susceptible to erosion, suggesting that the area is tectonically active.

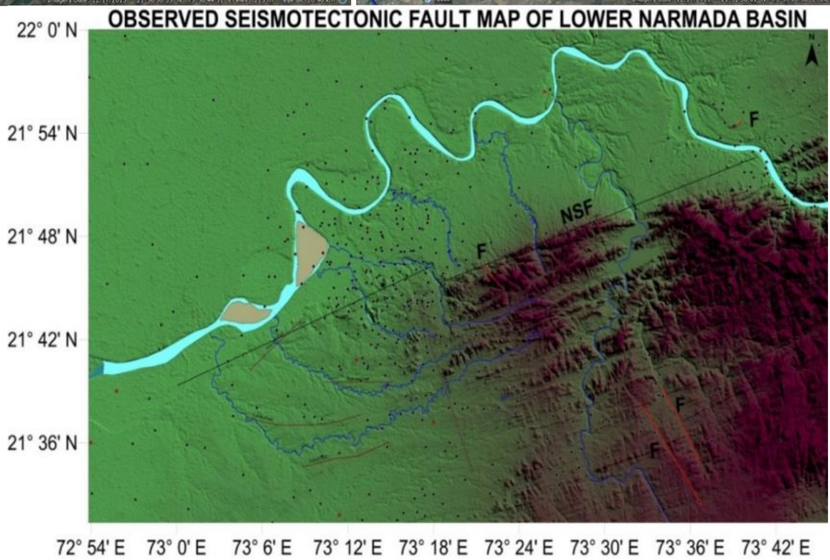

The study area has undergone structural disturbances due to the tectonics. On the basis of the faults observed topographically, a fault map has been prepared.

1.13 Identification of the traces of neotectonic activity in the vicinity of Sardar Sarovar reservoir

(Suraj Balan and Poorti Gosain)

The main lithology of the study area is the Deccan trap basalts, sedimentary sequence of sandstone, limestone, shale and mudstone (Blanford, 1869). The drainage pattern has been analyzed to understand the tectonic influence in the area. The data sets used include, satellite data (SRTM – one arc second resolution) and toposheets from survey of India. The morphometric analysis has been done for the correlation with tectonics.

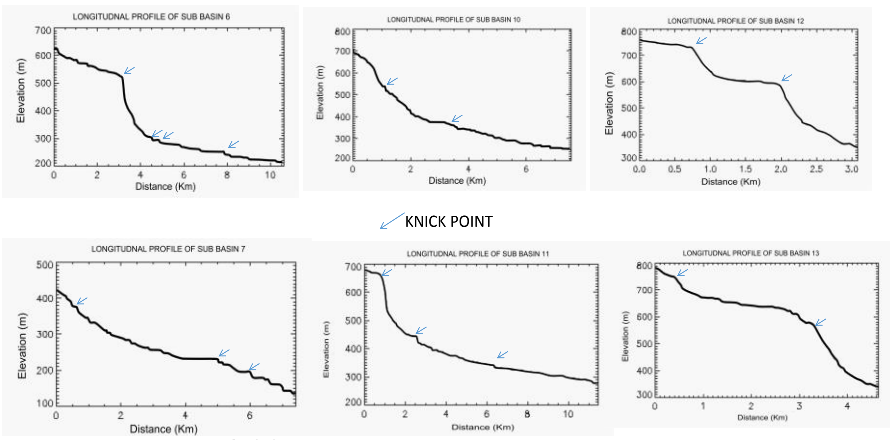

Figure 1.20: Longitudinal profiles of the sub basin

Longitudinal profiles of 13 sub basins have been prepared so that the knick points can be identified, which is the indicator of tectonics. The hypsometric integral has been calculated for the 13 sub basins to estimate the variation in hypsometric indices in each sub basin. Higher values indicate that the area is under tectonic influence.

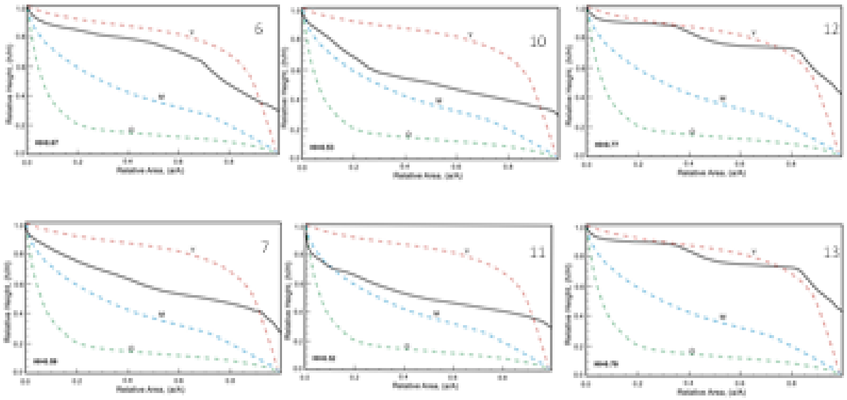

Figure 1.21: Hypsometric curves of the sub basin

Figure 1.22: A triangular facet is usually a remnant of a fault plane. The figure shows that the location has triangular facets and a stream flowing in straight line along the base of it.

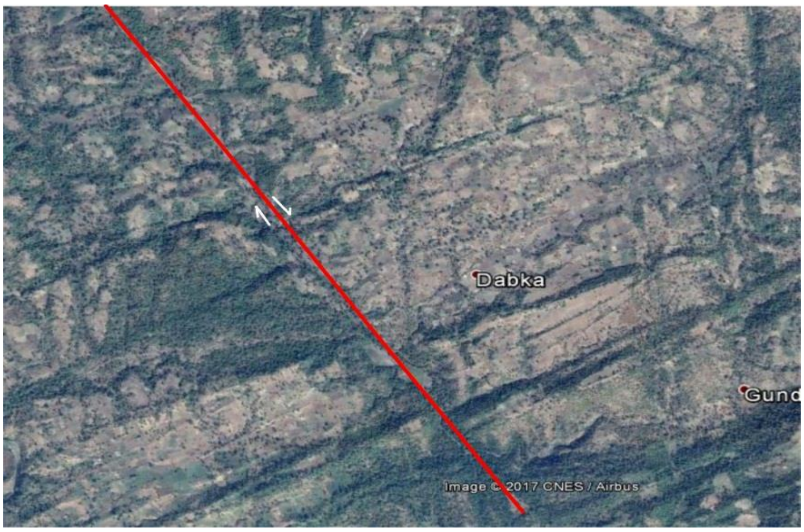

Figure 1.23: Figure showing ridges in the area displaced due to strike slip faulting.

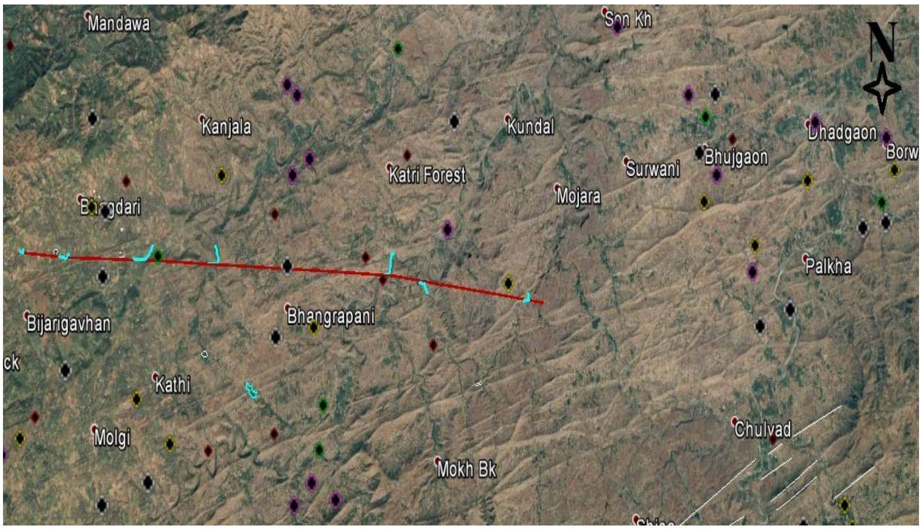

Figure 1.24: Observed offsets of channels. Ponding is present along a straight line. Seismicity is observed in the area along the line.

2 Seismic Hazard Assessment and Microzonation

2.1 Estimation of PGA and causes of building collapse during the 2001 Bhuj Earthquake

(Kapil Mohan, Sumer Chopra and Vasu Pancholi)

In Ahmedabad, 80 buildings with 1021 flats and 82 other houses collapsed (Mishra, 2004) during the 2001 Bhuj earthquake (Fig. 2.1). In Ahmedabad City, PGA values ranging from 82 to 125 cm/sec^2 are estimated for the far field earthquake scenario. The PGA estimated at the Passport office building due to this earthquake was found to be 100 cm/sec^2, closely matching with the recorded PGA value. Boreholes BH-01, 19, 08 and 17 were drilled in the vicinity of the collapsed building sites. Most of the collapsed buildings were close to BH-01 and BH-19 where Clay is present at the surface, with a very low N-value, low shear wave velocity and medium plasticity. The clay with interbeds of silty sand is present in the subsurface.

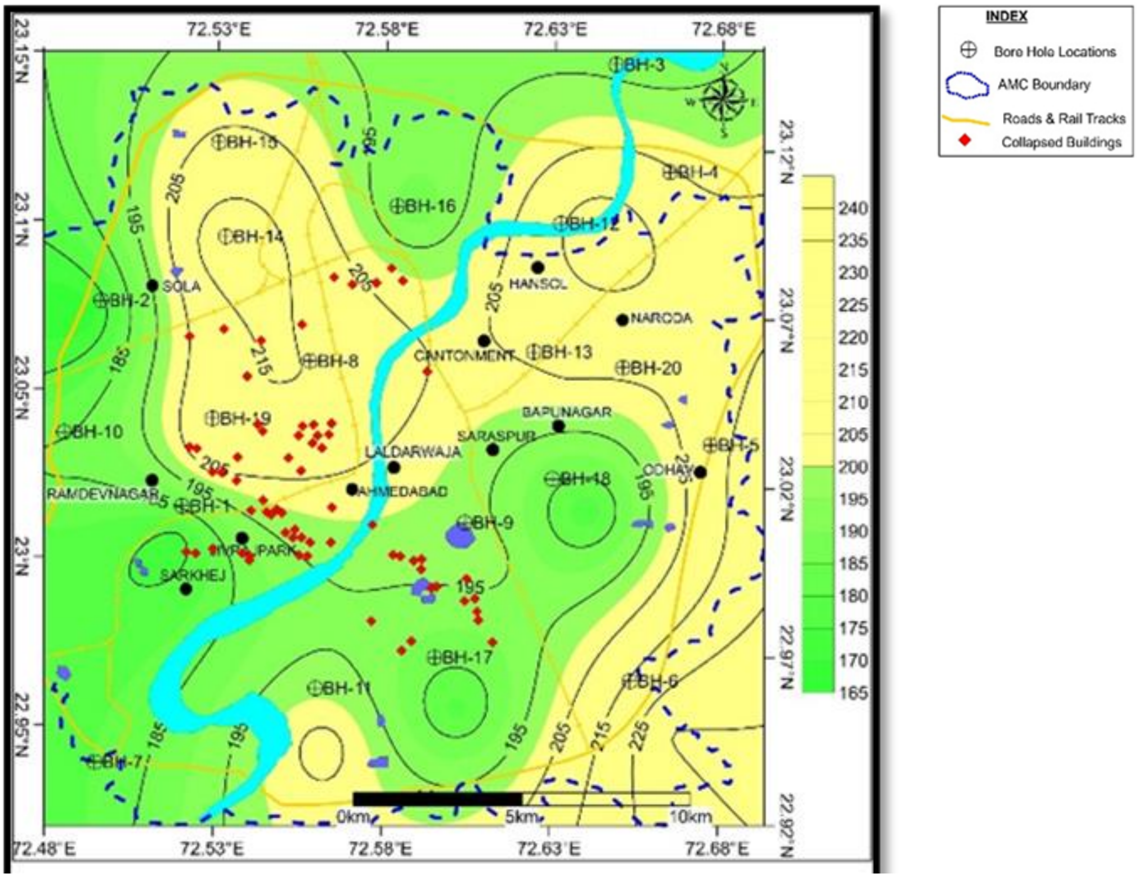

Figure 2.1: Map showing the spatial variation of PGA due to a farfield scenario earthquake, together with the locations of buildings collapsed during the 2001 Bhuj earthquake.

In the Loma Prieta earthquake (Ms 7.1) that occurred on October 17, 1989, the maximum (up to 80%) loss of life occurred about 50 miles away (at Treasure Island) from the fault rupture zone. Ferritto et al. (1993) from Naval Civil Engineering Lab, California have conducted the ground response analysis of the Treasure Island, which is a Naval base. The soil of Treasure Island consists of bay mud deposits, a high plasticity silty clay. It was concluded from the study that the high plasticity clay deposits can be a potential source of ground motion amplification. The Clay with Medium plasticity found at BH-01 and BH-19 may be one of the causes of devastation in the region.

2.2 Generation of Site specific Response Spectra at surface of IOCL Bongaigaon Refinery, Assam State, India using Probabilistic Seismic Hazard Assessment

(Kapil Mohan, Madan Mohan, Shruti Dugar and Sumer Chopra)

The methodology developed by Cornell (1968) for Probabilistic Seismic Hazard Assessment (PSHA) is applied for the estimation of seismic hazard at the Bongaigaon site in Assam, in terms of Peak Ground Acceleration (PGA) and Spectral Acceleration (SA) for 10% and 2% probability of exceedance in 50 years. The ground motion parameters are estimated at B/C boundary Sites (Vs=760 m/sec). Site Coefficients (NEHRP report, 2009) have been used to estimate the ground motion at B/C boundary sites for NDMA (2011) and Nath et al. (2012) relations and the other three relations to estimate the ground motions at B/C boundary sites. A logic tree approach was followed to obtain ground motion parameters. Maximum PGA values of 0.16g and 0.30 g are observed at 10% and 2% P.E in 50 years, respectively at B/C boundary sites (Vs=760 m/sec). The Uniform Hazard Spectra for 10% and 2% P.E in 50 years is obtained.

Due to unavailability of strong ground motion at the site, the Uniform Hazard Spectra (UHS) is estimated at the engineering bed layer (EBL) (Vs 760m/sec) for 2% Probability of exceedance and 10% probability of exceedance in 50 yrs. The Uniform Hazard Spectra (UHS) were scaled using two methods (i) strong ground motion data available at PEER site and (ii) the wavelets algorithm proposed by Abrahamson (1992) and Hancock et al. (2006) using recorded data. The matching of the response spectra generated by wavelet algorithm was found satisfactory for both 2% and 10% P.E. in 50 yrs. The matched spectra and the corresponding accelerograms at EBL for 2% P.E. and 10% P.E. in 50 yrs are given in Fig. 2.2.

The accelerograms generated at the EBL level through response spectra matching have been passed through the soil models prepared along all the eleven boreholes drilled at the site. The mean (within soil) PGA of 0.144g and 0.112g have been estimated for 2% and 10% P.E. in 50 yrs, respectively. The surface ground motion has been estimated at all the boreholes. Mean peak ground acceleration (PGA) values of 0.305g and 0.15g have been estimated at the surface for 2% and 10% P.E. in 50 yrs., respectively. The response spectra have been generated from the surface accelerograms using Newmark integration scheme (Newmark, 1959) applied in Seismosignal software. The Mean, Mean + Standard Deviation (SD), Mean-SD response spectra for damping of 0.5%, 2%, 3%, 4%, 5%, 7%, 10%, 20% and 30% at the surface are generated for both 2% and 10% P.E. in 50 yrs. The response spectra at 0.5% and 30% (at the surface) for 10% P.E. in 50 yrs. are shown in Fig. 2.3

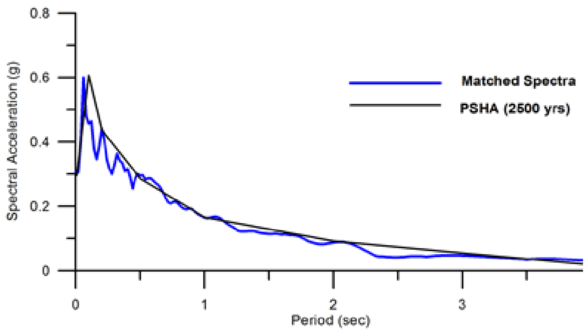

(a)

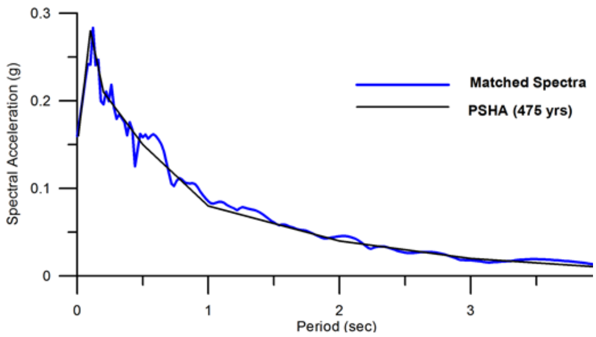

(b)

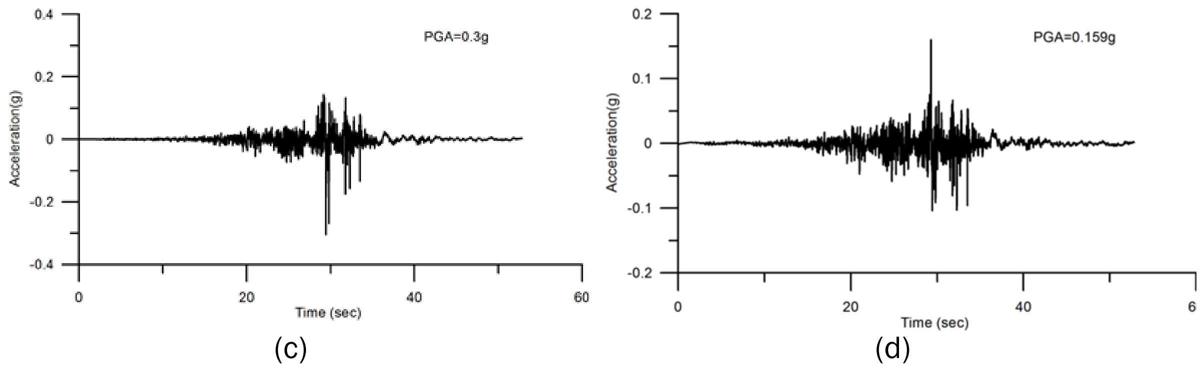

Figure 2.2: (a) The UHS and matched response spectra at 5% damping and (b) the accelerogram (outcrop motion) corresponding to the matched spectra at NEHRP B/C Boundary (Vs 760m/sec) for 2500 years (2% probability of exceedance in 50 yrs.), (c) The accelerograms (outcrop motion) and response spectra at 5% damping at NEHRP B/C Boundary for 475 years (10% probability of exceedance in 50 yrs).

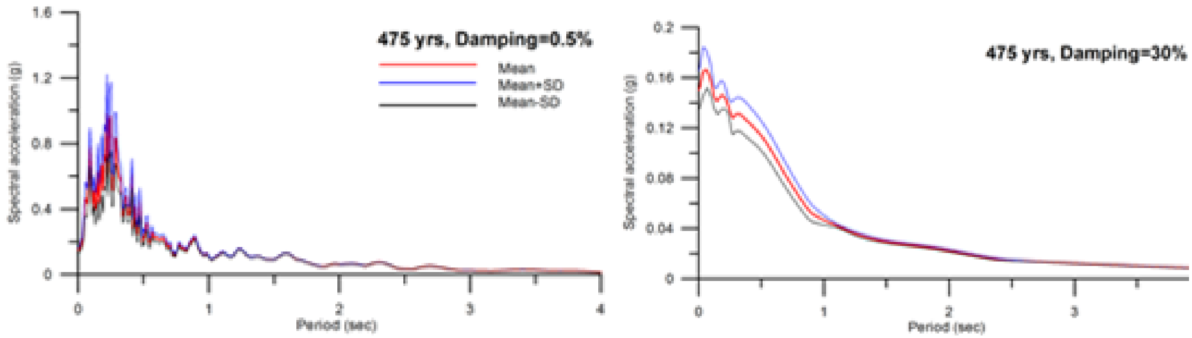

Figure 2.3: Response spectra at the surface level for different dampings (0.5% and 30%) for 475 yrs (10% probability of exceedance in 50 yrs)

2.3 Seismic Hazard Assessment of Devni Mori site, Sabarkantha, Gujarat

(Kapil Mohan, Naveen Kumar, B. Sairam and Sumer Chopra)

The Devni Mori site falls in Zone III of the seismic zoning map of India (BIS) where the maximum expected magnitude of an earthquake is 6.0. Seismic hazard analysis of this site is performed using the Stochastic Finite Fault Source Modeling (SFFSM) method by considering magnitude 6.0 as the scenario earthquake and the East Marginal Fault as the fault capable of generating a near field earthquake. The proposed heights of the structures range from 10 to 72m, and this high rise structure may be affected by the low frequency waves from a large earthquake in the Kachchh region. Hence, a scenario earthquake of Mw7.6 (2001 earthquake), along the eastern part of the Kachchh Mainland Fault (KMF) is also considered as the far-field source for hazard analysis. The strong ground motion is simulated at 310m/sec based on the MASW investigation conducted at the site. A PGA of 56.3 cm/sec^2 and PSA of 150.4 cm/sec^2 at 0.08sec (Fig. 2.4a) are estimated for the nearfield earthquake consideration. A PGA of 40.3 cm/sec^2 and PSA of 85.8 cm/sec^2 at 0.17sec (Fig. 2.4b) are estimated due to the far-field earthquake scenario.

The normalized response spectra (Sa/g) are also prepared for both (near field and far field) the earthquakes and shown in Fig. 2.5. A maximum Sa/g value of 2.67 is estimated at a period of 0.08 sec, in the case of a nearfield earthquake scenario. The site-specific response spectra are also determined for the site by anchoring the maximum PGA (56.45 cm/sec^2) estimated at the site with the maximum normalized acceleration (Sa/g) values at all the periods (Fig. 2.5). It is observed that the maximum value of spectral acceleration (150.3 cm/sec^2) is obtained at a period of 0.08 sec (Fig. 2.6). The proposed structures at the site are of 10m and 76m height, which correspond to natural periods of 0.4 sec and 2.5 sec.

(a) (b)

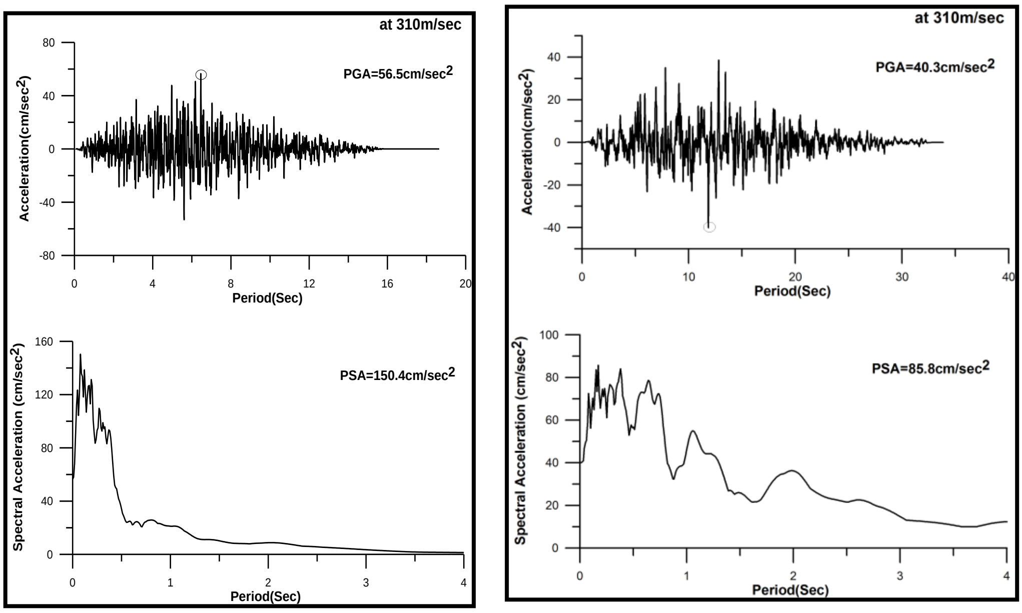

Figure 2.4: (a) Acceleration time history and response spectra at the Devni Mori Site at Vs of 310m/sec due to (a) near field earthquake and (b) far field earthquake

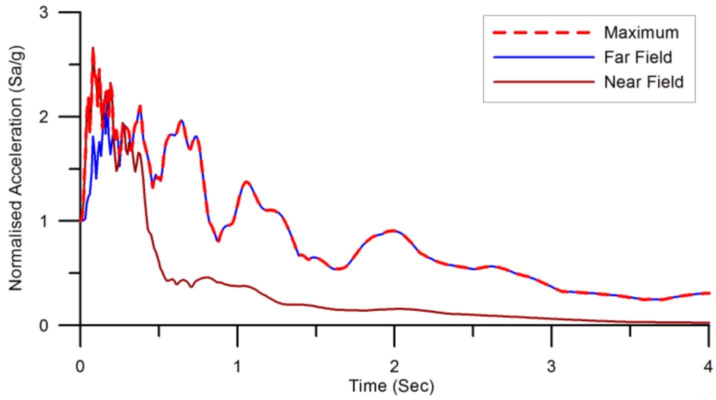

Figure 2.5: The normalized response spectra due to both near and far field earthquake consideration.

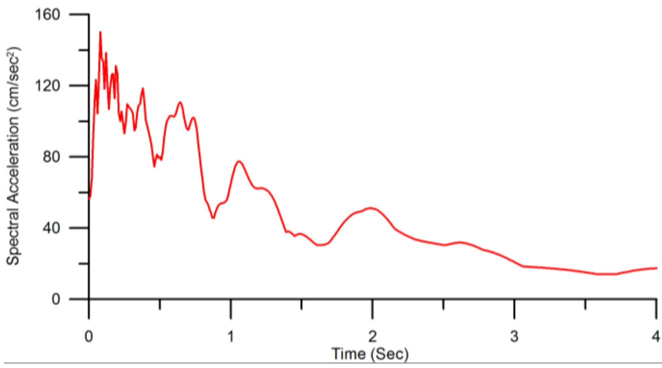

Figure 2.6: The site-specific spectra proposed for the site

2.4 Assessment of Seismic Hazard in Ahmedabad City incorporating parametric uncertainties

(Kapil Mohan, Shruti Dagur and Sumer Chopra)

The Ahmedabad City falls in Zone III of the seismic zoning map of India (BIS). In 1864, an earthquake of magnitude Mw 5.7 occurred 80km south of Ahmedabad city. The City lies in the Cambay basin surrounded by West and East Cambay faults. The seismic hazard analysis is carried out using the Stochastic Finite Fault Source Modeling (SFFSM) method by considering magnitude Mw 5.5, 6.0 and 6.5 as scenarios for the near field earthquake along the Cambay faults. Ahmedabad City has a number of high rise buildings and many were affected during the 2001 Bhuj earthquake. In this context, it is required to analyze the ground response from a future large earthquake from the Kachchh region also. Three scenarios of Mw 7.0, 7.6 and 7.8 along the eastern part of the Kachchh Mainland Fault (KMF) are considered as far-field sources for the hazard analysis. The ground response analysis is carried out considering soil data from the drilled boreholes. The Engineering Bed layer (EBL) (with V_s 520m/sec and N>80) is found varying from 24m to 54m.

The synthetic ground motions for a near field earthquake scenario (Mw 5.5, 6.0 and 6.5 along East Cambay Fault and West Cambay Fault) are generated. The quality factor proposed by Chopra et al. (2010) and Gupta et al. (2012) have been used. To overcome the uncertainity, stress drop values of 60, 80 and 100 bars and Kappa values of 0.02, 0.025 and 0.03 have been considered for generating the Near Field earthquake scenarios. A total of 54 input parameteric combinations have been considered for estimation of the ground motion at the EBL.

The ground response analysis is carried out at 20 boreholes varying in depth from 40 m to 80 m. The soil models for each borehole above the EBL have been prepared. The input earthquake motion when applied at EBL and allowed to pass through the soil column either gets amplified or de-amplified at the boundary of the layers. Finally, the response is observed at the surface in terms of PGA (from accelerogram) and spectral acceleration (from Response Spectra). This process is conducted using the SHAKE program. The input motion with mean PGA varying between 52.4 and 111.4 cm/sec^2 is applied at EBL. In case of a near-field earthquake, the PGA at the surface is estimated in the range 100.7-278.9 cm/sec^2 (Fig. 2.7). The response spectra at 5% damping on the surface at each borehole are estimated. A total of 1080 surface response spectra are generated for 20 boreholes. The response spectra generated at BH-20 is shown in Fig. 2.8. The mean PGA amplification factors are also calculated at all boreholes due to near field earthquakes and found varying from 1.6 to 3.3.

The synthetic ground motions for far field earthquake scenario (Mw 7, 7.6 and 7.8 along the eastern part of the Kachchh Mainland Fault) are generated. The quality factor proposed by Singh et al. (1999), Singh et al. (2004) and Bodin et al. (2004) proposed for mainland Gujarat have been used. To overcome the uncertainity, stress drop values of 140, 160 and 180 bars and Kappa values of 0.02, 0.025 and 0.03 have been considered for the far field earthquake scenario. A total of 81 input parameteric combinations are considered for estimating the ground motion at EBL for the far field earthquake scenario.

In case of a far-field earthquake, the input motion with mean PGA of 107.8 cm/sec^2 is applied at the EBL. The PGA is then calculated at the surface by passing the ground motion through the soil layers prepared for the area. The computed surface mean PGA is found to be varying from 118.4 to 161.5 cm/sec^2 (Fig. 2.9).

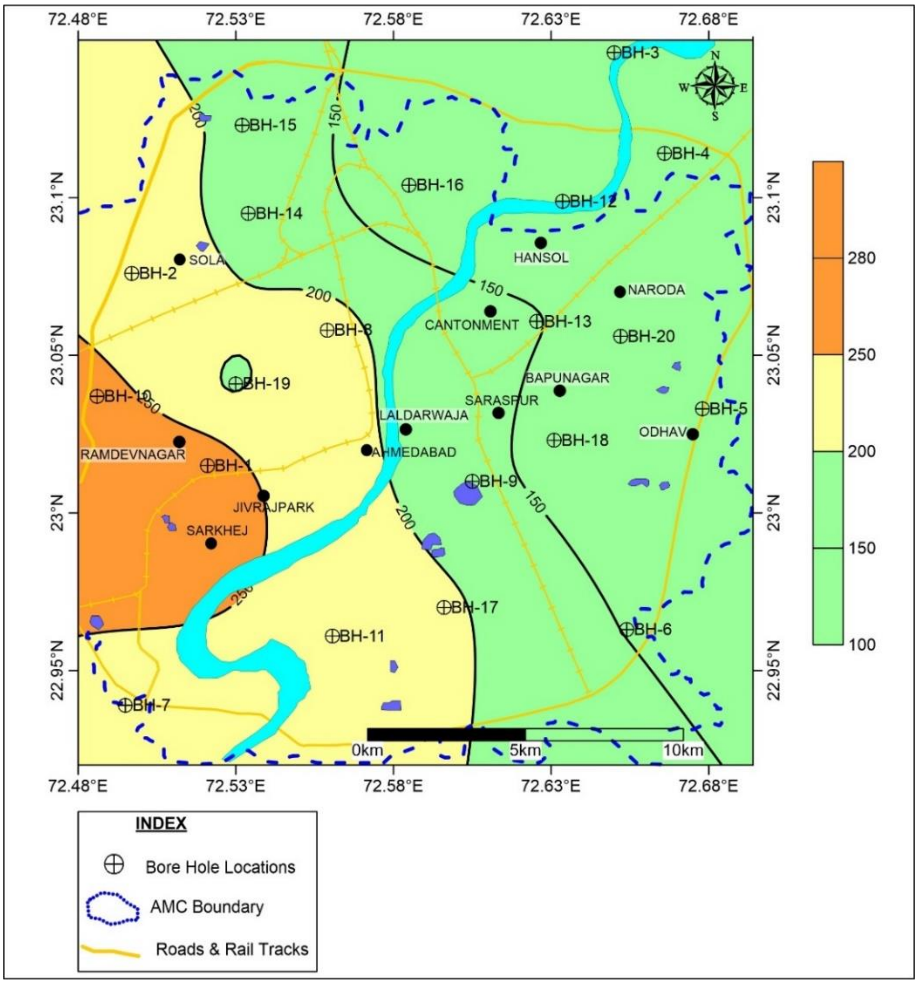

Figure 2.7: The surface peak ground acceleration distribution map of Ahmedabad city for a near field earthquake

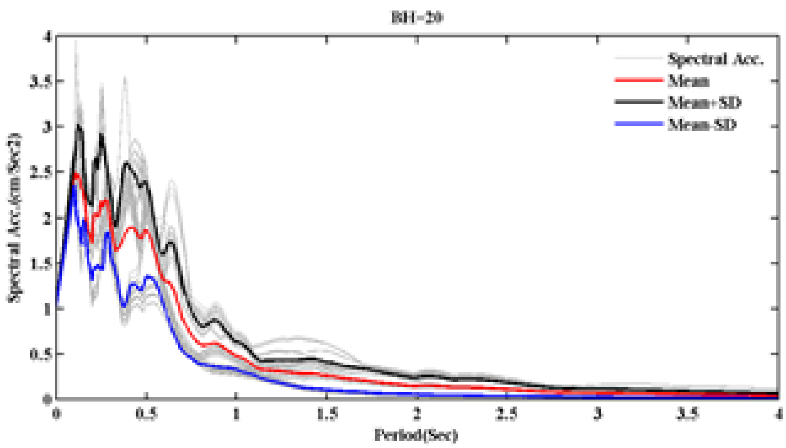

Figure 2.8: Spectral acceleration plot with mean and standard deviation for near field earthquake consideration at BH-20.

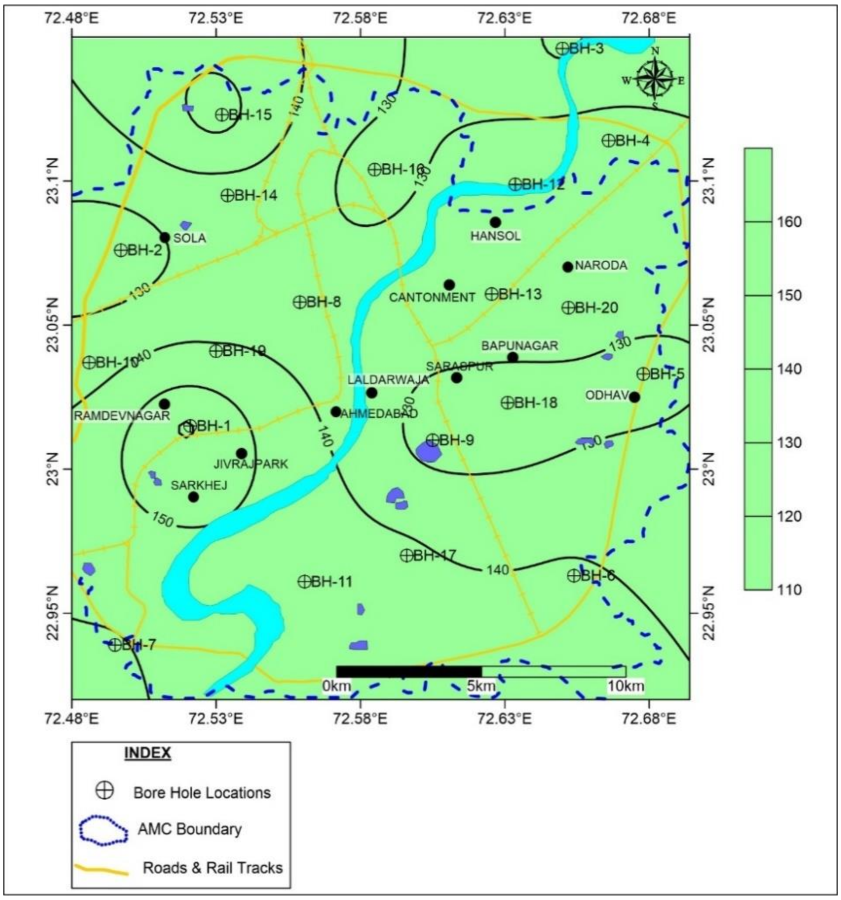

Figure 2.9: The surface peak ground acceleration (in cm/sec2) distribution map of Ahmedabad City for far field earthquake.

A total 1620 surface response spectra are generated for 20 boreholes.The mean PGA amplification factors are also calculated at all the boreholes due to far field earthquakes and are found to be varying from 2.2 to 3.0. The response spectra generated at BH-20 are shown in Fig.2.10.

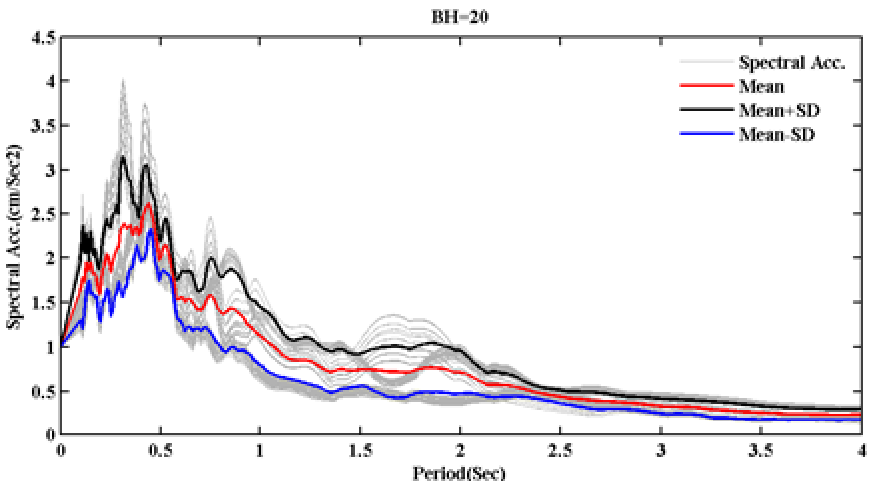

Figure 2.10: Spectral acceleration plots with mean and standard deviation for a near field earthquake at BH-20.

2.5 Assessment of Seismic Hazard in Gandhinagar City incorporating parametric uncertainties

(*Kapil Mohan, Shruti Dagur, Neha Tanwar and Sumer Chopra)*

Gandhinagar City (the Capital of Gujarat) falls under Zone III of the seismic zoning map of India, where an earthquake of magnitude 6 can be expected. To estimate the effect of soil on ground motion and to estimate the strong ground motion parameters at the surface, soil modeling and ground response analysis are conducted along uniformly distributed 14 boreholes drilled down to a depth of 50m. The methodology is divided into three parts (i) Estimation of depth of Engineering Bed layer (EBL) (a layer with a shear wave velocity 400m/sec≤Vs≤ 750m/sec, N value >80 and minimum soil variation below it) through soil modeling, (ii) Estimation of ground motion at EBL due to scenario earthquake at nearby active fault and (iii) Estimation of surface strong ground motion using 1D ground response analysis through SHAKE 2000 program. The EBL is found at a depth of 21 to 33m (shallower in central part and deeper in northern and southern parts). The Near Field scenario earthquakes of magnitude 5.5, 6.0 and 6.5 are considered along the East Cambay Fault located at about ~ 20km east of Gandhinagar and far field scenario earthquakes having magnitudes of 7.0, 7.6 and 7.8 are considered along the eastern part of the Kachchh Mainland Fault located ~270 km west of Gandhinagar. The quality factor given by Chopra et al. (2010) and Gupta et al. (2012) proposed for the mainland Gujarat have been used. To overcome the uncertainity, stress drop values of 60, 80 and 100 bars and Kappa values of 0.02, 0.025 and 0.03 are considered for the Near Field earthquake scenario. A total of 54 input parameteric combinations are considered for estimating the ground motion at EBL. Soil models are prepared utilizing data of the 14 boreholes. The estimated surface Peak Ground acceleration (PGA) is found in the range 150-290 cm/sec^2.

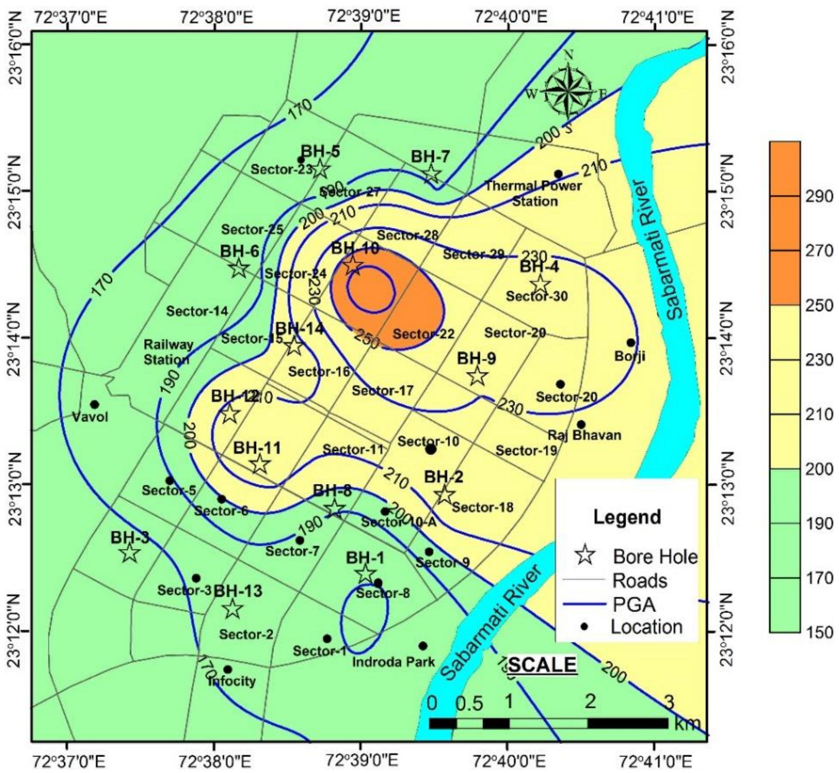

Figure 2.11: The mean surface peak ground acceleration distribution map of Gandhinagar city area for a near field earthquake scenario.

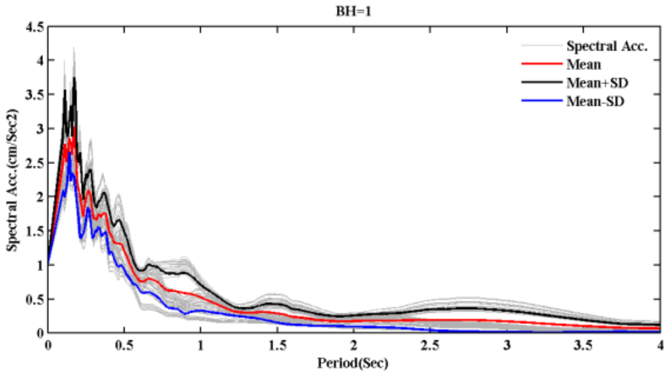

Figure 2.12: Spectral Acceleration plots with Mean and Standard Deviation for near field earthquake consideration at BH-01.

The synthetic ground motions for the far field earthquake scenarios (Mw 7.0, 7.6 and 7.8 along the eastern part of Kachchh Mainland Fault) are generated. The quality factor given by Singh et al. (1999), Singh et al. (2004) and Bodin et al. (2004) proposed for mainland Gujarat are used. To overcome the uncertainity, stress drop values of 140, 160 and 180 bars and Kappa values of 0.02, 0.025 and 0.03 are considered for the far field earthquake scenario. A total of 81 input parameteric combinations have been considered for estimating the ground motion at EBL. The mean surface PGA is found to be varying in the range 100-140 cm/sec^2 (Fig. 2.13). A total of 1134 surface response spectra are generated for 14 boreholes. The response spectra generated at BH-1 is shown in Fig. 2.14.

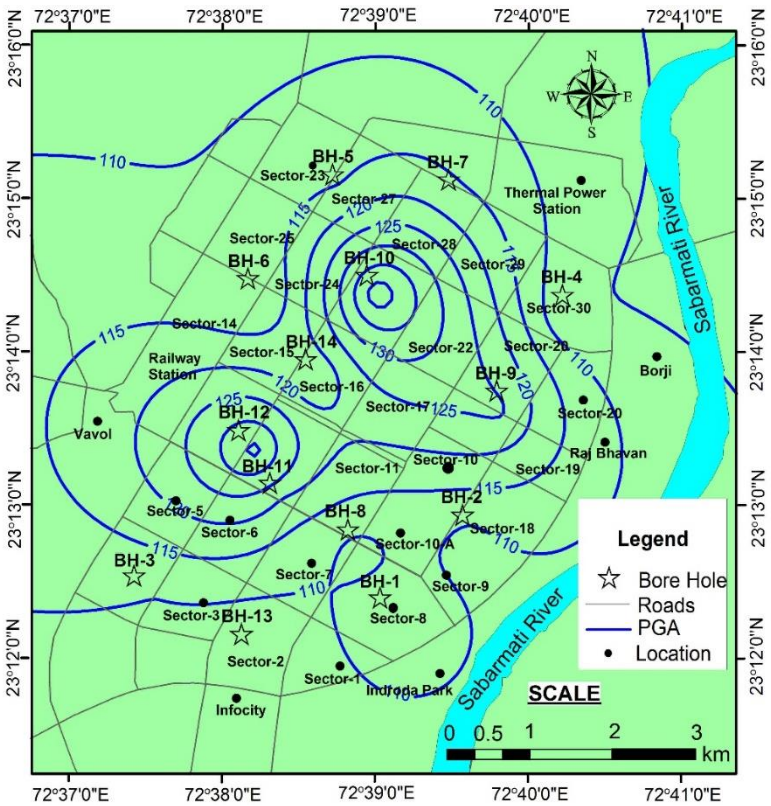

Figure 2.13: The mean surface peak ground acceleration distribution map of Gandhinagar city for far field earthquake scenario.

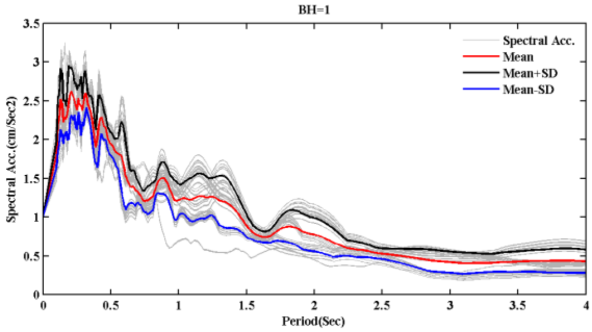

Figure 2.14: Spectral Acceleration plots with mean and standard deviation for far field earthquake consideration at BH-01.

2.6 Geological Map of the Dadra and Nagar Haveli (U.T)

(Naveen Kumar and Kapil Mohan)

The Dadra and Nagar Haveli and its surroundings is occupied by a thick succession of basaltic lava flows of cretaceous to Eocene age. The Deccan Trap flows of Dadra and Nagar Haveli are comprised of dense, medium to fine- grained, greenish grey to red, porphyritic to amygdaloidal Basalt, Trachyte and Rhyolite intruded by dykes of dolerite, basalt and gabbro. The dense, medium to fine grained, greenish grey to red, porphyritic to amygdaloidal Basalts are associated with Lower Ratngarh and Salher formations of Sahyadri Group of the Deccan traps. The Trachyte and Rhyolite intruded by dykes of dolerite, basalt and gabbro are mainly associated as intrusives. The vesicles/amygdales are circular and elliptical, the minerals in the amygdules comprise calcite and zeolites. The most prominent lineament trends are NNW-SSE to NE-SW. The Deccan basalt is overlain by Quaternary sediments comprising pebbly, gritty, silty and sandy clays (Fig. 2.15 and 2.16). The cross bedded gritty beds form terraces on both sides of the Damanganga and Ratakhadi rivers and their tributaries. The terrace sediments at most places along these rivers form the scarps and gullies, indicating that the drainage is structurally controlled. The NNW-SSE to NE-SW trending dykes form the oldest and very prominent lineaments in the area. Some of them trend towards N-S direction also. The contacts of these dykes with the Deccan Traps are sheared and faulted at places. The NNW-SSE to NW-SE lineaments represented by dykes also exhibit evidence of faulting at places. A huge Trachyte-rhyolite acidic complex is exposed (10km length and 4km wide) in the western part of the Dadra and Nagar Haveli. The leucocratic color makes it very prominent in the largely basaltic terrain. The flows are intruded by dykes of dolerite and basalt. The intrusions have north-south trends and are quite closely spaced. The geological map of Dadra and Nagar Haveli is shown in Fig. 2.17.

The findings of the study are given below:

The Dadra and Nagar Haveli region is covered by Deccan Trap basaltic flows with lateritic soil covers at higher hilly terrain and alluvial cover in the central portion in the vicinity of Silvassa and surroundings.

(a) The thick silty and sandy alluvium deposits on the right bank of the Damanganga River and downstream of the Madhuban dam suggests rejuvenation of the Damanganga river bed.

(b) The structural control of the streams in the vicinity of the Rhyolite-Trachyte complex is quite conspicuous. Damanganga River, which flows east-west in the major part of the area takes a sudden northerly trend near the acidic body. The flow of Dongarkhadi River is also controlled by the N-S trending fault.

N-S trending fault is inferred east of the trachyte-rhyolite complex. The following indirect evidence in the area suggests faulting:

a) Anomalous thickness of alluvium
b) Sudden change in the trend of Damanganga river
c) Incised course of Damanganga River with potholes and grooves, suggesting that the area has undergone tectonic adjustments
d) Unpaired and tilted terraces

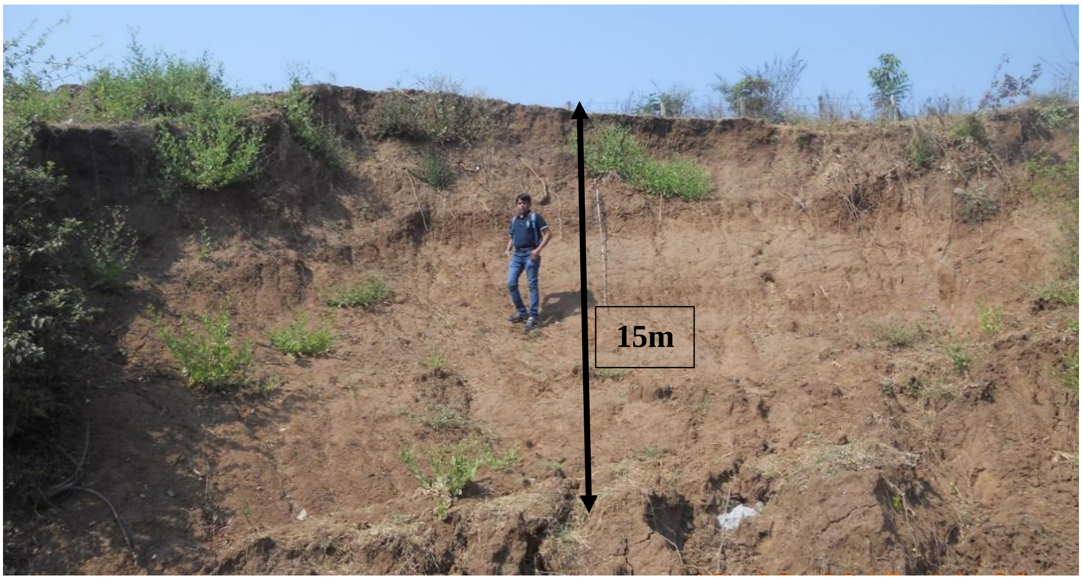

Figure 2.15: The figure shows the thickness of sediments (NW of Masat, near Cemetery)

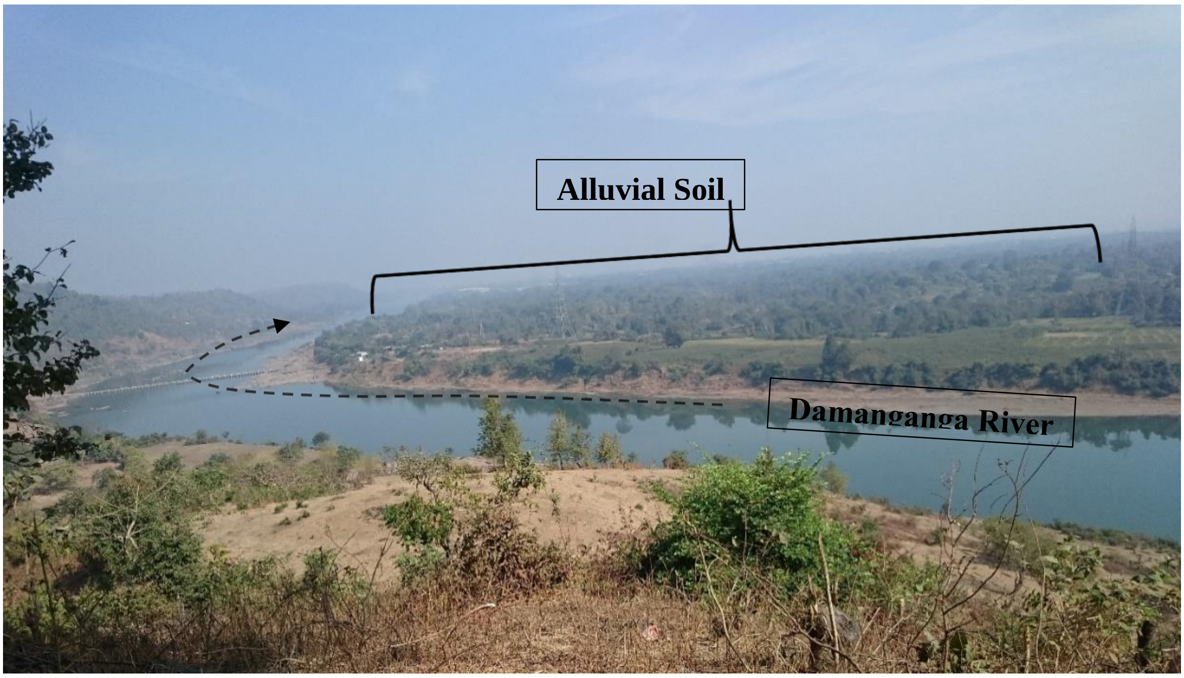

Figure 2.16: The figure shows flat alluvial and black soil terrain and Damanganga River

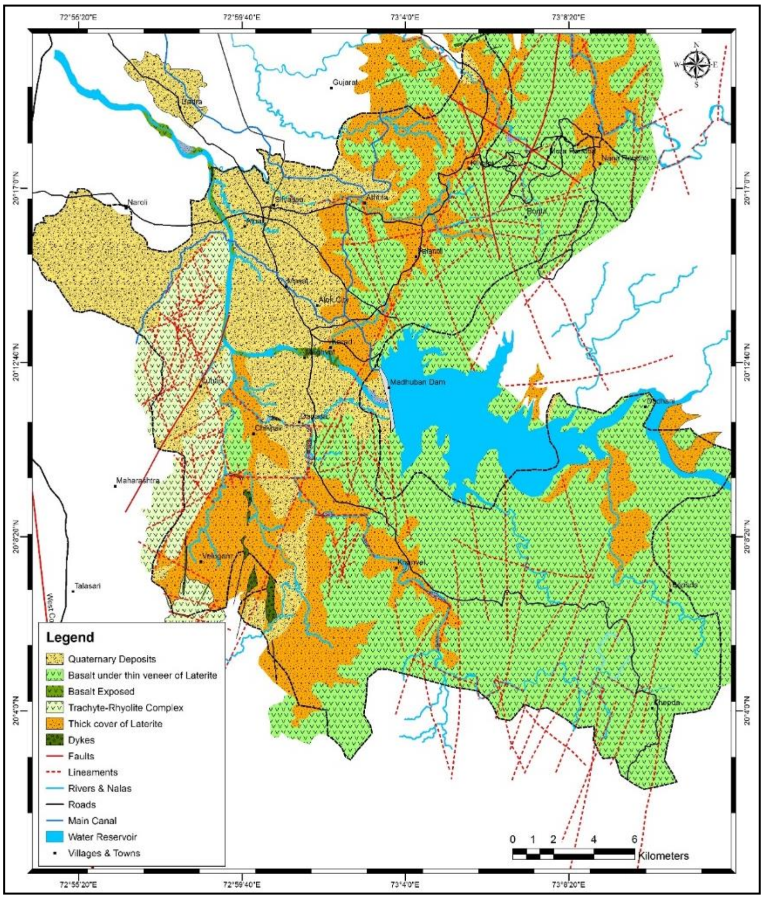

Figure 2.17: Geological Map of Dadra and Nagar Haveli.

2.7 Delineation of Palaeochannels in Dadra and Nagar haveli (U.T.)

(Naveen Kumar)

For delineation of palaeochannels, comprehensive mapping of the study area was carried out using LISS-III satellite image and Digital Elevation Model (DEM) of 30m resolution. The geocoded standard false colour composites (FCC) were generated using various spectral bands from the LISS-III data. The geometric and radiometric corrections were applied to reduce the errors in the image. The digital enhancement techniques, various multi sensor image fusion and DEM analysis were used for the recognition of palaeochannels in the study area. Palaeochannels were identified by their contrasting dark tone, the characteristic winding fashion of the channels in association with the cropping pattern, high reflectance of NIR bands, associated water bodies, well defined connectivity with the existing channel and associated lineaments

The Damanganga River is the major river in the study area which originates from the Sahyadri mountain range (elevation of 683m) and river Ratakhadi (elevation of 260m). A palaeochannel is identified by its contrast from the surrounding terrain, meandering, associated water bodies (sag ponds), the well-defined connectivity of meandering channel with existing channel in the form of identifiable inlet and outlet and most importantly, it is associated and developed with the trend of lineament and faults in the area (NNE-SSW & N-S in this case). During the study, it was found that these palaeochannels are developed due to the faulting or lineaments mapped along the channels of rivers (Fig. 2.18).

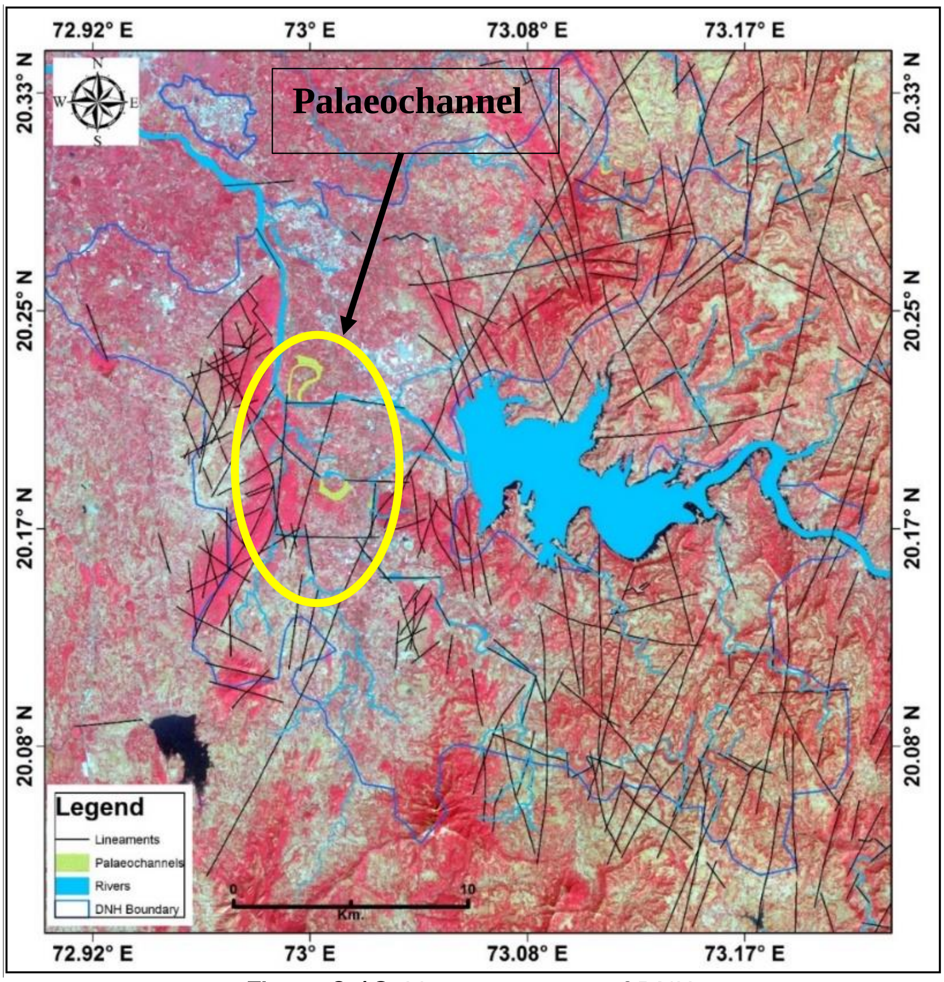

Figure 2.18: Lineament map of DNH.

2.8 Study of Deformation in Quaternary sediments in Dadra and Nagar Haveli (U.T.)

(Naveen Kumar, Kapil Mohan)

Unpaired, Tilted and Faulted River Terraces: The anomalous sediment depositional behavior, tilting of river terraces are the evidence of tectonic instability. At the east (right) bank of Damanganga River, near Dadra nd Nagar Haveli, the T1 to T3 level terraces are well exposed but on the west (left) bank of the river, only T3 terraces are developed. A Geological section has been prepared by conducting a topographical survey (Fig. 2.19). This section also confirms that there are unpaired terraces on the west bank of Damanganga River. The T3 terrace on the east (right) bank is found to be tilted in the east direction with a dip angle of 28^{o}-30^{o}. This terrace is comprised of alternate bands of sand, silty clay and sandy gravels. Presence of well-developed (T1 to T3) and tilted terraces on the east (right) bank reveal that the area has experienced neotectonic activities during degradation stage of the Damanganga river.

Palaeochannel Study: For delineation of signatures of neotectonism, comprehensive mapping of the study area was carried out using LISS-III satellite image and SRTM DEM. The standard false colour composite (FCC) images were produced using various spectral bands from the LISS-III data. The drainage anomalies were identified from DEM. The palaeochannels were delineated by their distinct dark tone, the characteristic meandering manner in association with the reaping pattern, high reflectance of Near Infrared bands, connected sag ponds, clear connectivity with current channel and associated lineaments.

Further detailed geological field investigations have been conducted to highlight the signatures of neotectonic deformations in the study area (i) at Damanganga River basin and (ii) Ratakhadi River Basin (Fig. 2.20).

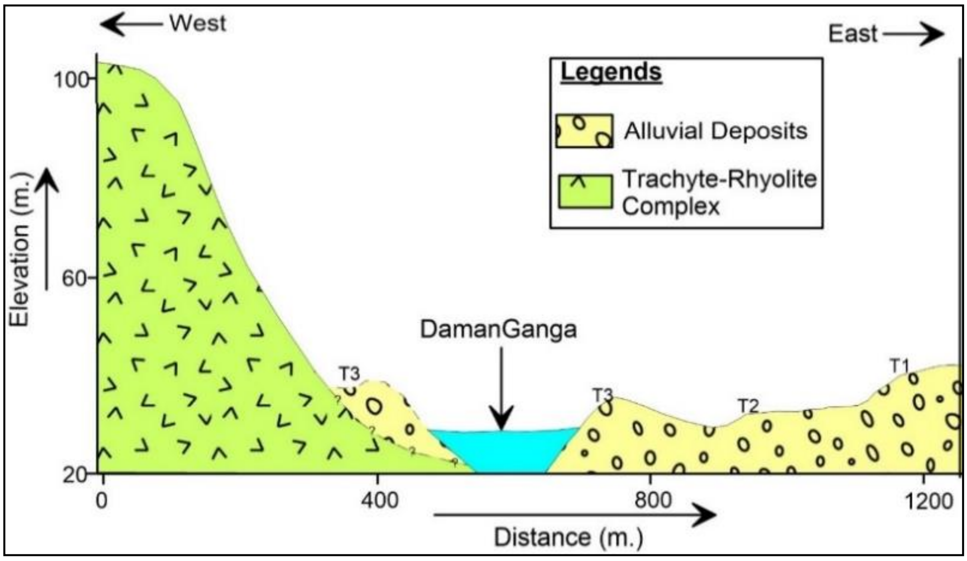

Figure 2.19: Longitudinal profile across the unpaired terraces

(i) Damanganga River basin

The Damanganga river channel is deflected at various locations along the structural discontinuities. The orientation of the lineaments and a fault (NNE-SSW) which is observed in the field as well as in satellite data and drainage anomalies in the area reveals their nature as strike slip. This could be a result of the readjustment of the present-day drainage due to the strike slip movement. The topographic profile along the current and palaeochannels reveals that there is a 10-15 difference in elevations of the current channel and palaeochannel. The palaeochannel and the adjoining area is covered by river sediments comprising sandy silty gravels. This hanging nature of the old river channel can be ascribed to neotectonic adjustment of the river channel.

(ii) Ratakhadi River Basin

The river channel is deflected near Bonta village and an offset of the river channel is observed along the fault and lineaments in this area. The present river channel is deflected 250m NE from the palaeochannels. The present river channel follows the trend of a WNW-ENE trending fault cutting across the river channel. The fault scarp is clearly visible in DEM and the topographic profile drawn across the present channel and palaeochannel. A longitudinal section drawn along the Ratakhadi river reveals a WNW-ENE trending normal fault along its current channel, due to which the channel is shifted in the NE direction (right). Due to this fault, several knick points are formed into the channel of the river. The longitudinal profile of the Ratkhadi river indicates that the river has a gradient of 2.5m/km in the study area. This could have been attained either by higher discharge through the channels or due to the presence of a weaker zone over which the Ratakhadi river flows, or both.

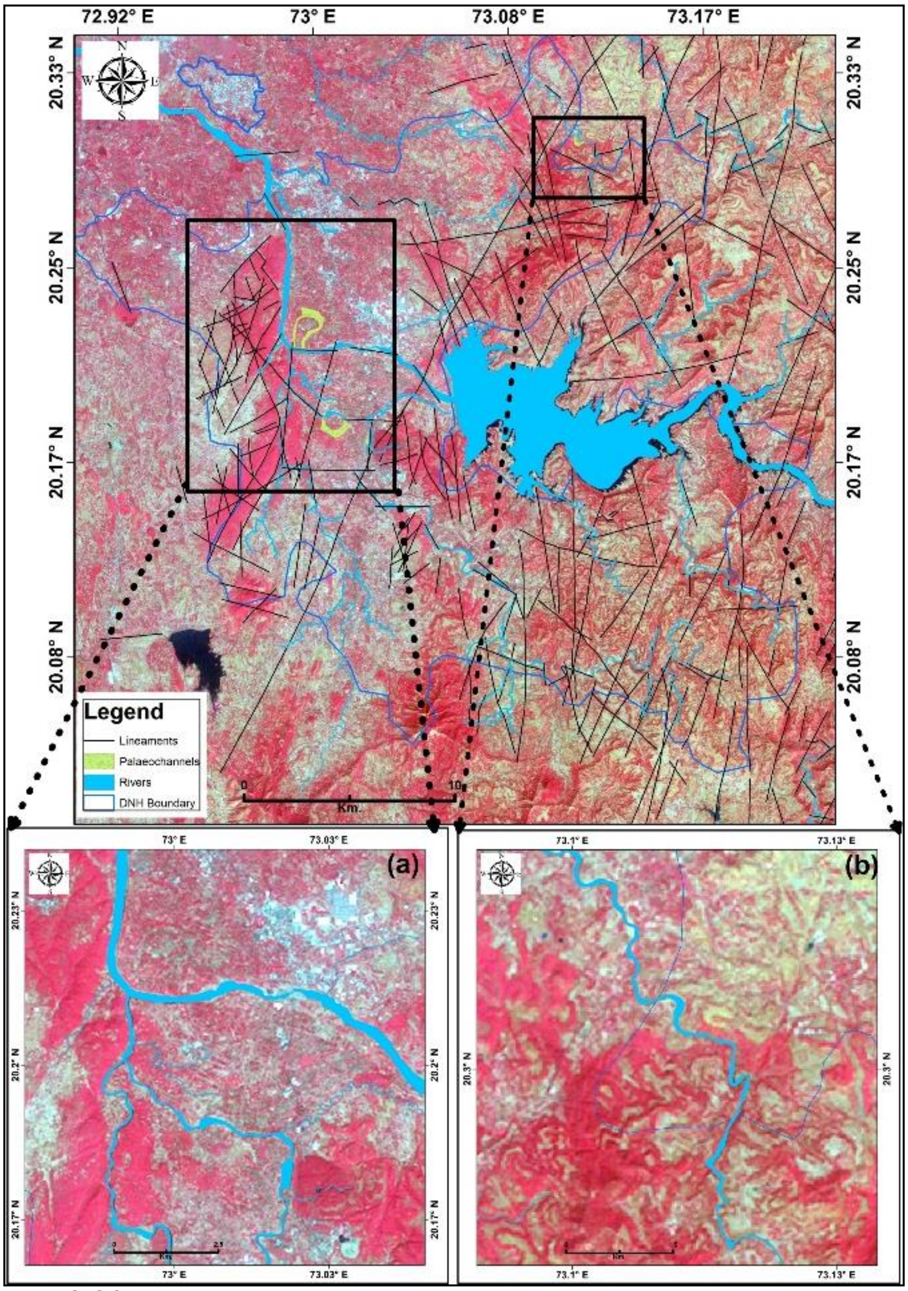

Figure 2.20: Deflected Drainages and Palaeochannels with associated Lineaments

2.9 Vulnerability Assessment in the Rambaug area of Ahmedabad

(*Russi Modi and Kapil Mohan)*

The seismic vulnerability assessment of the buildings consists of three steps- rapid visual screening, preliminary evaluation and detailed evaluation. Rapid visual screening was carried out on 100 RC frame buildings in Rambaug, Ahmedabad. Based on the rapid visual survey, several buildings from a dataset of 100 buildings were chosen for preliminary evaluation, which involves identification of the sizes of all columns and beams, existing strength of the concrete, reinforcement detailing and drawing of as-built plans. The preliminary evaluation of two buildings is shown in Fig. 2.21 & 2.22.

The details gathered during this evaluation, such as, the size of beam-column and building plan will be required for the detailed evaluation process.

Madhav Apartment

Jalsmruti Apartment

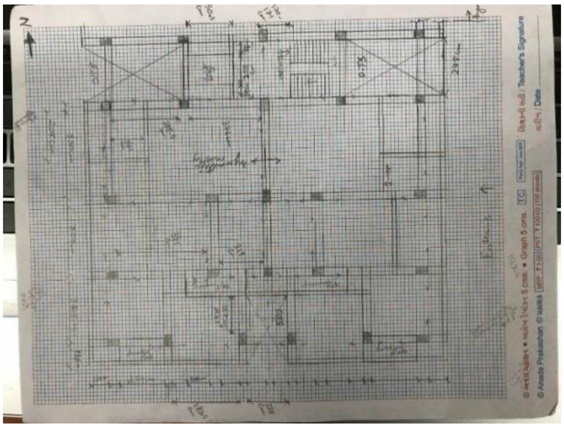

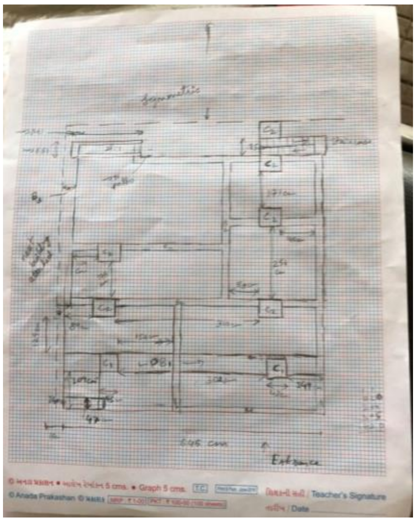

Figure 2.21: Built plan drawings of the Jalsmriti and Madhav Apartments in Ahmedabad

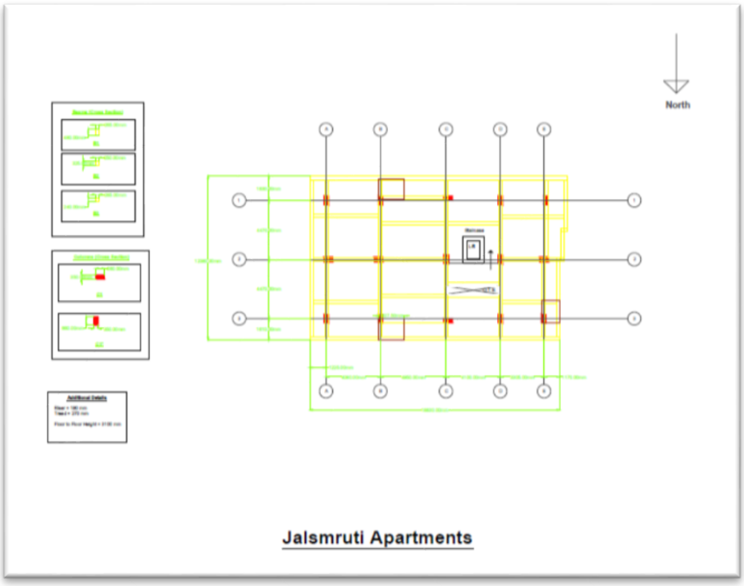

Figure 2.22: AutoCAD drawing of the Jalsmruti apartment

2.10 Rapid Visual Screening of Sector 2 and 23, Gandhinagar City

(Kapil Mohan, Akash Solanki and Russi Modi)

A web based application has been developed for Rapid Visual Screening (RVS) which can be loaded on a smart Phone. The application is hosted on www.rvs-isr.ml/admin. The URLs for generating excel files are:
All Buildings: www.rvs-isr.ml/excel/all
RC Buildings: www.rvs-isr.ml/excel/rc
Masonry Buildings: www.rvs-isr.ml/excel/ms
Hybrid Buildings: www.rvs-isr.ml/excel/hy

52 buildings were surveyed in sector 2, out of which 143 buildings were Masonry and 9 RC frame buildings. The sector 2 is a residential area and had very less commercial buildings. The vulnerability parameters observed during the survey are given in Fig. 2.24.

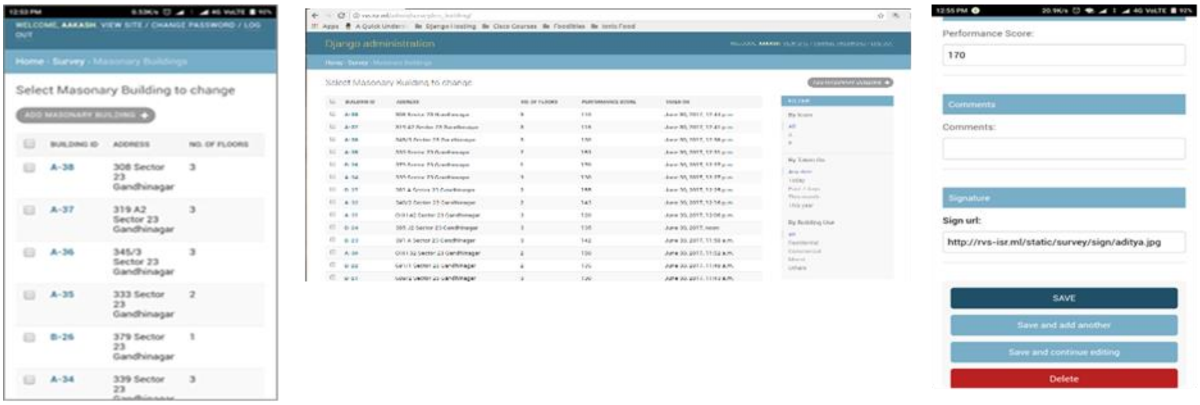

Figure 2.23: Mobile Interface and the data records.

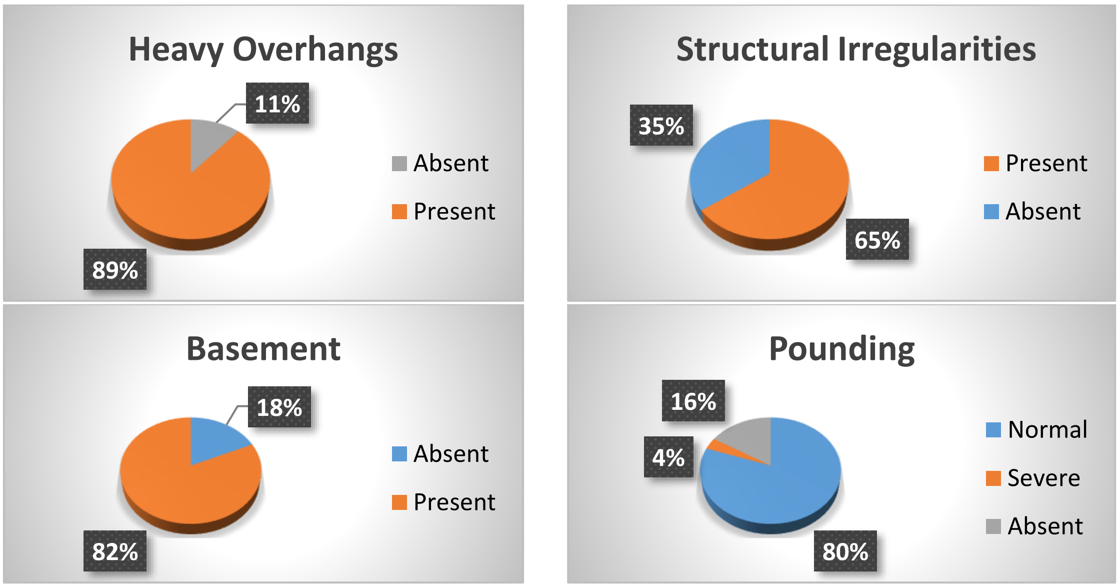

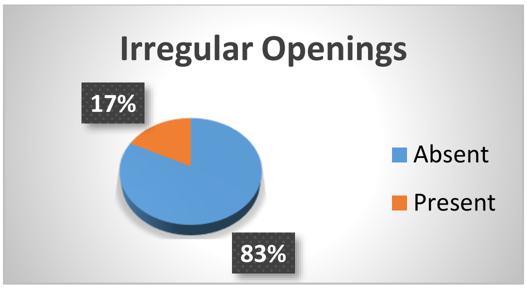

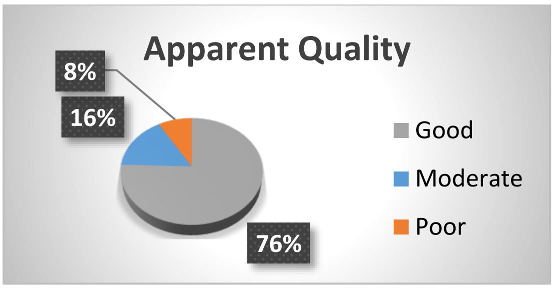

Figure 2.24: The vulnerability parameters present in the Masonry buildings of Sector 2.

It is clearly seen from the charts that most of the buildings contain heavy overhangs and almost all of them have a basement. 75% of the buildings have good quality of construction while 65% of them have structural irregularity. The total RVS score for masonry buildings varies from 170 to 85 with a mean score of 136. In case of 9 RC buildings, the RVS score varies from 150 to 100 (mean 125). In view of a good mean score, the chances of collapse are less.
The RVS survey has been conducted on 64 buildings in sector 23. The majority of the buildings are Masonry. It was observed that 51 buildings are masonry while 13 are RC frame buildings. The RVS score of the masonry building varies from 170 to 110 (mean 143). The RVS score of the RC frame buildings varies from 143 to 80 (mean 111). The mean score is good and chances of collapse are less.

2.11 Seismic Risk assessment in Bhachau city

(Akash Solanki, Russi Modi and Kapil Mohan)

A total of 3100 buildings were mapped in the Bhachau city (Fig. 2.25). The area of each building is calculated. The building inventory data of 359 buildings were collected during field work during February to March 2018. This data includes the wall type, roof type, no. of floors, location, utility, presence of slopy ground and population (day and night time population wherever available). Two most common roof types seen in the Bhachau city are (i) RC Slab and (ii) GI sheet. It was observed during this field visit that the wall type included a combination of load bearing masonry (consisting of burnt clay bricks or concrete blocks in cement mortar) wall with seismic bands (at sill level, plinth level and lintel level) along with Reinforced Concrete (RC) Columns for better seismic performance. Implementation of 135° hooks (Fig. 2.26) was seen at various local construction sites, which indicates awareness on seismic safety amongst the local population. The roof type mostly comprises of flat RC roof and Galvanized Iron (GI) (Fig. 2.27) sheet which were found to be present in combination as well in a few buildings (where the topmost storey had GI sheet as roof). The buildings are mostly found to be of one or two floors.

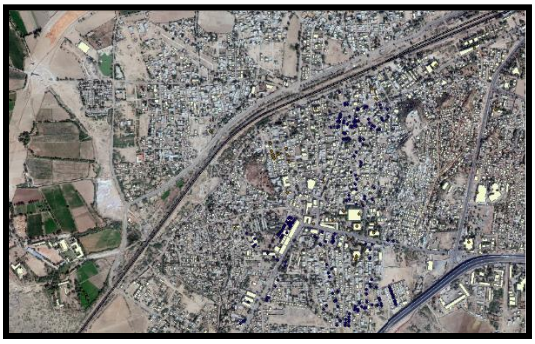

Figure 2.25: 3100 mapped buildings in Bhachau city

Figure 2.26: Construction site where 135° hooks were observed

Figure 2.27: Galvanized Iron (GI) Sheet as roof type in Bhachau city

2.12 Scenario based seismic risk assessment in the northern part of Gandhinagar City

(Akash Solanki and Kapil Mohan)

The quantification of the seismic risk and loss has to be prioritized in the important cities of India for future structural planning. The present study has been conducted to estimate the seismic loss using different seismic scenarios in the economically important sector 21 of the Gandhinagar city, Gujarat. Attenuation relation based five different hazard scenarios namely, (i) IS code based spectral shape with site-specific surface PGA (0.2g) (ii) Magnitude Mw 6.0 and focal depth 15 km, (iii) Mw = 6.0 and focal depth = 10 km, (iv) Mw = 6.5 and focal depth = 15 km, and (v) Mw = 6.5 and focal depth = 10 km were used to estimate the losses. The Response Spectra were generated based on the attenuation relationship given in NDMA 2010 report. A significant increase of seismic loss (29.63% increase at a focal depth of 15 km and 20.93% increase at a focal depth of 10 km) is observed when the magnitude is increased from Mw 6.0 to Mw 6.5 (Fig. 2.28). This increase may be due to the fact that Masonry buildings (63%) in the study area have shorter periods which coincide with the higher Spectral Acceleration (Sa) values observed in the demand curve, resulting in higher losses. The probabilities of damage grades 1 (slight), 2 (moderate) are higher in RC frame buildings than in Masonry buildings across all hazard scenarios (Fig.2.29). However, the probabilities of damage grade 3 (severe) for all buildings types are similar. The probabilities of damage grades 4 (complete) and 5 (collapse) are negligible for RC frame buildings while for Masonry buildings these probabilities rise significantly (maximum increase of 20% in probabilities of damage grade 4 in case of Masonry buildings), which is critical. It can also be concluded that the magnitude of an earthquake alone can have significant effects on the damage probabilities, especially for masonry buildings.

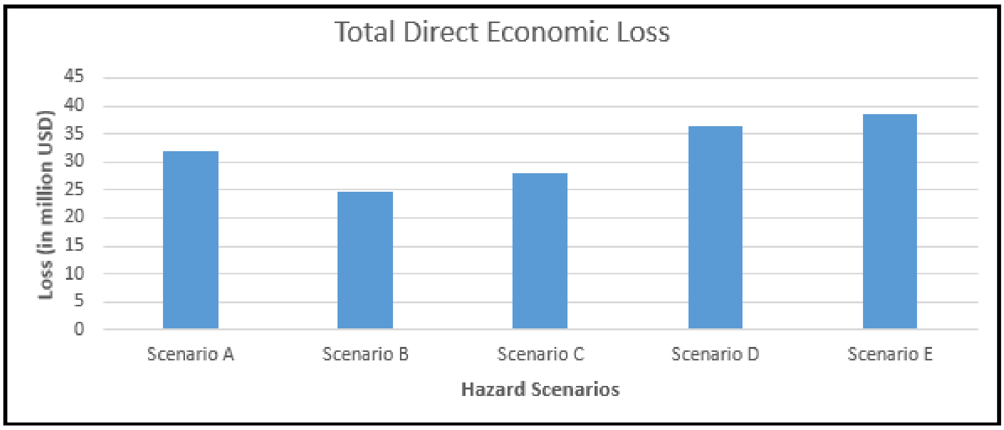

Figure 2.28: Comparison of Losses using different hazard scenarios

Figure 2.29: Comparison of Damage Grade Probabilities for different hazard scenarios

2.13 Rapid Visual Screening of RC frame buildings in Vasna area of Ahmedabad, Gujarat.

(Jay Patel, Russi Modi and Kapil Mohan)

A cluster of seven buildings that collapsed in Vasna, Ahmedabad were located on ground with the help of AMC and available literature. After locating the buildings, Rapid Visual screening was carried out to check the present day earthquake vulnerabilities of these buildings. The computed RVS scores of the 7 buildings range from 29 to 75. From the RVS, it was observed that the buildings of 4 to 6 storeys mostly showed presence of vulnerable parameters such as soft storey and heavy overhang.

Samayak Apartment

Vraj Apartment

Parasmani Apartment

Chandrama Apartment

Vardayini Apartment

Tagorpark Apartment

Figure 2.30: The buildings in the Vasna area, Ahmedabad, for which RVS was conducted.

2.14 Estimation of Source parameters of Mw 7.1 Central Mexico City Earthquake

(Neha Tanwar and Kapil Mohan)

An intra-plate earthquake of magnitude Mw 7.1 hit the Central Mexico City on September 19, 2017. The source parameters of the earthquake were calculated using the grid search method, which also includes the quality factor of the region.

Table 2.1: Estimated source parameters of Mw 7.1 Mexico earthquake

Source parameter	Values
Corner frequency, f_c(Hz)	0.11
Quality factor, Q	890±660
Source radius, r(Km)	16.04
Seismic moment, M_0(N-m)	(5.94±4.22)E+19

Size of rupture area, A(Km^2)	808.3
Stress drop, $\Delta\sigma$(Bars)	113±92
Average source dislocation(slip), D(m)	2.1
Moment magnitude, M_w	7.07±0.23

The values of M_0 and M_w are given to be 6.381e+19 Nm and 7.1 by USGS. In the present study, the values of seismic moment M_0 and moment magnitude M_w are found to be (5.94±4.22)E+19 N-m and 7.07±0.23, close to that given by USGS

2.15 Simulation of strong ground motion of Mw 7.1 Central Mexico City Earthquake

(Neha Tanwar and Kapil Mohan)

An intra-plate earthquake of magnitude 7.1 hit Central Mexico City on September 19, 2017. The source parameters of the earthquake were estimated. The validation of the estimated source parameters (Grid search method) has been conducted and the strong ground motion is estimated at one site (UNM) where the earthquake was already recorded. The simulation of the strong ground motion at this time has been conducted using Stochastic Finite-Fault Modelling Method. The input parameters are given in Table 2.2.

Table 2.2: The parameters used for simulation

Parameters	Values
Magnitude (Mw)	7.1
Kappa	0.038
Quality Factor	$100f^{0.34}$
Stress Drop	100 bars

The comparison of the recorded and simulated response spectra has been given in Fig. 2.31.

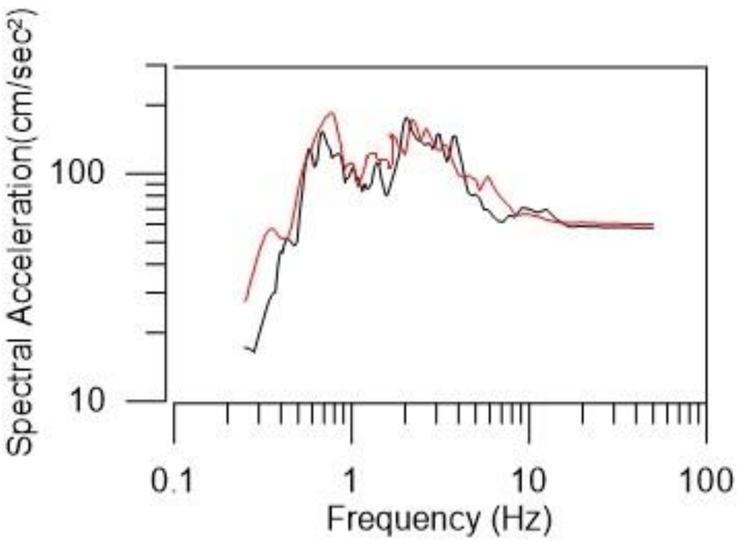

Figure 2.31: The simulated (red line) and recoded (black line) response spectra at 5% damping.

2.16 Probabilistic seismic hazard assessment of Bongaigaon, Assam, Northeast India

(Madan Mohan Rout)

The methodology developed by Cornell (1968) for PSHA is applied for the estimation of seismic hazard for Bongaigaon, Assam. The seismic events from 825-2008 were collected from the NDMA Report (2011), 2009 to 2014 events were collected from Nath et al (2017) and 2015 to 2017 events were collected from IMD. Six seismogenic zones were delineated on the basic of tectonics and seismicity. They are (I) Tibet Himalaya, (II) Eastern Himalaya, (III) Himalaya-2, (IV) Shillong Plateau, (V) Bengal Basin, (V1) Western part of Indo-Myanmar subduction zone. In this study, the declustering method of Gardner and Knopoff (1974) has been used to remove the foreshock and aftershocks. The seismic hazard parameters are computed using Entire Magnitude Range Method (EMR) modified by Woessner and Wiemer (2005). The ground motion equation published in NDMA (2011), Nath et al. (2012) for active intraplate margin of Shillong Plateau, Gupta (2010) for subduction zone, Boore and Atkinson (2008) and Campbell and Bozorgnia (2008) for tectonically active regions have been used in this study. The ground motion estimated at B/C boundary Sites (Vs=760 m/sec). Site Coefficients (NEHRP, 2009) have been used to estimate the ground motion at B/C boundary sites for NDMA (2011) and Nath et al. (2012) relations and the other three relations estimate the ground motions at B/C boundary sites. Probabilistic seismic hazard for Bongaigaon (26.52°N, 90.53°E) has been estimated using the seismicity parameters and the ground motion prediction equations with the given weightage discussed in Table 2.3. Maximum PGA of 0.16g and 0.30g is observed at 10% and 2% P.E in 50 years respectively.

Table 2.3: The ground motion prediction equations with the given weightage

Sr. No.	Seismogenic Zone	GMPE	Wt.
1	Tibet Himalaya	Boore and Atkinson (2008)	30
		Campbell and Bozorgnia (2008)	30
		NDMA (2011)	40
2	Eastern Himalaya	Boore and Atkinson (2008)	30
		Campbell and Bozorgnia (2008)	30
		NDMA (2011)	40
3	Shillong Plateau	Nath et al. (2012)	50
		NDMA (2011)	50
4	Bengal Basin	Nath et al. (2012)	50
		NDMA (2011)	50
5	Himalaya 2	Boore and Atkinson (2008)	30
		Campbell and Bozorgnia (2008)	30
		NDMA (2011)	40
6.	Western part of subduction zone	Gupta (2010)	60
		NDMA (2011)	40

2.17 A review of Seismic hazard assessment of Gujarat, a highly active intra-plate region of the world

(Pallabee Choudhury, Sumer Chopra and M Ravi Kumar)

Large intraplate earthquakes that occur in the interior of continental plates are rare and often very destructive. The Gujarat region of western India, that witnessed the deadly Mw 7.6 earthquake on January 26, 2001 and the Mw7.8 quake on June 16, 1819, is one of the most active intraplate regions of the world. The tragedy caused by the 2001 earthquake marked a turning point in the disaster awareness and preparedness in the region. In the aftermath of this earthquake, several workers investigated the important issue of mitigating seismic hazard through new knowledge based techniques of probabilistic and deterministic ground motion prediction, micro and macro zoning of vulnerable areas. This study reviews the results of seismic hazard estimation in the Gujarat region from different methodologies. We note that the probabilistic seismic hazard estimates by different workers are not consistent even within the same region because of uncertainties in constraining the hazard parameters, and it is observed globally. Using a logical approach, we evaluate all the ground motion predictions, estimated by different methodologies, and constrain the level of expected peak ground accelerations (PGA) by adjusting all values on a same platform. Our assessment says that the PGAs vary from 0.05 to 0.36g and 0.07 to 0.80g for 10% and 2% PE in 50 years at Vs=760 m/s in Gujarat (Fig. 2.32a and b). The deterministic values of PGA range from 0.02 to 0.90g at surface. Now, we see that within Gujarat, the ground motion values obtained by deterministic and probabilistic methodologies do not show much variations. We affirm that we need to undertake such a logical approach to arrive at a particular hazard value. Further, a comparison of the hazard values of Gujarat with those of other intraplate regions of the world reveals that the hazard level in Gujarat is higher than in Australia, Brazil and Western Europe and comparable to North China, Eastern Canada and New Madrid Seismic zone. The Kachchh region is one of the most active intraplate regions of the world that is undergoing high seismic activity at present.

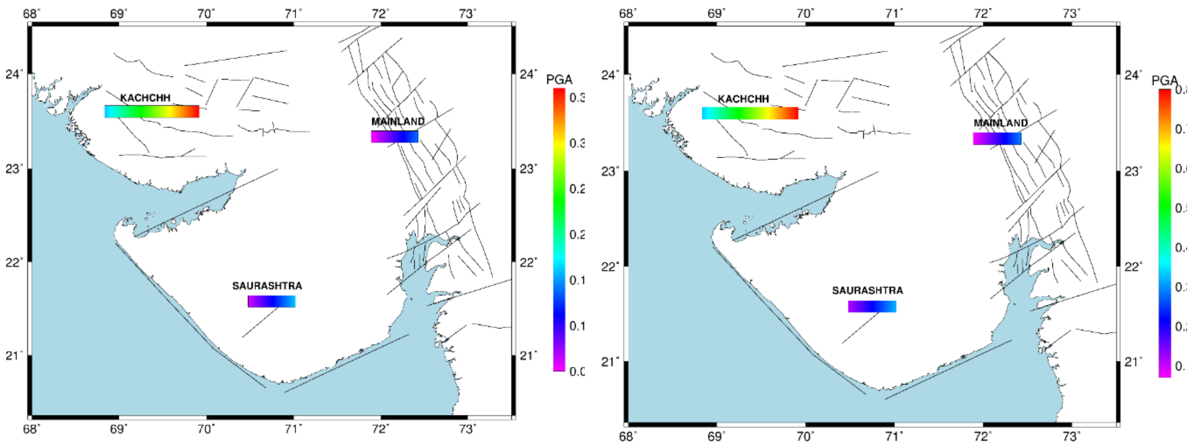

(a) (b)

Figure 2.32: The PGA range (in g) obtained in the present study in three different regions of Gujarat for (a) 10% (b) 2% of PE in 50 years.

2.18 Characterization of Kachchh Mainland Fault and Katrol Hill Fault in the western central part of Kachchh

(Kapil Mohan, Peush Chaudhary, Pruthul Patel and Sumer Chopra)

2D Magnetotelluric modeling was performed using data acquired at 17 sites in Dujapar village in the south to Shervo village in the north (Fig. 2.33). The 55km long profile with a station spacing of 2-3km, crosses the Kachchh Mainland Uplift (KMU).

The geoelectric section generated from 1D and 2D inversion of the MT data shows that the maximum sediment thickness is 2.3 km. The thickness is 2.2 km in the northern part near KMF and ~ 2.0 km between KMF and KHF. The Mesozoic sediment thickness of about 1.4 km is observed near Nirona village in the north and 1.8 to 2.0 km from Vedhar to Manjal villages (between KMF and KHF). A basement depth of about 2.3 km is observed near KMF and is found dipping south between KMF and KHF. A new deep-seated fault is observed between Ulat and Kotda villages (named as Ulat-Kotda fault) (conductor C2 in Fig. 2.34a), that dips near vertical down to 20 km depth and becomes listric (with a north dip) beyond 20 km depth (Fig. 2.34a). The KMU block is found to be tilting south, with the formation of a half graben between Ulat Kotda Fault (UKF) and KHF. The KMF is found dipping almost vertical up to 7-8 km and then dipping north afterwards, at an angle of about 45^{o}. The KHF dips south at an angle of ~60^{o} (Fig. 2.34a). In comparison with the past studies (Fig. 2.35), the KMF is found to be a north-dipping fault that dips south in the vicinity of transverse faults.

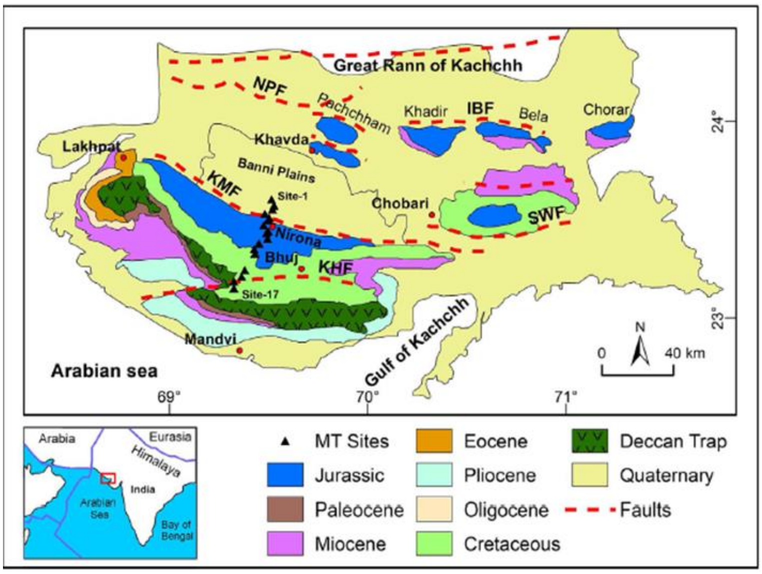

Figure 2.33: Location of the MT sites (marked as triangles) superimposed on the geology and tectonic map of the area (after Biswas, 2005). KMF: Kachchh Mainland fault, KHF : Katrol Hill fault, SWF : South Wagad fault, NPF : Nagar Parkar fault and IBF : Island Belt Fault.

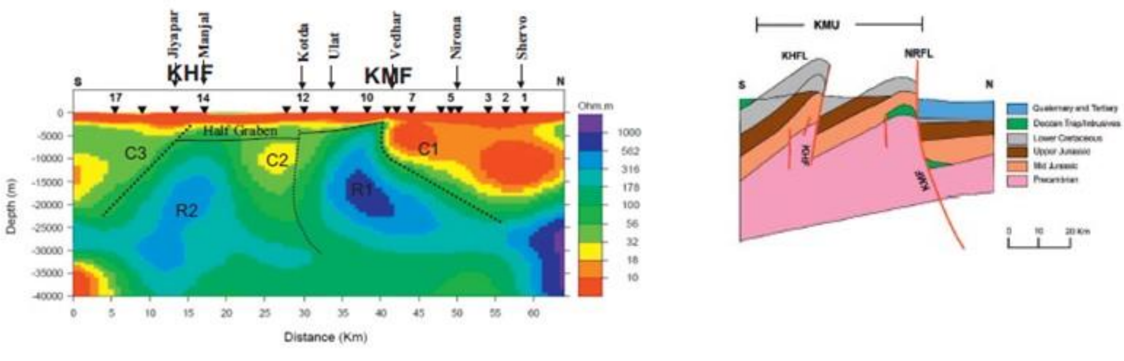

(a) (b)

Figure 2.34: (a) 2-D Geoelectric depth sections of TE+TM+HZ mode of the profile.C1: KMF and C3: KHF and (b) Geological cross section of the study area (after Biswas, 2005). KHFL : Katrol Hill Flexure and NRFL : Northern range Flexure.

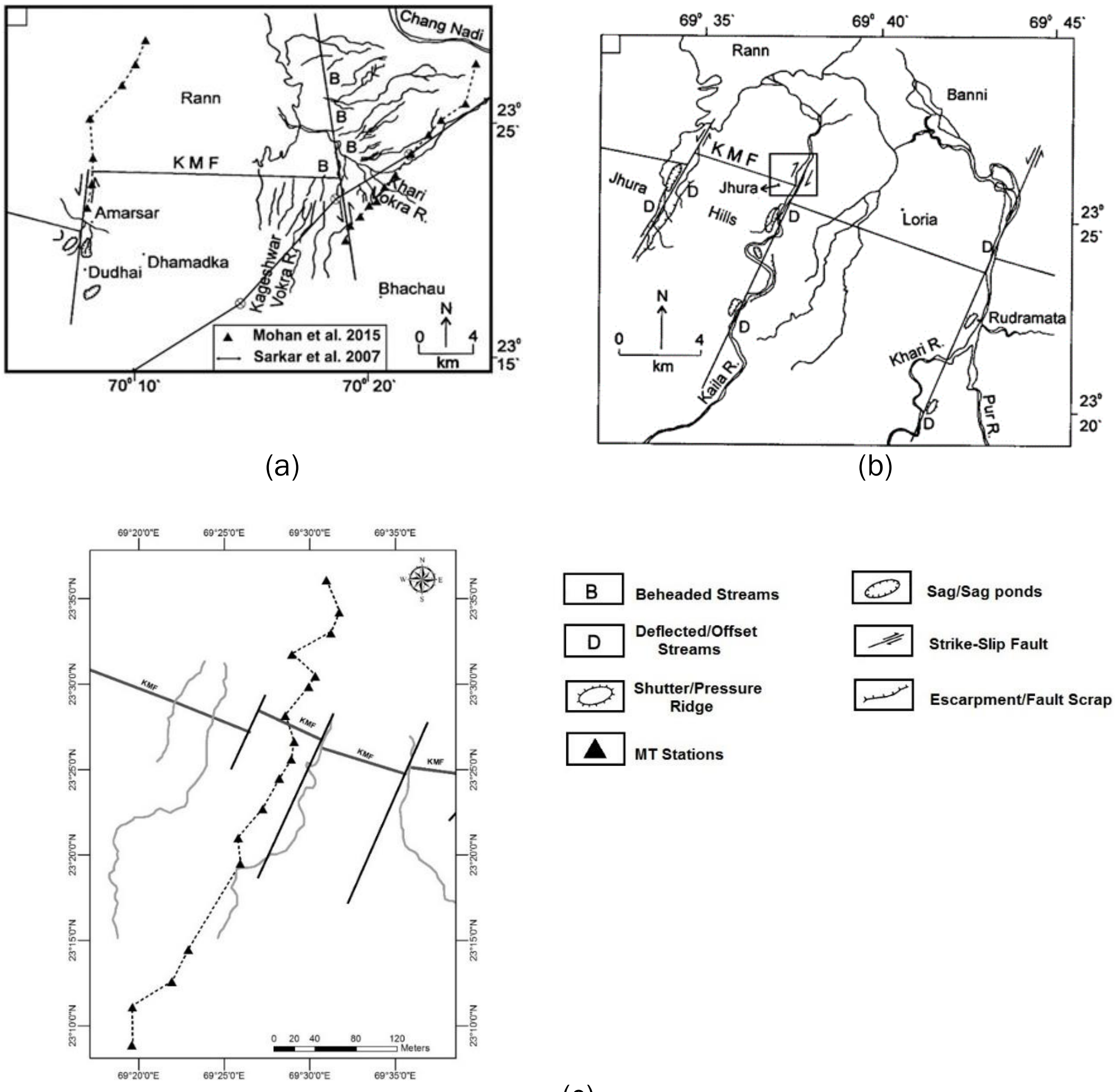

Figure 2.35: Map showing the transverse fault (a) across eastern part of KMF (after Maurya et al., 2003) overlapped by the MT sites and Seismic profile (b) across central part of KMF near Jhura. Square represents the study area of Morino et al. (2008) and (c) map showing the transverse faults (after Prizomwala et al., 2016) together with the MT profile acquired in the present study.

2.19 Magnetotelluric Study in the western part of Kachchh, Gujarat

(Kapil Mohan, Pruthul Patel, Dilip Singh and Vishal Vats)

An MT survey was conducted at 15 sites in a N-S profile for a recording period of 3-4 days from 22nd January 2018 to 14th February 2018 (Fig. 2.36). The profile runs from Hajipir in the north to Suthri village in the south. The aim of the survey is to characterize the Kachchh Mainland, Katrol Hill and Vigodi faults in the western part of the Kachchh region of Gujarat.

The dimensionality analysis was performed using Swift Skew, Bahr Skew and Caldwell methods. The value of Bahr skew is estimated less than 0.3, which indicates that the structure is 1D or 2D as shown in Fig. 2.37. The value of Swift skew is estimated less than 0.2 (Fig.2.37) which also indicates that the structure is 1D / 2D. The value of Skew angle beta is estimated less than 5 degree which is also a good indicator that the structure is 2D.

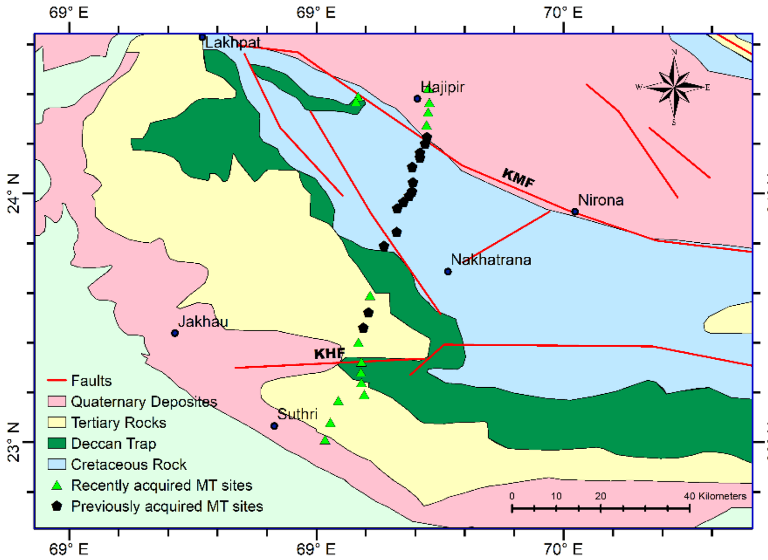

Figure 2.36: MT profile near Nakhatrana superimposed on a geological and tectonic map of Kachchh (after Biswas, 2005).

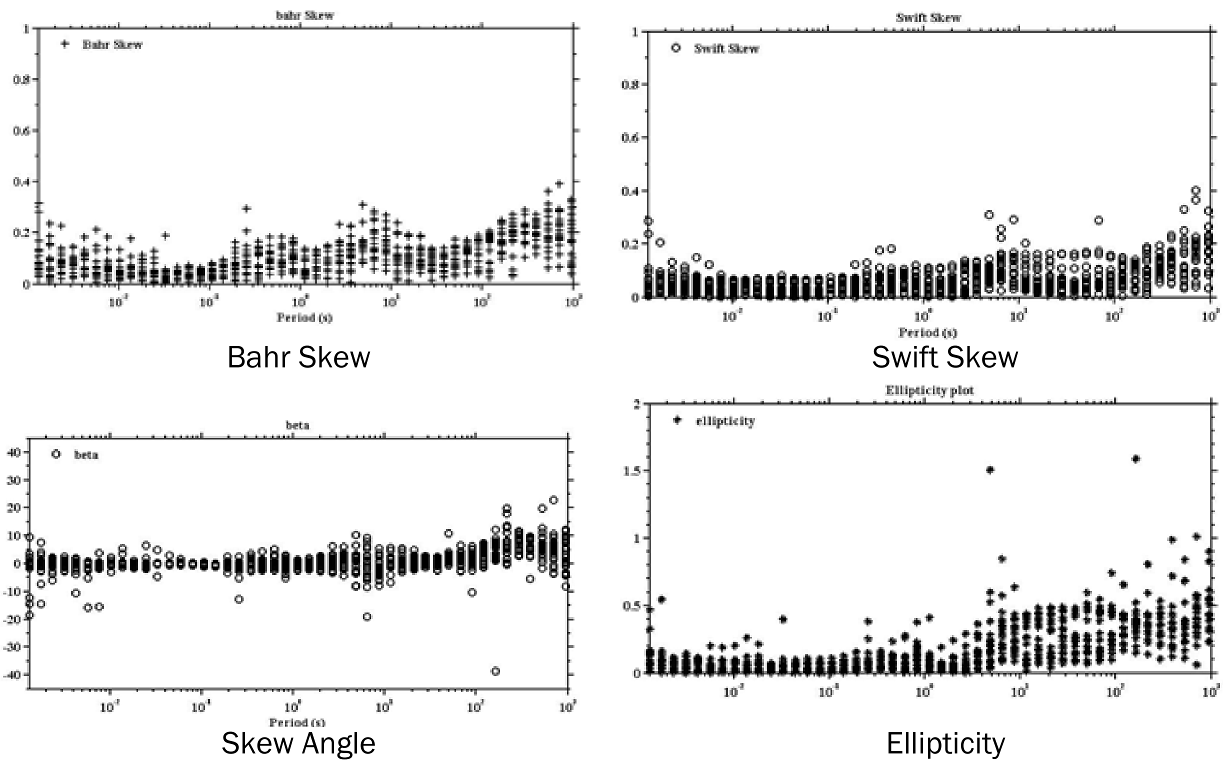

Figure 2.37: Diagram indicating values of Bahr Skew, Swift Skew, Skew Angle and Ellipticity, for all the stations

The strike analysis at the stations was conducted using the Caldwell (2004) method. The average strike values are found to be ~ -45 degree (Fig. 2.38) over a frequency band of 0.001 to 1000 sec. The value is in good agreement with the tectonic setting of the study area.

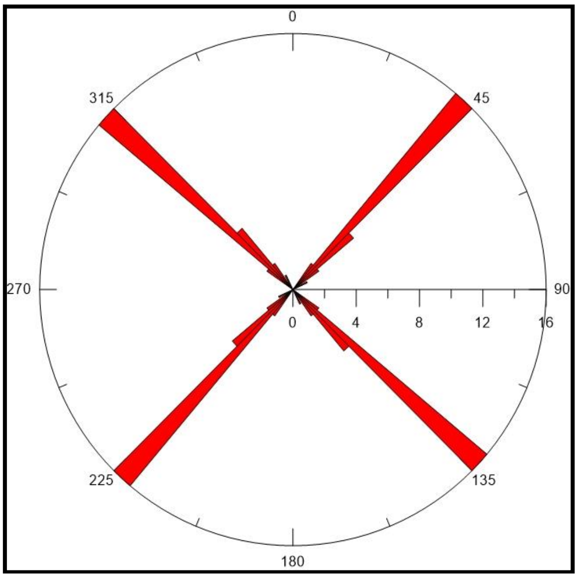

Figure 2.38: Diagram showing strike values for 0.001-1000 sec periods.

2.20 2-D subsurface model of little Rann area, Kachchh using Magnetotellurics

(Peush Chaudhary and Kapil Mohan)

2D MT inversion technique of Rodi and Mackie (2001) was used to generate a geoelectric depth section of the area, considering TE+TM mode (Fig 2.39). To check the robustness of the model features, sensitivity analysis and constrained inversion were carried out

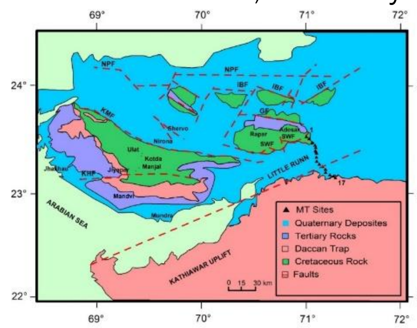

Figure 2.39: The location map of the MT profile.

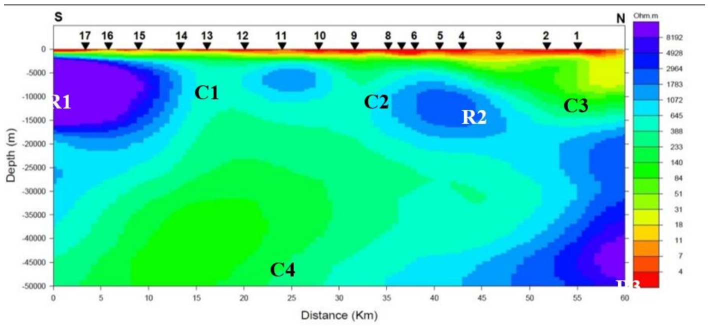

Figure 2.40: 2D geoelectric depth section of Adesar MT profile.

Following are interpreted from the final 2D section (Fig. 2.40)

1. Sedimentary thickness is found to be ~500m in the south and ~1200m in the north, which implies the thinning of sediments from north to south.
2. Three prominent conductive features C1, C2 and C3 and resistive zones R1, R2 and R3 are found (Fig. 2.37).
3. The location of the conductive feature C3 matches with the location of the Kanmer Fault
4. The conductor C4 at a depth of 20km may be indicative of fluid rich mafic/ultramafic body.

3 Solid Earth Geophysics

3.1 Geological and seismological field investigations at Navsari, Valsad and Silvas areas of South Gujarat

(Arjav Shukla and A. P. Singh)

During the months of October-December, people of some villages of Navsari and Valsad districts were panicked by faint earthquake tremors, ground vibrations and unusual sound. This phenomenon was also reported in the same time period in the same area in the year 2016. We carried out geophysical and geological surveys and public education/earthquake awareness programmes in Navsari, Vansda, Mandvakhadk, Zari, Kavdej, Keliya, Godvani, Limzar, Godmal, Lanchhakdi and Mota Randha areas of Navsari and Dadra Nagar Haveli. The landscape/area under investigation is divided into two segments, viz, alluvial plains, rugged highlands and lineaments trending E-W, N-S, NNE-SSW were identified. This physiographic division and crisscrossed orientation of lineaments and intrusive bodies in the landscape suggest tectonic control and geomorphic evolution of the region during the historic times. Though less or no evidence of neo-tectonic activity is found, the diversity and drastic change in topographic relief, fractured and jointed bedrock platforms and nature of river flow identified on the basis of satellite imageries emphases the scenario of tectonic activity.

Geologically, the area is dominated by different flows of Deccan trap basalt overlain by a thin cover of alluvial/fluvial soils deposited by Purna and other local rives. The different flows of basaltic lava were identified in form of small to large hill locks, plugs, dykes and lineaments. The areas around Navsari, Valsad and Dang districts fall under rain forest belt in the southern part of Gujarat. The areas under investigation lacks good outcrops and sections to study the geology and tectonic deformation, in detail. A highly dense vegetation cover and humid atmosphere have restricted the availability of good exposures and out crops for detailed investigation. The weathered and ductile, intact nature of country rock Basalt and development of highly pulverised ragolith cover over the rock beds do not preserve any good evidence of tectonic deformation observed in the road cutting and river sections. Fractured and joint bedrock was observed. An abrupt change in elevation is noticed SE of Navsari district. These elevated bodies and lineaments are probably the highly elevated dykes and plugs covered under dense forest vegetation. These highly elevated dykes and plugs can be seen cross cutting each other in the field and satellite imageries as well, which links their origin to tectonic deformation in the form of faults and fractures during the past. The entire region in vicinity of Navsari, Valsad and Dang districts seem to be highly controlled by the structural/tectonic phenomena. A number of small to large intrusive bodies, lineaments, fractures and joints, faults and other structural features are seen to have occurred in the region which is clearly observable in satellite imageries of the region.

Occurrence and orientation of structural features like dykes, fractures, joints and lineaments support the dominance of tectonic activity in the region. The nature of small faults and joint patterns documented in the region further support existence of both tensional and compressional tectonism and structural control in the region. It is also noticed that seismicity and earthquake swarm activity are majorly confined in the areas of highlands, in the SE direction of Navsari city. According to local residents and public perception, tremors and unusual sound are noticed and reported more near Keliya village/Keliya dam, especially in the months of October-December. This phenomenon leads to a conclusion that this swarm activity could be monsoon induced, in which the monsoonal rain water stored in reservoirs percolates down through the opened up fractures and joints of country rock Deccan basalt. To support this fact, annual rainfall data has also been collected from the Keliya dam site.

3.2 Local site effects estimated from Ambient Vibration measurements at Mehsana City, Western India

(Mayank Dixit and A. P. Singh)

Close monitoring of earthquake activity in the Gujarat region of northwestern Deccan volcanic province suggests that seismicity is still continuing with one or two magnitude 4-5 earthquakes every year. Most of the major cities in Gujarat are located on thick sediments of recent age, which amplify ground motion during a major earthquake. It is perceived that the ambient noise encapsulates the predominant frequency of the sediment layers. Therefore, to scrutinize the site characteristics in the vicinity of Mehsana city, a noise survey has been carried out at 63 sites using City Shark-II digitizers coupled to three component Lennartz LE3D (5s) seismometers to decipher the local site effects of the soft deposits. The analysis of the data shows plateau like peaks of the Horizontal to Vertical Spectral ratio (HVSR) curves in the frequency range 0.58-0.74 Hz with the amplitude values in range of 2.2 to 9.9. This may be attributed to the thickness of the upper soft soils of 270-345 m. Further, this study shows that the ground vulnerability index (Kg) at 48 sites in and around Meshana city is more than 10 which could be attributable to be the most vulnerable sites during any large earthquake. This investigation may be useful for future planning purposes as well as risk analysis and mitigation of earthquake in the study area.

3.3 Microtremor survey along the borehole sites located in Gandhinagar and Ahmedabad cities

(Arjav Shukla, A. P. Singh and Sumer Chopra)

In order to correlate the borehole and microtremor data and to validate the site specific information, a microtremor survey has been performed along 13 borehole sites in the Gandhinagar city with 60 minutes duration of recording. The H/V spectral ratios reveal that most of the sites in Gandhinagar have predominant frequencies around 0.6 Hz and the corresponding amplitude values at all the site are <4. Multiple peaks are also observed at some sites, indicating impedance contrast at different depths. The peak amplitude at low frequency may be associated with the Quaternary-Tertiary boundary in the area. The peaks are of plateau shaped in nature, indicating low contrast at depths.

3.4 Site response study in and around the Bhuj City

(Arjav Shukla and A. P. Singh)

During January to February 2018, we performed microtremor survey in different areas of Bhuj (Western Gujarat) as a part of microzonation of the city (Fig. 3.1). The main purpose is to delineate local site conditions and site response to ground motion considering the devastation caused by the 26th January 2001 Bhuj earthquake.

In present survey, microtremor data were recorded at nearly 42 sites/areas of Bhuj city and suburbs, considering local site conditions and geology. The survey was carried out using City Shark – II digitizer and recorder during early morning, evening and night time on continuous mode at a sampling rate 100 samples / sec. The data was recorded over a 40 minute time window. The H/V ratio curves obtained for all sites in Bhuj shows very close similarity in terms of their shape and spatial distribution. The shape and values of peak frequency and amplitude are nearly same for all the locations except a few, which is due to monotonous geology of the city. The resultant HVSR curves are matching with local geological conditions at a site. It is observed that most of the curves exhibit broad, plateau shaped peaks at very flat, low to moderate amplitude values in a confined low frequency range between 0.4 to 2.0 Hz. These sites with observed low amplitude values at lower frequencies <3 Hz suggest that the sites are situated on a compact platform of Cretaceous sandstone of Bhuj formation with no other soft rock deposits lying over or in contact with it. A few high amplitude values (>4) indicate soft and unconsolidated Quaternary deposits over hard rock platforms, including fluvial and alluvial deposits.

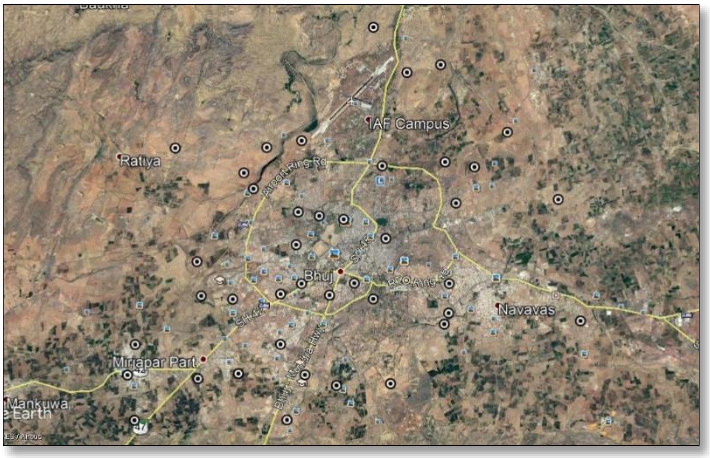

Figure 3.1: Satellite imagery of Bhuj area showing locations of microtremor survey (Black and white circles)

3.5 Subsurface structure in the Eastern Indian Shield region using ambient vibration

(A. P. Singh and Rashmi Singh)

Ambient vibration and earthquake recordings are used for understanding stability of HVSR and subsurface structure of the Eastern Indian Shield region, which is tectonically *stable* and *less* vulnerable to *earthquake* activities. The microtremor data have been analyzed at 9 permanent seismological observatories to determine the site amplification corresponding to the amplified frequencies and the relevant shear wave velocity profile of the EIS. The measurements at all sites were recorded at three components of broad band seismograph (120s). HVSR at all the sites indicate that frequencies remain unchanged; while amplification changes slightly with the season. The resonant frequencies observed at stations ISM, BKR, CAL, BHW, GTK, VAL, VAR, BLS and SHB are 1.2, 1.2, 0.7 ,2.0 4.8, 4.0, 0.5, 4.1 and 5.0 Hz, respectively. The H/V ratios using BBS earthquake records show amplification of 2.75-3.5 and 4.0-6.02 in the frequency band of 1.0-2.0 Hz and another at 4.0-6.0 Hz respectively. There is no amplification below 1 Hz frequency, which may be due to the moderate size earthquakes used in the present study. We estimated shear wave velocity model using a two layer model as the initial model for the inversion. It is seen that the upper most layer up to 20 meters has a low shear velocity between 400-850 m/s. The second layer at the depth of 80-100 meters has a shear velocity of 850-1200 m/s. These layers are Quaternary sediments and granite-gneiss. There is less variation of structure and properties. The first layer is stiff soil or sediments while the second layer is a soft rock. The results of microtremor measurements and earthquake recordings have been compared with the results from other geophysical and geological information. The estimated site effects of the deep soil in the area shows a good correlation with geomorphological data.

3.6 Shallow Subsurface Imaging of Eastern Kachchh using Transient electromagnetic studies

(Pavan Kumar, Indu Chaudhary, Mehul Nagar, Himanshu Chaube, Rakesh Nikam, Dinesh Singh, Durga Prasad and Siddhartha Prizomwala)

To Image the deep groundwater aquifers, we carried out Transient electromagnetic (TDEM) investigations in the close vicinity of the KMF as well as surrounding areas. A total of 48 TDEM sites have been acquired in a in-loop configuration. At each site, a 100m transmitter loop was laid and ~9.2 amp of current was injected in to the loop with different transmitter current frequencies (32,16,8,4,2,1 Hz). The induced voltage due to sudden change in the transmitter current was measured at the centre of the loop as a function of decay time using a magnetic coil. The apparent resistivity estimated from the induced voltage at each site is used for one dimensional modelling of the data. The resistivity sections across the KMF show sharp resistivity contrast that reflects the contact between Mesozoic (5-100 Ohm.m) and Quaternary group of formations (> 20 ohm.m).

The resistivity section across the KMF imaged a confined aquifer (~10 ohm.m) at a depth of 70-80m from the surface with a thickness of 30-40m. The depth of the aquifer decreases towards the KMF and terminated in the in KMF zone. Since the northern side of the KMF is consists of quaternary banni sediments mostly composed of clay, clayey-sand, which is highly impermeable and anisotropic, we infer that the groundwater flow through the aquifer is restricted to the zone due to tectonic sediment mixing and clay smear in the unlithified rock in the fault zone resulting in a reduction in permeability across the fault zone. This strengthens the concept that the fault can behave as a barrier for across-fault flow, while it can also act as conduit for fault-parallel flow when a fault zone is composed of sand, together with or instead of clay beds. In this case, the permeability of the fault zone will be enhanced, since beds of permeable material along the fault zone will form conduits for the migration of fluids along the fault zone. The process of permeability will also depend on the continuity and thickness of this permeable material in the fault zone. Multidisciplinary interpretation combining geophysical, structural geological and hydrological data shall give a better understanding on the behaviour of the fluid flow across a fault zone.

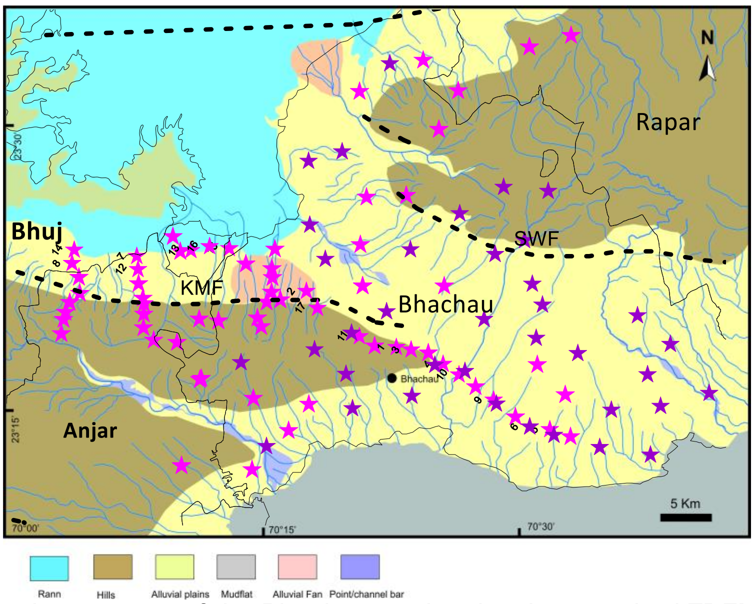

Figure 3.2: Geomorphology map of the Bhachau taluka showing acquired TDEM points and major faults

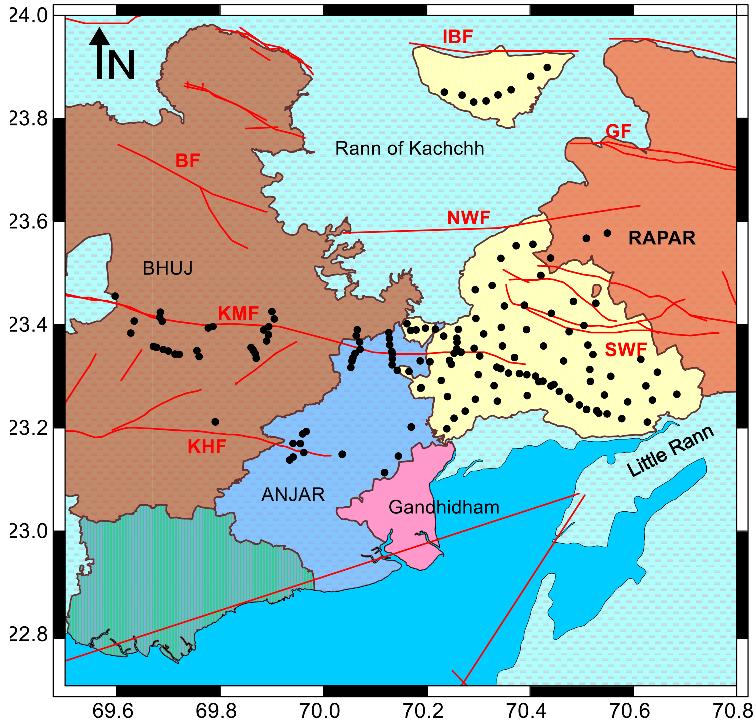

Figure 3.3: Map showing the acquired TDEM points in Eastern Kachchh

3.7 Shallow subsurface imaging of Kachchh Mainland Fault (KMF)

(Pavan Kumar and Indu Chaudhary, Mehul Nagar)

We analysed the time domain electromagnetic data at 52 sites (Fig. 3.4), distributed along seven traverses across the KMF zone. The study not only demarcates the KMF but also reveals presence of splays and transverse features in the area (Fig. 3.5). The subsurface structure of the fault zone suggests segmented nature of the KMF with the activity increasing from the western to the eastern part. Some of the splays portray a negative flower structure, suggesting localized trans-tensional geometry of the region. The presence of buried colluvial wedges can be deduced based on high conductive zones in the hanging wall side of the fault, indicating neotectonic activity in the study region. The estimated thickness of the Quaternary sediments is 105 m (Fig. 3.6).

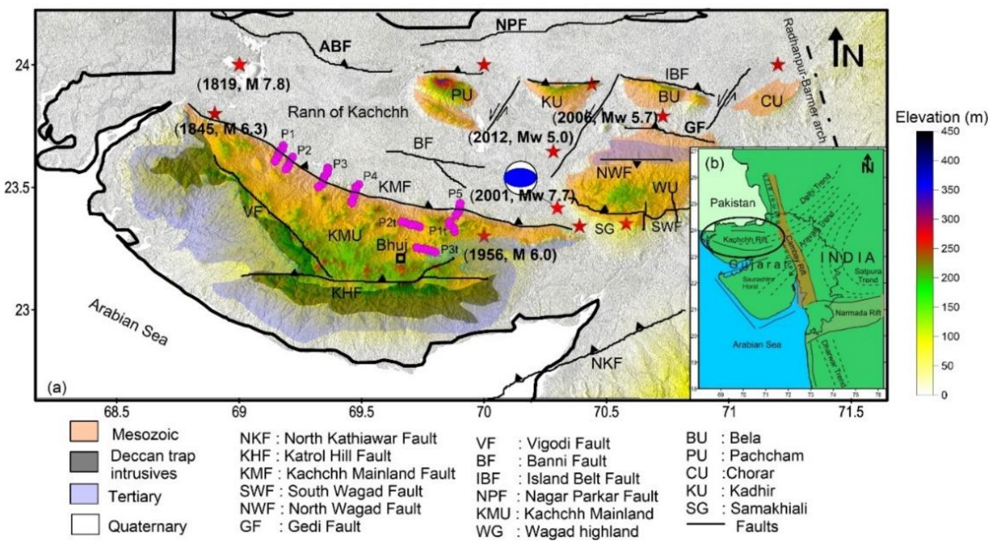

Figure 3.4: Geological map of the Kachchh region showing TDEM sites

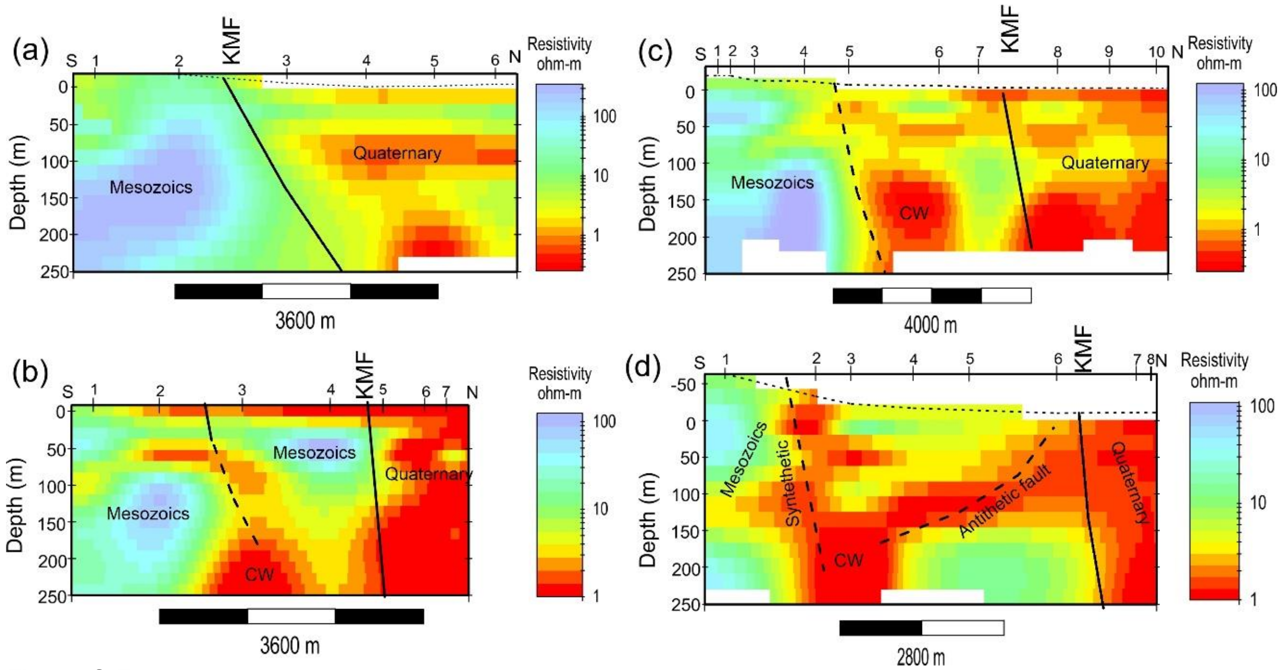

Figure 3.5: Geoelectric resistivity sections along four profiles that cut the KMF.

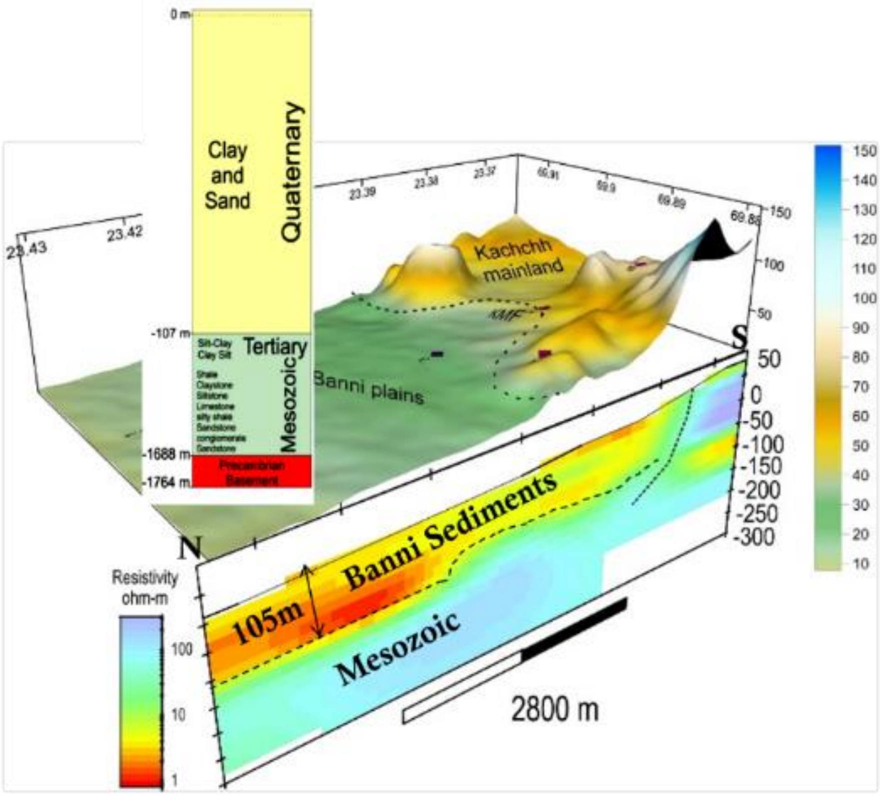

Figure 3.6: Shallow resistivity image at Lodai village of the Kachchh district.

3.8 Magnetotelluric investigations in the Eastern part of the Kachchh rift basin

(*Pavan Kumar, Mehul Nagar, Rakesh Nigam and Himanchu Chaube)*

To understand the crustal electrical resistivity structure of the eastern Kachchh region, we acquired MT data at 15 locations across the KHF and KMF, in a broad frequency range

(0.01-4096s) with 4 days recording duration. The interstation spacing is about 3-4km. The acquired MT sites are shown in figure. 3.7. Data of 15 sites have been processed and earth response functions are estimated. The processed data are then analysed for amount of distortions. The geoelectric strike direction is calculated as N71E.

The one-dimensional inversion of the data is carried-out to estimate sedimentary thickness and the basement architecture. The 1-D section along the profile (Fig.3.8) shows that the northern portion is more conductive compared to the southern side. The high conducive zone (C1) (< 5 ohm.m) observed in the model could represent quaternary and tertiary sedimentary deposits (Clay and sand) in the region. The moderate conducive zone (C2) underlain over the quaternary and tertiary sediments might indicate the presence of the Mesozoic formations comprising of sandstone and shale. In the northern portion, the sedimentary layer is overlain on a resistive layer ((~500 ohm) representing the basement. The high resistive zone (R2) (>1000 ohm.m) at a depth of 6-7km might indicate a basaltic intrusion, representing the remanance of Deccan Volcanism that occurred about 65My ago. In the southern portion of the profile, we observed a resistive layer (R3 &R1) at shallow depths indicating the presence of Deccan traps in the region. Interestingly, the 1-D model yields two conductive zones (C3, C4) down to greater depths (~10km). The surface location C3 coincides with the Kachchh Mainland Fault (KMF). We therefore suggest that the C3 zone represents the subsurface image of the KMF. In the southern portion, we observed a good resistive contrast (R3 &C2) that represents the presence of Katrol Hill fault (KHF). The model also shows a high conductive zone at 8km below the KHF zone. We speculate that this conducive zone might be a fluid filled fracture zone. However, detailed 2D/3D modelling will be required to further confirm the presence of this high conductive zone.

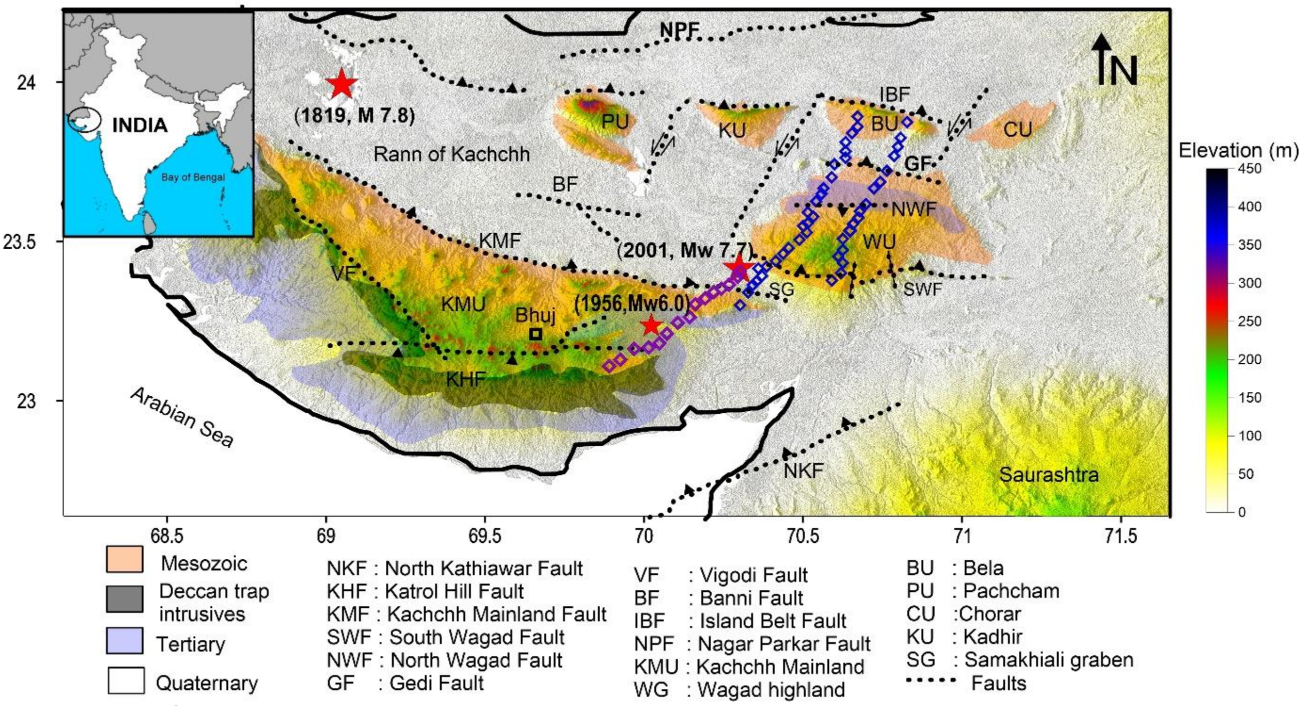

Figure 3.7: Map showing locations of the acquired MT sites (violet coloured symbols)

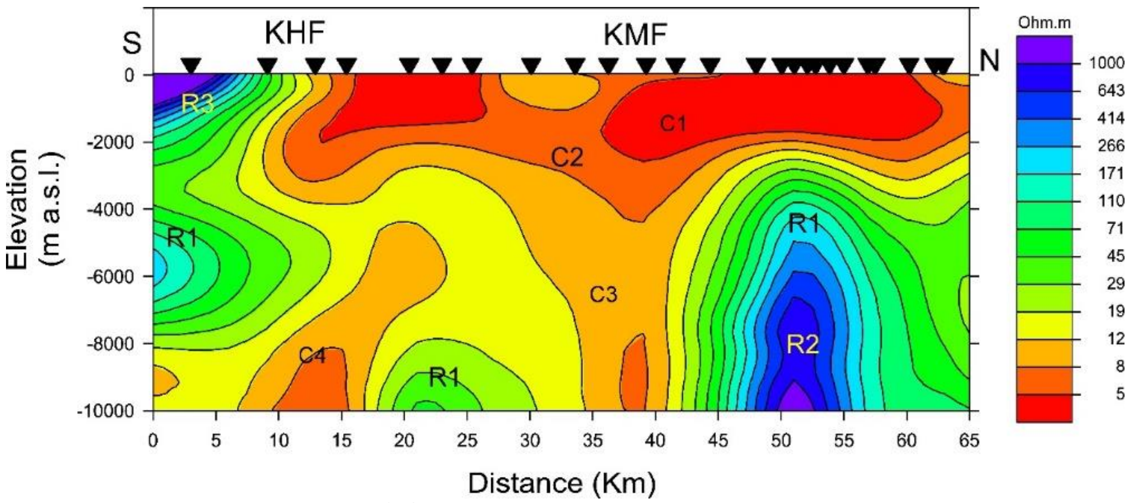

Figure 3.8: Resistivity section across the profile

3.9 Assessment of base metal mineralization in Banaskantha District using Joint geological and geophysical Investigations (AMBAJI)

(Avinash Chauhan, Dinesh Singh, Himanshu Chaube, Rakesh Nikam and Pavan Kumar)

Multi-disciplinary geophysical studies have been initiated in the Amabji area of Banaskatha district for assessing the mineral potential of the region. Different corrections, like elevation, lat, long, free air, diurnal and IGRF are made for analyzing the gravity and magnetic data. For shallow gravity exploration, regional and residual separation was performed. The observed magnetic data are corrected for Remanent and Induced magnetic field components. The resultant residual gravity and magnetic anomaly maps of the study region are shown in figure 3.9.

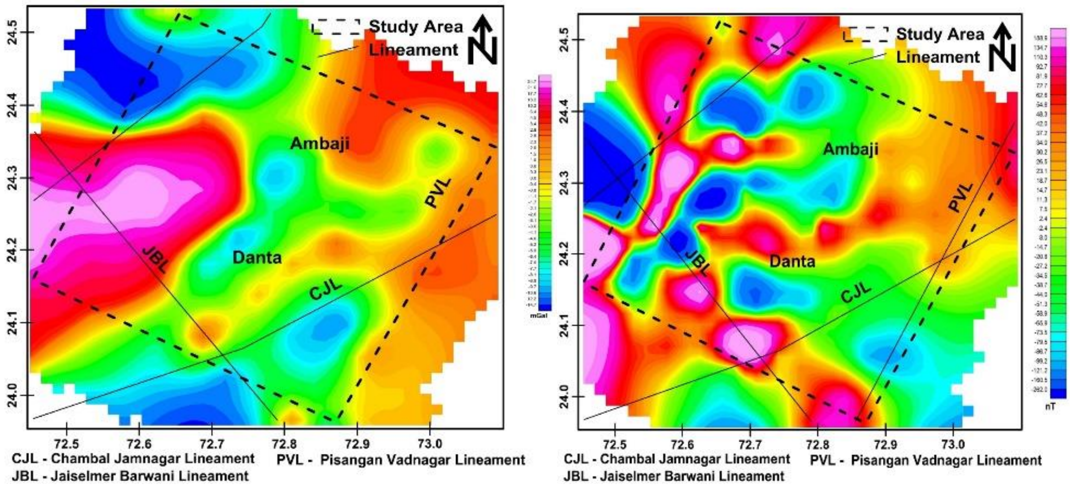

Figure 3.9: Residual gravity and magnetic anomaly map of the study region

We also collected TDEM data at 15 sites in the study region to map the shallow resistivity structure. The locations of the TDEM sites are shown in figure 3.10.

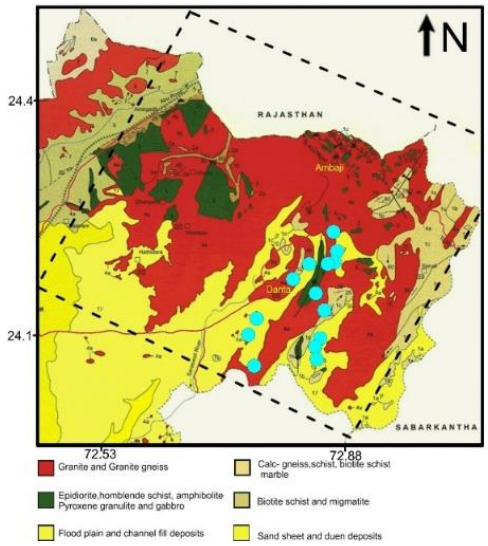

Figure 3.10: Geological map of the Ambajji area showing acquired TDEM sites

3.10 Delineation of structural features over Ambaji mineralization zone, Gujarat, NW India using gravity and magnetic data

(Avinash Kumar Chouhan, Dinesh Singh, Himanshu Chaube, Rakesh Nikam, Mehul Nagar and G. Pavan Kumar)

To understand the complex tectonic setting and its linkage to origin of mineralization of the Ambajji and its surrounding area, gravity (~ 450 points) and magnetic data (~200 points) are collected at a station interval of 1-5 km and analysed. Bouguer gravity anomalies are obtained using a Bouguer slab of density 2.67 gm/cc. Bouguer anomaly (BA) values range from -30 to 30 mGal (Figure 3.11a). The total magnetic anomaly values are calculated after correcting for diurnal variation and International Geomagnetic Reference Field (IGRF) which show a variation from -770 to -30 nT (Figure 3.11b). Upward continuation of gravity data is performed to image the subsurface extension of regional tectonic features. Gravity and magnetic data have been analysed for the delineation of structural features using different derivative techniques like total horizontal derivative (THD), Tilt angle derivative, Theta map and Analytical Signal techniques.

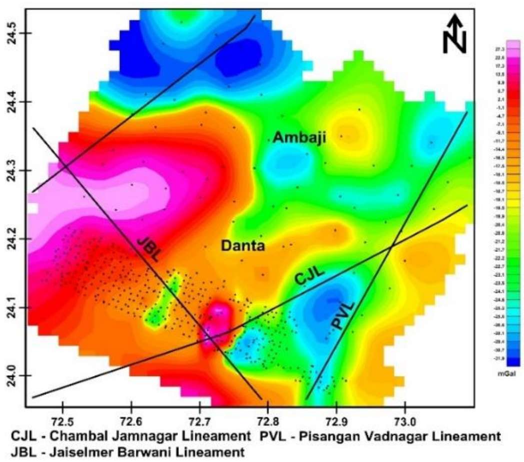

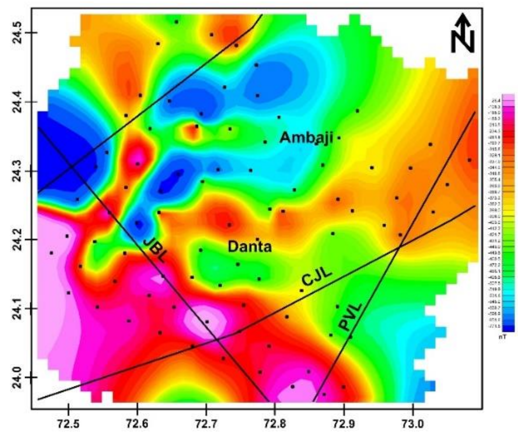

Figure 3.11: (a) Bouguer anomaly map of the Ambaji area. (b) Magnetic anomaly map of the Ambaji area. CJL-Chambal Jamnagar Lineament, JBL- Jaiselmer Barwani Lineament, PVL- Pisangan Vadnagar Lineament. Dots show the gravity and magnetic stations.

The derivative analysis delineated major NE-SW trending lineaments- Chambal-Jamnagar Lineament (CJL), Pisangan-Vadnagar Lineament (PVL) and the NW-SE oriented Jaisalmer-Barvani Lineament (JBL). The high gravity anomalies in the western part of the study region suggest a shallow basement. The residual Bouguer anomaly obtained by subtracting the regional field from the observed anomaly shows a pattern almost similar to the observed BA with little changes in the amplitude. The Magnetic high in the south-western part, correlating with the JBL possibly indicates a deep rooted nature of the lineament. An E-W structural trend appears to be continued from the northeastern part of the region, representing the Delhi-Aravalli trend. The presence of the Aravallis below the northern alluvial plains is also supported by previous regional geophysical studies in the region.

3.11 Crustal studies over the northern Cambay basin using high resolution gravity measurements

(Avinash Kumar Chouhan, Dinesh Singh and Pallabee Choudhury)

To study the crustal structure and tectonic trend of the northern Cambay basin, gravity data is acquired and a Bouguer anomaly map is prepared (Figure 3.12). To study the crustal architecture, gravity data has been acquired along five profiles and modeling is under process. To study the lineaments/contacts, filtering and derivative analysis will be done.

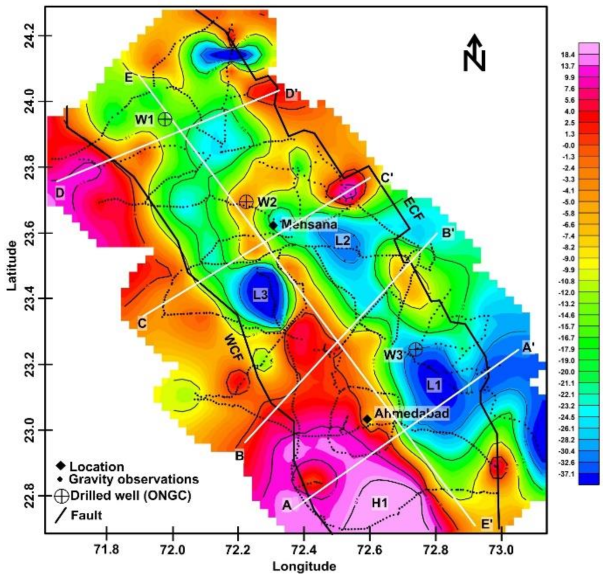

Figure 3.12: Bouguer anomaly map of the North Cambay basin. Circular dots show the gravity observation points. Square dots indicate the major locations in the study area. Black lines trace the Eastern Cambay fault (ECF) and the Western Cambay fault (WCF). AA', BB', CC', DD' and EE' are the gravity profiles selected for modelling. H1 represents gravity high and L1, L2 and L3 represent the gravity lows. W1. W2 and W3 are the locations of wells drilled by ONGC (after Kaila et al., 1989).

3.12 Astronomical and Meteorological Earthquake precursors in the Kachchh Rift Basin, Northwestern India

(*Mayank Dixit)*

Seasonal fluctuations in the observed seismicity of the Kachchh Rift basin, Gujarat was studied using the earthquake catalog data compiled for the period 2010 to 2016. During this period, approximately 7000 earthquakes of magnitude greater than or equal to 1.4

were recorded by a very dense seismic network established and maintained by the Seismic Data Analysis Center (SeiDAC), Institute of Seismological Research (ISR). In this investigation, the impact of seasonal and diurnal variation, the effect of tides, Supermoon phenomenon and land surface thermal anomalies on the seismic activity was studied for Kachchh region. A significant drop in the seismic activity was observed during the Indian Monsoon (June-September). A thorough analysis of the recorded earthquake data indicated higher seismic activity during the night and early morning hours when compared to the daytime. This behavior has been observed for all events of magnitude beyond the detection threshold. Further, the Dholavira earthquake (2012) of magnitude 5.0 was analyzed for identifying the variations in the land surface thermal anomalies. It can be interpreted that the land surface temperature shows an increase seven days prior to the said earthquake.

We also observed no clear correlation between the lunar phases and earthquake clusters. Another interesting observation made during the 27th and the 1st lunar day is an increase in seismicity rate above the average value, in the magnitude range of 1.4-2.9 and 3.0 to 5.0 which was found to be 23% and 43% respectively. This behavior is mostly attributed to the effect of tidal forces. Significant clustering of earthquakes was found before and after the 30th Jan 2010 and 19th March 2011 Supermoons, but during other supermoons, no such fluctuations were observed for the earthquakes of intraplate nature. This study aims to create awareness about the fluctuations in the natural phenomenon which could be considered as indicators of an upcoming earthquake, thereby improving the earthquake preparedness and disaster mitigation strategies.

3.13 Discrimination of quarry blasts from micro earthquakes in the Surendranagar region of Saurashtra province, Northwestern India

(Mayank Dixit, A. P. Singh)

The complex and covert phenomenon undergoing in the earth's interior is revealed by the seismic waves propagating to the surface. The main objective of this study is to capture the difference in the nature of waves transmitted due to quarry blasts and earthquakes and differentiate the tremors caused by these two. A total of 1100 ground motions ($M \geq 1.1$) recorded from different regions of Saurashtra, during 2012-2016 were considered for the study. These recordings have been obtained from the seismic network established and maintained by Seismic Data Analysis Center (SeiDAC), ISR. In this investigation, ground motions of frequency greater than 1Hz were considered and statistical method (maximum of P to S waves ratio) was applied for four frequency bands such as, 2- 4, 4-6, 6-8, 8-10 and a common bin from 1 to 10 Hz. The outcome of this investigation suggested that 6% of the examined ground motion records were caused due to quarry blasts and the rest as a consequence of earthquakes. Application of coda decay rate method revealed that the coda decay rate Qc^{-1} is significantly higher for quarry blasts than earthquakes, in the frequency range of 1.5 to 3.0 Hz. Spectrogram analysis affirms the distinction between quarry blasts and earthquakes in terms of varying frequency content. The detailed investigation brought forward an intriguing remark about mining-induced seismicity as more seismic activity was observed during the daytime than night. The findings of this investigation may contribute to the existing knowledge base on earthquakes in addition to creating a distinction between the natural and manmade earthquakes.

3.14 Remotely triggered tremors in Kachchh region, Northwestern India following large teleseismic earthquakes

(Mayank Dixit)

The static stress variation caused by an earthquake can trigger seismic activity in its vicinity but a fluctuation in dynamic stress can trigger micro earthquakes even at remote distances. Most of the remotely triggered tremors have been found along major plate boundaries but for intraplate regions, this phenomenon is stil elusive. This study focuses on demonstrating the possibility of remotely triggered tremors in the seismically active intraplate Kachchh rift basin due to large amplitude and long duration transient signals. Systematic analysis of waveforms of 30 significant earthquakes recorded at 35 broadband seismic stations affirms clear triggered tremors in the region. We identified many high frequency seismic signals during the passage of Love waves. The outcome revealed that the triggered tremors were mostly located along the Kachchh Mainland Fault (KMF), North and South Wagad fault, in the epicentral zone of the 2001 Bhuj earthquake (Mw 7.7). This study is an attempt to understand the less investigated remotely triggered tremors in the intraplate region.

3.15 Source characteristics for the Gujarat region

(Jyoti Sharma)

In this study, we present a comprehensive account of the source characteristics of moderate earthquakes (M_L 3.5-5.0) which occurred in the Kachchh region. Such studies are important to understand the nature of newly active faults. Moreover, some of these earthquakes of Gujarat viz., the 2007 and 2011 Talala earthquakes (M_w 5.0) of Saurashtra were well felt in the state, and damaged many adobe type houses.

Source and fault plane parameters namely Moment tensor (MT), Moment magnitude (Mw), Strike, Dip, Rake of Nodal planes (NP1 and NP2), Corner frequency (fc), High frequency spectral fall-off factor (γ), Stress drop (Δσ), and Radius of rupture (rd) were determined in the present study. Moment tensor and fault plane solutions of all the nine earthquakes were estimated using full waveform inversion. The source parameters were determined by spectral analysis of the transverse components of the earthquake records at different source azimuths using the most popular and convenient Brune's model (Brune, 1970). The distribution of broadband seismic stations used in present study is shown in Figure 3.13. To estimate source parameters, transverse component of the recorded displacement spectra is iteratively correlated with the Brune's displacement spectra, $D(f,R) = \dfrac{\pi_o G(R,d)\exp(\frac{-\pi ft}{Q_s})\exp(-\pi\kappa f)}{\left[1+\left(\frac{f}{f_c}\right)^{\gamma}\right]}$ within 0.1 to 20 Hz, until the best possible minimum value of the objective function is achieved by a grid search method. To identify the best solution, L2 norm of the log difference between observed and modeled spectra was used as an objective function. Here, $\dfrac{\pi_o}{\left[1+\left(\frac{f}{f_c}\right)^{\gamma}\right]}$ and $G(R,d)\exp(\frac{-\pi ft}{Q_s})\exp(-\pi\kappa f)$ represent the source and path terms, respectively. The derived spectral parameters are then used to calculate seismic moment, stress drop and radius of rupture using Brune's (1970) equations for circular model. The moment magnitude (M_W) was calculated using Kanamori (1977), and Hanks and Kanamori (1979) relation, M_W= 2/3 log (M_o) - 10.7. The spectral fit between the observed and Brune's displacement spectra at two seismic stations (CHA of Kachchh and UNA of Saurashtra) is shown in figure 3.14.

The moment tensor inversion performed in the present study is based on the extended Kikuchi and Kanamori (1991) technique for the regional and local data. The modified technique is based on the full wavefield analysis using discrete wavenumber method of Bouchon (1981) and Coutant (1989). This technique of iterative deconvolution for both single and multiple point sources (Kikuchi and Kanamori, 1991) is called as ISOLA (Isolated Asperities) (Sokos and Zahradnik, 2008). In the present study, a good waveform match between observed and synthetic displacement seismograms has been obtained for all the studied earthquakes. The waveform match for an event is shown in figure 3.15.

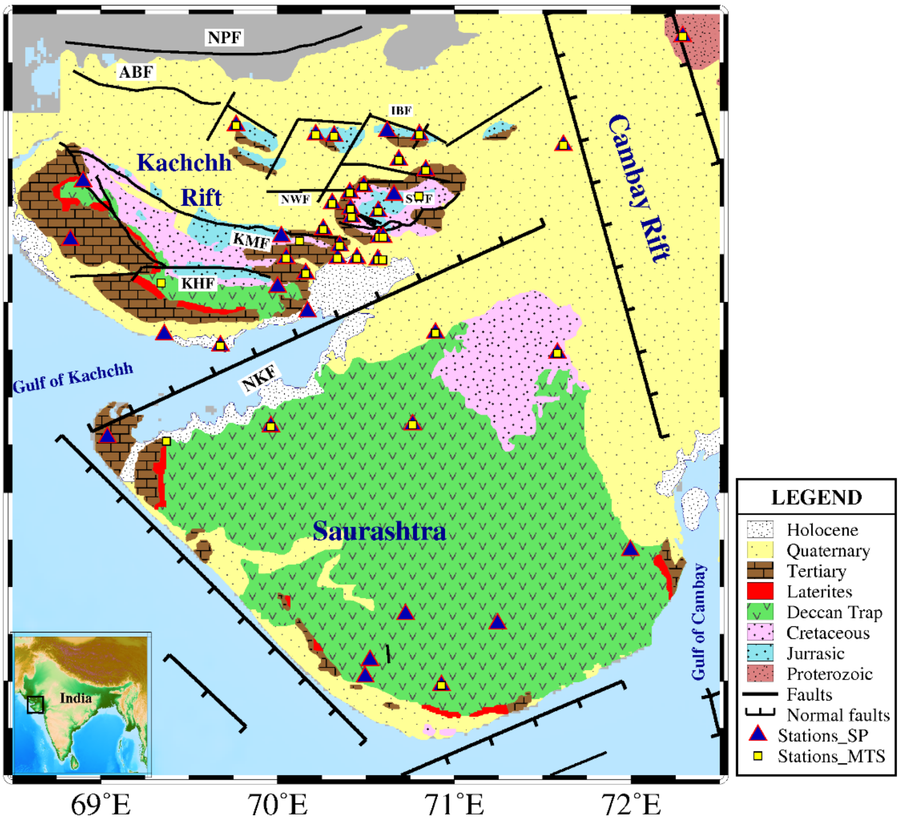

Figure 3.13: Distribution of ISR broadband seismic stations used in source characteristics analysis of earthquakes recorded in Kachchh region of northwestern Deccan Volcanic Province.

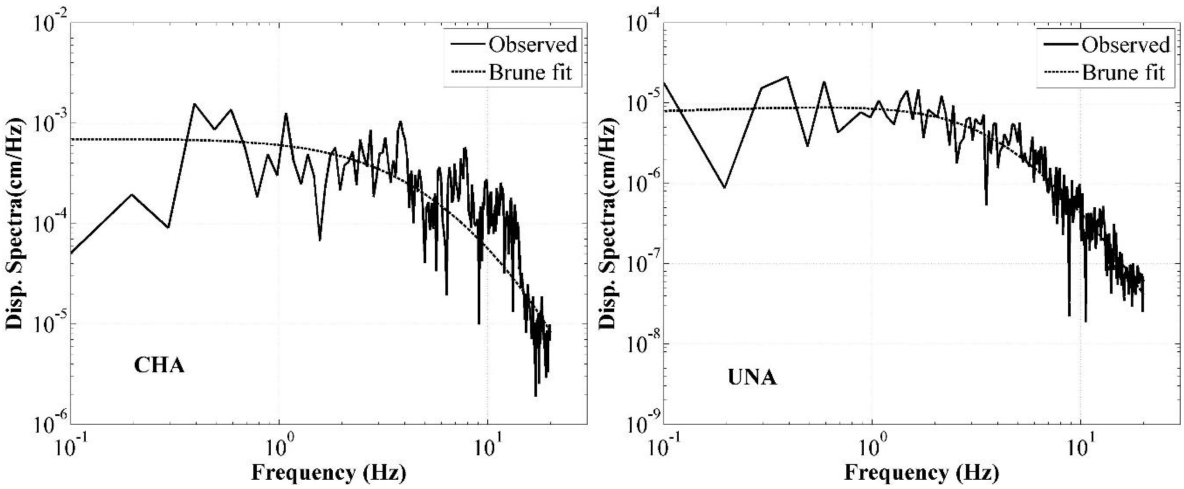

Figure 3.14: The S_H-wave spectral fit between observed and Brune's (1970) spectra for an event in Kachchh recorded by different seismic stations of ISR.

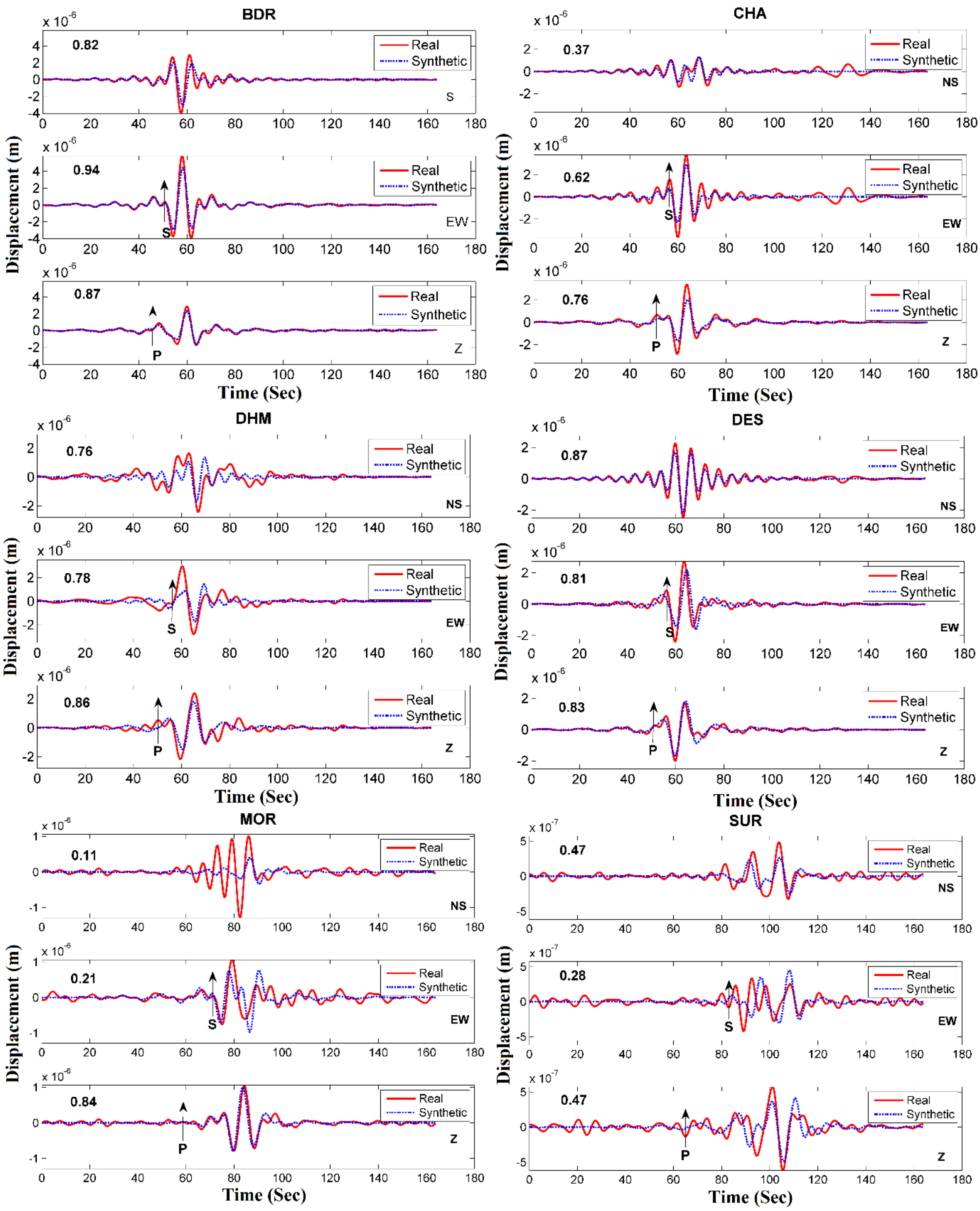

Figure 3.15: Waveform match between the observed (red) and synthetic (blue) filtered displacement seismograms at different stations of ISR.

3.16 Seismic evidence for décollement plane beneath the Arunachal Himalaya

(A. P. Singh)

We obtained a high resolution 3-D velocity structure of the Arunachal Himalaya by inverting a large number of high quality arrival times. We applied the 3-D tomographic inversion method of Koulakov (2009) and Koulakov et al. (2010) to 11,860 P- waves and 10,323 S- wave arrivals from 1492 earthquakes. It is an iterative algorithm for simultaneous inversion of P- and S-arrival times from local and regional events resulting in three dimensional distributions of P- and S- wave velocity and source coordinates. We parameterized the subsurface using a grid of nodes distributed in the study volume, according to the ray density, using an algorithm described by Koulakov et al. (2006). For improving the results of local earthquake tomography, we used some events out of the network. The crustal seismic velocities and physical properties reveal a large difference in the upper and lowermost portions beneath the Arunachal Himalaya. Significant increase of the seismic velocity at around 20 km is interpreted as a décollement plane in this area. The Eastern Himalayan Syntaxis is imaged as a low velocity down to a depth of 40 km where great Himalayan and the Indo-Burmese Arc meet.

3.17 3-D seismic structure beneath the Shillong Plateau area of Northeast India

(A. P. Singh, O. P. Mishra)

The north east India is bounded by the Himalayan arc to the north and the Burmese arc to the east. The Shillong Plateau and Assam Valley lie at the boundary zone of the two arcs. Microearthquake surveys were conducted in this area from 2009 to 2013. We have applied a tomographic method to about 7370 high quality P- and S-wave arrival times from 363 local earthquakes in the magnitude range 2.0 to 4.0 recorded by 11 temporary seismic stations, to determine the 3 D seismic structure of the crust and upper mantle in this region (Fig. 3.16). The results reveal significant lateral heterogeneities in the study area. The high velocity zones in the uppermost crust act as a geometric asperity where interseismic strain and stress-build up. The low velocity zone in the lower crust could have played a major role in accommodating stress and caused the great earthquake (Fig. 3.17). The tomographic images obtained in this study are compatible with the major tectonic features such as active faults and seismic trends.

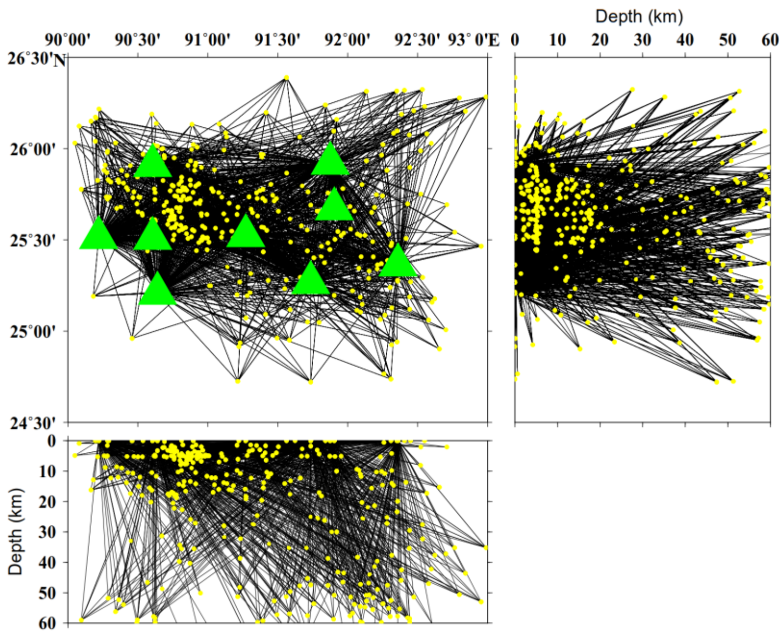

Figure 3.16: The spatial distribution of seismic ray of 363 from the earthquake is shown in the lateral and vertical directions. Every path between an epicentral and a station is drawn as one straight line. Green triangles show seismic stations that recorded the arrival times

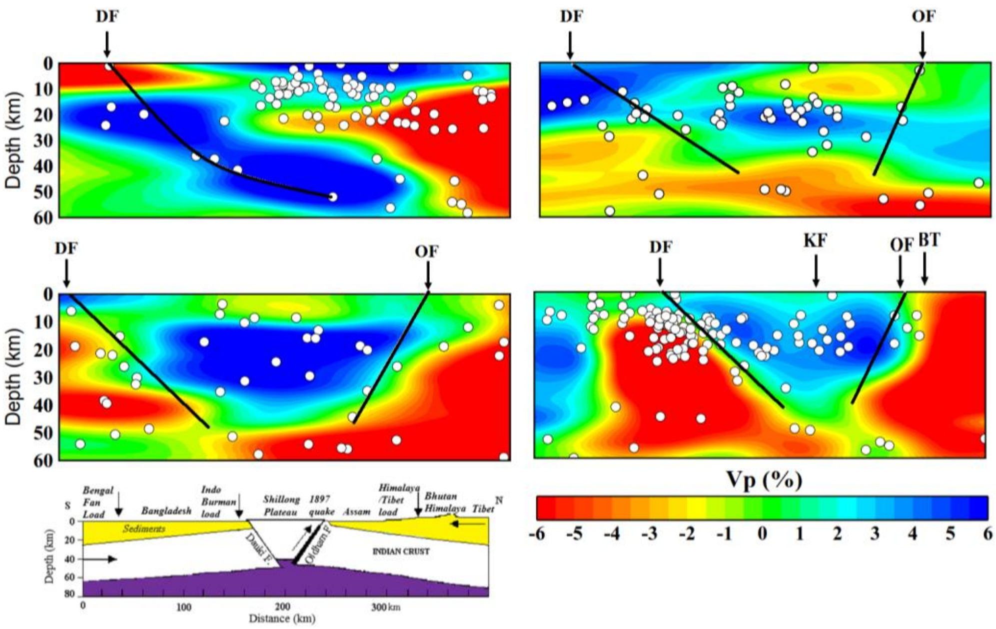

Figure 3.17: N-S and E- W Vertical cross sections of P- wave velocity models The geological faults are also marked. The lower figures show the pop-up tectonic model of the Shillong Plateau (After Bilham and England, 2001).

3.18 Estimation of shear wave velocity contrast ($\delta\beta_M$) across the Moho in Gujarat Region

(C. Haldar, P.Kumar and M.Ravi Kumar)

$\delta\beta_M$ across the Moho beneath Gujarat varies from 0.19 to 0.97 km/s (Figure 3.18). This large variation suggests that the lower crust in this region experienced a large gradation in the Moho, which implies that the crust mantle boundary does not evolve in an identical condition in the geological past. $\delta\beta_M$ for Kachh rift varies from ~0.45 to 0.67 km/s; ~0.19 to 0.41 km/s for Saurashtra and ~0.25 to 0.54 km/s for Gujarat Mainland (Figure 3.18).

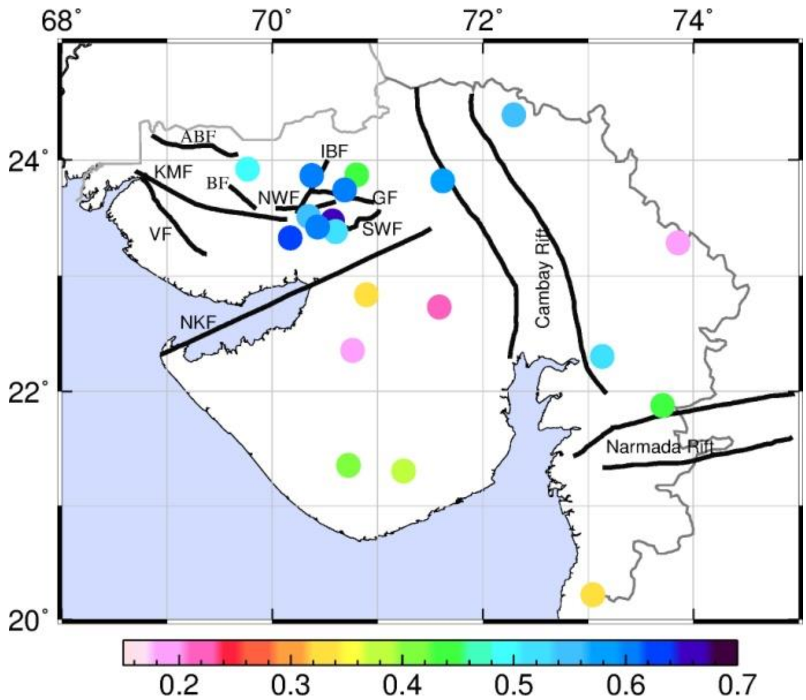

Figure 3.18: $\delta\beta_M$ map across Gujarat Moho. Color scale indicates δβM (km/s) variation

3.19 Seismic evidence for secular evolution and alteration of Archaean crust in the Indian shield

(C.Haldar, P.Kumar, M.Ravi Kumar, L.Ray and D.Srinagesh)

The mechanisms through which the Archaean continental crust evolved are debatable. The end member models advocate horizontal accretion of island arcs or vertical accretion due to differentiation of magmatic material above hotspots. Whether both the processes operated together or separately is hard to ascertain. Also, there is no consensus on the processes that govern secular change in the character of the crust in Archean, as revealed by the seismological and petrological data. In order to address these key issues, we use converted wave data to extract the bulk crustal properties of the Indian cartons. Our analysis dominated by data from the Dharwar craton, reveals that most of the crust is formed in the early Archean. Soon after its formation, it gradually altered, making it mafic-to-intermediate in bulk composition. Further, the present day heat-flow values, which are higher in late-Archaean compared to the early, correspond to regions of thinner crust, implying that the crustal formation prevails at much higher temperatures predominantly through vertical accretion initially and then by slab melting. This suggests that some form of plate tectonics was in operation even in the Archean time. However, in the later stage, horizontal accretion dominantly contributes to crustal evolution. During this stage, large part of the lower crust seems to be degenerated making it thin and intermediate in composition. The age and bulk crustal thickness of the Indian shield derived from receiver function studies are anti-correlated. Our observation reveals that most of the crust is formed in the early Archean and subsequently altered, making it more evolved in composition. The present day higher heat-flow values correspond to regions of thinner Achaean crust. The crust was initially accreted dominantly by vertical accretion mechanism and then shifted to horizontal process.

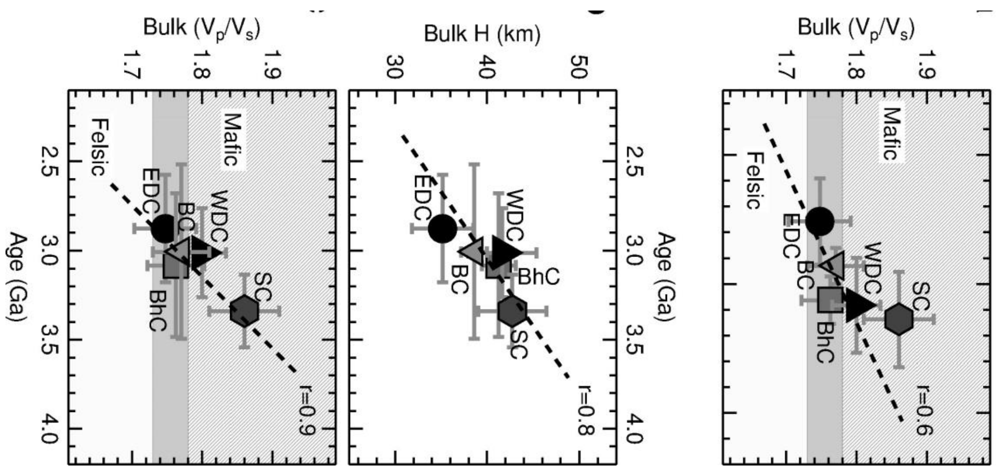

Figure 3.19: Clustering and temporal distribution of bulk crustal properties for the Indian cratons. All the available parameters for the single cratons are averaged out with the error bar as shown by the bar lines. a) variation of bulk crustal thickness with respect to bulk Vp/Vs, and b) temporal variation of crustal thickness and Vp/Vs respectively. The labeling inside the subplots are the abbreviations for the cratons, e.g., EDC: Esatern Dharwar craton, WDC: Western Dharwar craton, BC: Bastar craton, SC: Singhbhum craton and BhC: Bundelkhand craton. The dashed line represent the best fit regression line with regression coefficient of r.

3.20 Estimating the thickness of the crust of Gujarat using PmP phases

(Himangshu Paul)

The Moho undergoes a large impedance contrast between the lower crust and the upper mantle. Owing to this fact, the travel time of Moho reflected phases like PmP can give a good estimate of the thickness of the crust. However, PmP phases are not easily identified on a seismogram. We, therefore, calculated theoretical travel time of PmP phase using an average velocity model of Gujarat and then search for the observed phase in the vicinity of the predicted pick. The phases being emergent were still unrecognizable in most of the seismograms. Therefore, another methodology is being adopted in which P-amplitude-normalized seismograms are stacked to visualize the PmP phase clearly. For this, a larger dataset is prepared. An even distribution of events is made by dividing the catalog into bins of narrow range of latitude, longitude, depth and magnitude and then by selecting the largest earthquake from each bin. In total, 2880 events were selected with an average of 13 stations per event.

3.21 A review on the role of mantle convection in geoid anomalies

(Himanshu Paul)

Geoid is an equipotential surface coinciding with the mean-sea level of the earth. In a rigid earth, presence of local excess of mass in a region warp the geoid upward resulting in a geoid high while local deficit of mass leads to a geoid low. However, geoid anomalies are also dependent on the dynamics of the mantle when the latter is taken into account. Density anomaly in the interior of the earth (mantle) owing to temperature perturbation gives rise to a convective current. Convection deforms boundaries like the upper surface of crust, transition zones, the core-mantle boundary etc. They are pushed upward over rising current and pulled downward over sinking current. This deformation of the boundaries (especially the upper surface) has a major effect on the geoid. In case of a negative density anomaly (high temperature, low density then ambient), boundaries are pushed upwards. Positive contribution to the geoid due to the rise of the upper surface is counteracted by negative contribution from the low density anomaly. The residual of these two effects is the resultant geoid. Similar observations are also made in case of positive density anomaly. It is seen that for a uniform mantle viscosity, the geoid due to boundary deformation is larger compared to that due to the density anomaly itself, resulting in a net negative geoid corresponding to positive density anomalies and vice-versa. Therefore, the role of mantle dynamics must be considered in any interpretation of long-wavelength geoid anomalies.

4 Earthquake Precursory Research

4.1 Preliminary results of magnetic pulsations during the storm occurred on 8th Jan 2015

(Prasanna Simha and K M Rao)

In this study, we considered a magnetic storm which occurred on 08th Jan 2015. We have taken magnetic data of three days covering one day before and one day after the storm in order to see various geomagnetic signatures in the ULF range. The signal is found to vary in the range -3.0-2.5; -0.5-1.5 and -0.5-1.5nT for Bx, By and Bz. Because of various influence of ULF and ELF signals, the salient features have been traced by applying the fast Fourier transformations. The spectral variations are derived from the above three days of data. Figure 4.1 represent the frequency variation of the data during the storm time regime.

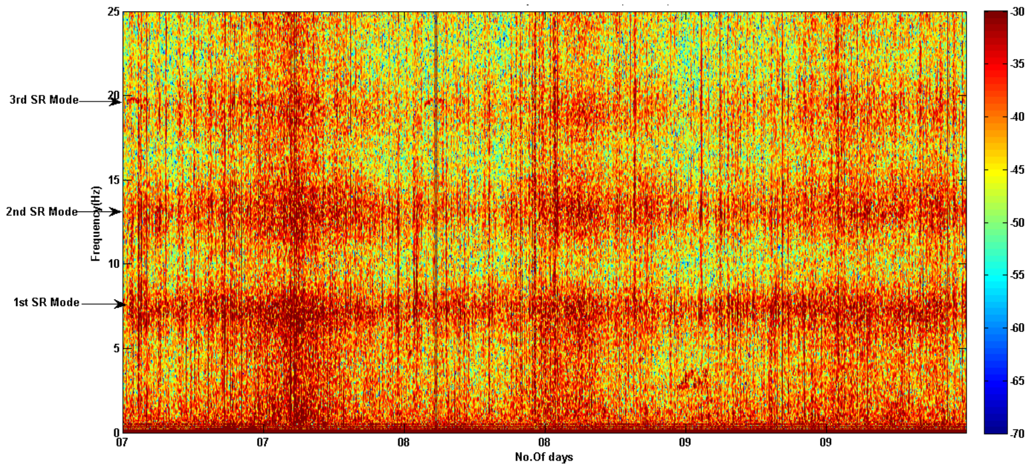

Figure 4.1: Spectral Variations of N-S component of LEMI over the three days.

The clear indication of 1st and 2nd mode of Schumann resonance has been observed during the three days. The spectral variations of N-S component after applying the bilinear transformations is shown in figure 4.2. The patch where the wavelet type of distribution has been observed, shows the pulsation continuous and sudden rise and fall of the amplitudes are pulsation irregular (Figure 4.2).

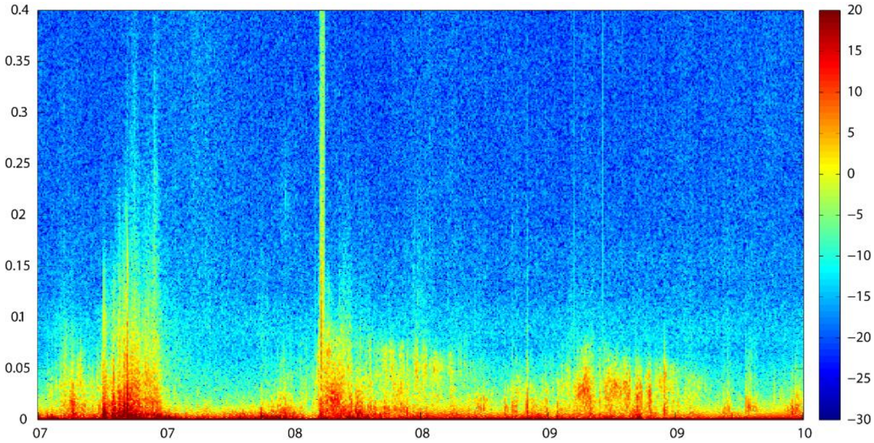

Figure 4.2: Hourly Variations of N-S Spectra variations during 07-09 Jan 2015.

4.2 Empirical Mode Decomposition based Hilbert Huang Transform on Soil Radon (Rn^{222}) data of Kutch, Gujarat, India: Identification of daily quasi-periodic oscillations and Earthquake precursors

(Sushant Kumar Sahoo and K M Rao)

The soil radon concentration has been monitored continuously at the Desalpar station of Kachchh, Gujarat by using the SARAD (RTM2100) instrument for identification of daily and quasi periodic oscillations and earthquake precursors. Data from 29th September, 2011 to 29th November, 2011 are selected for this analysis. The recorded data of the monitoring station exhibits periodicity due to the impact of the other soil parameters like temperature, pressure and humidity. Empirical mode decomposition method has been applied to the soil Radon (Rn^{222}) time series to identify and extract the periodicities into different oscillatory modes, known as the intrinsic mode function (IMF). We compared the harmonic periods of radon with other meteorological parameters in order to separate the physically significant IMFs. These physically significant IMFs which are not having any periodic oscillations are considered as input for the Hilbert Huang Transform (HHT). The distribution of the Instantaneous Energy with respect to time has been correlated with the seismic activities during the study period. Fig. 4.3 depicts the raw data of the Radon, pressure, temperature and humidity at Desalpar station.

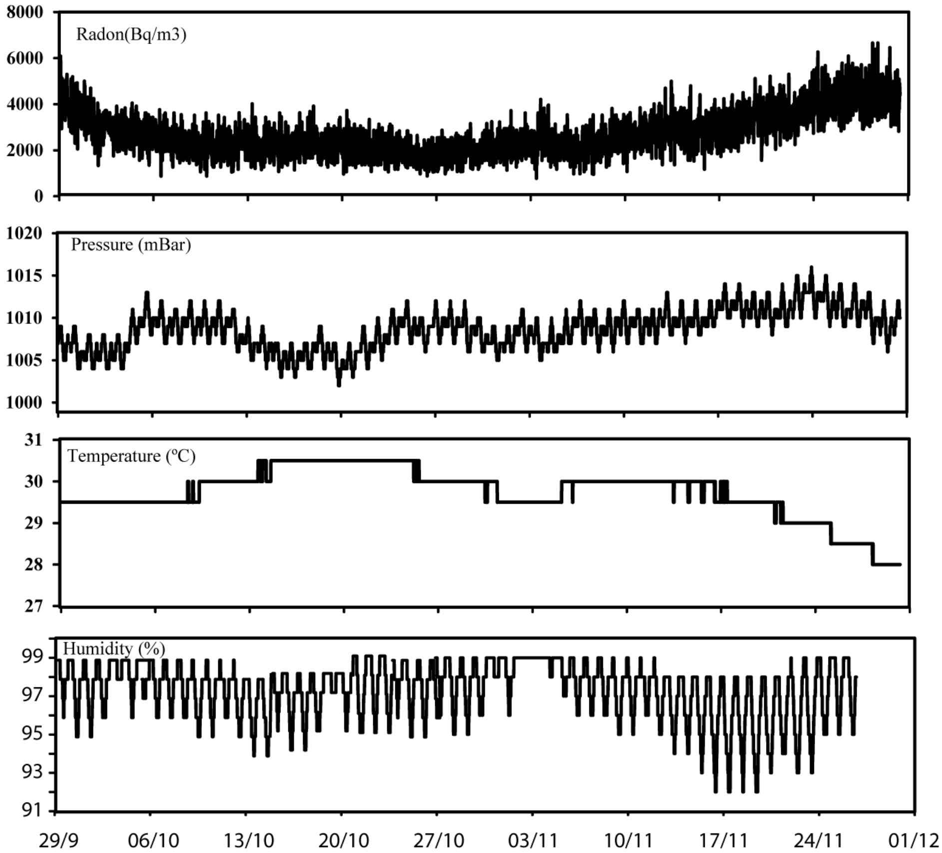

Figure 4.3: Raw data plot of Radon, Pressure, Temperature and Humidity at Desalpar

The oscillatory modes in the Radon and other parameters are identified by the periodograms obtained from the Fast Fourier Transform (FFT). It is a basic requirement towards the selection of the significant intrinsic mode functions, obtained from the empirical Mode Decomposition method, for further analysis. The FFT periodograms of the soil radon (Rn^{222}), soil pressure and temperature at Desalpar (Fig. 4.4) depicts three harmonic modes with periods 23.04, 72.3 and 167.8 hours. The soil pressure shows a harmonic mode with a period of 23.97 hours and the soil temperature shows a period of 24.38 hours. From this analysis, it can be observed that many harmonic modes of the soil radon time series coincide with the harmonic periods of the other soil parameters and this similarity provides a clear indication of the influence of the soil parameters towards the soil radon emission. Therefore, it is necessary to remove these effects from the soil radon data before further analysis.

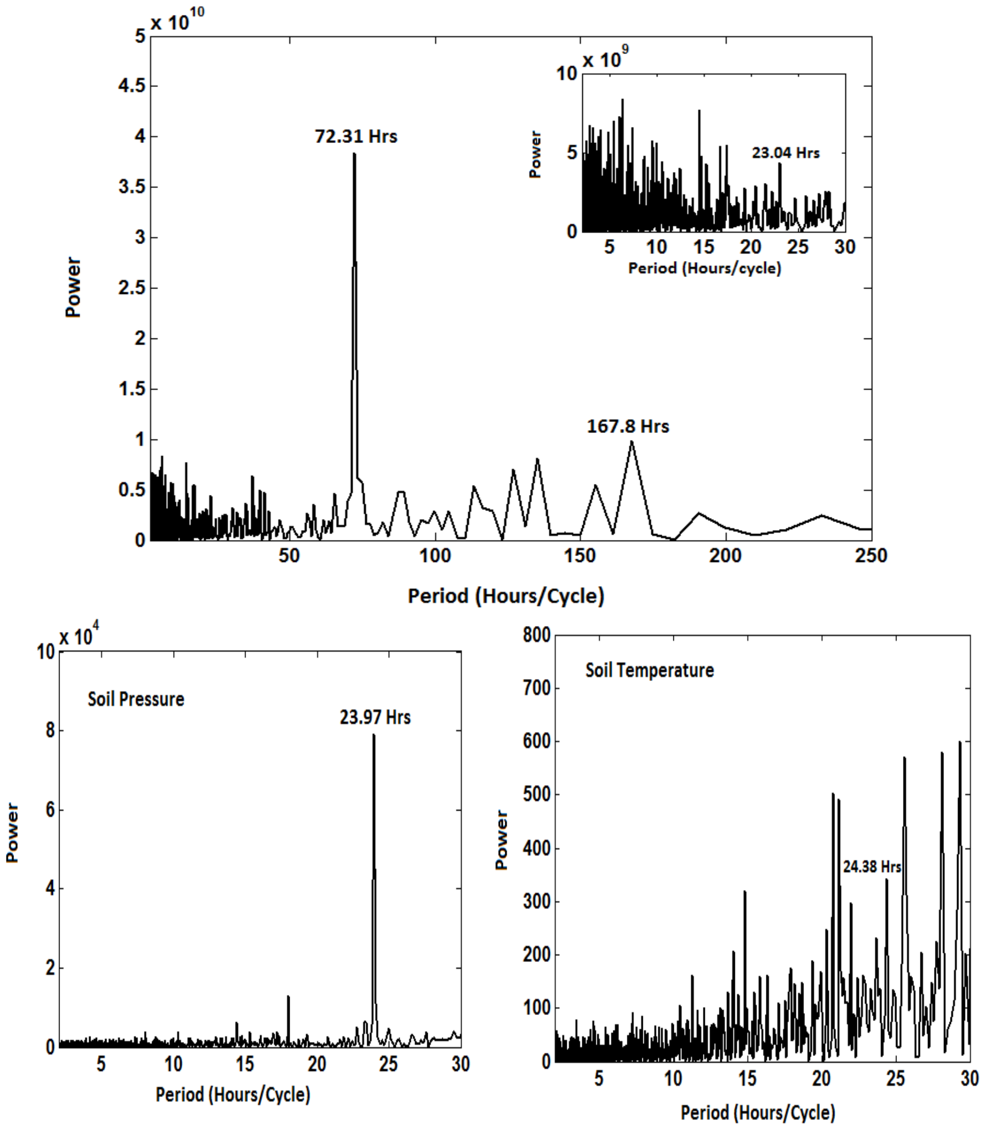

Figure 4.4: FFT periodograms of Radon, Soil Pressure and Temperature at Desalpar

Fig. 4.5 shows the empirical mode decomposition of the soil radon time series. The soil radon gets decomposed into 11 intrinsic mode functions. During the process of the decomposition, due to the interpolation of the cubic spline in the local extrema, there may be chances of the occurrence of swings. In the successive iteration process, it can propagate inside to form pseudo-IMFs. Therefore, cross correlation between the extracted IMFs and the corresponding measured soil radon (Rn^{222}) has been conducted in order to detect those pseudo-IMFs. The Intrinsic mode functions having correlation coefficient more than 0.1 have been considered as significant and selected for further analysis. As per the process of decomposition, each intrinsic mode function obtained through EMD is having a specific oscillatory period. Therefore, those harmonic periods are determined by calculating the periodicities of all the significant IMFs by the process of Fast Fourier Transform (FFT). Table D1 depicts the harmonic periods of the IMFs for Desalpar.

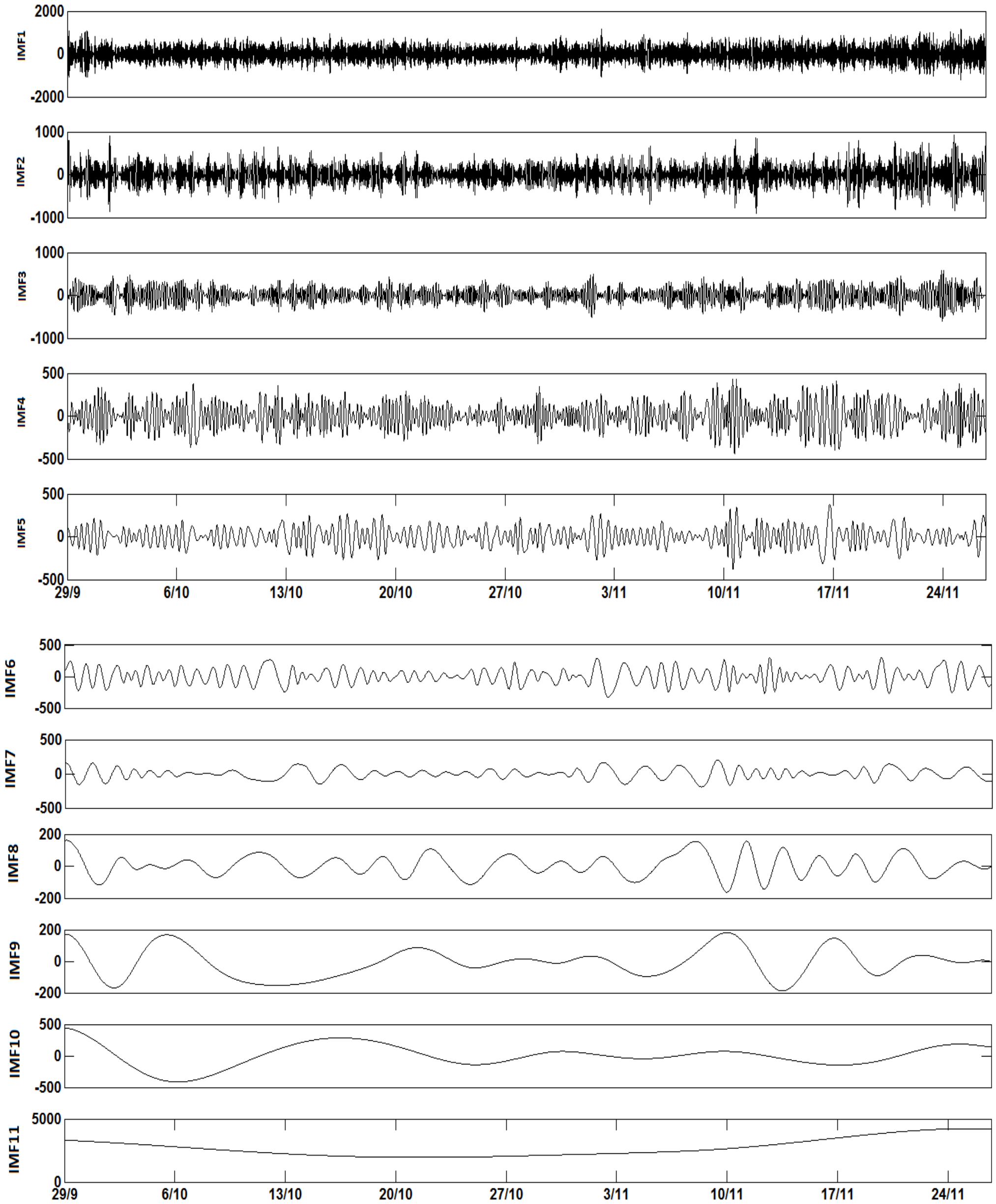

Figure 4.5: Empirical Mode Decompositions of Soil radon (Rn^{222}) at Desalpar

Table 4.1: Harmonic modes obtained for the IMFs at Desalpar

IMF No	1	2	3	4	5	6	7	8	9	10	11
Harmonic Period	2.81 Hrs	7.43 Hrs	12.48 Hrs	17.4 Hrs	1 day	3 days	6.98 days	9.73 days	29.46 days	58.78 days	176.24 days

The first four IMFs show the harmonic modes with periods of 2.81, 7.23, 12.48 and 17.4 Hours and are regarded as instrumental noise. Again, the harmonic mode of the fifth IMF gets coincided with that of the diurnal variation. Hence it is discarded. The 9th and 10th IMFs are having the harmonic modes of periods of 29.46 and 58.78 days respectively. These values are of the multiples of 15 and therefore these are regarded as the tidal periodicities and are discarded. The 11th IMF is having harmonic mode of high periodicity of 176.24 days. This is nothing but the trend of the data and therefore, this is also discarded. Finally, we arrived at a conclusion that the 6^{th}, $7^{th}$and 8^{th} IMF are significant and taken for the further analysis.

Figure 4.6 show the unwrapped phases of the IMFs for Desalpar station. From this figure, it is observed that the phases are getting decreased with the decreasing order of the IMFs. Due to the variation of the instantaneous frequencies as shown in the figure, it can be confirmed that the Hilbert Huang transform can detect the non stationarity in the soil radon (Rn^{222}) datasets. To avoid the arrival of spurious harmonics and see the true representation of the time-energy-frequency distribution, Hilbert-Huang Transform are determined for physically significant IMFs of the Soil Radon (Rn^{222}) as shown in fig. 4.7.

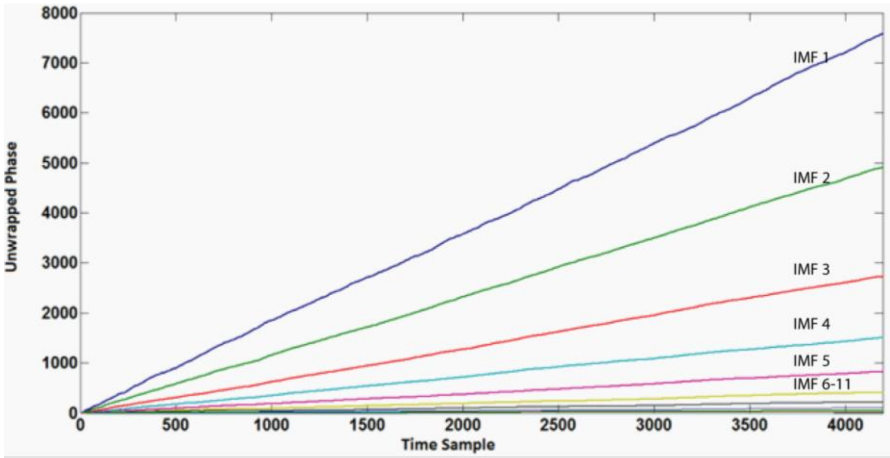

Figure 4.6: Unwrapped phases of IMFs at Desalpar

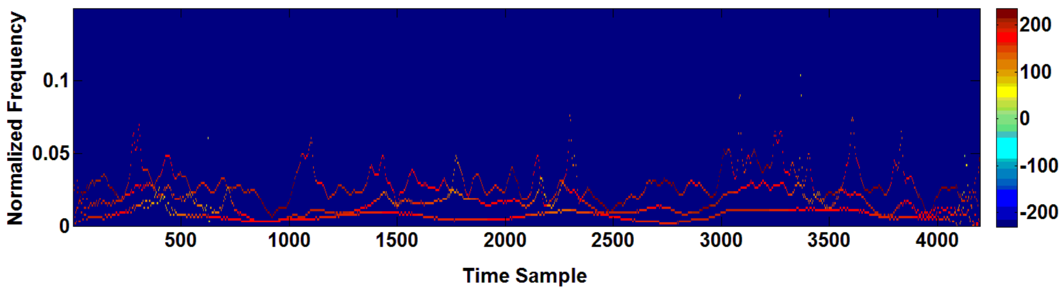

Figure 4.7: HHT spectrum of soil radon data of Desalpar

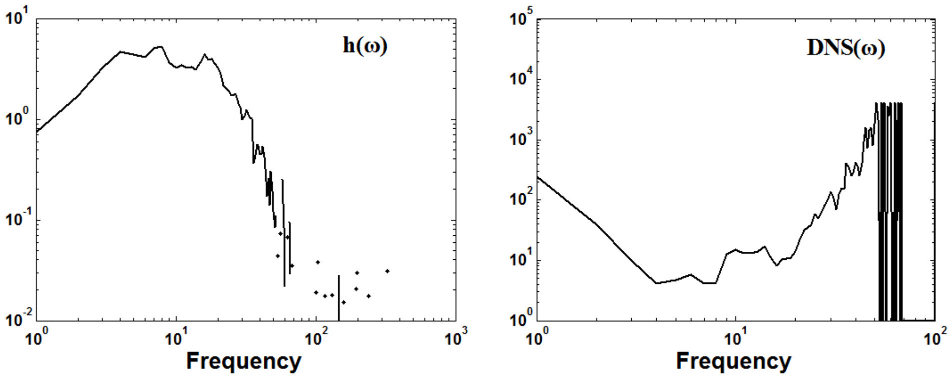

Figure 4.8: (a) The mean marginal spectrum and (b) The Degree of non-stationary spectrum at Desalpar

The mean marginal spectrum and DNS spectrum obtained from the Hilbert Huang spectrum are shown as fig. 4.8. From this figure, it can be observed that the marginal spectrum shows higher fluctuation in the high frequency range (> 20 Hz). The frequency components of more than 20 Hz are found to be non-stationary leading to the conclusion that the intermittency increases with increase in frequency.

The Instantaneous energy IE(t), which provides the distribution of energy with respect to time, has been correlated with the local earthquakes during the study period (Fig. 4.9).

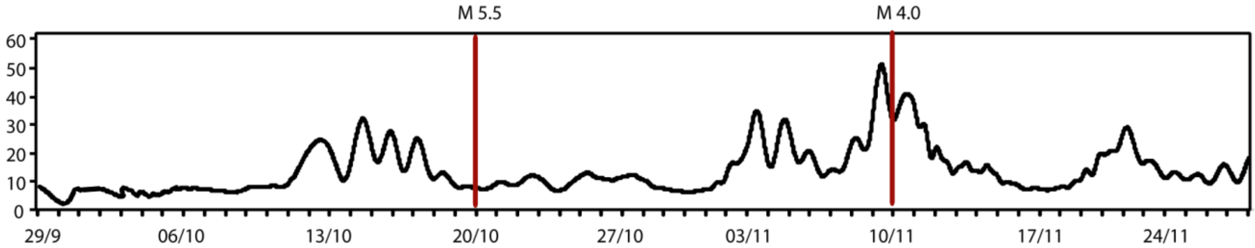

Figure 4.9: Instantaneous Energy of Desalpar

There were two moderate earthquakes of magnitudes 5.5 and 4.0 on 20th October and 10th November 2011 respectively, within an epicentral distance of 400 km from the Desalpar observatory. From this figure, it can be seen that the energy gets enhanced during 13-19 of October, before the moderate event on 20th October (M 5.5) and the energy gets enhanced during 8-10 of November (M 4.0) before the event of 10th Nov 2011.

4.3 Application of the Artificial Neural Network (ANN) on the Soil Radon (Rn^{222}) time series for identifying Earthquake Precursors in Kutch, Gujarat

(Sushant Kumar Sahoo and K M Rao)

Artificial Neural Network (ANN) method has been applied to the soil Radon time series at Desalpar station of Kachchh region in order to identify the earthquake precursors. Among the different types of the neural network configurations, the Multi-layer perceptron (MLP) feed forward method has been chosen for the soil radon data analysis. Pressure, Temperature and Humidity are taken as the inputs whereas the Soil Radon as the output. Error back algorithm has been applied for the processing of the MLP. 4195 datasets are considered for the analysis which are divided into two parts, i.e., training (70%) and test (30%). Complex computation has been conducted by the hidden layers by extracting the valid features from the input layers. 16 hidden layers are obtained in our analysis. The measured radon concentration and the radon time series predicted by the application of ANN are shown in Fig. 4.10. The trend of both the measured and predicted radon are similar, with a correlation coefficient of 0.669, but the fluctuation of the time series is much more reduced in the predicted radon. The predicted radon can be considered for identifying the precursors.

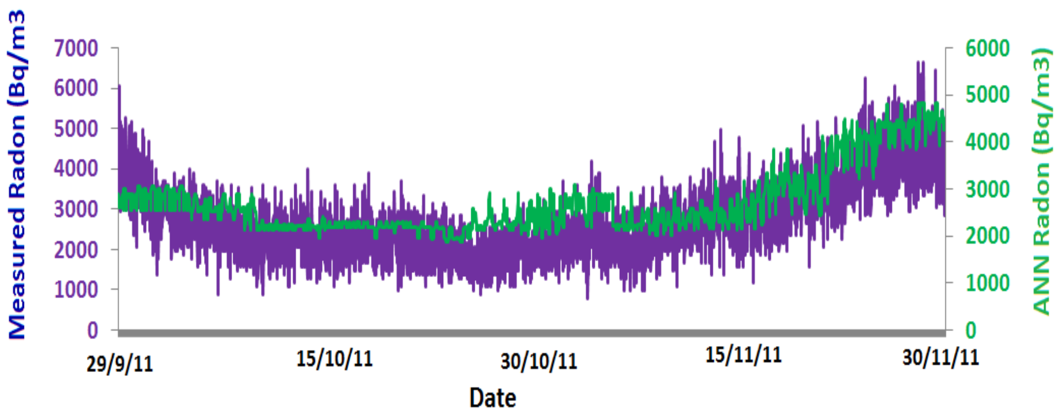

Figure 4.10: Measured radon concentration at Desalpar and the radon time series predicted by ANN.

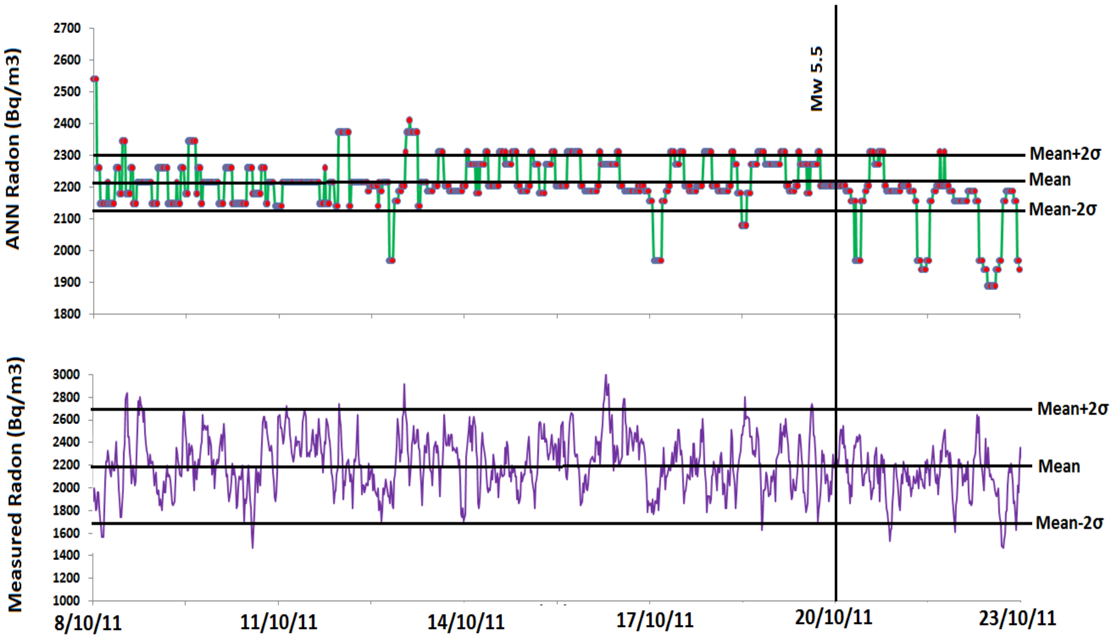

Figure 4.11: Predicted radon time series and Measured radon concentration with ±2 standard deviation.

We have selected two earthquakes of magnitudes 5.5 and 4.0, that occurred on 20th October and 10th November 2011, respectively that come well within the earthquake preparatory zone. Fig. 4.11 depicts the measured radon and predicted radon during the period of investigation. A total of 5 radon peaks were observed in both predicted and measured radon time series which are crossing the ±2 standard deviation. Amongst these radon peaks, there are two peaks of radon concentration which crossed ±2SD on 13th and 16th October in both the time series, might be related to the 20th October event (M 5.5).

4.4 Spatial and temporal behaviour of Ionospheric VTEC during the shallow earthquake of New Zealand (M 7.8) occurred on 13th November 2016

(C.P.Simha, K.M.Rao and R.K.Dumka)

We report the results of the Ionospheric VTEC during October 01 to December 31, 2016, to see the anomalous changes during the New Zealand earthquake of M 7.8, that occurred on 13th Nov 2016. The data of 25 IGS stations are used for this analysis (Fig. 4.12). These IGS stations cover both the near and far distance from the epicenter of the earthquake, where we can expect significant ionospheric variations in association with this shallow significant earthquake. Results of our study in terms of the global planetary index, Dst, Solar Irradiance and AL reveal signatures of small magnetic activity during October 01-November 05, 2016. We considered the data of the period November 6-20, 2016, which covers the duration of 7 days before and after the earthquake to study the pre and post seismogenic effects.

Spatial TEC maps have been generated from the 25 IGS stations for every half an hour using Kriging interpolations to see the spatial variations of VTEC during the event. The clear enhancement of the signal has been noticed just few hours before the event. The TEC values have increased to 37 TECU within the non EIA zone which give the scope of existence of some ionospheric precursory anomaly which is rapidly varying just before few hours of the event. We plotted the diurnal variations in TEC along various longitudes during the disturbed and quiet period (Fig. 4.13).

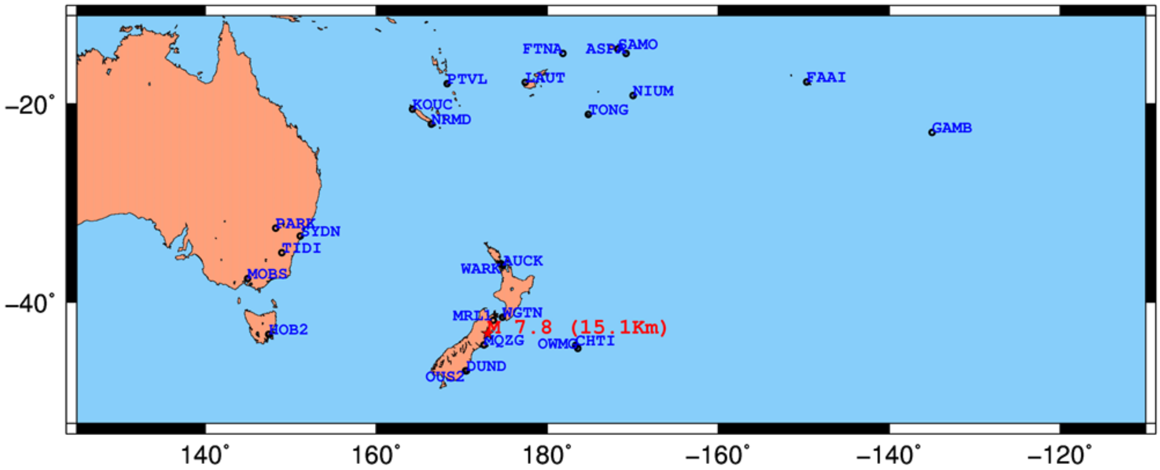

Figure 4.12: Location of the earthquake occurred on 13th November 2016 and the IGS stations

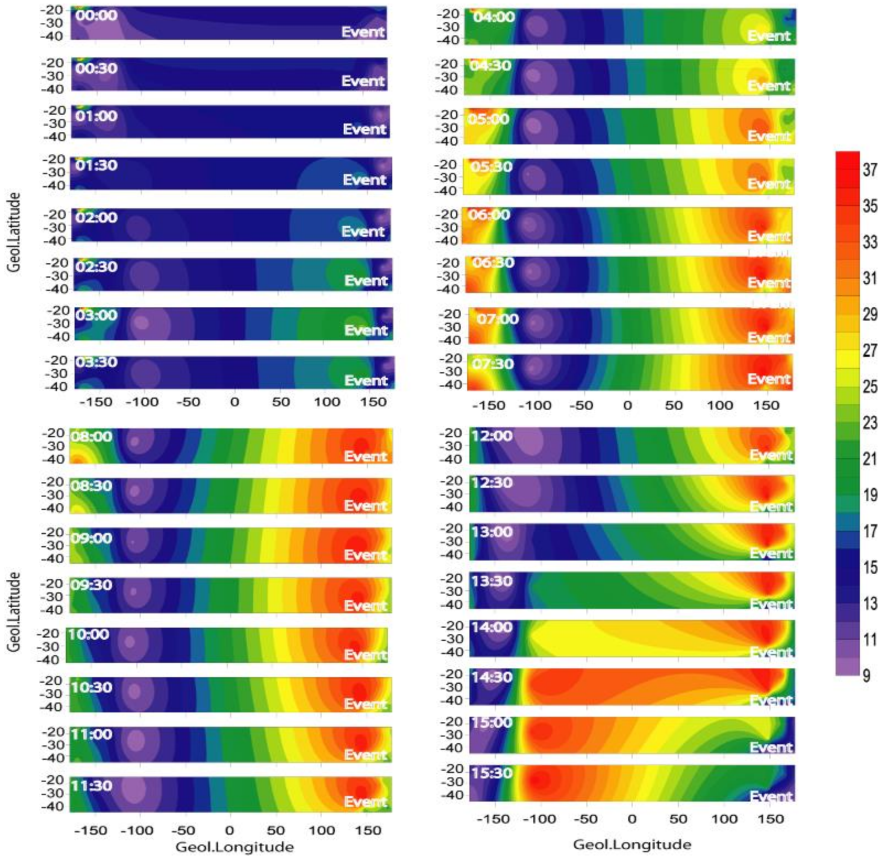

Figure 4.13: Spatial variations of VTEC observed in GPS stations located near the New Zealand earthquake epicenter.

The diurnal variations of GPS-TEC during Nov 12-14, 2017 are considered as seismically active period and Nov 6-8, 2017 is considered as Geomagnetically quiet period (Fig. 4.14). We can clearly observe the enhancement of signal in the stations near the epicenter and see the negative anomalies with the far stations. Moreover, we also can infer that the variations in VTEC are minimal during the quiet period than seismically disturbed days. Spatial variation of VTEC is observed to be enhanced at nearest stations than far stations. In order to see the temporal variations of VTEC, we determined Upper Bound (UB) and Lower Bound (LB) of VTEC time series. We observed more enhancement of LB over the observed VTEC at the nearest stations than far stations.

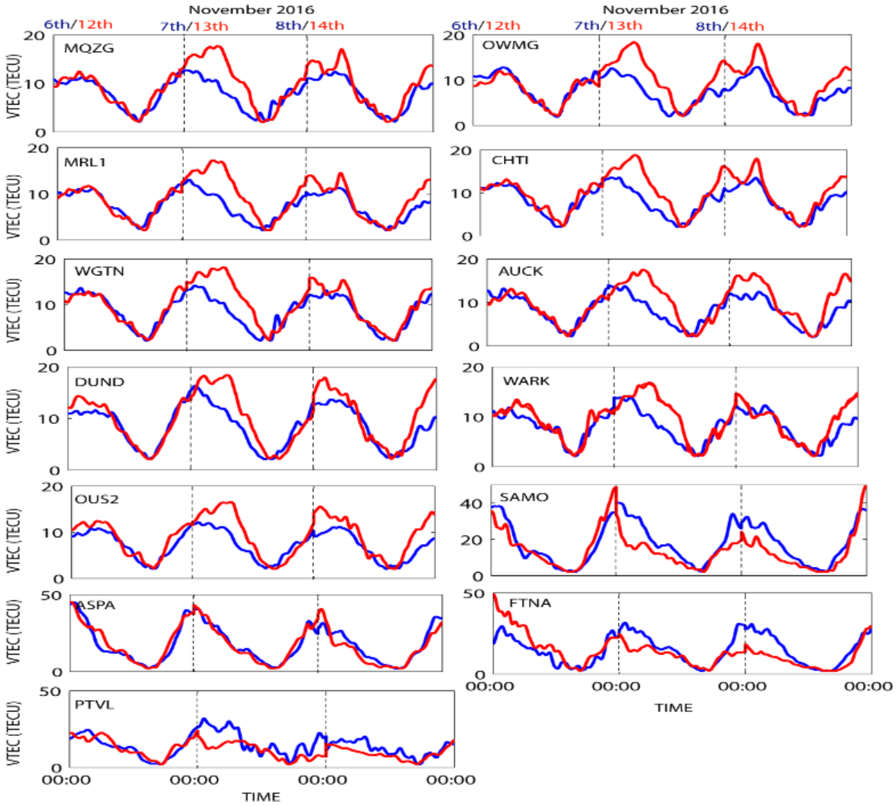

Figure 4.14: The diurnal variations of GPS-TEC with respect to the event regime. The blue curves are the quiet time mean variations of TEC and red curves represent the seismic time mean variations of TEC

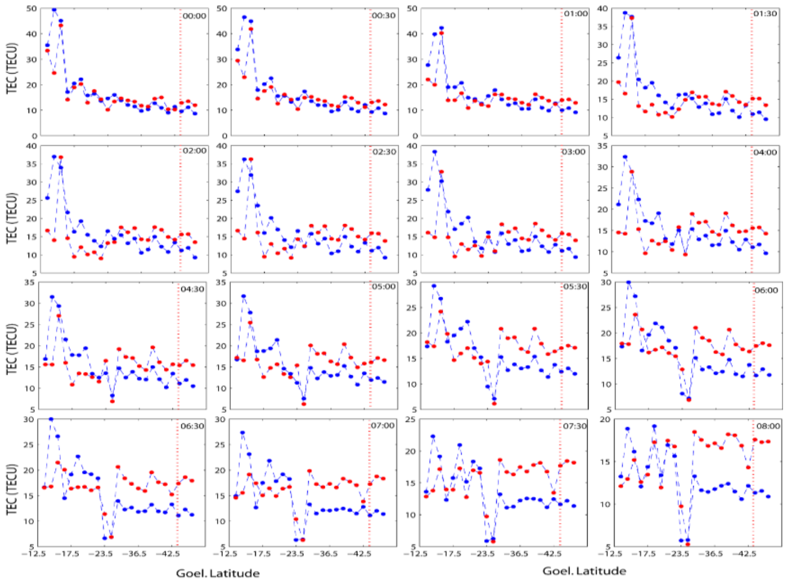

Figure 4.15: Latitudinal variations of VTEC at each 30 min interval from 00:00 to 15:30 UT on 13th Nov 2017 (red) and 12th Nov 2017 (blue) over the epicentral region of the New Zealand event.

Dynamic spectra and temporal variations at different frequency bands show a strong band at 22 to 30 mHz, which may indicate the rise of 5th Schumann resonance band before the event time. Latitudinal variations of VTEC at each 30 min interval from 00:00 to 15:30 UT on 13th Nov 2017 and 12th Nov 2017 from -12.5 to 44.5^0 latitudes over the epicenter of New Zealand event are compared (Fig. 4.15), which clearly indicate the enhancement of the TEC signal just before the earthquake. The TEC values seem to be normal during 00:00 to 04:30 hrs and later show an increasing trend. The TEC is found to reach the maximum value around 08:30 UT onwards till earthquake time (11:03 UT).

4.5 The effect of geomagnetic storms on the magnetic field observed at four Indian stations

(Shivam Joshi and K.M.Rao)

The main focus of the present study is to examine the influence of solar wind parameters (density and pressure) on the magnetic field measurements at low latitude magnetic stations of India. Here we have studied two severe geomagnetic storms, that occurred during the solar activity period of current solar cycle-24 (Year 2015). The first storm was during March 17-18, 2015 (Dst= -223nT), the most intense geomagnetic storm (G4) of the current solar cycle and the other storm was during June 22-23, 2015 (Dst= -204 nT). The data of four complete days (96 hours) are considered, which in general, comprise SSC, initial, main and recovery phase. Analysis of coherence between the solar wind and IMF Bz on the H-field of the magnetic field recorded by the Digital fluxgate magnetometers at Four Indian Magnetic Observatories (Jaipur (IIG), Desalpar (ISR), Alibag (IIG) and Hyderabad (NGRI), reveal their direct impact at low latitudes. The solar wind Pressure, Density and IMF Bz are found to be more influencing parameters during the storm since they have a coherence >0.6. The correlation of solar wind velocity with total magnetic field is found to be 0.79 during the June 2015 storm. Dynamic spectra (Fig. 4.16) are prepared using the magnetic field recorded at different Indian magnetic stations and satellite derived solar wind and IMF parameters.

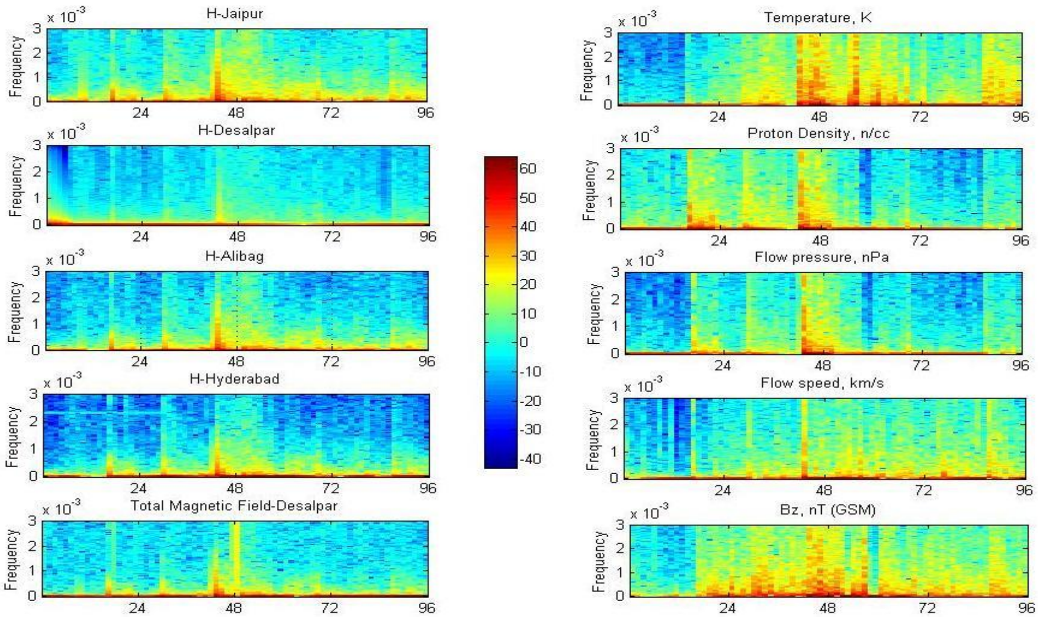

Figure 4.16: Dynamic spectra of the June 2015 storm

4.6 ULF magnetic field variations before a moderate Earthquake (M 4.0) in Kachchh, Gujarat, India

(M.S.B.S.Prasad, Sushant Kumar Sahoo and K.M.Rao)

In this work, we carried out the study of power spectral density, polarisation ratio and fractal dimension to analyse the seismo-electromagnetic emissions associated with a moderate earthquake (M 4.0) that occurred on 13th June 2017, using the data of 3 component Fluxgate magnetometer installed at Desalpar and Vamka in Kachchh, Gujarat. This earthquake occurred about 19 and 39 km from the Vamka and Desalpar observatories, both of which are located within the preparatory zone. In order to avoid the day time cultural noise and diurnal variations, the night time data (18-21UT) is taken for further analysis. Power spectral densities (PSD) are calculated using FFT technique in five frequency bands, i.e., f1 (0.001–0.005Hz), f2 (0.005–0.01Hz), f3 (0.01-0.05Hz), f4 (0.05-

0.01Hz) and f5 (0.1-0.5Hz). We found an enhancement in power spectral density in different frequency bands before this earthquake and this specific enhancement is found in frequency band 0.5-1.0 Hz just 15-17 hours prior to this earthquake. The polarization ratios (Z/G, Sqrt (Z)/G, Sqrt (Z/G), Z/X) in five frequency bands f1 (0.001–0.005Hz), f2(0.005–0.01Hz), f3(0.01-0.05Hz),f4(0.05-0.01Hz) and f5(0.1-0.5Hz) are determined as shown in Fig. 4.17.

Generally, it is believed that if this ratio crosses 1, then there is a lithospheric influence, otherwise, there is a global magnetic influence on the signal. The vertical dotted line indicates the day of the earthquake. The polarisation ratios are found to cross 1 before this earthquake. The minimum polarization values are found to be 0.2 in Z/G on 6th June and the polarization increased during 7-11 June, i.e., few days prior to the earthquake. After the earthquake, the polarization value goes down to 0.5-0.8. The most characteristic frequency of the observed Seismo-ULF emissions is found in F1-F3 bands, similar to the results obtained by previous researchers (Kopytenko et al., 1990 and Hayakawa et al., 1996). The possible explanations for higher polarizations might be micro fracture electrification (Molcahnov and Hayakawa, 1998) and inductive seismo-electromagnetic effect (Molcahnov et al, 2001). The corresponding Kp and Dst are also plotted and they are found to be lower during this period which may indicate that the influence of global magnetic effects is minimal. We found an enhancement in polarisation ratio before this earthquake.

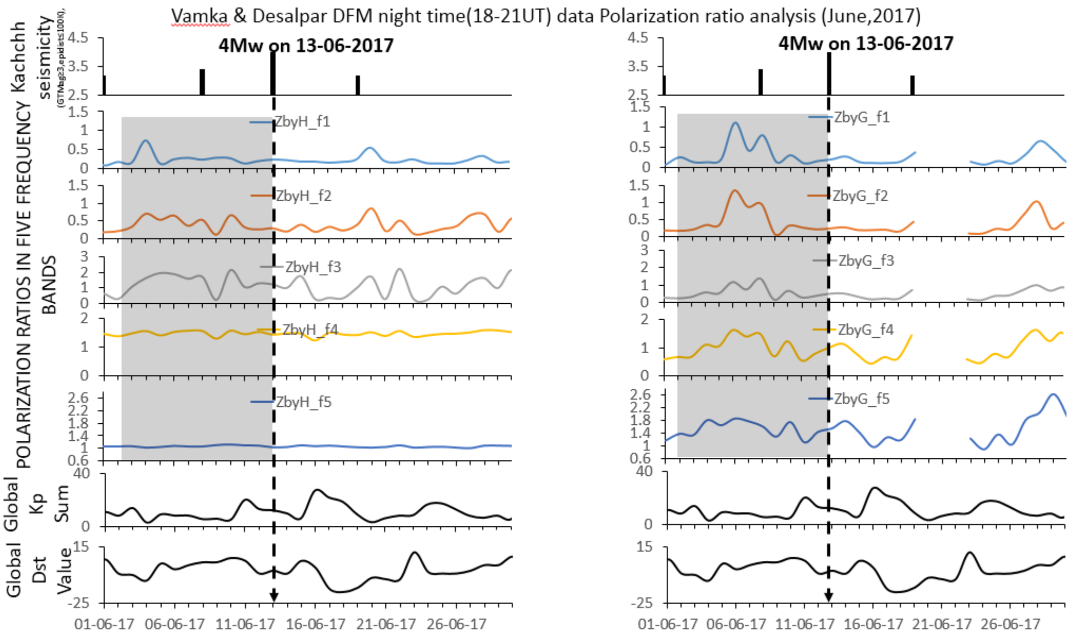

Figure 4.17: Polarisation ratios at Vamka and Desalpar in different frequency ranges along with the no. of local earthquakes, Kp and Dst.

4.7 Geomagnetic anomalies possibly linked with 2001 Bhuj, Gujarat earthquake (Mw 7.7): a study on earthquake precursors

(Shivam Joshi and K.M.Rao)

at 08:46 (IST) in Kachchh region which killed around 14,000 people in Gujarat and is considered as the most destructive natural hazard in the history of Gujarat. In this study, we attempted to study the ULF geomagnetic anomalies associated with the 2001 Bhuj earthquake of Mw 7.7. We analyzed the geomagnetic data from 21 to 31 Jan 2001 (11 days) with sampling rate of 1 minute (Fig 4.18) recorded at the Alibag station (Geographic latitude 18.64^{o}N, longitude 72.87 ^{o}E). In order to reduce the manmade and atmospheric perturbations, we consider the data during the mid-nights (18-21UT). The effect of geomagnetic storm activity, planetary index (Kp) and Dst (nT) index are also analyzed in the corresponding periods. Total Magnetic Field values varied from 42231 to 42246 nT. Similarly, H component varied from 38078 to 38090 nT and Z component varied from 18496 to 18503 nT. We can clearly see a sudden drop of 13 nT in both TMF and H-component, 3 hours and 16 minutes prior to the occurrence of this earthquake. The PSD analysis has been carried out in four frequency bands, f1(0.001-0.005Hz), f2(0.005-0.01Hz), f3(0.01-0.05Hz) and f4(0.05-0.1Hz) on H, D, Z components of the magnetic data. The Z Component shows a rise in different ULF range. The rise is observed before the main event too. The Kp values are quite normal during the time of this earthquake and the peaks before this earthquake might be correlated with this earthquake. A rise of 40- 50% of the signal has been observed before the seismogenic effects. We can clearly see the distinct increase of signal in response to this earthquake. The polarization ratios (Z/G) and (Z/H) in four frequency bands f_1(0.001–0.005Hz), f_2(0.005–0.01Hz), f_3(0.01-0.05Hz) and f_4(0.05-0.01Hz), are shown in Fig 4.19.

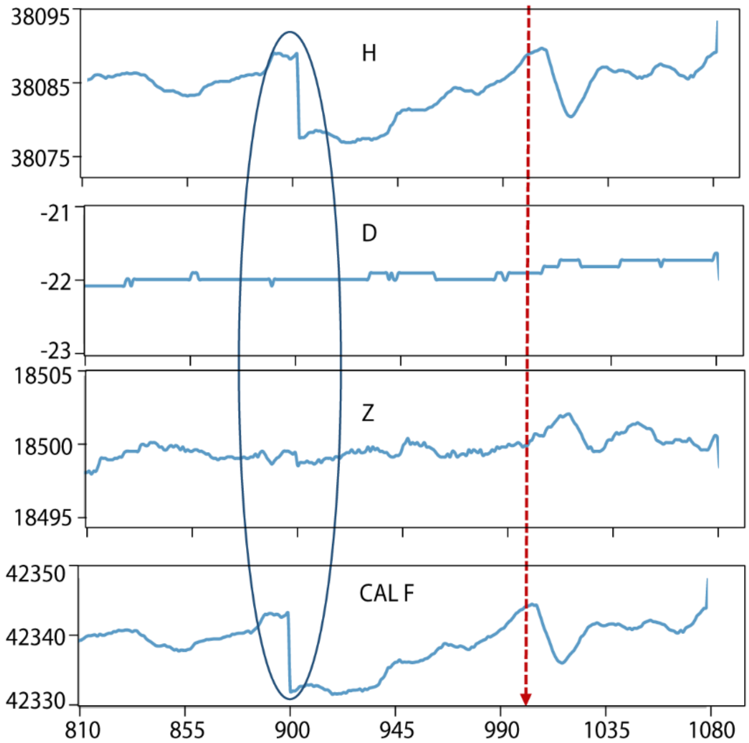

Figure 4.18: H, D, Z-field and Total magnetic field before the main event.

It can be seen from Figure 4.19 that both Z/X and Z/G enhanced before this earthquake. However, major enhancement appears in the first frequency band f1 but other frequency bands also show enhanced ratios during the same period with some reduced intensities. The most characteristic frequency of the observed Seismo-ULF emissions is found to be in the range 0.01-0.5Hz, similar to the results obtained by previous researchers for Spitak (Kopytenko et al., 1990); Loma Prieta (Fraser-Smith et al., 1990); Guam (Hayakawa et al., 1996); Biak (Hayakawa et al., 2000) earthquakes. The analysis of polarization at this characteristic frequency has shown that the polarization ratio increased significantly 6-7 days before this earthquake. This type of ULF increase before one week seems to be consistent with earlier works (Hattori, 2004). The increased trend of polarization ratio is also continued after the occurrence of earthquake, which may be an indication of post seismic adjustments. Our observations are similar to the previous case studies like Guam (Hayakawa et al., 1996) and Biak (Hayakawa et al., 2000) earthquakes. So, this phenomenon appears to be a precursor to the Bhuj earthquake.

There are various possible explanations for high polarization ratio, (i) increased vertical magnetic field, which can be associated to direct mechanisms acting in the crust like micro fracture electrification (Molcahnov, O. and Hayakawa, M, 1998); (ii) decrease of horizontal magnetic field, which can be related to indirect mechanisms like lithosphere-atmosphere-ionosphere coupling effects (Gokhberg, M.B. et al, 1995; Molcahnov, O et al, 2004; Sorokin, V., et al, 2004); and (iii) inductive seismo-electromagnetic effect (Molcahnov, O. et al, 2001). It is expected that EM emissions generated from any of these mechanisms may propagate very easily at the observing station, which is located in the preparatory zone. This analysis proved to be very good for the precursory study. The enhancement is shown in all the four ULF frequency ranges of both the parameters Z/G and Z/H.

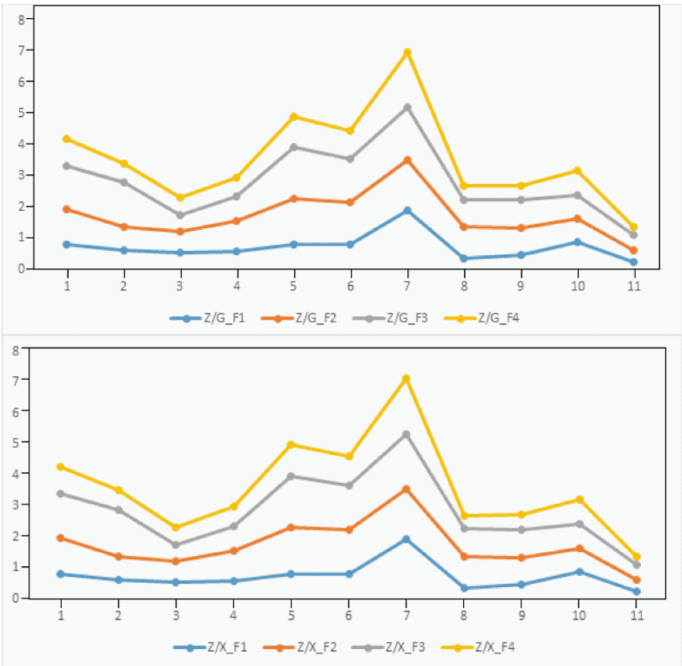

Figure 4.19: Polarization ration (Z/G and Z/H) analysis in four frequency bands.

4.8 Empirical Mode Decomposition based Hilbert Huang Transform to the Soil Radon (Rn^{222}) time series during Jan-Dec 2017

(Sushant Kumar Sahoo and K.M.Rao)

The soil radon concentration has been monitored continuously at Badargarh station in Kachchh to identify the earthquake precursors. The data from Jan 1 to Dec 31, 2017 recorded at Badargarh have been chosen for the analysis (Fig 4.20). In the first step, we checked whether the radon data shows normal distribution or not. In general, the soil data is following the fundamental laws of geochemistry which are usually normally distributed (Ahrens, 1954). In order to check this, we performed the probability plot (P-P plot) of radon time series. From this plot, it can be observed that the soil radon is normally distributed. In order to identify and extract the periodicities, Empirical mode decomposition (EMD) technique has been applied to the soil Radon (Rn^{222}) time series in which the observed time series gets decomposed into several intrinsic oscillatory modes known as the intrinsic mode function (IMF). In order to separate the physically significant IMFs which are not having any periodic oscillations, we follow two steps. 1) the IMFs are correlated with raw data and 2) the harmonic modes of each IMFs are also compared with periodicities of temperature, pressure, humidity and tidal variation. Three IMFs of both the stations are found to be physically significant and are considered to be free from any external influence.

These IMFs are taken as input for the Hilbert Huang Transform (HHT). The HHT became a successful tool for extracting the time-frequency-energy distribution, which can be utilized for the analysis of the complex non-stationary soil radon time series (Fig 4.21).

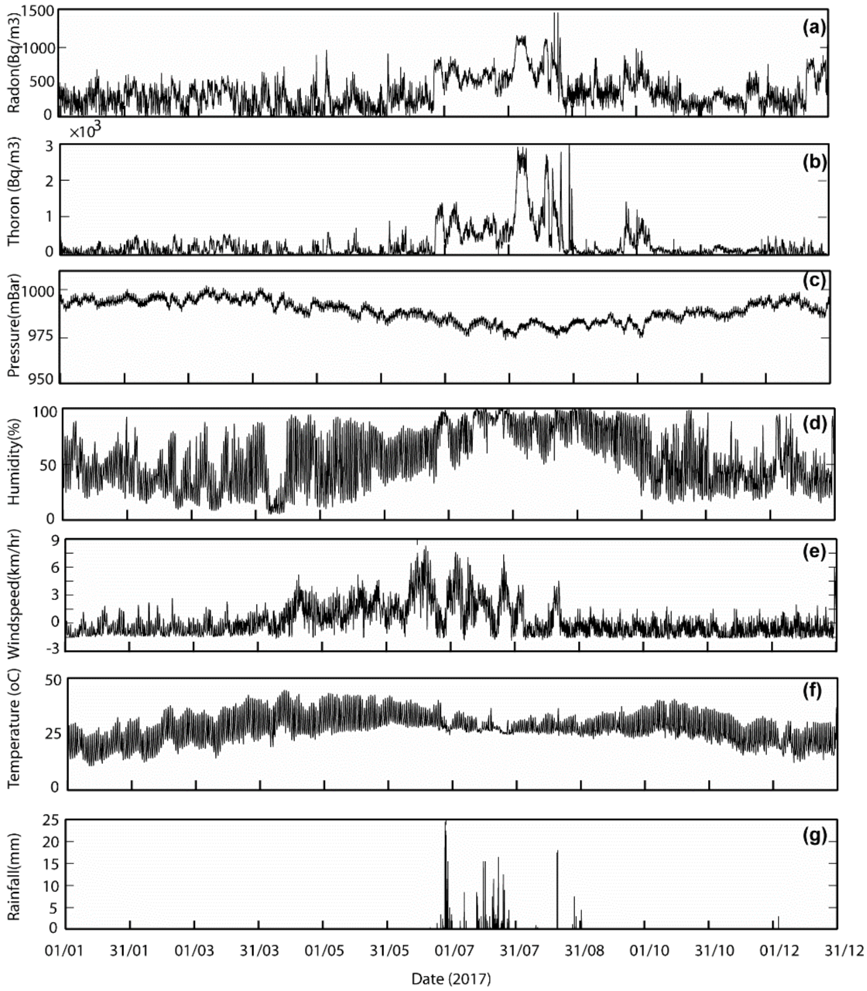

Figure 4.20: Time series of Radon, Thoron, Pressure, Humidity, Wind speed, Temperature and Rainfall during Jan-Dec, 2017

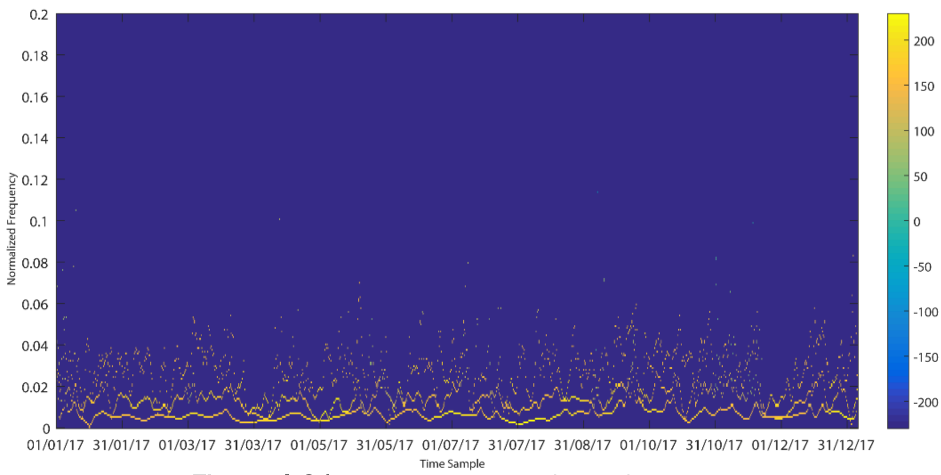

Figure 4.21: HHT spectrum of significant IMFs

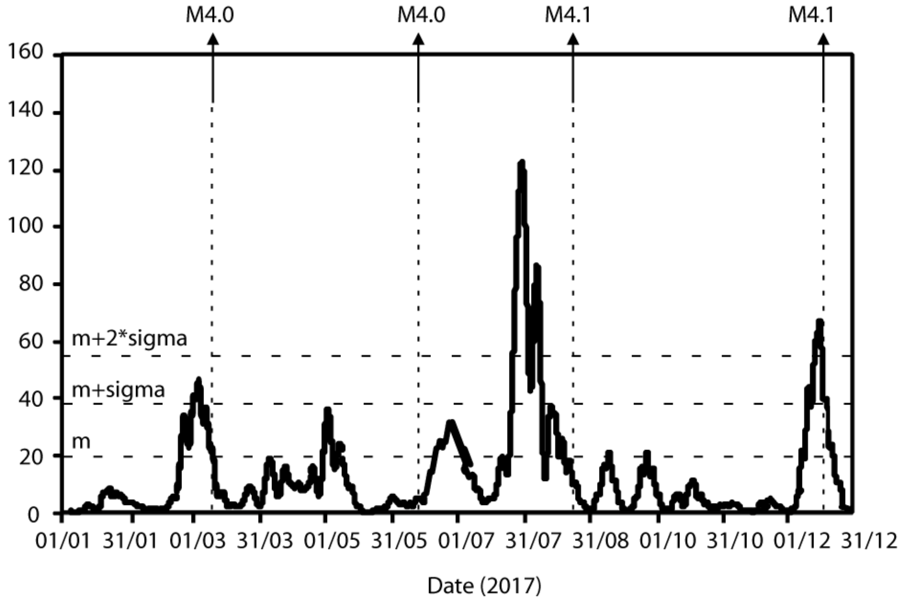

Figure 4.22: Instantaneous energy of significant IMFs along with the local earthquakes

It is observed that the instantaneous phases are getting decreased with the increasing order of the IMFs. The distribution of the instantaneous energy with respect to time has been correlated with the occurrence of the local earthquakes during the study period (Fig. 4.22). Four local earthquakes that occurred on 05/03/2017 (M 4.0); 13/06/2017 (M4.0); 23/08/2017 (M 4.1); 11/12/2017 (M 4.1) near to the observatory in Kachchh are considered for this study. The instantaneous energy gets increased prior to some of these earthquakes. The detailed analysis of correlation with local earthquakes is under process. The EMD-HHT method is proven to be useful in identifying the earthquake precursors in radon time series.

4.9 Geomagnetic and Geochemical anomalies before a moderate earthquake of M 4.8

(Sushant Ku Sahoo, Shivam Joshi and K.M.Rao)

The Geomagnetic field and soil radon have been continuously monitored at Badargadh in Kachchh region of Gujarat to study the precursors of local earthquakes. In this study, the geomagnetic field (N-S, E-W and Vertical components) of duration 1st January- 6th April, 2018 has been analyzed. Polarization ratio, variation of Fractal Dimension, power spectral density along with empirical mode decomposition of radon time series were studied to identify the precursors of three moderate earthquakes that occurred on 29/03/2018 (M 4.8), 25/02/2018 (M 4.1) and 16/01/2018 (M 4.1). The time evolution of the polarization ratio (Z/G, Z/H and Z/D) in the range of ULF band (0.001-0.01 Hz) has been observed for the entire study period and it has been found that Z/G shows an enhancement seven to ten days before the occurrence of all the three moderate earthquakes. Again, the basic dynamics of the Earthquake process have been studied by using the time evolution of the fractal dimension of Earth’s magnetic field. The fractal dimension of the vertical component of the geomagnetic field increased before the moderate seismic events that occurred during the study period. The planetary index (Kp sum) has been analyzed during the study period for discriminating the influence of the ionosphere and magnetosphere activities due to the solar coronal mass ejection. The Kp value was below 30 for the entire monitoring period, showing a quiet condition.

Geomagnetic data analysis: The components (N-S, E-W and Vertical) of the Earth’s magnetic field have been measured using the Digital Fluxgate Magnetometer (DFM). The evolution of polarization ratio and the fractal dimension of the geomagnetic field with time have been checked for this study (Fig. 4.23).

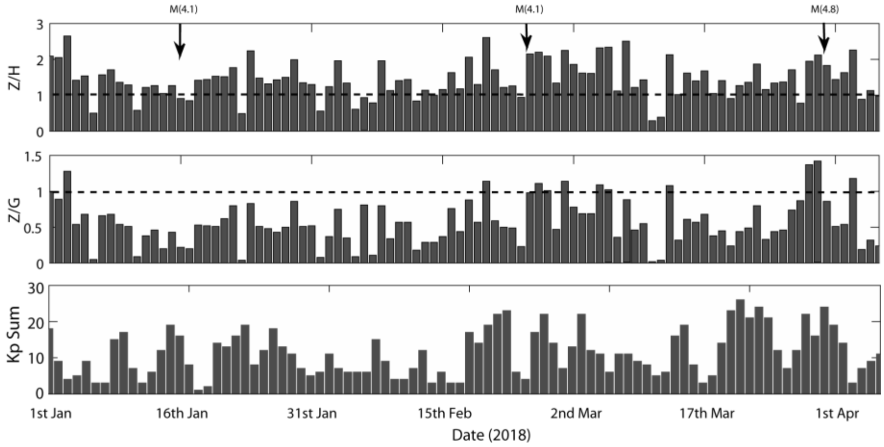

Figure 4.23: Polarization ratios Z/H and ZG along with Kp values during the study period

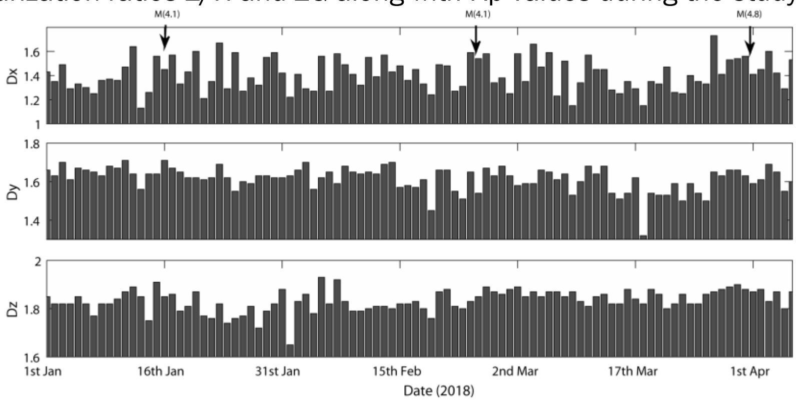

Figure 4.24: Fractal dimensions of X, Y and Z components during study period

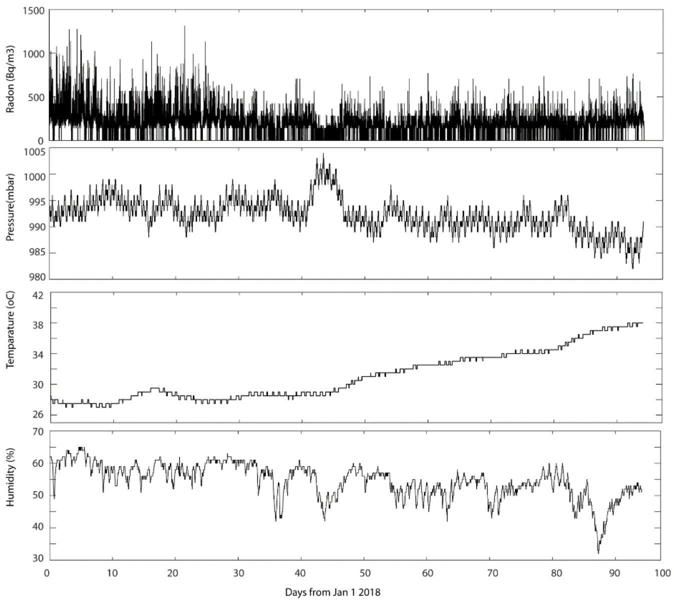

Figure 4.25: Time series of Radon, Pressure, Temp and Humidity during Jan1-April 4, 2018

Among the three seismic events occurred during study period, it has been observed that the ratio started decreasing before the Earthquake (M 4.1) occurred in 16th Jan, 2018 showing that there was no anomaly, but there was an enhancement of the polarization ratio prior to the earthquakes (M 4.1 and 4.8) occurred on 25th February and 29th March, 2018 respectively. The increase in this ratio indicates dominance of the contribution of the vertical magnetic field over the horizontal and thereby showing the contribution of the emission of the electromagnetic emission prior to these earthquakes. Again, for confirmation regarding the discrimination from the activities of the ionosphere, the planetary index (Kp) has been plotted during the study period and it has been found that for the total monitoring duration, the Kp value was below 30, which shows a quiet condition.

Fractal Dimension analysis: The obtained fractal dimensions of x, y and z components have not shown considerable changes before these earthquakes (Fig. 4.24)

Soil Radon Analysis: Empirical mode decomposition based Hilbert Huang Transform has been applied to the soil radon (Rn^{222}) concentration that has been monitored continuously at Badargadh station in Kutch, Gujarat with sampling interval of 10 minutes for the study of short-term geochemical precursor of earthquakes. In this study, the raw data of the duration of 96 days (from 1st January, 2018 to 6th April, 2018) has been taken for analysis (Fig. 4.25).

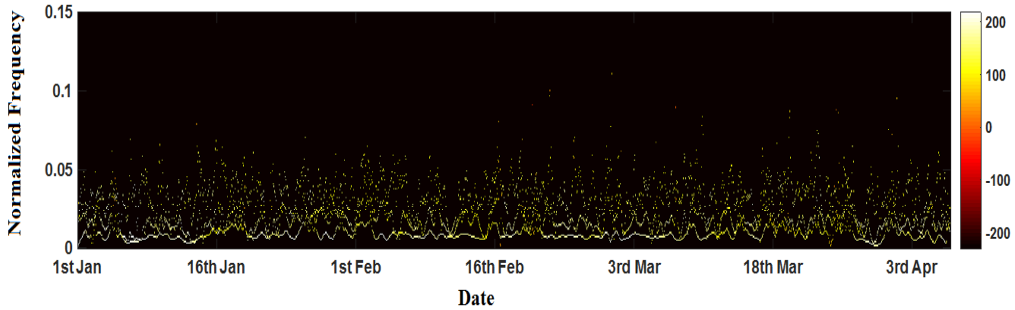

Figure 4.26: HHT spectrum of significant IMFs

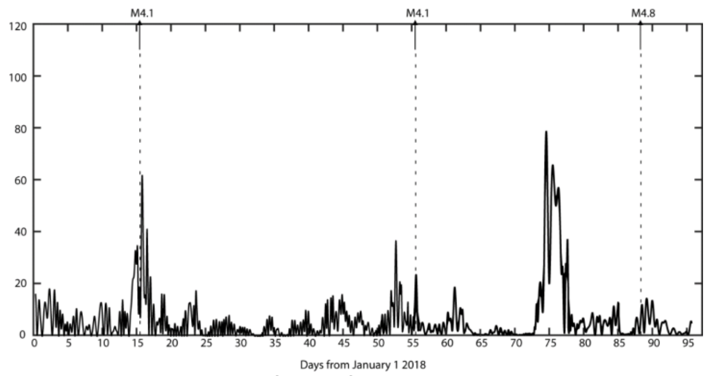

Figure 4.27: Instantaneous energy of significant IMFs along with the local earthquakes

The power spectrum analysis has confirmed the presence of diurnal and semi-diurnal periodicities in the soil radon, temperature and pressure. We applied the EMD technique on this radon time series and obtained 13 IMFs. These IMFs are mono-frequent, that is, each IMF represents a single oscillatory mode with a single frequency, as is exhibited by the unwrapped phases of the IMFs. We applied the HHT to physically significant IMFs (Fig 4.26). Apart from the instantaneous frequency, there are other important statistical parameters, like the mean marginal spectrum, degree of non-stationary and instantaneous energy, which are also obtained from the Hilbert spectrum. The time evolution of the Instantaneous energy for the study period has shown some anomalous enhancement prior to the three moderate earthquakes (M>4) that occurred in the monitoring location (Fig. 4.27).

4.10 Observation of Magnetic pulsations during quiet and disturbed times

(Prasanna Simha and K.M.Rao)

In this study, we tried to identify the pulsations of geomagnetic field components in H, D and Z components during quiet days (KP~0-1) and highly disturbed days (Kp~4-9). We used the Induction coil and Fluxgate data for this study. The induction coil data is highly sensitive to small type of variations, so we tried to compare the lower frequency (Pc3, PC4, Pc5 and Pi2) with Fluxgate data. We also tried to examine the higher frequency pulsations (Pc1 and Pc2). The long period pulsations Pi2 decreases with increasing geomagnetic activity levels. Yagova *et al.* (2017) presented various statistical and case analysis of night time Pc3 from middle to equatorial latitudes ,which are observed during the period of fast solar wind (V>500 km/s). Various activities of magnetosphere with and without influence of solar activities have been identified by the geomagnetic pulsations. Hence, we have selected some days which include quietest days and highly disturbed days during Jan-Apr 2015.

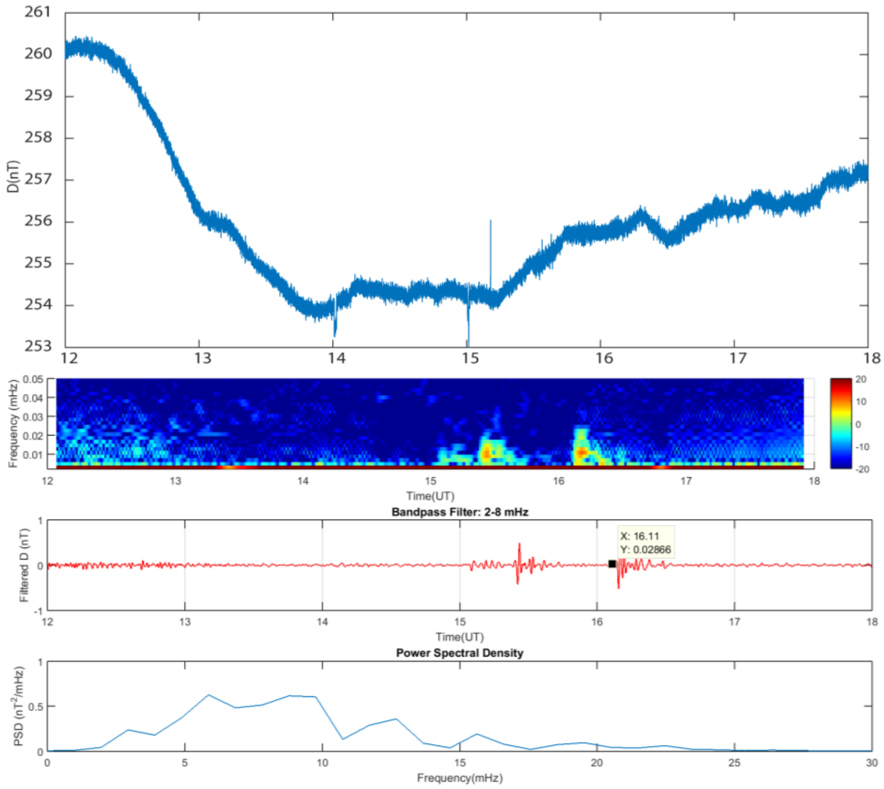

Figure 4.28: LEMI 30 Raw Data, Spectral, Filter, PSD variations of Y component during 12-18UT

The following steps have been adopted to identify the pulsations:

- Thorough inspection of raw data to check if the Geomagnetic pulsations exist or not.
- Spectral distribution of frequency of Geomagnetic field component to justify the signal strength of the event and to quantify the noise in the instruments.
- Applying a band pass filter as per the lower and cut-off frequencies obtained from the spectral distribution.
- Variations of Power Spectral Density with frequency to see at what frequency the signal has appeared.

The Fig. 4.28 depicts the Y component geomagnetic pulsations in LEMI-30 data during 30th March 2015 which is the quietest period (Kp~0-1). In the above figure, when we make frequency distribution of the temporal geomagnetic data, we noticed two pi2 at 15:05 UT and 16:17 UT at 19 mHz in ICM data. In order to confirm this observation, we applied the above procedure on fluxgate data of Hyderabad. Here, we clearly identified the signature at 16.03UT around 13mHz. This indicates that the peak observed around 15.05UT is not Pi2, but artificial noise.

5 Active Tectonics

5.1 Defining the geometrical characteristics of the fault scarp from topographic profiles and fault bedding

(Raj Sunil Kandregula and Girish Ch Kothyari)

Fault parameters are critical for studying the tectonic evolution, deformation characteristics, active tectonism, and seismic hazards. Analysis of fault displacement, paleoseismic recurrence intervals, and models of fault motion have been widely used to study the active tectonics during the late Quaternary (100-120 ka). In the present study, we attempted to understand the crustal deformation and the tectonic evolution of the KMF by defining the geometrical characteristics of the fault scarp with the help of measurements from topographic profiles and fault bedding.

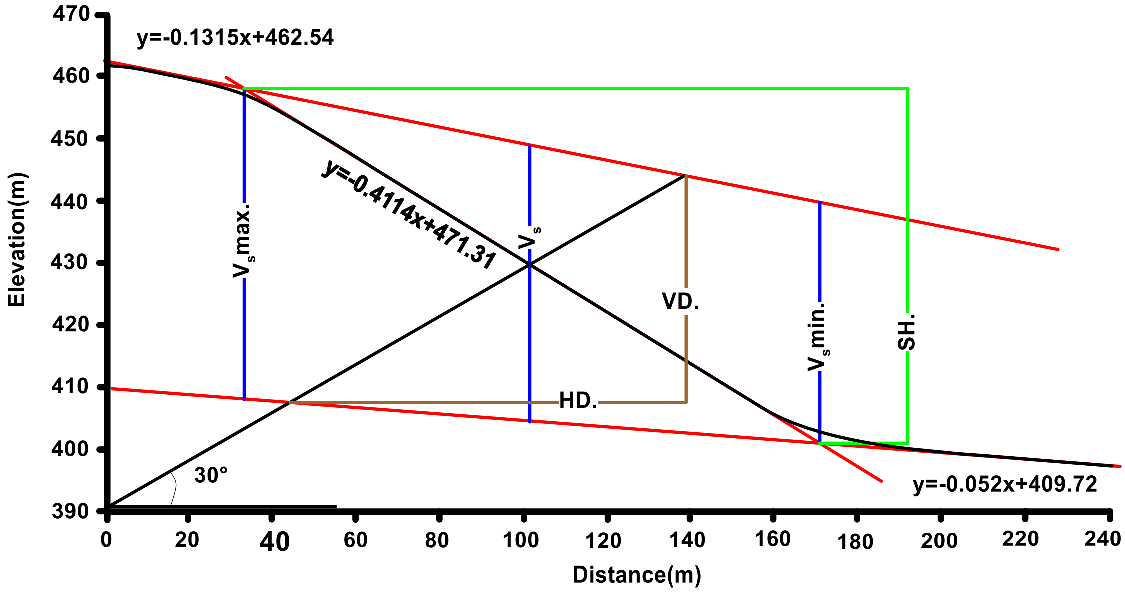

Figure 5.1: Diagrammatic sketches of calculation of the fault parameters across the fault scarp. VS: Vertical separation of ground surface; VS min: minimum vertical separation of ground surface; VS max: maximum vertical separation of ground surface; SH: scarp height; DS: dip slip of fault; HD: horizontal displacement of fault; VD: vertical displacement of fault.

5.2 Satellite data analysis to delineate Geomorphology of the KMF

(Raj Sunil Kandregula and Girish Ch Kothyari)

We used LANDSAT-8 data to delineate the lineaments in the vicinity of the Kachchh Mainland Fault(KMF). Based on the Lineament map derived from satellite data, the western KMF line and several major lineaments are identified and visually verified. The search for faults associated with the KMF was carried out along the identified fault line through visual inspection of satellite data.

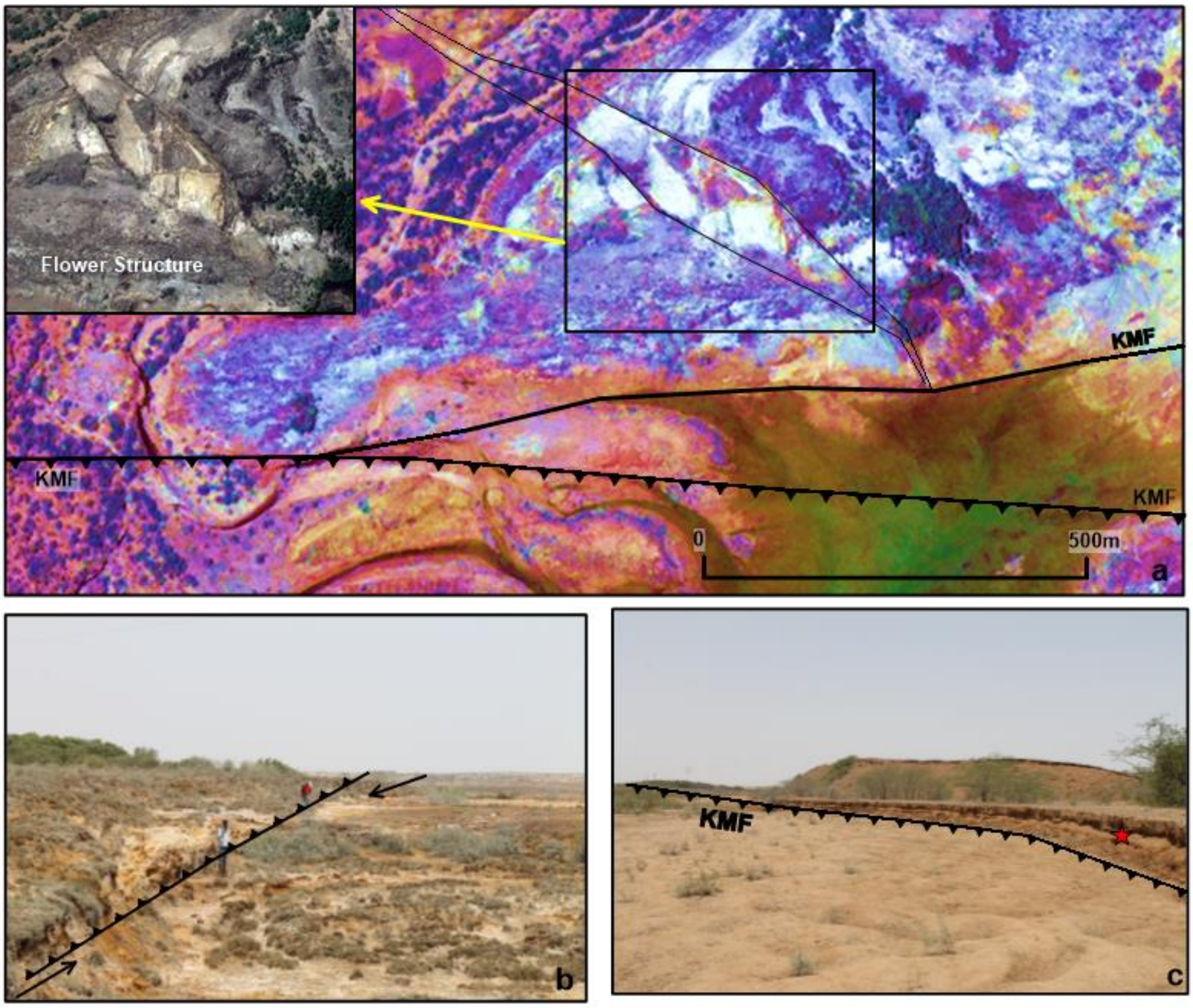

Figure 5.2: (a) Google satellite image shows presence of two strands of KMF in the area. Positive flower structure is associated with the southern strand of KMF (b) Field photo of steeply south dipping reverse fault (c) Uplifted Holocene sediments forming broad abandoned terrace surfaces and shutter ridges developed in the area.

5.3 Neotectonics and Paleoseismic Investigations along the Kachchh Mainland Fault Zone, Western India: Implications for Seismic Hazard Assessment

(Raj Sunil Kandregula and Girish Ch Kothyari)

The present study is aimed to characterize the seismogenic potential of the Kachchh Mainland Fault Zone (KMF) of the Kachchh region using detailed neotectonic history and paleoseismic investigations. The E-W trending fault systems in the Kachchh basin are zones of accumulation of compressive stresses evidenced by the association of several morphotectonic features, viz, anticlines, half anticlines, synclines and domal structures associated with faults. However, a detailed study of tectono-morphology and Quaternary stratigraphy along the faults is essential for understanding their seismogenic potential. Further, the sequence of neotectonic reactivation of the fault and their chronology may provide crucial data for understanding seismotectonic nature of Kachchh basin. The seismicity of Kachchh clearly demonstrates the role of active intrabasinal faults in accumulating and releasing the tectonic stresses. However, critical geological database for effective seismic hazard estimation and identification of earthquake prone zones is scarce. Very few studies related to the neotectonics and paleoseismic investigations were done in various parts of mainland region of Kachchh. The neotectonic evolutionary history and paleoseismicity are still not yet clearly understood in this region. The proposed work deals with the detailed study of nontectonic evolution and paleoseismic investigations along the KMF zone.

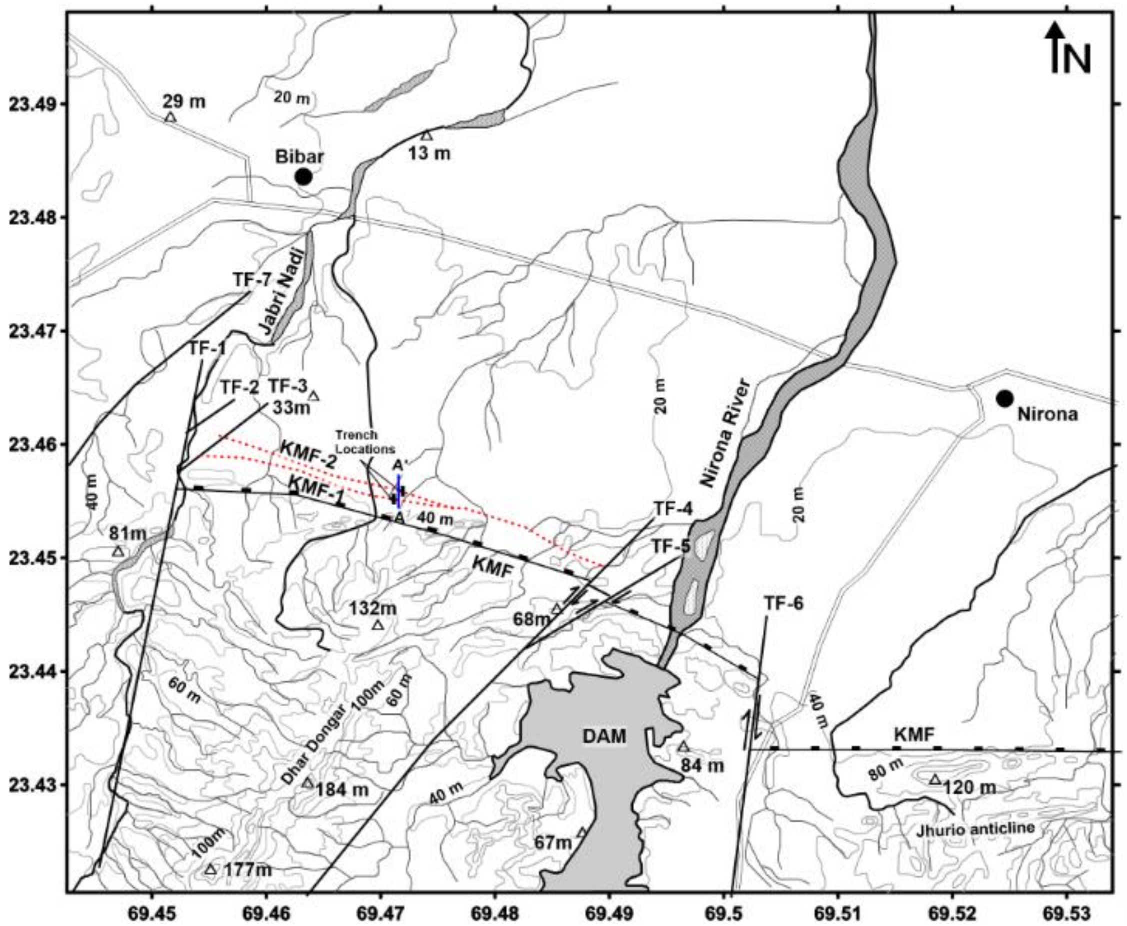

Figure 5.3: Topographic map of the study area. Contour lines are marked by grey lines with a contour interval of 20 m, elevation peaks are shown by black triangles, and transverse faults are shown by black solid lines. Traces of active fault are marked by red dotted lines. Double solid black lines indicate roads.

5.4 Gradient anomaly for rivers of Kachchh (for ~100 river channels) to determine the tectonic subsidence and uplift associated with the major active faults

(Raj Sunil Kandregula and Girish Ch Kothyari)

High resolution digital models, combined with GIS or other terrain modelling software, allow many new possibilities in geoscience. In this work, we adopted the Gradient Length Anomaly (GLA) method to detect the active tectonic uplift or subsidence along river courses. It is a modification of Hack's SL-index method in order to overcome the disadvantages of the latter. The core assumption of the GLA method is that over geological time, river profiles quickly adjust to follow an exponential decrease in elevation along the river course. Any large deviation can be attributed to active tectonic movement, or disturbances in erosion/sedimentation processes caused by an anthropogenic structure (e.g. artificial dam). This method was applied to the entire river drainages of the Kachchh Mainland Zone crossing over all the major faults to detect active tectonic uplift and subsidence.

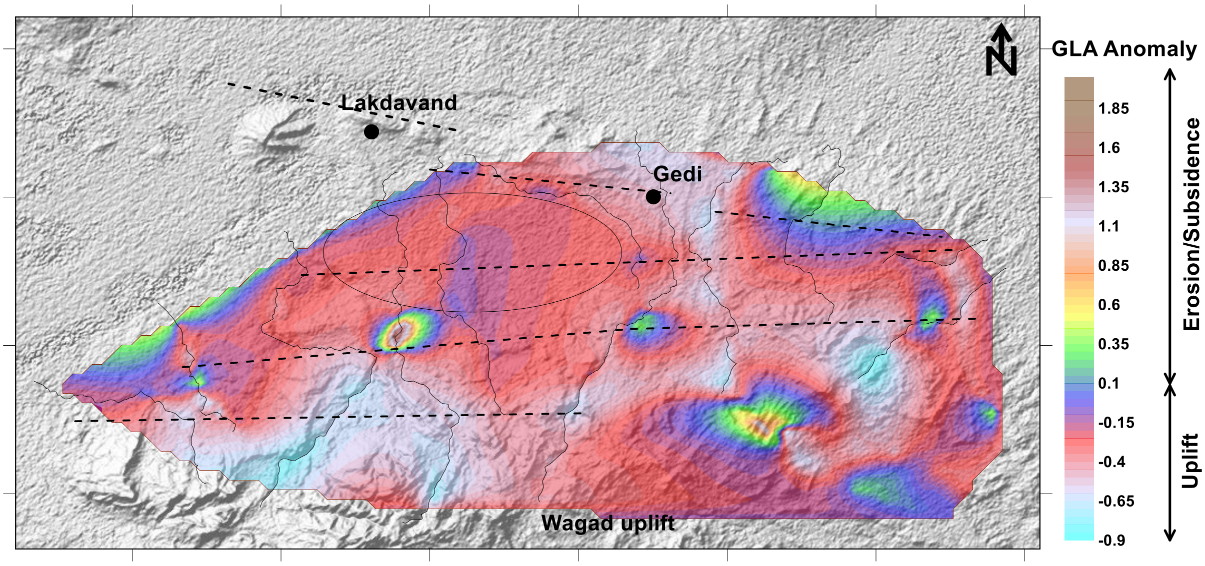

Figure 5.4: Gradient length Anomaly (GLA) distribution pattern of northern Wagad area shows regions of uplift and subsidence

5.5 Evolution of drainage in response to brittle-ductile dynamics and surfaces processes in Kachchh Rift Basin, Western India

(Girish Ch Kothyari, A. P. Singh, Sneha Mishra, Raj Sunil Kandregula, and Indu Chaudhary)

The eastern part of Kachchh basin and northern part of Wagad upland got seismically active after the 2001 Bhuj (Mw 7.7) and the 2006 Gedi (Mw. 5.7) earthquakes, respectively. Recent studies suggest that the eastern part of Kachchh is active. The area of present investigation is located between the Bharudia Fault/NWF, GF, and Island Belt Fault (IBF) in the northern part of Wagad upland. We present the geomorphic evidence along the surface traces of active faults in the northern part of Wagad and Bela upland regions. Development of tectonic landforms, namely, active fault scarps, shifting of drainage, uplifted ridges, and drainage offset reveal the active nature of the terrain. Three major faults controlling uplifts were identified within the surface rupture zone of GF. These uplifts were developed in a step-over zone of the GF, and formed due to the compressive force generated by the left-lateral motion within the segmented blocks. We primarily employed conventional morphometric analysis and several geomorphic parameters, e.g., stream length gradient index (SL), steepness index (Ks), hypsometry integral (HI), asymmetry factor (AF), and basin shape (BS) have been calculated. Based on these parameters, a single index of relative active tectonics (RIAT) has been evaluated to show the degree of activeness.

We corroborated the estimated parameters with the shallow to deeper fault natures as revealed by the earlier studies. Several E-W oriented deeper and shallower faults have been identified based on tomography and drainage pattern analysis. Drainage offset is the remarkable geomorphic expression observed in the area, associated with the deeper and shallower E-W oriented faults. From the drainage offset and seismic tomogram analysis, it is reasonably inferred that the area is having high heterogeneities. Furthermore, based on geomorphology and terrace stratigraphy supported by optical chronology, two major phases of enhanced uplift have been quantified, dated to 8 ka and 4ka. The younger event of enhanced uplift was responsible for the incision of the older valley fill sediments and the Tertiary bedrock. These ages suggest that the average rate of uplift ranges from 0.3 to 1.1 mm/yr during the last 9 ka.

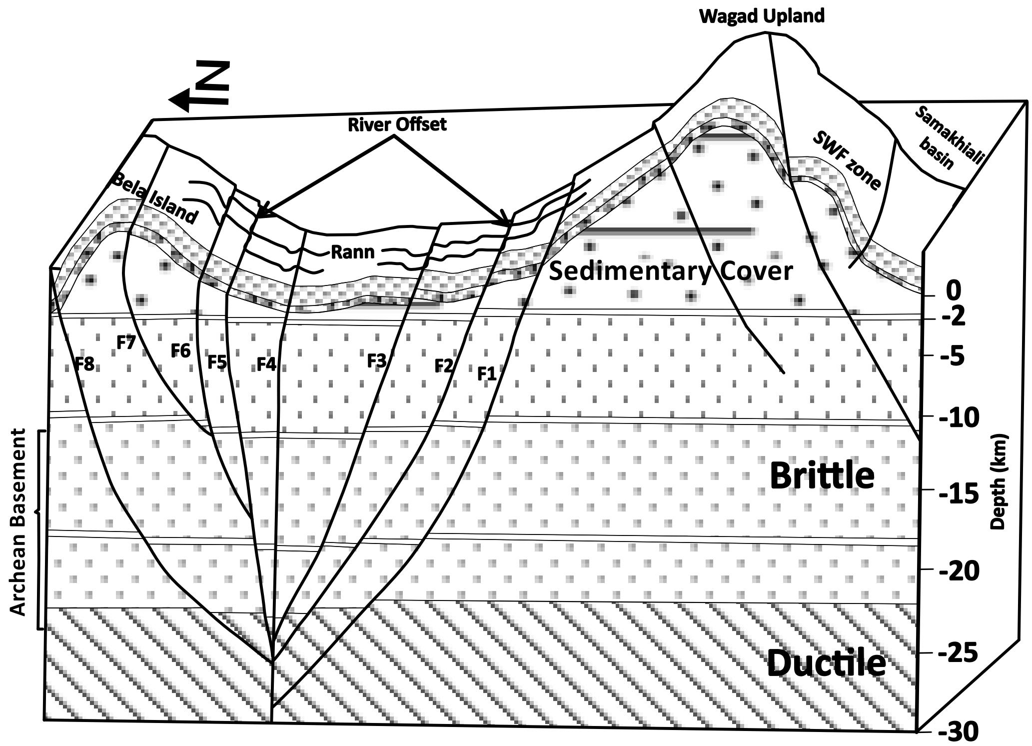

Figure 5.5: Three Dimensional block model of northern Wagad area showing development of negative flower structure at deeper level as inferred from seismic structures. The faults on the top surface are marked by stream offset pattern.

5.6 Palaeoseismological Investigation along the Back thrust of HFT, Soan Dun, Northwest Himachal Himalaya, India

(Neha Joshi and Girish Ch. Kothyari)

The Himalayan belt has experienced many devastating earthquakes in the historical past including the CE 1505, CE 1803, the 1905 Kangra earthquake (Mw 7.8); 2005 Balakot event (7.6); and the 1555 Kashmir event (M 7.6). The area of present investigation is located towards the hinterland of Januari anticline, where approximately 110 km long intermontane Quaternary basin has developed. The fault related fold growth, where several folds are interlinked, gives rise to a single ~100km long anticline. The NW-SE oriented Soan dun is controlled by the back thrust to the southwest and Soan Thrust to the northeast. Several geomorphic features such as, linear offset of streams, vertical displacement of alluvial fans and fluvial terraces with linear mountain fronts, ponding of streams, back tilting, and triangular facets have been identified in the area. Conventional morphometric indices such as SL, Ks, and AF are used to evaluate the tectonic scenario of Soan valley. High resolution satellite (CARTOSAT-1) data have been used for mapping of active landforms. We carried out Paleoseismic studies to identify the paleoearthquake. The exposed section along the back thrust shows 2.5m displacement of sediments along a SW dipping thrust fault. Based on the stratigraphic offset of sedimentary units, two traces of NNE-SSW oriented NE dipping normal fault with 53cm slip have been identified. A trench excavated across the back thrust revealed evidence of at least two palaeoseismic events during the Late Holocene. The trench investigations suggest that the earthquake during the recent past were accompanied with surface rupture. Studies show that the crustal shortening between MBT and HFT is ~ 11 ±5 mm/yr to 21 ±5 mm/yr. The integrated results revel that the landform development within the Soan dun area is controlled by the vertical tectonic forces generated by crustal shortening between the MBT and HFT.

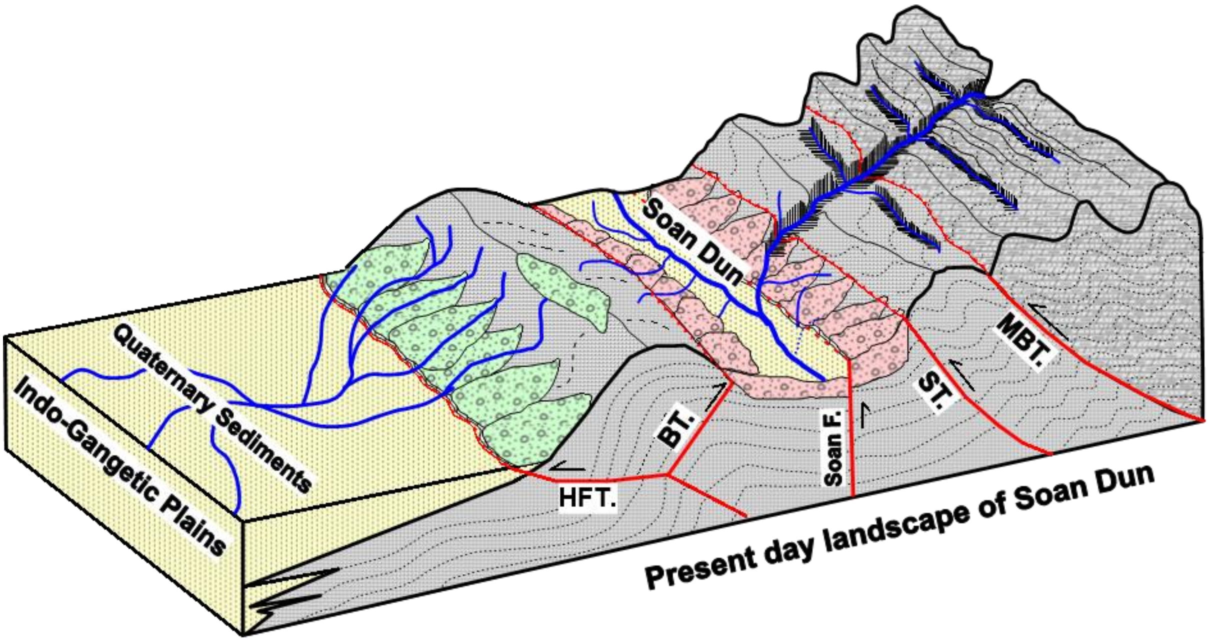

Figure 5.6: Schematic diagram of Soan dun of NW Himalaya shows evolution of tectonically induced landform features.

5.7 Evaluation of Neotectonic variability along major Himalayan thrusts within the Kali River Basin, Central Kumaun Himalaya, using the geomorphic markers

(Riyanka Talukdar, Girish Ch. Kothyari and Charu C Pant)

We have analyzed the geomorphic signatures in aggregation with the geomorphic indices with respect to hinterland and foreland neotectonic variability across the major Himalayan thrust system along the Kali valley of eastern Kumaun Himalaya. The valley floor morphology in the vicinity of the major thrust gave rise to the accommodation space for aggradation of the recent fluvial sediments. Along the 212 km longitudinal length between the South Tibet Detachment (STD) and Himalayan Frontal Thrust (HFT), the valley has preserved significant aggradational landforms. These landforms are physically examined to explain the spatial and temporal variability in phases of aggradation /incision in response to the tectonic activity during the late Quaternary. Fossil valleys and associated epigenetic gorges, cut-and-fill terraces with thick alluvial cover, debris flow terraces, bedrock strath terraces and alluvial fan terraces are the significant aggradational landforms observed within the valley that provide signatures of tectonic activity and past climatic records. To assess tectonic activities in the area, various geomorphic indices, namely, stream-gradient index (SL), steepness index (Ks), longitudinal profile, hypsometric curve and Index (HI), and assymmetric factor (AF) have been analyzed to map the spatial variability in tectonic processes across the major thrusts. We applied GLA analysis to deduct uplift and subsidence at the intersection between the drainage basin and active thrusts. The results of morphometric indices corroborated with the GLA anomaly and field observations, suggest that the area has undergone active deformation between the MCT and HFT, which is attributed to the regional compression. The results of geomorphic and morphometric data are validated with the focal mechanisms of moderate earthquakes. The geomorphic analysis suggests that the hinterland part of eastern Kumaun is comparatively more active than the foreland region.

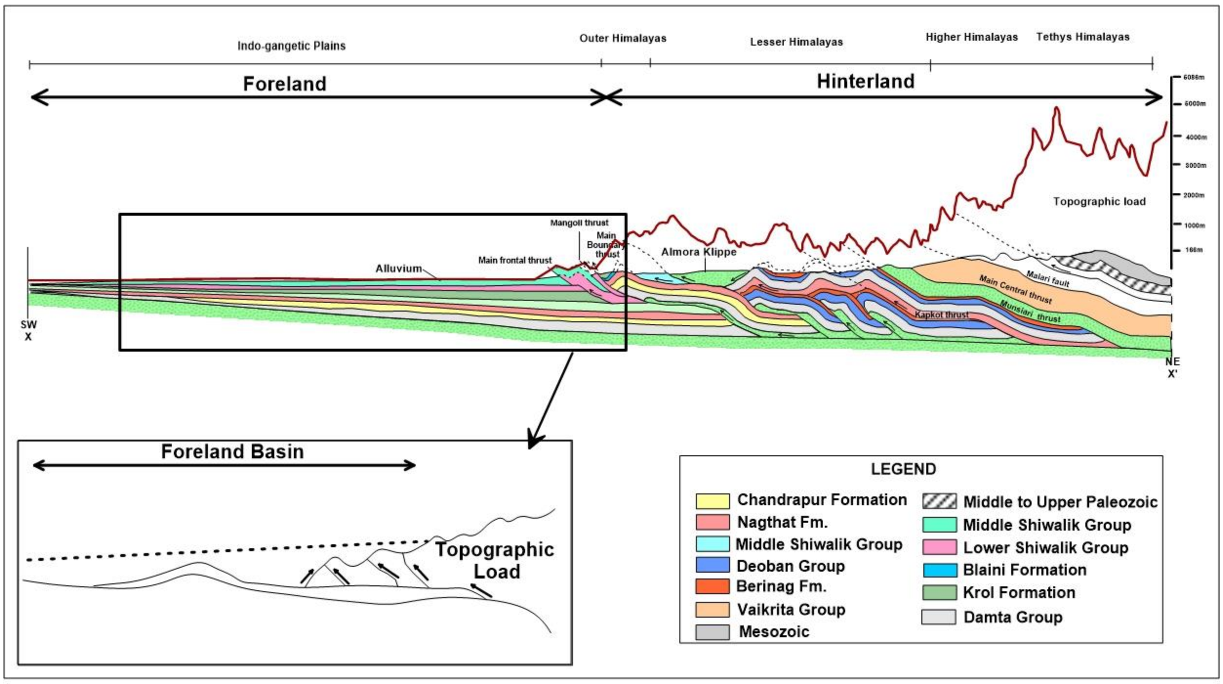

Figure 5.7: Cross-section shows thrust controlled topography of eastern Kumaun Himalaya (Modified after Shrivastava and Mishra, 1994).

5.8 Quaternary landform developments and climatic variability in a tectonically active region of Central Kumaun Himalaya, India

(Riyanka Talukdar and Girish Ch Kothyari)

The fluvial landforms in the Saryu, Pindar, Ramganga, Goriganga and Kali river valleys of central Kumaun Himalayan region were investigated to understand the role of temporal variability in climate and the spatial changes in crustal deformation. In present work, we employed geomorphological, sedimentological, geochemical concepts, supported by optical dating. Three major phases of valley-fill aggradation separated by phases on non-deposition are discerned. These river valleys have preserved cut-and-fill terraces with a thick alluvial cover, debris flow terraces, bedrock strath terraces, and fossil valleys associated with the epigenetic gorges that provide signatures of tectonic activity and climate. The available chronological data from Pindar, Saryu and Alakananda river basins suggest that the oldest phase of aggradation within these basins occurred between 33 and 45 ka, during a relatively strengthened ISM corresponding to the later part of pluvial Marine Isotopic Stage-3 (MIS-3). However, the sedimentation impersistently continued until and around 21 ka, during the declining phase of the ISM. The major phase of valley fill is dated between 13 and 22 ka. The youngest phase of aggradation dated at early and mid-Holocene (9-3 ka), represents a transitional climate during which sporadic high sediment fluxes, both from the upper catchment and tributary streams, led to the development of fossil valleys.

The monsoon and glacial dominating rivers in the Himalaya are the best archives that preserve the records of past climate and tectonic processes. Provenance study helps to estimate the amount of sediment derived from a given source and is mostly based on the concept that the bedrock provides us the sediment which is distinguished from one another in different parts on the basis of their chemistry, geochronology or tectonic evolution. These differences are finally transferred from the bedrock to the sediment in the rivers, which help us in understanding their source and the rate of erodibility of the rocks. The sediment dispersal along the valley and geochemical analysis provides us the period of high and low precipitation, which can cause the large scale deposition. The sedimentological, geochemical and chronological study together suggest that the sediments within these basins are primarily regulated by monsoon precipitation and glacial melt. However, the post depositional landform modification is modulated by tectonic forcing.

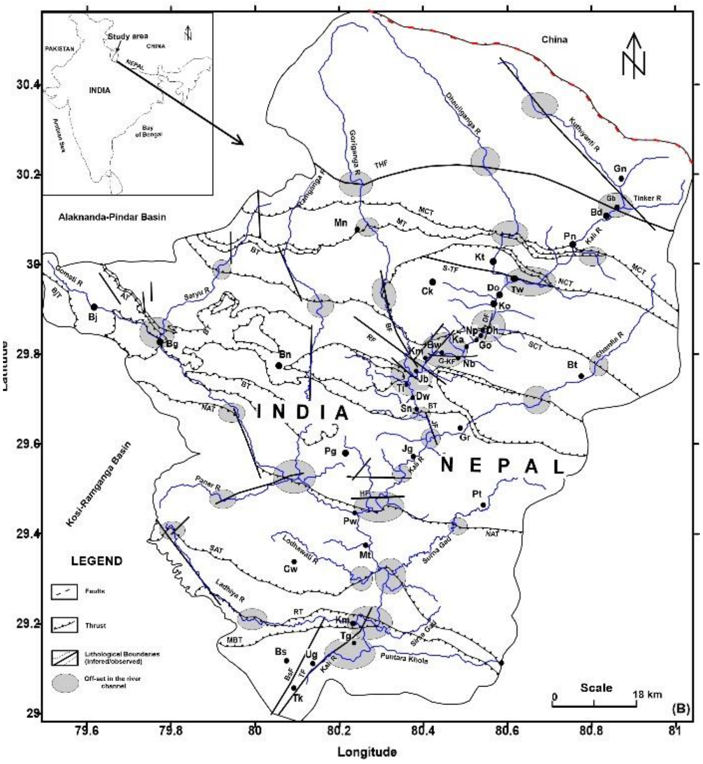

Figure 5.8: Drainage map and major structural discontinuities of eastern Kumaun Himalaya. Offset of drainages are marked by grey ellipses

5.9 Morpho-structural evidence of neotectonic movement along Vigogi fault: Kachchh Rift Basin

(Sneha Mishra, Girish Kothyari, R K Dubey)

The Kachchh rift basin is situated in the western margin of India, which is composed of thick Mesozoic sediments of Late Jurassic period. The western part of the Kachchh basin was activated after the 1819 Rann of Kachchh Earthquake (Mw 7.8) and the 1956 Anjar earthquake (Mw 6.0). Recent studies suggest that the western part of Kachchh is potentially active for generation of a future earthquake. The area of present investigation, the Vigodi fault, is located between the Kachchh Mainland Fault (KMF) and the Katrol Hill Fault (KHF) in Kachchh. The NW-SE trending Vigodi Fault is an extension of the KHF and is wrench type in nature. The fault splays out into several branches, creating Vigodi-Gugriana-Khirasra fault complex, sub parallel with oblique conjugate faults. In this work, we present geomorphic evidence along the surface traces of neotectonically active faults in North Western part of the Vigodi fault. Development of neotectonically induced landforms like starth terrace in upthrown part of fault, filled terrace in downthrown part of fault, fault scarps, warping in quaternary sediments, incision in sediments and slit canyon, knick points and river offset. We also investigated the tectonically deformed areas like the fault plane in the contact zone between Mesozoic and Tertiary formations, Faulted joints, slicken sides, bunches of mini strike-slip faults and conjugate type of faulting along the Khari river, which reveal that the area is disrupted by neotectonic activity. We primarily used conventional morphometric analysis and several geomorphic parameters like, stream length gradient index (SL) and steepness index (Ks). Based on these parameters, the area has been evaluated to see the degree of activeness. We also calculated the GLA, which is a modified version of Stream Length Gradient Index. The calculated positive and negative values show the upliftment and subsidence in the area. The various tectono-geomorphic features and geomorphic indices suggest that the Vigodi fault is neotectonically active in the Quaternary period.

5.10 GPS measurements of deformation caused by the seasonal filling and emptying cycles of four hydroelectric reservoirs in India

(Rakesh Dumka, Pallabee Choudhury, V. K. Gahalaut, Kalpna Gahalaut, Rajeev Kumar Yadav)

We present GPS measurements of crustal deformation due to seasonal filling and emptying of four surface reservoirs of varying dimensions, located in various geological domains of India. We report that all the reservoirs, including the smallest Dharoi reservoir with a storage capacity of 0.1 km^3 only, cause deformation in the neighbouring region. Such deformation leads to stress change and depending upon the availability of critically stressed faults in the region, the reservoir may trigger earthquakes which can be detected if a local seismological network is in place in the region. Interestingly all the three, the Tehri, Koyna and Ukai, reservoirs have triggered earthquakes in their vicinity. Thus, we suggest that there appears to be no lower threshold on the size of the reservoir to cause deformation in the surrounding medium and to trigger earthquakes, as long as the faults are critically stressed.

5.11 Reconstructing climate-tectonic signatures from terraces of central and eastern Northern Hill Range (NHR)

(Siddharth Prizomwala, Gunjan Yadav, Tarun Solanki and Archana Das)

The salient findings of the study are:

- The northerly draining fluvial sequences exhibit a variety of valley fill, channel fill and strath terrace sequences over the hanging wall block of the (KMF).
- Based on detailed stratigraphy and OSL chronology, we identified three cyclic phases of aggradation and incision during the last 24 ka period.
- The NHR experienced three aggradation phases during 24-10 ka, 8-4 ka and < 4 ka period in response to climate change.
- The KMF experienced at least two phases of uplift 1) > 24 ka and < 4 ka which led to landscape modification at regional scale of terrace formation.

5.12 Geomorphic Expressions of Active Strike-slip faulting (Girnar Fault), Saurashtra, Western India

(Tarun Solanki, S. P. Prizomwala)

The Talala region of Saurashtra in Western India has been rocked by three moderate seismic events of Mw 4.8 (2007), Mw 5.0 (2007) and Mw 5.1 (2011). Despite several seismological observations, which hint at monsoon being responsible for triggering swarm type activities, the moderate events may have another causal mechanism. There is limited data available pertaining to geomorphic / surface expression of faults in the region, which is crucial for understanding the crustal deformation in this seismically active intraplate region. In the present study, we report the geomorphic evidence of active left-lateral strike-slip movement with presence of oblique slip component along a fault (Girnar Fault). The zone of the fault extends for about 60 km in length in the NE-SW direction. Nevertheless, the seismological observations suggest that the seismicity is only restricted to a length of

40 km. The drainage network of Hiren and Shetrunji rivers shows anomalous pattern in the form of offset channel, deflected streams and straight channels, which are characteristic signatures of strike-slip faulting, apart from aligned drainages and linear valleys. Unpaired terraces present in the study area indicate presence of dip slip component along the fault. These factors along with the monsoon-triggering, present and active in the region, might have played a role in causing moderate earthquakes.

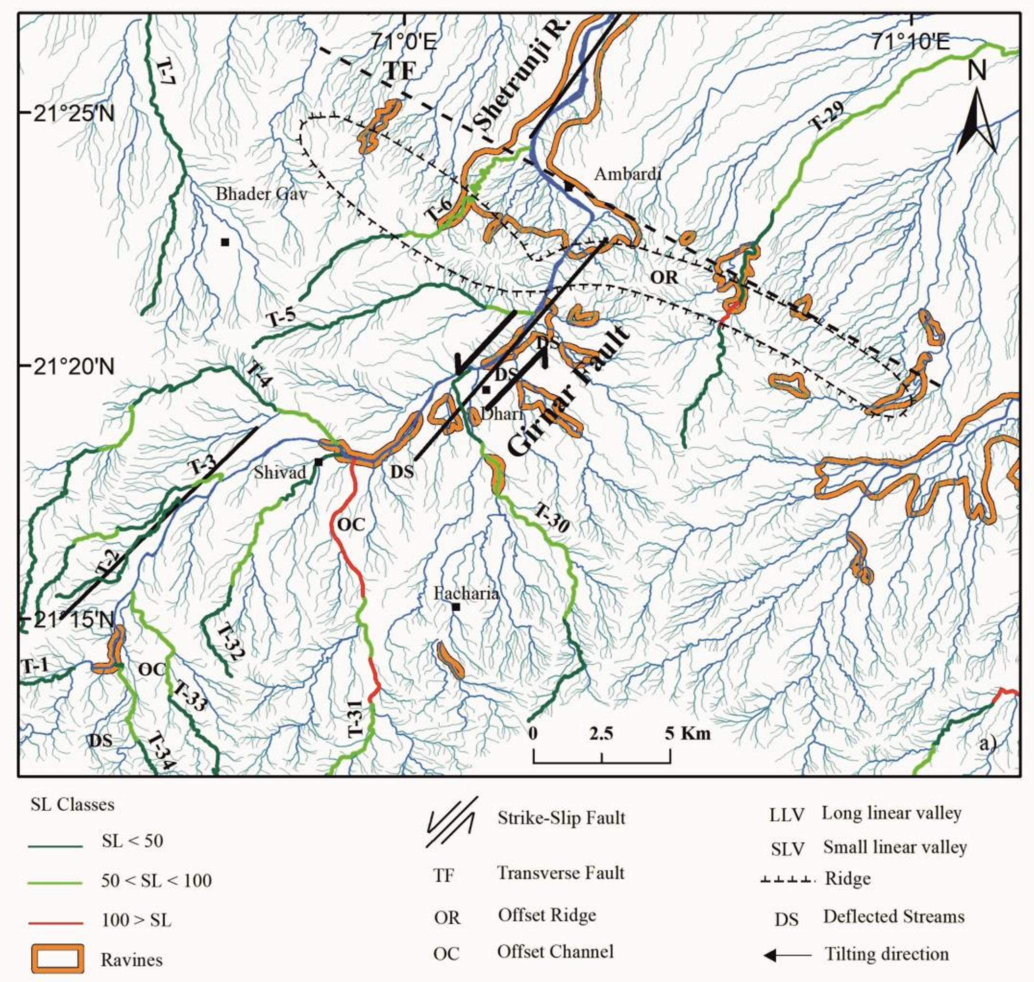

Figure 5.9: Geomorphic and morphostructural signatures showing the signature of the Girnar Fault

5.13 Signatures of middle to late Holocene high sea level/paleo environmental/paleoclimatic changes from the Banni plain, Rann and its linkage with the declination of past civilization

(Nisarg Makwana, S. P. Prizomwala, Chintan Vedpathak)

The present study attempts to reconstruct the evolution of Banni Plains of the Kachchh region, which has remained a hotspot for Harappan civilization. We employed a host of multiproxy techniques, namely, sedimentology, sediment geochemistry, magnetic susceptibility along with OCL and AMS chronology, to deduce the palaeoenviornmental changes experienced by the Banni Plains. The OSL and AMS chronology suggest the Banni trench site spans from 2.9 ka to present, with a mean sedimentation rate of 1.4 mm per annum. The enhanced chemical weathering intensities suggest that the last two millennia witnessed two phases of relatively warm and humid climatic conditions, which coincide with the Roman Warm Period and Little Ice Age. Also, the Banni Plains evolved owing to the Middle Holocene high sea stand and subsequent fall during the last 2 ka period. The extent of high sea stand upto 2 m above MSL also corroborated well with the ancient port settlements of the Late Harappan period. This implies that the Harappan civilization was indeed influenced and affected by the sea level change. Nevertheless, this cannot be the sole reason for the demise of the mighty civilization.

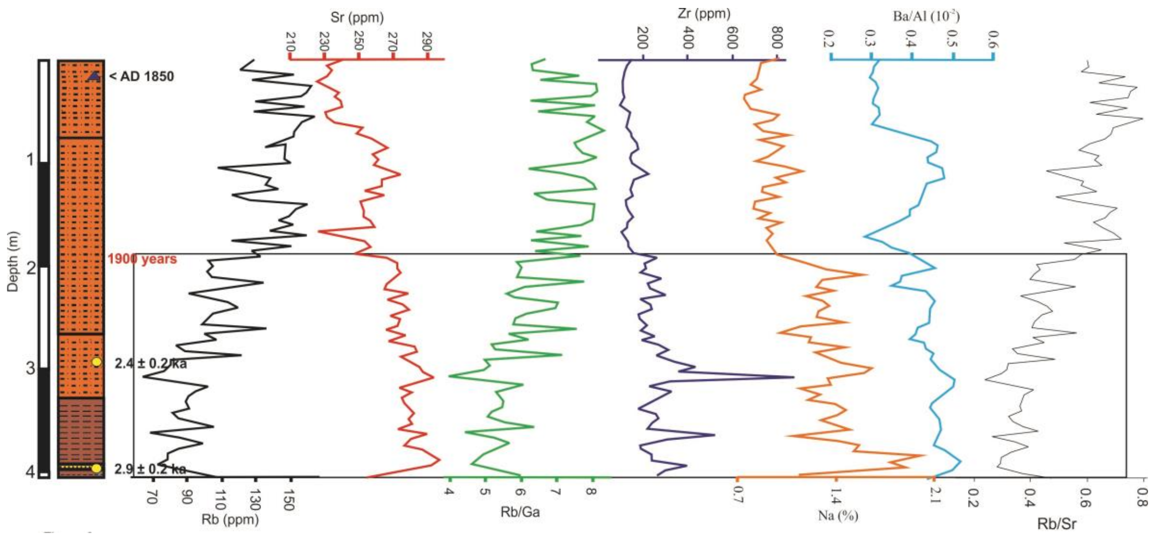

Figure 5.10: Temporal variation in trace elements showing palaeoenvironmental changes during the Late Holocene period

5.14 Geological evidence for AD 1008 tsunami along the Kachchh coast, Western India: Implications for recurrence along the Makran Subduction Zone

(S. P. Prizomwala, Drasti Gandhi, Nisarg Makwana)

The 2004 Sumatra-Andaman tsunami emphasized the catastrophic nature of such disasters and exposed our knowledge gap of the historical and palaeo events. In the aftermath of this deadly event, the thrust in palaeotsunami studies were restricted to areas in the Indian Ocean, affected by this Tsunami. The northern Arabian Sea, which hosts a similar tsunamigenic source, i.e., the Makran Subduction Zone (MSZ), has so far remained 'Terra-Incognita'. Here, for the first time, we report the geological evidence of the 1008 AD tsunami, also mentioned as 'an enigma' in the historical reports, by identifying a >250 km long sand sheet with a landward extent of more than 250 m from the Indian coastline. Detailed sedimentology and geochemistry reveals an offshore origin of this sand sheet, from where it was eroded by a high energy wave and deposited in a supratidal environment. Optical and AMS ^{14}C chronology constrains its age of deposition around 1000 AD. The regional impact of the 1008 AD tsunami suggests a 1000-year reoccurrence for the major tsunamigenic events along MSZ. The results of our study also highlight the potential of the western MSZ to produce major tsunamigenic thrust earthquakes, with longer reccurrence interval compared to the Sumatra Subduction Zone. The proximity of this sand sheet does not discount the role of extremely unlikely large storms as its causal mechanism.

5.15 Sedimentological, geochemical and chronological constraints from a palaeochannel near Lothal ~ a Harappan dockyard: Implications for palaeoenvironmental changes during the Middle to Late Holocene period

(Archana Das, S. P. Prizomwala, Chintan Vedpathak, Aashima Sodhi, Nisarg Makwana)

Lothal is situated on the bank of the Bhogavo River, which is now a palaeochannel of the Sabarmati river basin. It has been stated that Lothal was a Dockyard/Riverine port. The Harappans got collapsed/ deurbanised at 4.2 ky. Thus, certain questions are raised related to the collapse of such advanced civilization. Therefore, in order to address those questions scientifically, we excavated a 3.8m trench at Lothal. Based on the multiproxy datasets used, our results suggest that the area was under the high sea level stand which later got regressed and the river got defunct, causing deurbanisation. One such chronological age is also in accordance with the Little Ice age. Thus, it can be inferred that the settlement responded to the fluctuating climatic and sea level condition.

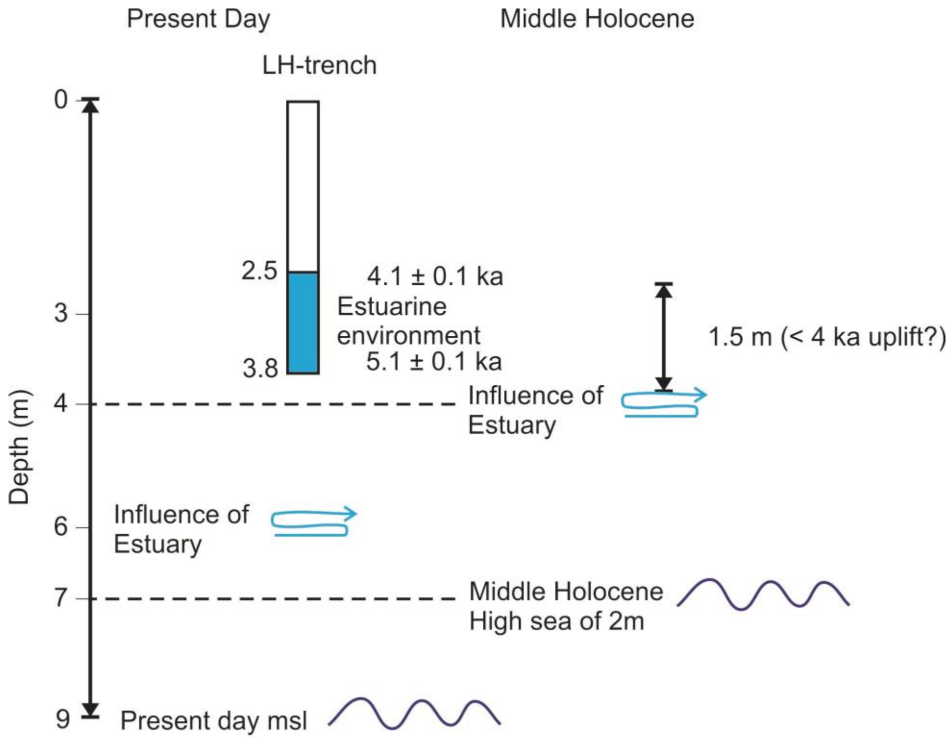

Figure 5.11: Schematic scenario of estuarine deposition during the present day and Middle Holocene period near Lothal, Western India

6 Commercial Research and Development

6.1 Estimation of strong ground motion at surface level and design spectra in the coastal region of Odisha near Dhamra

(Kapil Mohan, Sumer Chopra, Naveen Kumar, Vandana Patel and B. Sairam)

Under a commercial research project, the bedrock and surface strong ground motion are estimated in coastal Odisha, Near Dhamra. The magnitude corresponding to a return period of 475, 2475 and 4975 years are estimated. A magnitude Mw 5.7 is assigned for a return period of 475 years, 6.2 for 2475 years and 6.5 for 4975 years in the zone where the Dhamara site is located. The approach suggested by Mohan (2017) is adopted to estimate the surface strong ground motion parameters. In this approach the process of strong ground estimation is divided in three parts: (i) Estimation of Engineering Bed layer (EBL) from the shear wave velocity data from down hole, MASW survey and geotechnical data from the boreholes, (ii) Estimation of Ground motion at Engineering Bed Layer by Stochastic Finite Fault Source Modeling (SFFSM) (Motazedian and Atkinson, 2005) and (iii) Estimation of ground motion at surface by ground response analysis.

A total of 10 boreholes (BH-01 to BHL-10) are drilled in the study area; two boreholes were drilled up to 90m depth and 8 boreholes up to 75m depth. In majority of the boreholes, clay is found upto 20 m depth to maximum 45m depth followed by yellowish brown fine to medium sand.

On the basis and interpretation of soil data, four numbers of subsurface profiles are prepared. The subsurface profile data of all boreholes reflects that the yellowish brown clay of stiff to firm strength along with intermittent bands of silty clayey yellowish brown sand of loose to medium dense strength is present upto 28.5m depth. From depth 28.5 to 90m, yellowish brown fine to medium grained sand of very dense strength along with thin intermittent bands of yellowish brown to grey silty clay of stiff to firm strength are present. As per the SPT N value, the soil falls under soft to hard (in case of Clay) and loose to very dense (in case of Clayey, Silty, and Poorly graded sand). In all the bore holes, the ground water level is encountered at 0.5m depth from the actual ground level.

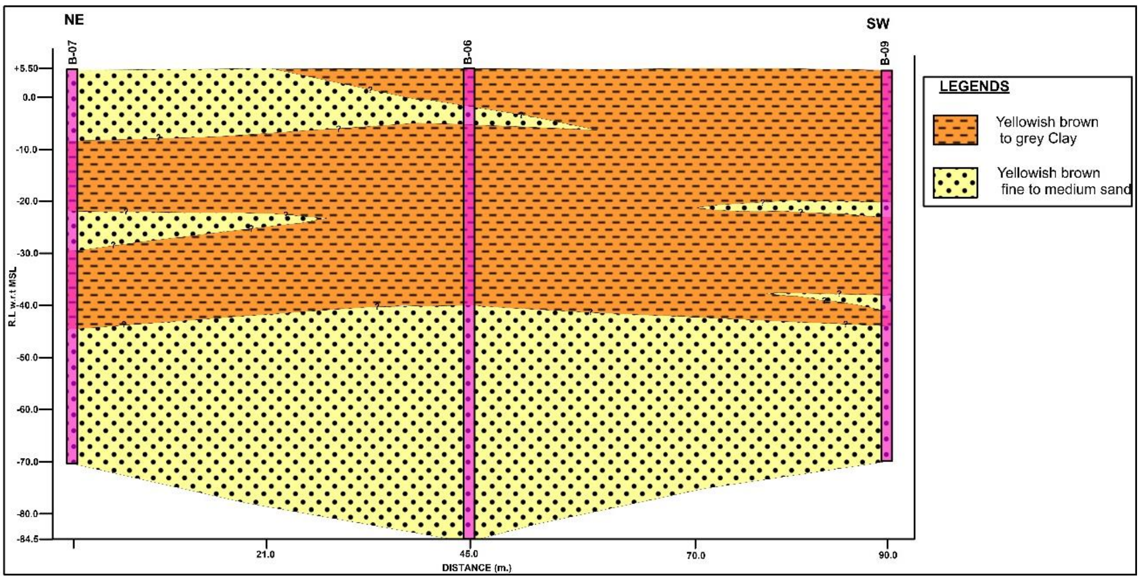

Figure 6.1: The subsurface profile along the boreholes

Soil models for all the ten boreholes are prepared based on the above-mentioned soil classification using corrected $(N_1)60$-values, moisture content and wet density and shear wave velocity estimated from down hole data and MASW survey data. The layer with a shear wave velocity of 760m/sec is found at a depth of 48 to 64.5m with refusal in N-value. The layer is considered as Engineering Bed layer (EBL). The ground motion is estimated at the EBL (Vs 760m/sec) for all the three magnitudes, corresponding to return periods of 475 years, 2475 years and 4975 years, using the Stochastic Finite Fault Modeling Technique (SFFMT) (Motazedian and Atkinson, 2005) and is given in Fig. 6.2.

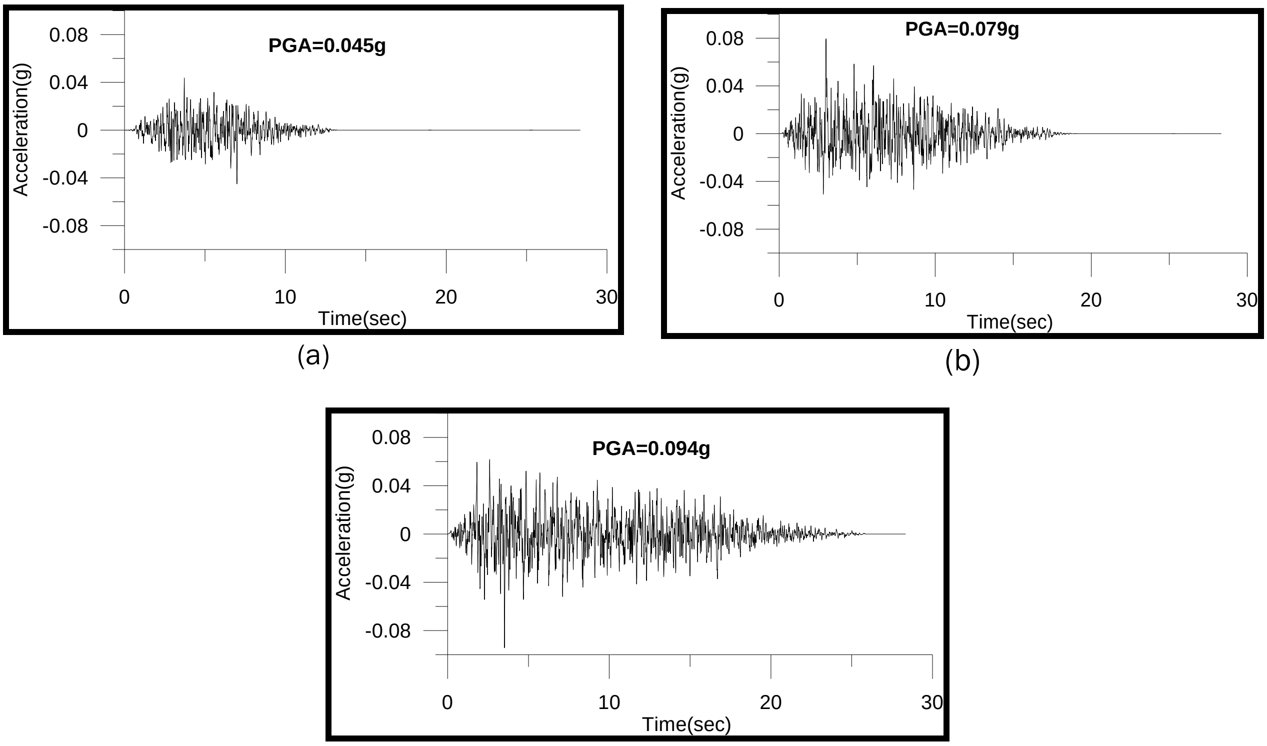

(a) (b)

(c)

Figure 6.2: The strong Motion estimation at surface for scenario earthquake of Magnitudes (a) Mw 5.7, (b) Mw 6.2 and Mw 6.5.

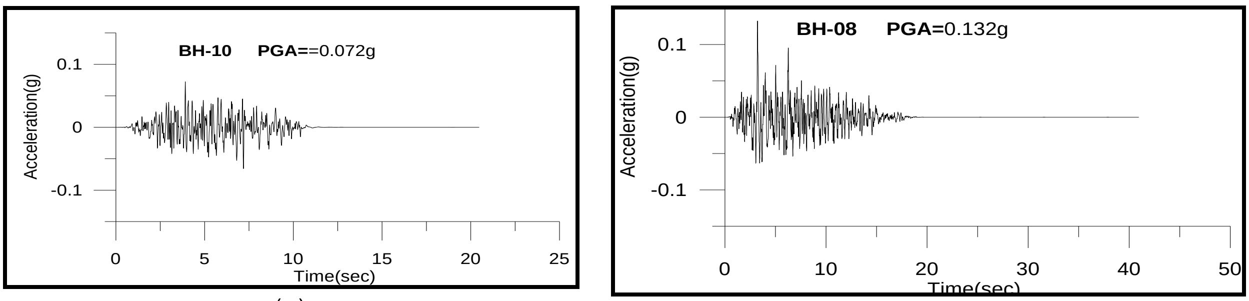

(a) (b)

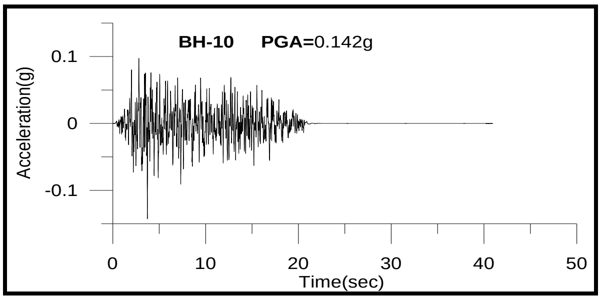

(c)

Figure 6.3: Strong motion estimation at surface for (a) Nearfield, (b) Farfield earthquake scenarios.

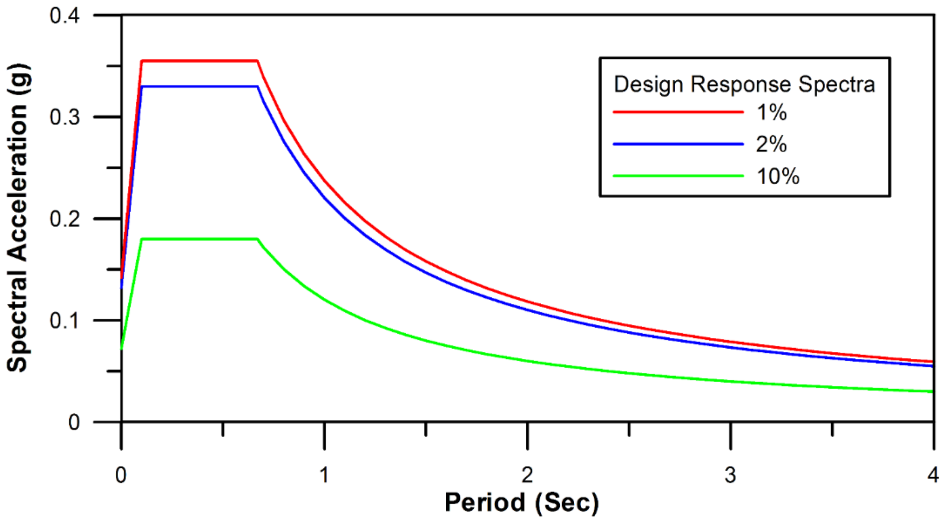

Figure 6.4: Design spectra at 5% damping at ground surface

The ground response analysis is conducted using geotechnical data to estimate the surface strong ground motion parameters. The maximum surface PGA of 0.072g **is** estimated due to magnitude Mw 5.7; 0.132g, due to Mw 6.2 and of 0.142g due to an earthquake of magnitude Mw 6.5 (Fig. 6.3). The design spectrum as per BIS (2002) is proposed for the study area (Fig. 6.4). The soil is found prone to liquefaction to a depth of 13.5m (from EGL) (mostly sandy soil).

6.2 Seismic Hazard Assessment at LPG treatment facility Bongaigaon

(Kapil Mohan, Naveen Kumar, Shruti Dagur and Sumer Chopra)

M/s L&T- Chiyoda has requested the ISR to conduct seismic hazard assessment of Indmax FCC unit including LPG treatment facility in LSTK-1 at Bongaigaon Refinery, IOCL, Assam. The Soil Testing Report of 11 boreholes down to depth of 20m conducted by M/s SKM Geosurvey at the site was provided for the analysis.

ISR has prepared the geological and seismotectonic map of the area from the available resources. It is found that the area is located in one of the most active seismic regions of India and is assigned zone V by Bureau of Indian Standards (BIS). Three great earthquakes (M>8) have occurred around the region in the last 120 years. To arrive at the site-specific response spectra, the 1950 Assam earthquake of Mw 8.7 (epicenter located ~650 km NE of the site) along with the 1934 Bihar Nepal earthquake of Magnitude Mw 8.1 (epicenter located ~ 360km west of the site) are considered as far-field earthquakes. The 1897 Shillong earthquake (epicenter about 90km south of the site) of magnitude Mw

8.1 and a scenario earthquake of M7.0 (about 55km north of the site) are considered as the near field earthquakes (Fig. 6.5).

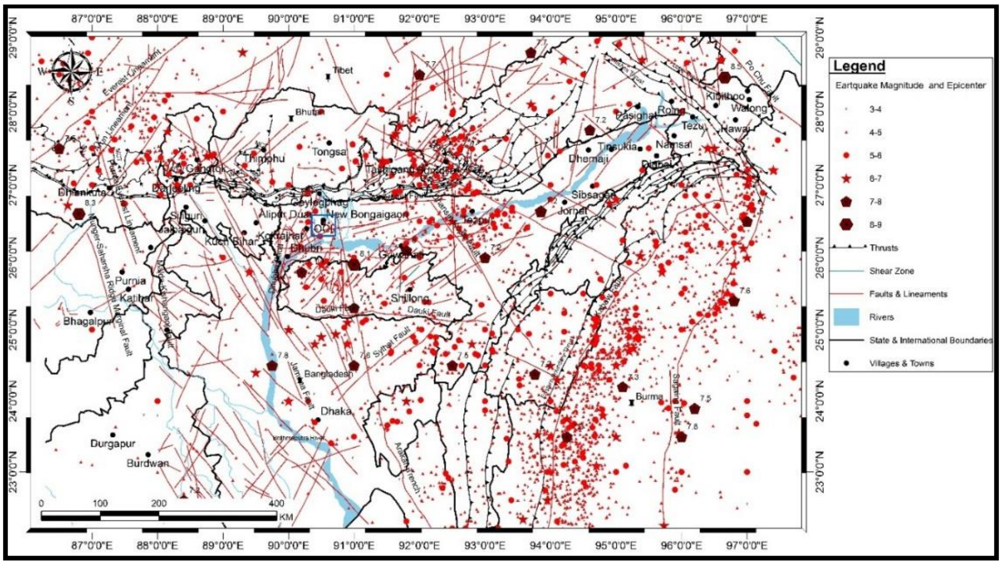

Figure 6.5: Seismotectonic map of NE India

The soil models for each borehole have been prepared using the soil profiles (Fig. 6.6) and ground response analysis has been conducted to estimate the surface strong ground motion parameters (peak ground acceleration, response spectra at 5% damping). The site specific response spectra have been proposed using the deterministic seismic hazard approach. The maximum surface Peak Ground Acceleration (PGA) of 0.346g is estimated at the site (Fig. 6.7). The PGA value is little lower than the PGA expected (0.36g) for Zone V, as given by BIS. The normalized response spectra from all the four considered earthquakes is shown in Fig. 6.8. The normalized site-specific response spectrum is anchored with the PGA. The maximum Peak Spectral Acceleration (PSA) of 1.6 g is found at 0.06 sec.

The Liquefaction potential at the site is estimated using a PGA of 0.346g. The possibility of liquefaction is seen from 0 m to 14.5 (maximum) where loose to medium dense silty sand is present.

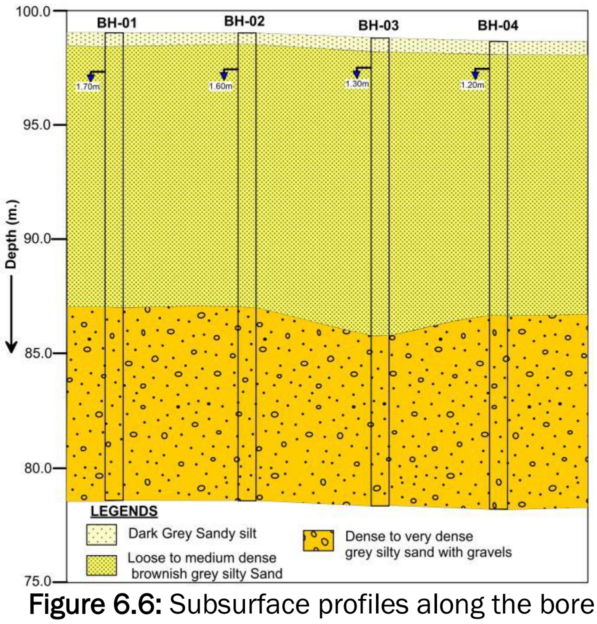

Figure 6.6: Subsurface profiles along the boreholes

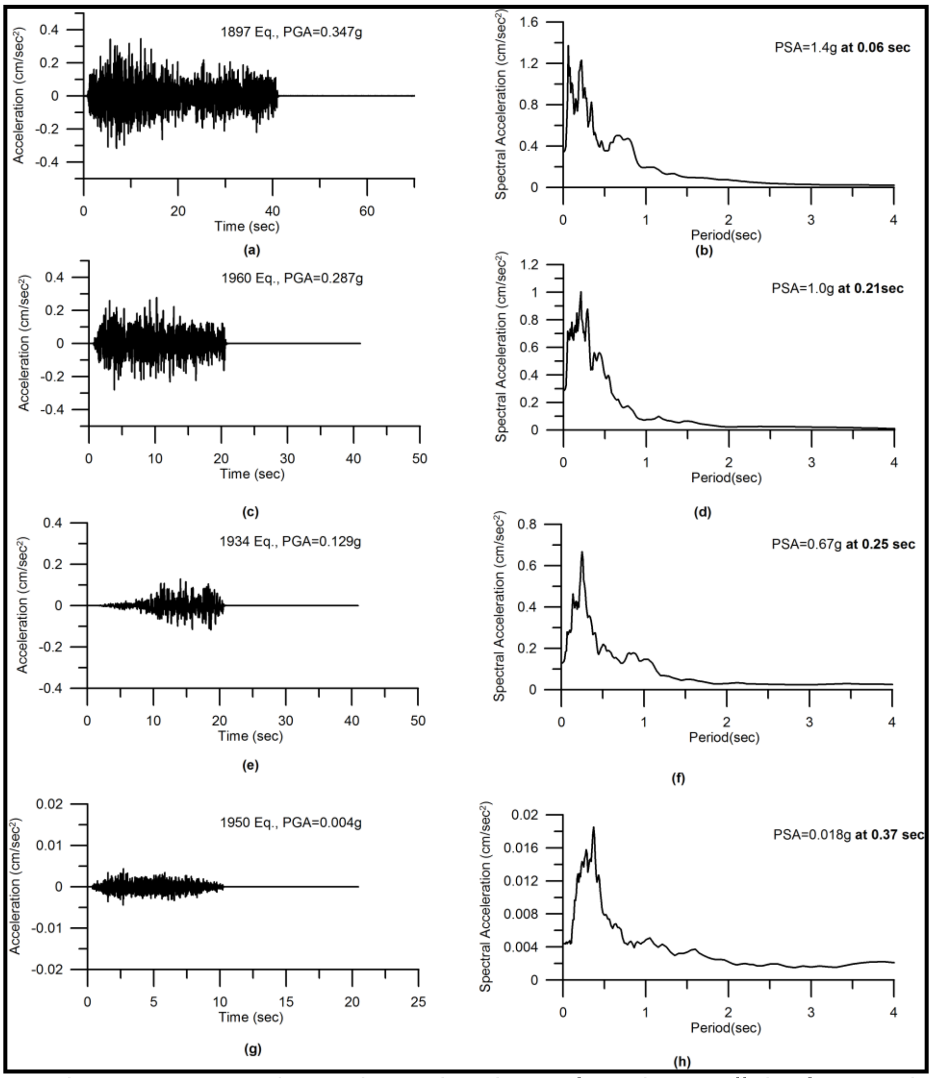

Figure 6.7: The maximum strong motion estimated at the surface due to all the four earthquakes

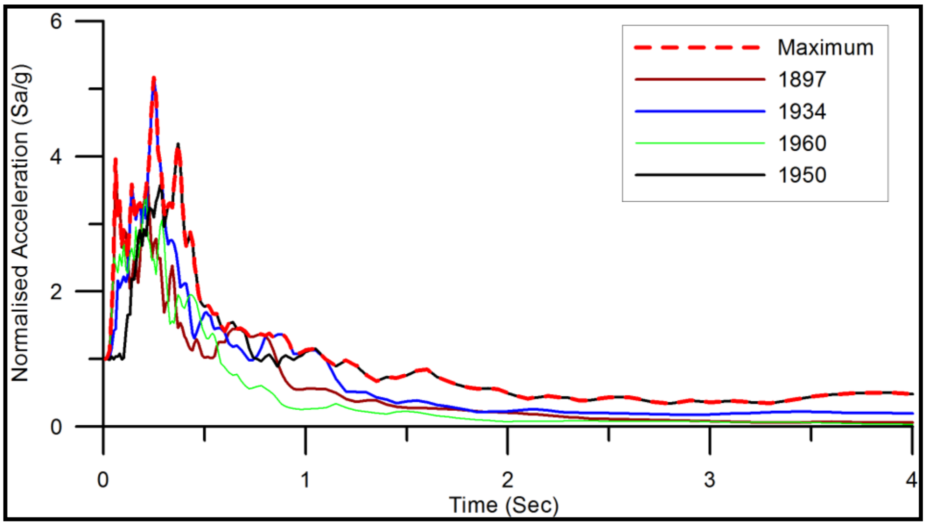

Figure 6.8: The normalized response spectra due to all the four earthquakes. The maximum among all four is also plotted.

6.3 Seismic hazard assessment of mounded LPG bullet plant at Bongaigaon Refinery, IOCL, Assam.

(Kapil Mohan, Naveen Kumar, Shruti Dagur and Sumer Chopra)

M/s Parsan Overseas (P) Limited, New Delhi has requested the Institute of Seismological Research to conduct seismic hazard assessment of mounded LPG bullet plant at Bongaigaon Refinery, IOCL, Assam.

The Soil Testing Report of 5 boreholes to a depth of 25m conducted by M/s Turnkey Investigating & Consulting Agency, Kolkata at the site was provided for the analysis. The geophysical survey comprising of ReMi was carried out by M/S Parsan Overseas (P) Limited and provided to ISR to constrain the engineering bedrock.

ISR has prepared the geological and seismotectonic maps of the area from the available resources. It is found that the study region is located in one of the most active seismic regions of the world and is assigned zone V by Bureau of Indian Standards (BIS). Three great earthquakes (M>8) have occurred around the region in the last 120 years (Fig. 6.9).

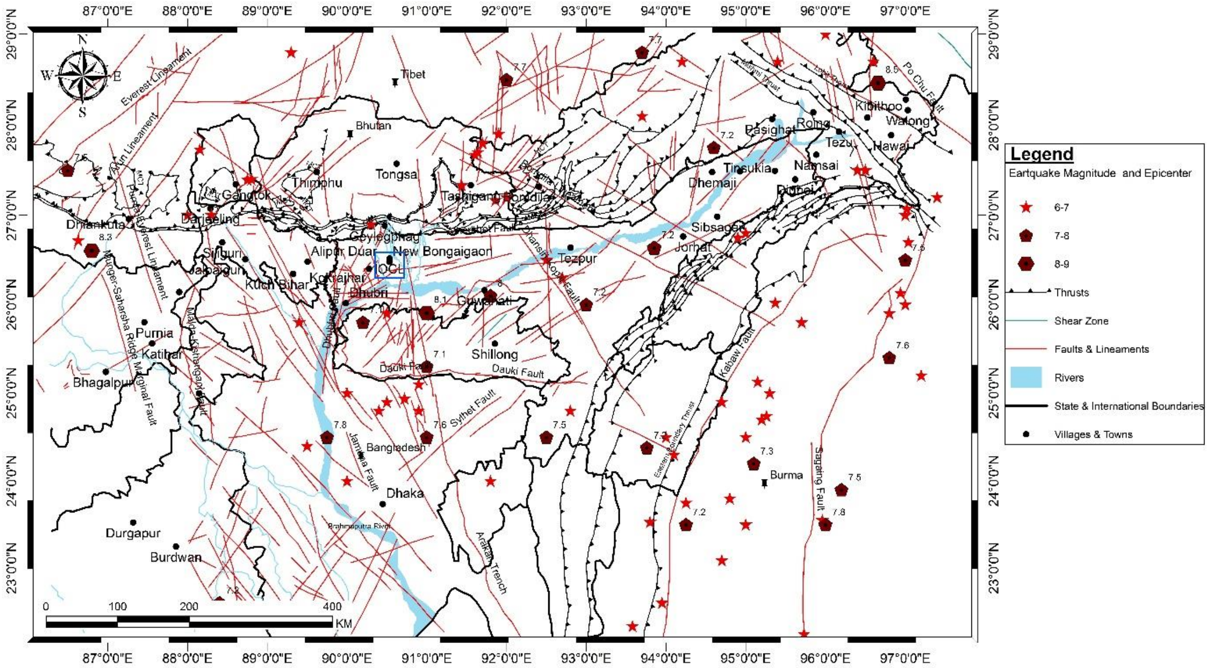

Figure 6.9: Seismotectonic Map of North-East India showing earthquakes M_W >6

The soil profiles of the 5 boreholes are shown in Fig. 6.10. The project site is located in the foothills of NE Himalaya to the south of the Main Boundary Thrust (MBT). In the drilled boreholes, clay is found down to a maximum depth of 7.5 m followed by dense to very dense Sand with Mica till termination depth (Fig. 6.10). In all the five boreholes, at about 25m, the N value reaches ~ 80 in soils comprising of very dense sand with Mica. Therefore, the EBL for the analysis is considered at 25m depth.

The dynamic corner frequency based stochastic finite source simulation method (Motazedian and Atkinson, 2005) is used in the present work to perform the deterministic seismic hazard analysis. This method effectively models large earthquakes too. In this modified method, the rupture history controls the frequency content of the simulated time series of each sub-fault. Raghukanth et al. (2008), Chopra et al., (2013) applied the same technique to estimate the ground motions in NE and Western India, respectively. Mohan et al. (2017) used the same technique to estimate the strong motion at bed layer level in the coastal locations of Gujarat. We have adopted this stochastic finite modeling technique to estimate the strong motion for a layer having Vs=760 m/sec because engineering bed layer is decided having this velocity.

The synthetic ground motions are estimated for (a) Far Field and (b) Near field earthquakes on the site. The 1950 Assam Earthquake (AS1950) of Mw 8.7 (epicenter located ~650 km NE of the site) and the 1934 Bihar Nepal earthquake of Magnitude Mw 8.1 (BN1934) (epicenter located ~ 360km west of the site) are considered as far-field earthquakes. The 1897 Shillong earthquake (SH1897) (epicenter about 90km south of the site) of magnitude Mw 8.1 and a scenario earthquake of M7.0 (epicenter of the 29th July 1960 earthquake, about 55km north of the site) (MB 1960) are considered as near-field earthquakes in the modelling of strong ground motions.

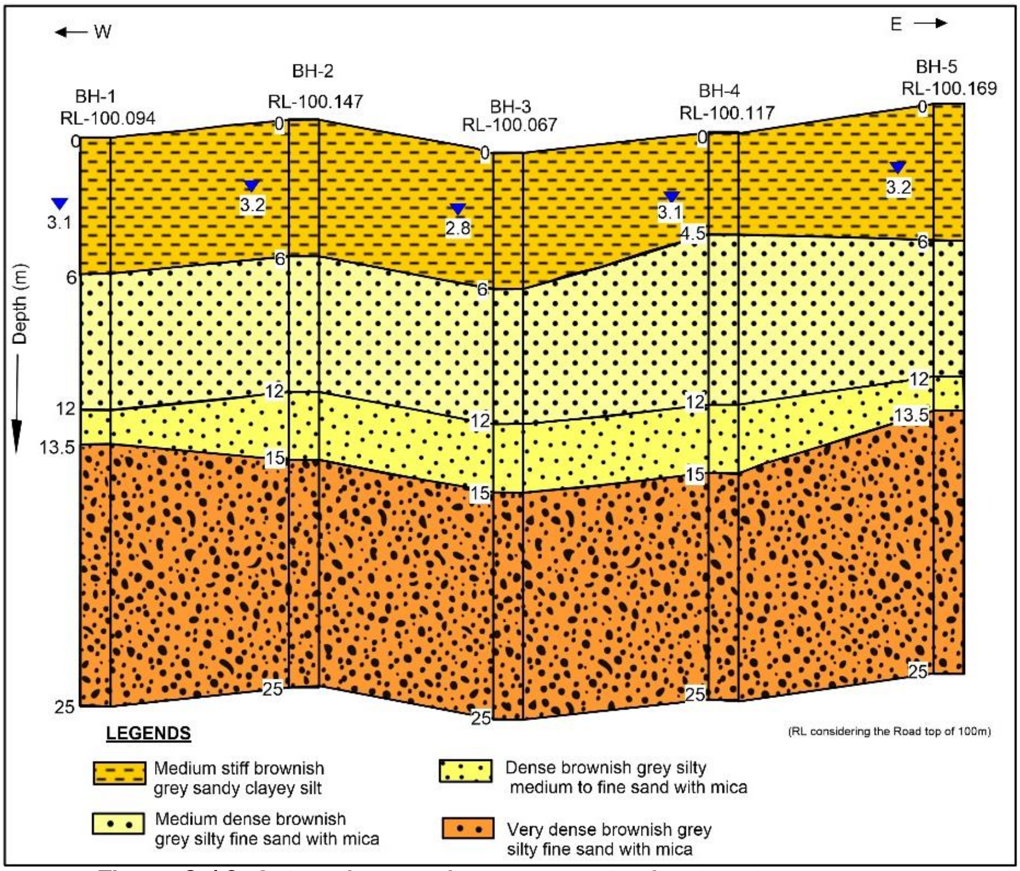

Figure 6.10: Subsurface profile along all the five boreholes.

The soil models at each borehole are prepared and ground response analysis is conducted to estimate the surface strong ground motion parameters (Peak Ground Acceleration, response spectra at 5% damping). The accelerogram and response spectra estimated at surface for 5% damping are given in Fig. 6.11. The normalized response spectra are determined for all the four earthquakes and the maximum at each period is considered to arrive at the site-specific response spectra. At the sites, the estimated maximum surface Peak Ground Acceleration (PGA) is 0.356g and the maximum Peak Spectral Acceleration (PSA) of 1.61 g is found at 0.24 sec. The Liquefaction potential at the site is estimated using PGA of 0.356g. The possibility of liquefaction is seen at a depth of 7.5-10.5m where medium dense silty fine sand is present.

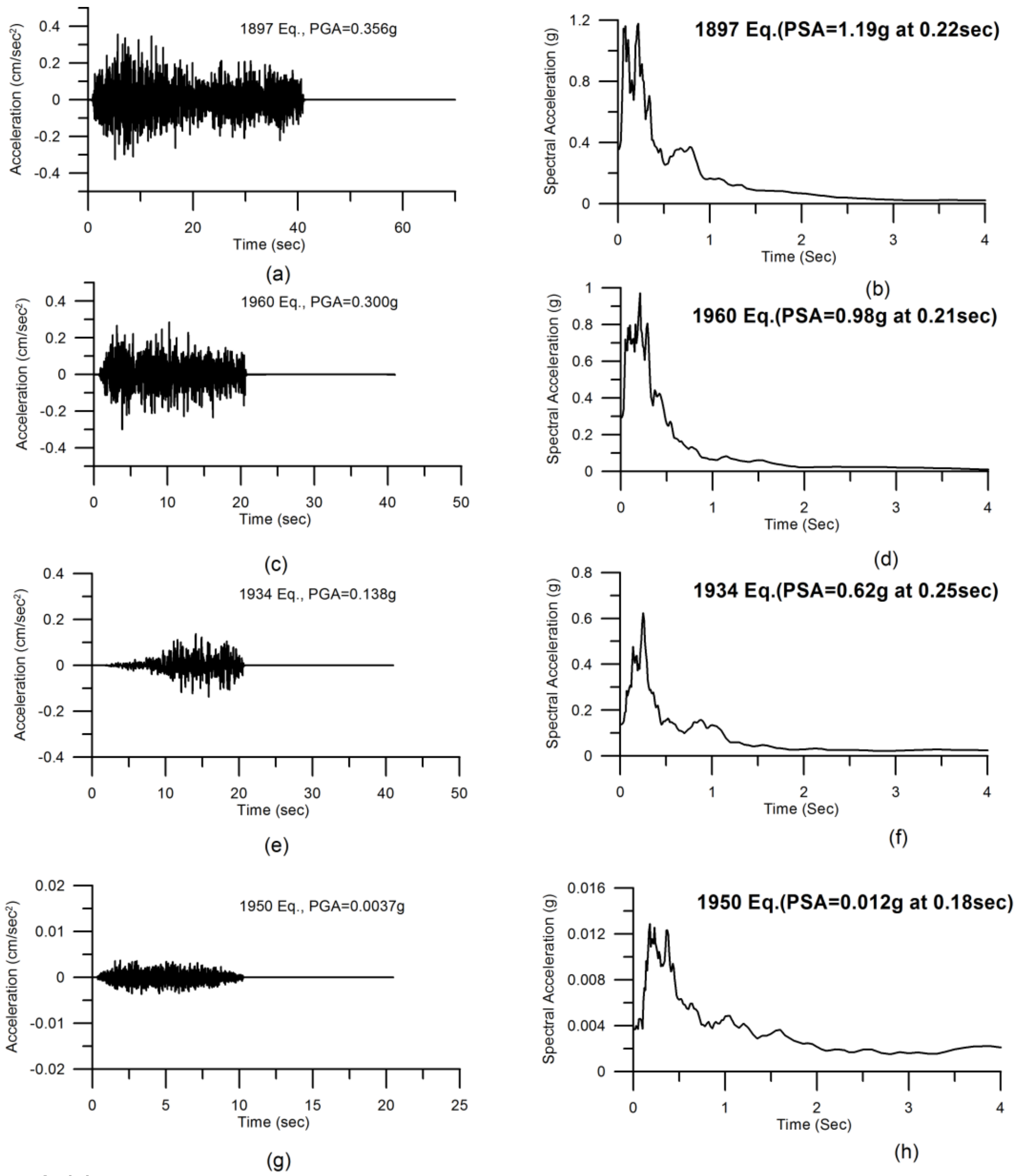

Figure 6.11: The Maximum Strong Motion estimated at surface due to all four earthquakes

6.4 Estimation of Mesozoic sediment thickness in the eastern part of Kachchh, Little Rann region

(*Kapil Mohan, Pruthul Patel and Peush Chaudhary)*

Magnetotelluric data was acquired at 23 sites along a profile starting from Adesar in the north to Dhangadra in the south (Fig. 6.12). The 1D resistivity section obtained from 1D Occam inversion is shown in Fig. 6.13. From this inversion, five different layers are identified down to 5km. The first layer with resistivity 1 to 3 Ohm.m has been observed with thickness varying from 400m followed by a layer of resistivity 3 to 5 Ohm.m having thickness of ~ 200m. The third layer with resistivity 7 to 11 Ohm.m with a varying thickness of about 1 km is observed in the north near Adesar village and ~200-300m in the south. The first layer is interpreted as Quaternary + Tertiary sediments followed by Miocene deposits. The fourth layer is interpreted as Mesozoic sediments. The basement is found below Mesozoic sediments, dipping to the north.

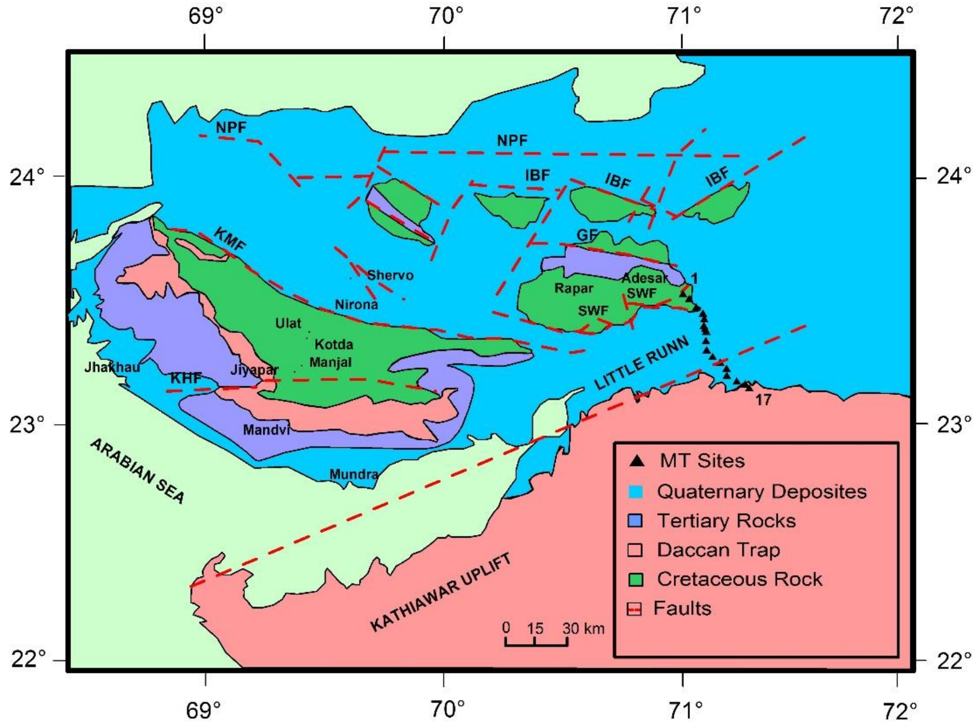

Figure 6.12: The location map of the MT profile (sites shows as black triangles).

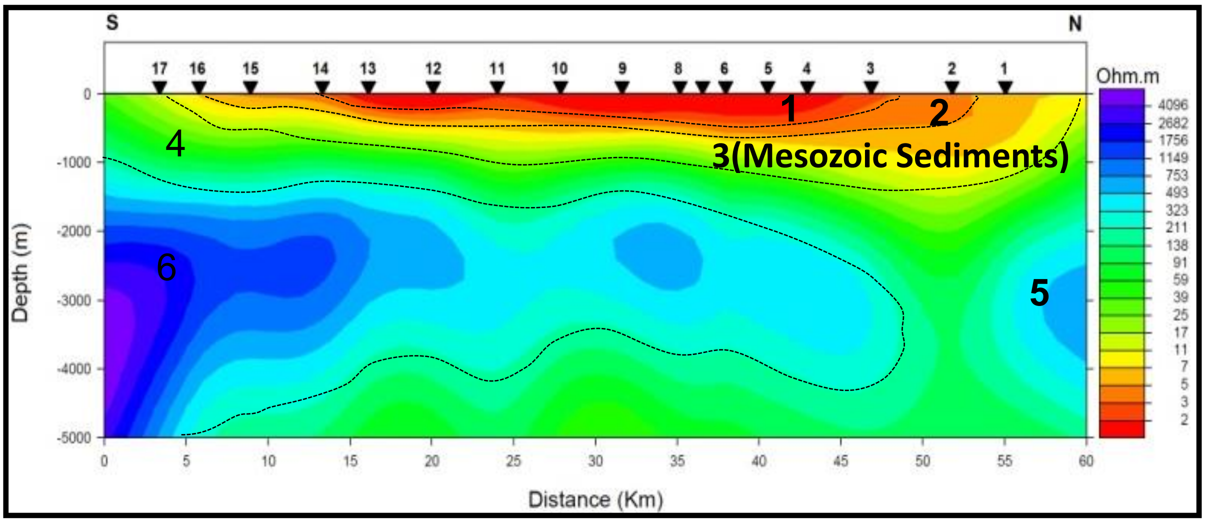

Figure 6.13: 1-D resistivity section along the profile. 1. Quaternary + Tertiary, 2.Miocene, 3.Mesozoic Sediments, 4.Basement.

6.5 Possible Geothermal process in the Tuwa Godhra region

(Kapil Mohan, Peush Chaudhary, G. Pavan Kumar, Girish Ch Kothyari, Virender Choudhary, Mehul Nagar, Pruthul Patel, Drasti Gandhi, Dilip Kuswah and B.K.Rastogi)

Usually, groundwater flows through a regional lithostratigraphic slope through permeable rocks (Todd and Mays, 2005). Presence of non-porous granitic body west of the contact zone barricades the groundwater to flow further west towards the regional slope. However, the groundwater might penetrate further down through the fissures and cracks. According to Singh and Chandershekharam (2010), the Tuwa thermal springs have high chloride concentrations. Stratigraphically, the Godhra granite rests over Paleoproterozoic carbonate rocks of Udaipur Formation and the Lunavada Group of

Aravalli supergroup is present in the east, separated by a contact zone (Figs. 6.14a & b). The Lunavada Group consists of quartzites and metapelites (chlorite schists, and garnet mica schists) (Gupta et al., 1992). The Champaner group of rocks have been inferred below the Godhra granite (Fig. 6.14b and c). The contact zone rocks of Lunavada and Champaner groups might become weathered (chemical weathering occurred) due to water percolation from the surface as suggested by Todd and Mays (2005). The contact zone becomes rich in chloride owing to the chemical reaction of water with the Lunavada group of rocks i.e. chlorite schists, and garnet mica schists. The presence of chloride in hot water from thermal spring samples might be driven from the weathered schistose rock of Lunavada group as illustrated in Fig. 6.14c. Tuwa has a very high geothermal gradient of 70°C/km (Chandrasekhar and Chandrasekharam, 2009) that can also generate a very high subsurface temperature. As the groundwater comes in contact with Paleoproterozoic rocks of Udaipur formation, it might react with the carbonate rocks and thereby be generating heat beneath the subsurface level (Fig. 6.14b). Due to the high geothermal gradient, the temperature becomes very high beneath 8 km depth level. The temperature generated by chemical reaction and the subsurface temperature might be responsible for heating and evaporation of groundwater (Fig. 6.14c). Hence, the hydrostatic pressure generated below 8 km depth may result in upward migration of groundwater through faulted and fractured litho-units in the form of hot springs. The hot spring in the area is present ~10 km southwest of the site C8 (Fig. 6.14a and Fig. 6.14c) at the contact zone of Godhra granite and basalt. The slope of the area follows the western trend (Fig. 6.14a), therefore, the water comes at the surface through the contact zone of Godhra granite and basalt, ~10km SW of the study area.

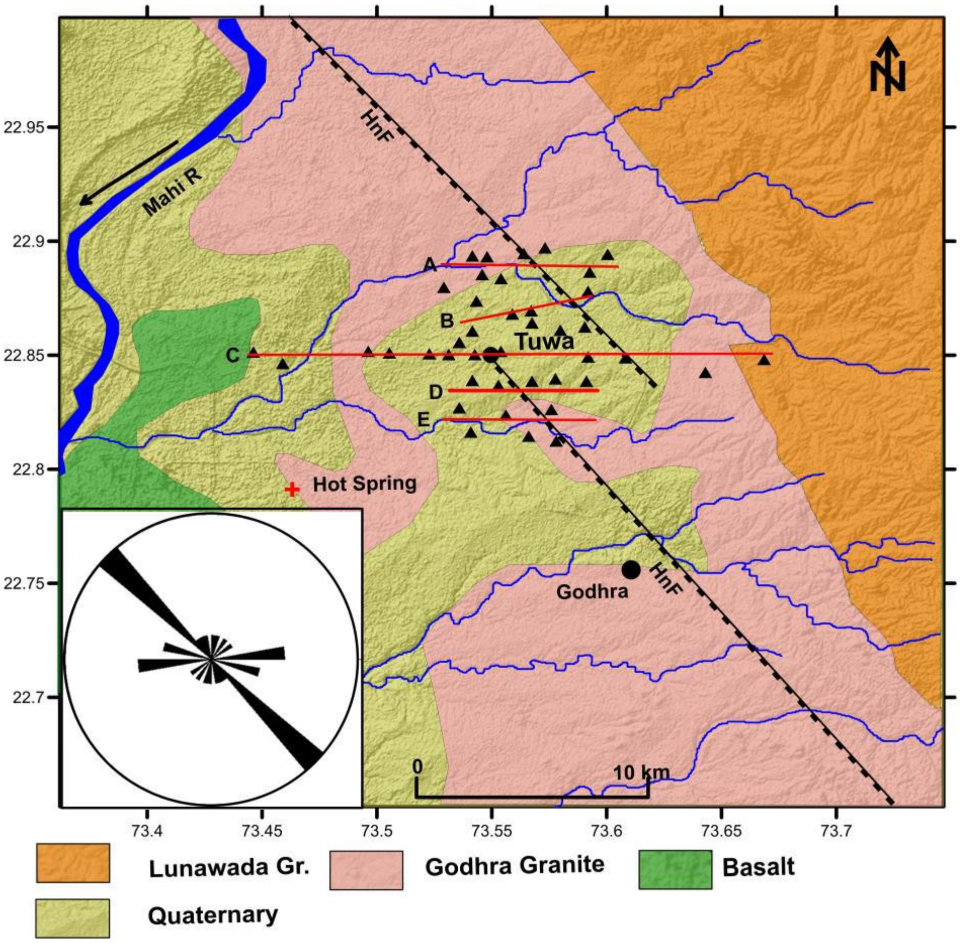

(a)

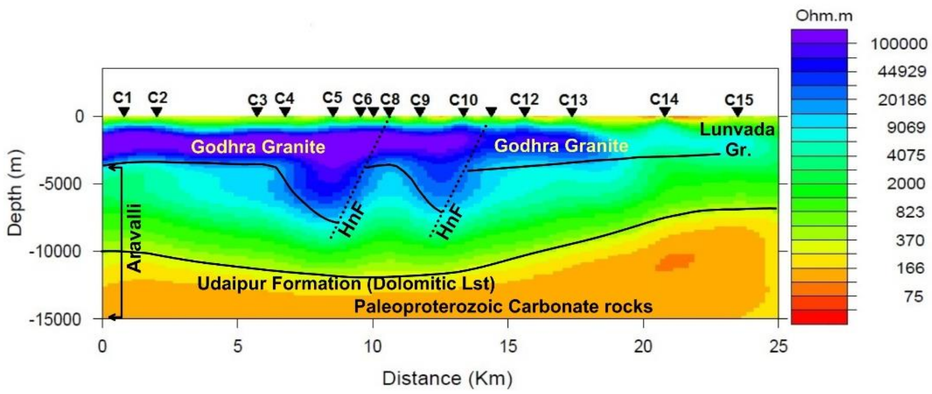

(b)

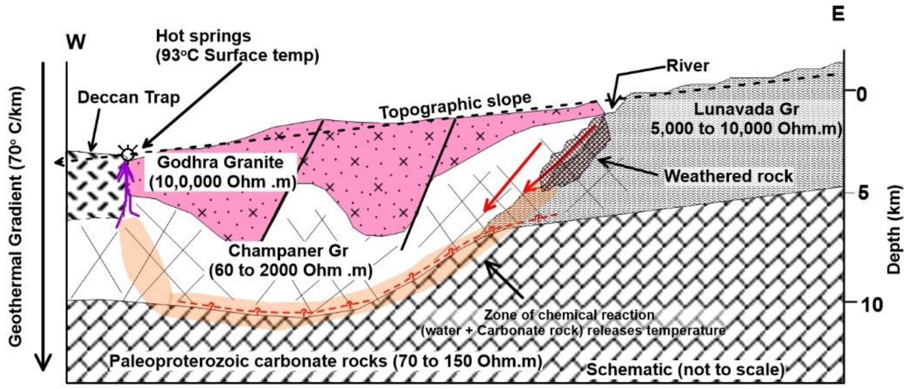

(c)

Fig. F14: (a) Geological and Tectonic map of Tuwa and surroundings, (b) geoelectric depth section and (c) the schematic diagram showing subsurface geothermal process.

PUBLICATIONS

Published

- Bhatt S., Shah R.D., Pancholi V., Dwivedi V.K., Bhatt N.Y. (2017), Index properties of soil of Sabarmati River, Gandhinagar district, Gujarat, Indian Journal of Scientific Research 16(1):144-150.
- Bhattacharya F., Shukla A.D., Patel R.C., Rastogi B.K., Juyal N. (2017), Sedimentology, geochemistry and OSL dating of the alluvial succession in the northern Gujarat alluvial plain (western India) - A record to evaluate the sensitivity of a semiarid fluvial system to the climatic and tectonic forcing since the late Marine Isotopic Stage Geomorphology 297, 1-19.
- Chingtham P., Prajapati S.K., Gahalaut V.K., Chopra S. and Roy P.S. (2017), Forecasting seismicity rate in the north-west Himalaya using rate and state dependent friction law, Geomatics, natural hazards and risk, doi: 10.1080/19475705.2017.1369168
- Chopra S., Kumar V., Choudhury P., Yadav R.B.S. (2017), Site Classification of Indian Strong Motion Network using Response Spectral Ratios, Jour. of Seismology, DOI: 10.1007/s10950-017-9714-9.
- Dubey R. K., Dwivedi V. K., Pancholi V., and Rastogi B. K. (2018), Relative Index of Seismic Hazard (RISH) and it's Implication in first order Seismic Hazard Assessment of Sabarmati River Basin, Gujarat, India, Indian Geophysical Union (IGU) 52-59.
- Dwivedi V.K., Dubey R.K., Thockhom S., Pancholi V., Chopra S. and Rastogi B.K. (2017), Assessment of Liquefaction potential of soil in Ahmedabad Region, Western India published in J. Ind. Geophys. Union, 21, (2), 116-123
- Haldar C., Kumar P., Kumar M.R., Ray L. and Srinagesh D. (2017), Seismic evidence for secular evolution and alteration of India crust: Precambrian Research, 304, 12-20.
- Imsong W., Bhattacharya F., Lochan R., Mishra S., (2017), Geomorphic Evidence of Late Quaternary Displacement of the Karakoram Fault in Nubra and Shyok valleys, Ladakh Himalaya. Current science 112(11):2295-2305.
- Jade S., Shrungeshwara T.S., Kumar K., Choudhury P., Dumka R.K. and Bhu H. (2017), India plate angular velocity and contemporary deformation rates from continuous GPS measurements from 1996 to 2015, Scientific Reports, 7: 11439, DOI:10.1038/s41598-017-11697-w.
- Joshi S., Simha C.P., Rao K.M. and Prasad M.S.B.S. (2017), Variations of total magnetic field before two small earthquakes during 2014 in Kachchh, Gujarat, India. J. IGU .21(3), 183-190.
- Joshi V., Chopra S., Mahesh P. and Santosh K. (2017), Joint Modeling of Velocity Structure and Hypocentral Locations in the Seismically Active Kachchh, Saurashtra, and Narmada Regions of Western India: An Active Intraplate Region. Seismological Research Letters, doi: 10.1785/0220160203
- Joshi V., Rastogi B. K., and Santosh K. (2016), Intraplate Seismicity along the Gedi fault in Kachchh rift basin of western India, Journal of Seismology, 21, 1641-1655
- K. Mohan, Gayatri P.K., Chaudhary P., Choudhary V.K., Nagar M., Khuswaha D., Patel P., Gandhi D. and Rastogi B.K. (2017) Magnetotelluric investigations to

identify geothermal source zone near Chabsar hot water spring site, Ahmedabad, Gujarat, Northwest India, Geothermics, 65, 198-209.

- K. Mohan, Chaudhary P., Patel P., Chaudhary B.S., Chopra S. (2018), Magnetotelluric study to characterize Kachchh Mainland Fault (KMF) and Katrol Hill Fault (KHF) in the western part of Kachchh region of Gujarat, India, Tectonophysics 726, 43-61.
- Kothyari G.C., Chopra S. and Kumar M.R., Shallow subsurface investigations for resource exploration and hazard estimation, CURRENT SCIENCE, VOL. 113, NO. 380 3, 10 AUGUST 2017
- Kothyari G.C., Singh A.P., Mishra S., Kandregula R.S., Chaudhary I., Chauhan G. (2018), Evolution of drainage in response to brittle - ductile dynamics and surface processes in Kachchh Rift Basin, Western India, Tectonics Book.
- Kumar M.R., Singh A., Bhaskar Rao Y.J., Srijayanthia G., Satyanarayanaa H.V. and Sarkar D., Vestiges of Precambrian subduction in the south Indian shield? – A seismological perspective, Tectonophysics 740–741 (2018) 27–41
- Pancholi V., Kothyari G.C., Prizomwala S., Sukumaran P., Shah R.D., Bhatt N.Y., Chauhan M. and Kandregula R.S. (2017), "Morphotectonic of Sabarmati-Cambay basin, Gujarat, Western India", J. Ind. Geophys. Union, v.21, no.5, pp: 371-383
- Prajapati S.K., Dadhich H.K., Chopra S., Isoseismal map of the 2015 Nepal earthquake and its relationships with ground-motion parameters, distance and magnitude, Journal of Asian Earth Sciences (2016), http://dx.doi.org/10.1016/j.jseaes.2016.07.013
- Rohilla S., Kumar M.R., Rao N.P. and Satyanarayana H.V.S., Shear-Wave Velocity Structure of the Koyna–Warna Region, Western India, through Modeling of P-Receiver Functions, Bulletin of the Seismological Society of America, Vol. XX, No. XX, pp. –, – 2018, doi: 10.1785/0120160395
- Sahoo S.K., Rao K.M., Shaji J.P., Murali Krishna K.S., (2018), 'Influence of meteorological parameters on the soil-radon (Rn^{222}) emanation in Kutch, Gujarat, India', Environmental Monitoring and Assessment, 190:111, pp 1-20, https://doi.org/10.1007/s10661-017-6434-0
- Saikia S., Baruah S., Chopra S., Singh U.K., Gogoi B. and Gohain H.B., Study of crustal structure and geological implications of southwestern margin of Northeast India, J Seismol, DOI 10.1007/s10950-017-9701-1
- Saikia S., Chopra S., Baruah S., and Singh U.K., Shallow Sedimentary Structure of the Brahmaputra Valley Constraint from Receiver Functions Analysis, Pure Appl. Geophys., DOI 10.1007/s00024-016-1371-3
- Sairam B., Singh A. P., Kumar M.R. (Accepted: October 09, 2017), Comparison of Earthquake Source Characteristics in the Kachchh Rift Basin and Saurashtra horst, Deccan Volcanic Province, Western India, Journal of Earth System Science, DOI: 10.1785/0120160276
- Satyavani N., Kumar M.R. and Sain K., Wavefield decomposition of multi-component obs data to enhance the seismic signal, N.Satyavani, M.Ravi Kumar and Kalachand, v.22, no.2, pp: 138-142
- Singh A.P., Parmar A., Chopra S. (2017), Microtremor study for evaluating the site response characteristics in the Surat City of western India, Natural Hazards, DOI: 10.1007/s11069-017-3012-2
- Thokchom S., Bhattacharya F., Durga Prasad A., Dogra N.N., Rastogi B.K. (2017), Paleoenvironmental implications and drainage adjustment in the middle reaches

of the Sabarmati River, Gujarat: Implications towards hydrological variability, Quaternary International, 454, 1-14.

- Thokchom S., Rastogi B.K., Dogra N.N., Pancholi V., Sairam B., Bhattacharya F., and Patel V. (2017), "Empirical correlation of SPT blow count vs Shear wave velocity for different soil in Dholera", Natural Hazard doi:10.1007/s11069-017-2744-3
- Thokchom S., Rastogi B.K., Dogra N.N. and Pancholi, V. (2017), Geotechnical investigations in the southern part of Ahmedabad district, Gujarat, India published in J. Ind. Geophys. Union, 21(2), 105-115
- Thokchom S., Pancholi V., Rastogi B. K., and Dogra N. N. (2018), Liquefaction potential mapping in Dholera region of western India. Natural Hazards. https://doi.org/10.1007/s11069-018-3214-2

Under review/ communicated

- Azeez A., K. Mohan, Veeraswamy K., Rastogi B. K., Gupta A.K., Harinarayana T., 3D crustal resistivity structure beneath the Wagad aftershock zone of the 2001 Bhuj earthquake, Kutch, India: Heterogeneous resistivity structure controlled by widespread fluid infiltration and clues to aftershocks pattern submitted to Tectonophysics.
- Bhatt N., Bhatt N.Y., Pancholi V., Kothyari G.C. (March-2018), Geomorpho-Tectonics evolution of Sabarmati basin, Gujarat, Western India, Conference on Emerging trends in Geophysical Research for Make in India (ETGRI), pp194, 9-11, March-2018.
- Chaudhary P., K. Mohan and Chaudhary B.S., Magnetotellurics study to identify subsurface structure in the eastern part of Kachchh (Little Rann area) of Gujarat, India, submitted to Pure and applied geophysics.
- Chauhan A. (2017), New insight of crustal structure of Cambay basin using EIGEN-6C4 gravity data, J. Asian Earth Sciences (Under review)
- Das A., Prizomwala S.P., Chauhan G., Solanki T., Makwana N., Thakkar M. G. (2017), Are dryland fluvial systems ~ a plausible archive for palaeoclimatic reconstruction during the Late Quaternary Period? A review from the Southern Kachchh Mainland, Western India, Sedimentary Geology (Under Review).
- Das A., Prizomwala S. P., Solanki T., Chauhan G., Chopra S., Chauhan A., Thakkar M. G., Bhatt N.Y. (2017), Katrol Hill Fault (KHF): Seismic landscape from Southern Kachchh Mainland, Western India: Restraints from Geomorphometry and Seismology in an Intraplate Environment (Geological Magazine, Submitted).
- Das A., Prizomwala S.P., Vedpathak C., Sodhi A., Makwana N. (2018), Sedimentological, geochemical and chronological constraints from a palaeochannel near Lothal ~ a Harappan dockyard: Implications for palaeoenvironmental changes during the Middle to Late Holocene period, Quaternary International (Under Review)
- Dubey R.K., Dwivedi V.K., Pancholi V. and Rastogi B.K., Relative Index of Seismic Hazard (RISH) and its implication in first order Seismic Hazard Assessment of Sabarmati river basin, Gujarat, India. (In Press).
- Dumka R.K., Choudhury P., Gahalaut V. K., Gahalaut K., Yadav R.K. (2017) , GPS measurements of deformation caused by the seasonal filling and emptying cycles of four hydroelectric reservoirs in India, communicated to BSSA.
- Dwivedi V.K., Dubey R.K., Pancholi V., Singh P. and Chopra S. (March-2018), Geotechnical characteristics of soils to identify sub stratification of Ahmedabad

city, Gujarat, Western India. Conference on Emerging trends in Geophysical Research for Make in India (ETGRI), pp107, 9-11, March-2018.

- Gahalaut K., Gupta S., Gahalaut V.K., Mahesh P., (2017), Influence of Tehri reservoir impoundment on local seismicity of NW Himalaya, BSSA (Under review).
- Gandhi D., Prizomwala S. P. and Bhatt N.Y. (2017), From remote sensing to coastal processes: An integrated approach for hunting extreme wave events, communicated to Geomorphology.
- Geoelectrical investigation for groundwater resources and aquifer characteristics at parts of Ahmedabad and Gandhinagar cities, Gujarat, Current science (Under Review).
- Haldar, C., P. Kumar, M. R. Kumar., L. Ray, On the nature of Indian Moho, Tectonophysics, 2017 (Under Review)
- Joshi N., Singh S., Pant P. D., Kumar M., and Kothyari G. C. (2017), Polyphase Kinematics and Quaternary reactivation of Baijnath Klippe: Western Kumaun Himalaya. Communicated to Geological Journal, Willy library GJ-17-0418 (under review)
- Joshi V., Chopra S. and Santosh K. (2017), A Local Magnitude Scale ML for the Kachchh rift basin: an active intraplate region, Gujarat, India. Bulletin of the Seismological Society of America (BSSA).
- K. Mohan, Chaudhary P., Pavan Kumar G., Kothyari G.C., Choudhary V., Nagar M., Patel P., Gandhi D., Kuswaha D. and Rastogi B.K., Magnetotelluric investigations in Tuwa-Godhra region, Gujarat (India), Revision submitted to Pure and Applied Geophysics in Jan. 2018.
- K. Mohan, Rastogi B.K., Pancholi V. and Gandhi D. (2017), Seismic Hazard Assessment at Micro Level in Gandhinagar (the Capital of Gujarat) considering soil Effects, communicated to Soil Dynamics and Earthquake Engineering.
- Kothyari G.C., Joshi N., Taloor A., Kandregula R.S., Pant C.C. (2018), Deduction of surface deformation in Soan Dun area of 1905 Kangra earthquake zone in NW Himalaya: A geomorphic approach, Communicated to Geological Society of American Bulletin.
- Kothyari G.C., Kandregula R.S., Chauhan G. (2018), Geomorphic and Paleoseismological evidence of North Dipping active Kachchh Mainland Fault, Kachchh, India, Communicated to Arabian Journal of Geosciences.
- Kothyari G.C., Kandregula R.S., Pancholi V., Shah N. (2018), Identification of fluvial stratigraphy using shallow subsurface geophysical and field investigations: A case study from Sabarmati River terraces, Mainland Gujarat, communicated to Pure and Applied Geophysics.
- Kothyari G.C., Prizomwala S.P., Kandregula R.S., Desai B.G. (2018), Quaternary Landform development in the Central segment of tectonically active Kachchh Mainland Fault zone, Western India, Communicated to Open Quaternary.
- Kothyari G.C., Shirvalkar P., Kandregula R.S., Rawat Y., Dumka R.K. (2018), Holocene tectonic activity along Kachchh Mainland: Impact on Late mature Harappan Civilization, Kachchh, Western India, Communicated to Quaternary International.
- Kothayri G.C., Singh A. P.¸ Mishra S., Kandregula R.S., Chaudhary I., Chauhan G. (2018), a book chapter Evolution of drainage in response to brittle - ductile dynamics and surface processes in Kachchh Rift Basin, Western India: Tectonics
- Makwana N., Prizomwala S.P., Chauhan G., Phartiyal B., Thakkar M.G. (2018), Late Holocene palaeo-environmental change from the Banni Plains, Kachchh, Western India, Quaternary International. (Under Review)

- Naveen K., K. Mohan, Dumka R.K. and Chopra S., Evidence of neotectonism in Quaternary sediments from Dadra and Nagar Haveli, Western India, submitted to Quaternary International.
- Observation of Free Oscillations after the 2010 Maule and 2011 Tohoku earthquakes by superconducting gravimeter in Kutch, Gujarat, India, Cryogenics (under review)
- Pancholi V., Bhatt N.Y., Dwivedi V.K., Thokchom S., Choudhury P., Chopra S. (2018), Assessment of liquefaction hazard in Gandhinagar city, Gujarat, Western India, Bulletin of Engineering Geology and Environment (under review).
- Pancholi V., Dwivedi V.K., Choudhury P., Thokchom S., Sairam B., Chopra S. and Bhatt N.Y., Engineering Geological Mapping of Gandhinagar city, Gujarat, Western India. Abstract submitted to Indian Geotechnical Conference 2017, which will be held in December 2017.
- Paul H., Kumar M.R., Tiwari V.M., Singh A., Chadha R. K. and Srinagesh D. (2017), Density contrast across the Moho beneath the Indian shield: Implications for isostasy, Journ. of Asian Earth Sci. (Under review,)
- Pavan Kumar G., Chaudhary I., Nagar M., Chouhan A., Prizomwala S.P. and Mahesh P. (2017), Transient Electromagnetic investigations in a tectonic domain of the Kachchh intraplate region, western India: A morphotectonic view of splays and colluvial wedges. Tectonics (Revision submitted)
- Pavan Kumar G. and Mahender E. (2017), Trasnsient electromagnetic imaging of Khari River Palaeochanel, Bhuj, Western India. Near Surface Geophysics. (under reveiw)
- Pavan Kumar G., Nagar M., Chaudhury V., Mahendhar E. et al. (2017), Shallow subsurface imaging of the Wagad active fault system (Kachchh, northwestern India) by time domain electromagnetic studies. J. Earth Sys. Sci. (Under review)
- Prizomwala S. P., Gandhi D. , Bhatt N.Y., Winkler W. , Kumar M.R., Makwana N., Bhatt N. (2018), Geological evidence for AD 1008 tsunami along the Kachchh coast, Western India: Implications for recurrence along the Makran Subduction Zone, Nature Scientific Report (Under Review)
- Prizomwala S.P., Yadav G., Solanki T., Chauhan G., Makwana N., Das A. (2018), Style and stages of valley fill aggradation-incision cycles in the Northern Hill Range, kachchh, Western India, Sedimentary Geology (Under Review)
- Rout M.M., Chopra S. and Sairam B. (2018), Probabilistic seismic hazard assessment at surface level for Gujarat state, Western India-an active intraplate region. Bulletin of Earthquake Engineering Journal (under review).
- Rout M. M., Das J. D. and Kamal (2018) Probabilistic seismic hazard for Himalayan region using Kernel Estimation Method (Zone Free Method) (under revision).
- Sahoo S.K., Rao K. M., Kumar C. and Barman C. (2017), Empirical Mode Decomposition based Hilbert Huang Transform on Soil Radon (Rn^{222}) data of Kutch, Gujarat, India: Identification of Daily quasi-periodic oscillations and Earthquake precursors, Earth, Planets and Space (under review)
- Sahoo S.K., Rao K.M., Shaji J.P., Murali Krishna. K.S., 'Influence of meteorological parameters on the soil-radon (Rn^{222}) emanation in Kutch, Gujarat, India', Environmental Monitoring and Assessment.
- Sahoo S.K., Rao K.M., Simha C.P. and Prasad M.S.B.S. "Removal of Diurnal and Semi-diurnal variations in Soil Radon (Rn^{222}) time series for the study of the short-term geochemical precursor to Earthquake at Kachchh, Gujarat, India", Acta Geophysica.

- Sairam B., Singh A.P. and Kumar M.R. (2018), Comparison of Earthquake Source characteristics in the Kachchh Rift Basin and Saurashtra horst, Deccan Volcanic Province, Western India, Journal of Earth System Science (Accepted).
- Sairam B. , Singh A. P., Patel V., Pancholi V., Chopra S., Dwivedi V. K. and Kumar M.R. (2018), Influence of Local Site Effects in the Ahmedabad Mega city on the Damage Due to Past Earthquakes in Northwestern India. BSSA, (under review).
- Santosh K., Dinesh K., Rastogi B.K. and Singh A.P. (2018), Kappa model for Kachchh region of Western India, Geomatics, Natural Hazards and Risk, 9:1, 442-455, DOI: 10.1080/19475705.2018.1447025 (Accepted)
- Simha C.P., Rao K.M., Dumka R.K., Spatial and Temporal behaviour of ionospheric VTEC during the shallow earthquake of Newzealand (Mw 7.8) on 13th November 2016, Advances in Space Research (under review)
- Simha C.P., Rao K.M., Prasad M.S.B.S. and Dumka R.K., "Observation of Atmospheric and Ionospheric anomalies for the Nepal Earthquakes on 25th April and 12th May 2015, submitted to Earth Planetary Science (EPS) journal
- Solanki T., Das A., Makwana N., Prizomwala S.P., Solanki P. M., Fluvial response of dryland rivers to sea level changes in western India: Late Pleistocene-Holocene period, Sedimentary Geology (Under Review).
- Solanki T., Prizomwala S. P. and Solanki P. M. (2018), Geomorphic Expressions of Active Strike-slip faulting (Girnar Fault), Saurashtra, Western India, IGU (Minor revision submitted).
- Solanki T., Solanki P.M., Makwana N., Prizomwala S.P., Kothyari G.C. "Geomorphic response to neotectonic instability in a Deccan volcanis province, Shetrunji River, western India: Insights from remote sensing and field investigation", Geological Journal (Under Review).
- Talukdar R., Kothyari G. C. and Pant C. C. (2017), Evaluation of Neotectonic variability along major Himalayan thrusts within the Kali River Basin using geomorphic markers; Central Kumaun Himalaya, Geological Journal, Willy library GJ-17-0479 (under review).

Technical Reports

- Final Report "Seismic Hazard Assessment of LNG Terminal at Dhamra, Odisha", ISR Technical Report No. 112. Project PI: Dr. Kapil Mohan; Project coordinator: Dr. Sumer Chopra; Major contributors: Sh. Naveen submitted, Ms. Vandana Patel, Dr. Madan Mohan Raut and Dr. B. Sairam submitted to M/s Dhamra LNG Terminal Pvt. Ltd., Ahmedabad and submitted in May 2017.
- Mahesh, P, A.P. Singh, Aadil Hussain, Santosh Kumar, M. Ravi Kumar & Sumer Chopra., (2018). Local earthquake tomography (LET) studies around the dam site of Bursar project, Jammu & Kashmir, NHPC ltd., ISR Tech. Rep.
- Seismic Hazard Assessment of mounded LPG bullet plant at Bongaigaon Refinery, IOCL, Assam, ISR Technical Report No. 114. Project Principal Investigator Dr. Kapil Mohan; Project coordinator: Dr. Sumer Chopra; Co- PI: Sh. Naveen Kumar, contributor: Ms. Shruti Dugar, submitted to M/s M/s Parsan Overseas (P) Limited, New Delhi, in July 2017.
- Report on "Generation of Site Specific Response Spectra at IOCL Bongaigaon Refinery, Assam State, India, ISR Technical Report No. 115. Project Principal Investigator Dr. Kapil Mohan; Project coordinator: Dr. Sumer Chopra; Co- PI: Sh.

Naveen Kumar, contributor: Ms. Shruti Dugar, was submitted to M/s L&T Chiyoda, Vadodara, in August 2017.

- 2nd Report on " Seismic Hazard Assessment of Devni Mori Site", ISR Technical Report 116, Principal Investigator Dr. Kapil Mohan; Project coordinator: Dr. Sumer Chopra; Co- PI: Dr. B. Sairam and Vasu pancholi; Major Contributors: Dr. Pavan Gayatri, Mr. Naveen Kumar, Mr. Mayank Dixit, Ms. Vandana Patel; Mr. Project Contributor: Mr. Dheerendra Mani Tripathi, Mr. Mehul Nagar and Mr. Pritesh Chauhan submitted to Tourism Corporation of Gujarat Ltd., in August 2017.
- Mahesh, P., Santosh Kumar, Ravi Kumar, M., Chpora, S., (2017). Earthquake data processing and interpretation of MEQ data collected during Jan. to Dec. 2016 for study the of Seismogenic sources around the Subansiri lower H.E. project, ISR, Tech.Rep.117.
- Final project report (ISR Technical Report-118) "3-D surface wave group velocity distribution and attenuation Structure of the Gujarat, India" (Project No.:- SR/FTP/ES-69/2013; Date: - 22.04.2014) was submitted to Science and Engineering Research Board, New Delhi by Dr. A. P. Singh, Principal Investigator.
- Final report (ISR Technical Report-119) of DST-RFBR research project "Study of 3D seismic structure of the crust and upper mantle beneath the Kachchh region of western India using seismic tomography and its geodynamic interpretation" (Ref. INT/RUS/RFBR/P-208: Dated 08.10.2015 was submitted to Department of Science and Technology, Government of India by Dr. A. P. Singh, Principal Investigator.
- Final Indo-Taiwan research project (ISR Technical Report-120) report "Full 3-D waveform tomography and Lg attenuation for Kachchh, Gujarat, India" (GITA/DST/TWN/P-62/2014; Dated April 30, 2014) was submitted to Department of Science and Technology, Government of India by Dr. A. P. Singh, Principal Investigator.
- Draft Final report of the project entitled "Generation of Site specific Response Spectra at IOCL Bongaigaon Refinery, Assam State, India" submitted to L&T Chiyoda. PI: Dr. Kapil Mohan, Project Coordinator: Dr. Sumer Chopra, Co-PI: Naveen kumar and contributiors: Dr. Madan Mohan and Ms. Shruti Dugar, ISR Technical Report No.122, submitted in February-2018.
- Progress Report of the project entitled "Operational definition of seismic risk and intervention Technique for strategic buildings: an integrated system on HPC platform" submitted in June 2017 by Dr. Kapil Mohan.
- Progress Report of the project entitled "Seismic Hazard Assessment of Dadra & Nagar Haveli (U.T.), Project PI: Dr. Kapil Mohan; Project coordinator: Dr. Sumer Chopra; Project Co-PI: Naveen Kumar; Major contributors: Sh. Vandana Patel; Participant: Sh. Pruthul Patel submitted to Dadra and Nagar Haveli Disaster Management Cell in April 2017.
- Annual Progress Report of the project entitled "To map the subsurface nature and extension of the Kachchh Mainland Fault (KMF) through magneto-telluric and geoelectrical methods along the entire length of the KMF zone" PI: Dr. Kapil Mohan; Co-PI: Mr. Pavan Gayatri and Dr. Rakesh Dumka submitted to Ministry of Earth Sciences, Govt. of India.

NOTABLE EVENTS

Awards/Recognition

- Dr. Arjav Shukla has been awarded a PhD degree from Department of Geology, Kachchh University. The title of his thesis is **Site response study and seismic hazard mitigation in some urban areas of kachchh intra plate basin**.
- Ms. Drasti Gandhi defended her PhD viva and received the provisional degree.
- Science, Technology and Innovation (STI) Policy for the Gujarat state prepared with the participation of ISR scientists is approved by Hon'ble Chief Minister of Gujarat. The Government released this STI Policy (2018-2023) and it is a GR. Now, it is implemented in Gujarat and Crores of Rupees are expected to be invested in Science, Technology and Innovation.
- Dr. K.M. Rao represented DST, Government of Gujarat during the Indian Science Congress held at Imphal, Manipur during March 16-20, 2018. He received the award for best among all the states in Indian Science Congress-2018. The award was given by Hon'ble Governor of Manipur Dr. Najma Hepthulla
- Ms. Aashima Sodhi was awarded the prestigious “Inspire Fellowship”

MoU’s Signed

- An MoU was signed with the Faculty of Technology, CEPT University, Ahmedabad on 15th September 2017.
- An MoU has been signed between ISR and Gujarat Technical University on 09.01.2018 for mutually beneficial cooperation in the areas of seismology, disaster preparedness and civil engineering related to Heritage structures of Gujarat to implement joint research projects for overall sustainable development and improvement of Heritage Tourism in Gujarat.

Meetings/ conferences attended/ papers presented

- Following papers/ posters were presented during the 54th Annual Convention of Indian Geophysical Union (IGU), held during 03.12.2017 to 07.12.2017 at NGRI, Hyderabad
  - Mahesh, P., G. Pavan Kumar and M. Ravi Kumar. Fluid driven earthquakes in the intraplate region of Kachchh, Northwestern (NW) India: An insight from local earthquake tomography.
  - B. Sairam, A. P. Singh, Vandana Patel, Sumer Chopra and M. Ravi Kumar, Soil classification and VS30 mapping for seismic site effect estimation in Gujarat region, Western India.
  - A.P. Singh, M. Ravi Kumar and Santosh Kumar, Seismic Tomography in Deccan Volcanic Province of Western India: Crust-Mantle Velocity Structure and Intraplate Seismicity.
  - B. Sairam, A. P. Singh, Vandana Patel and Sumer Chopra, Soil classification and V_{S30} mapping for seismic site effect estimation in Gujarat region, Western India.

  - Pavan Kumar, M. Ravi Kumar and P. Mahesh. Are trapped fluids transported from deep crustal depths responsible for microseimic activity in the Kachchh intraplate region?
  - Thokchom S., Sairam B., Pancholi V., Patel V. and Chopra S, Evaluation of Liquefaction Resistance based on Shear Wave Velocity in Southern Region of Ahmedabad, near Gulf of Cambay.
- Following papers/ posters were presented during the National conference on "Emerging Trends in Geophysical Research for Make in India (ETGRMI-2018)" held at Indian Institute of Technology (ISM), Dhanbad during 09.03.2018 to 11.03.2018.
  - Haldar, C., Kumar, P. and Santosh Kumar, Estimation of shear wave velocity contrast across Moho in Gujarat Region.
  - Smita Mishra, A. P. Singh, Santosh Kumar and G. Mohan, Hypocenter relocation using a 3D seismic velocity model in the Northwest Deccan Volcanic province of India.
  - Rashmi, A. P. Singh and P. K. Khan, Subsurface structure in the Eastern Indian Shield region using ambient vibration.
  - Chouhan, A. K., Singh, D., Chaube, H., Nikam, R., Mehul Nagar and G. Pavan Kumar, *Delineation of structural features over Ambaji mineralization zone, Gujarat, NW India using gravity and magnetic data*.
  - Chaube, H., Indu Chaudhary, A. Durga Prasad, Rakesh Nikam, Dinesh Singh and G. Pavan Kumar, *Shallow subsurface image of the Katrol Hill and its subsidiary branch faults, Kachchh using Transient electromagnetic investigations*.
  - NiKam, R., Singh, D., Indu Chaudhary, Himanchu Choube, Durga Prasad and Pavan Kumar, *Is faults act as barrior for vertical groundwater flow? Case study from Kachchh, NW India*.
  - Riyanka Talukdar attended presented a paper "Geomorphic Evidences of Neotectonic activity, inferred from the River Offset and Paleolake, in the Lower Goriganga River: Higher Central Kumaun Himalaya".
  - Sneha Mishra presented a poster on "Morpho-Structural evidence of neotectonic movement along Vigogi fault: Kachchh Rift Basin".
- Dr. Kapil Mohan has attended Meeting with L& T Chiyoda, Vadodara representative Mr. Chaitanya Marjadi on 06.04.2017 on project work entitled "Generation of Site Specific response spectra at Bongaigaon IOCL refinery".
- Pallabee Choudhury delivered a talk on "Seismology and Seismic hazard" at GSDMA on 12.04.2017.
- Dr. Kapil Mohan delivered an Invited talk on "Importance of Geological, Geophysical and Geotechnical Investigation for Seismic Resistant Designing" at Department of Civil Engineering, CHARUSAT University, Changa, Anand on 12.04.2017.
- Dr. Kapil Mohan attended meeting with Mr. Abhishek Basu, Head Engineering and Project Manager, LPG Dhamra project related to Site specific study to generate site specific response spectra at LPG Dhamra site, Odisha project progress on 12.04.2017.
- Dr. Kapil Mohan delivered an expert talk on "Earthquakes and its effects on buildings" at Gujarat State Disaster Management Authority (GSDMA) on 13.04.2017

- Dr Kapil Mohan attended a meeting on 12.07.2017 with Dr. Dhara Shah and Dr. Komal from Department of Civil engineering, CEPT University for possible research collaborations.
- Falguni Bhattacharya presented a paper on “Late-Quaternary fluvial landforms and their response to the regional stress scenario in the Kachchh peninsula, Western India presented” at Asia Oceania Geosciences Society (AOGS) held during 06.08.2017 to 14.08.2017 in Singapore.
- Dr Kapil Mohan attended Scientific Advisory committee meeting of ISR and presented “Site Specific study to generate response spectra for proposed critical structures in Eastern, Northeastern and Southern India”, held on 11.09.2017 at ISR Gandhinagar.
- Shivam Joshi presented a poster on “Relation between Solar wind Parameters &Geomagnetic storm Condition during the current Solar Cycle 24” during the SAC meeting of ISR held on 11.09.2017.
- Dr. Kapil Mohan delivered a talk “Site specific studies for Seismic Resistant Designing –with some case studies” in Training Programme on “Disaster Resistant Construction Technologies” on 20.09.2017.
- Falguni Bhattacharya presented a paper on “A preliminary attempt to understand the first order cumulative signature of landform degradation with the help of the Mars Colour Camera (MCC) images in the Valles Marineris” at Mars Orbiter Mission (MOM) - Science Meet Programme held at ISRO, Bangalore on 25.09.2017.
- Pavan Kumar Gayatri presented a paper titled ‘Efficiency of time domain electromagnetic method for delineation of the deep freshwater aquifers’ in the workshop on "Water Conservation and Related Issues" under ”Jal Kranti Abhiyan” organized by Central Ground Water Board.
- Vasu Pancholi delivered a talk on “Importance of the Geotechnical studies for Earthquake resistant building” to the South Asian Association for Regional Co-operation (SAARC) participants at ISR.
- Dr. G. Srijayanthi attended an invited lecture on Sub-slab anisotropy controlled by slab dip? at IIT Roorkee
- Nisarg Makwana went to BSIP Lucknow for 13 days for analysing 200 samples from the Lothal and Rann sequences for geo-magnetic studies.
- Riyanka Talukdar presented a poster at “International Meeting of Sedimentalogist” held at Toulouse, France in October 2017.
- Dr. Kapil Mohan attended the 13th Meeting of CGPB Committee -IX on Geoscientific Investigations which was scheduled on 09.10.2017.
- Raj Sunil Kandregula participated in the Field workshop on Active Fault Mapping during 23.10.2017 to 28.10.2017.
- Pallabee Choudhury delivered an invited lecture organized by Dept of Physics, GDC & Indian Science Congress Association, Tripura at Govt. Degree College, Dharmanagar, Tripura on 25.10.2017.
- Dr. Kapil Mohan has attended a three days (from 26.10.2017 to 28.10.2017) field workshop on active fault mapping in Kachchh, Gujarat which was organized by MoES, New Delhi.

- Dr. Kapil Mohan delivered progress presentation of the project "Seismic hazard assessment of Dadra and Nagar Haveli (U.T.)" at Collectorate, Dadra and Nagar Haveli (U.T.) on 06.11.2017.
- Archana Das attended and presented a paper on Dryland fluvial response to Late Quaternary Climate, Tectonic and Sea level changes from the Southern Kachchh Mainland, Western India: Insights from Optical Chronology, Sedimentology and Geochemistry in the 9th International Conference on Geomorpgology held at Delhi, Vigyan Bhawan during 06.11.2017 to 11.11.2017.
- Dr. Kapil Mohan participated in the community program on earthquake awareness in a Village near Silvassa on 07.11.2017.
- Raj Sunil Kandregula attended workshop on Geochronology at IUAC, New Delhi during 15.11.2017 to 17.11.2017.
- Drasti Gandhi attended a workshop on Geochronology at Inter University Accelerator Centre, New Delhi during 16.11.2017 to 17.11.2017.
- Riyanka Talukdar attended a Refresher course on "Theoretical structural geology, crystallography, mineralogy, thermodynamics, experimental petrology and theoretical geophysics'' held at in IISc Bangalore in November 2017.
- Dr Kapil Mohan delivered a talk on "Seismic Microzonation and Site Specific studies" on 20.12.2017, visit of Dr. Rajnikanth Patel, Director, RCSC, Gujarat Technical University for possible collaboration with ISR.
- Dr. Santosh Kumar delivered a lecture on Seismicity monitoring and reporting by ISR on 28.12.2017 at GIDM, Gandhinagar.
- Dr. Kapil Mohan has attended a 2 day conference (from 01.01.2018 to 02.01.2018) on Reducing hazards of earthquakes and disasters for persons with disabilities and the elderly in Hilly regions of India" and delivered a talk on Micro Seismic Hazard Assessment – Some Case studies.
- Dr. A. P. Singh delivered a lecture as Resource Person titled Planning for mitigation and response in coastal areas on 04.01.2018 in the training program at Gujarat Institute of Disaster Management (GIDM), Gandhinagar.
- Dr. Kapil Mohan delivered a presentation on "Seismic Hazard Assessment of Heritage structures" at the MoU signing ceremony with Gujarat Technical University on 09.01.2018. The V.C., GTU, Registrar, Director, Smart City project and Advisor, GTU were present.
- Dr. Kapil Mohan presented progress of the project entitled "Seismic Hazard assessment of Devni Mori" to Principal Secretary, Tourism on 12.01.2018.
- Dr. A. P. Singh delivered a lecture as Resource Person titled Building vulnerability and site response analysis on 22.01.2018 in the workshop at Shankersinh Vaghela Bapu Institute of Technology, Gandhinagar, Gujarat
- Dr.Sumer Chopra delivered series of lectures for post graduate students in Department of Civil Engineering, National Institute of Technology (NITK), Surathkal, Karnataka on Basics of seismology, Seismic microzonation, Seismic site characterization, Site response studies and seismic hazard assessment 29.01.2018 to 31.01.2018.

- Pallabee Choudhury delivered a keynote talk on “Seismic Hazard assessment” in the National Workshop on “Reducing hazards of Earthquakes and Disasters for persons with Disabilities and the Elderly in Hilly regions of India”, held at ISR during 01.02.2018 to 03.02.2018.
- Vasu Pancholi delivered a talk on “Importance of the Geotechnical Investigations in Seismic Hazard assessment” in the National Workshop on “Reducing hazards of Earthquakes and Disasters for persons with Disabilities and the Elderly in Hilly regions of India”, held at ISR during 01.02.2018 to 03.02.2018.
- K. M. Rao and Sushanta Ku Sahoo attended the workshop on Radon Measurements at Centre for Advanced Research in Environmental Radioactivity (CARER), Mangalore University, Mangalagangothri - 574 199, Mangalore, INDIA during 22.02.2018 and 23.02.2018.
- Sh. Pruthul Patel and Sh. Dilip Singh demonstrated SYSCAL pro switch 72 (acquisition, processing and interpretation) to map the ground water aquifer in “Importance of geophysical techniques in ground water exploration” near Shamlaji, Himmatnagar, Gujarat from 26.02.2018 to 28.02.2018.
- Dr. Pavan Kumar, Sci. B delivered a talk on ‘Electromagnetic methods in groundwater exploration’ during a national level seminor on Importance of Geophysical methods for groundwater mapping’ held during 26.02.2018 to 28.02.2018 at GIDM, Gandhinagar
- Pallabee Choudhury delivered a talk related to “Seismology and Seismic hazard assessment” at Department of Geology, MLS University on 09.03.2018.
- V.K. Dwivedi has attended the Conference on “Emerging trends in Geophysical Research for Make in India” (ETGRI) held at IIT-ISM Dhanbad during 09.03.2018 to 11.03.2018.
- Dr. Santosh Kumar participated in table top exercise and Mock Exercise on 15.03.2018 and 16.03.2018 at Gandhinagar.
- Dr. Kapil Mohan attended meeting with Sh. Navneet Gautam, DGM-Geophysics, M/s Mercator Petroleum, Mumbai Dtd. 16.03.2018 regarding MT data Acquisition, processing and Interpretation near Bharuch.
- Dr. Santosh Kumar delivered two lectures in GIDM on 16.03.2018 and 21.03.2018 regarding seismicity monitoring and reporting.
- Dr. Kapil Mohan attended a meeting with Sh. Tushar Shah, AE Narmada Water Resource, KALPSAR Project regarding site specific seismic study on 21.03.2018.
- Dr. Santosh Kumar delivered a talk on "Seismicity Monitoring and Estimation of epicentral, and Source parameters" on 23.03.2018 at Gujarat University.

Distiguished Visitors

- Officials of Narmada Control Authority visited ISR on 19/04/2017
- Shri S.N. Tyagi, GSBTM, visited ISR on 02/05/2017
- Dr. R. Gopichandran, Director, Vigyan Prasar visited ISR as the Chief Guest of the foundation day celebration on 20/05/2017
- Dr. Surendra Nadh Somala, IIT Hyderabad visited ISR on 21/05/2017
- Shri P.K. Taneja, Director General, GIDM visited ISR on 03/10/2017
- A delegation of 20 officers from Nepal visited ISR on 13/10/2017
- Lt. Gen. N.C. Marwah, (Member) NDMA visited ISR on 28/10/2017
- Dr. Afroz Ahmad, Member, Narmada Control Authority visited ISR on 16/02/2018
- Prof. Barbara Romanowicz, renowned Seismologist from the Institut de Physique du Globe de Paris (IPGP), Paris and Professor, University of Berkeley visited ISR and delivered the 5th CEFIPRA Annual Lecture on "Seismic Imaging of the Earth's deep interior" on 22/02/2018

Visit of Student Groups

- A group of 50 students from SVIT-Vasad visited ISR on 18/08/2017.
- A group of 24 students of Structural Engineering Department from CEPT University visited ISR on 19/08/2017.
- A group of 47 students of Civil Engineering Department from L.C.I.T, Bhandu visited ISR on 29/08/2017.
- A group of 52 students of 7th Sem Civil Engineering Department from Gujarat Power Engineering and Research Institute, Mevad, Mehsana visited ISR on 07/09/2017.
- A group of students from B.H. Gardi college of Engineering and Technology, Rajkot visited ISR on 21/09/2017.
- A group of students of M.E. Civil Engineering Department and Geotechnical Engineering from Indus University visited ISR on 25/09/2017.
- A technical visit of 15 students of M.Tech in Geotechnical Engineering, Department of Civil Engineering, along with 3 faculty members Dharamsinh Desai University, Nadiad, visited ISR on 13/11/2017.
- A group of 29 students, M.Sc. Geology final year along with their faculty (Prof. S.K. Pandita and Dr. Yudhvir Singh) from Jammu University, Jammu and Kashmir, visited ISR on 17/01/2018.
- A group of students of Civil Engg. Department come along with their faculty members from G.H. Patel College of Engineering and Technology (GCET), Vallabh Vidhyanagar visited ISR on 27/02/2018.
- A group of 18 students of Civil Engineering Department from Nirma University visited ISR on 20/03/2018.

SOCIETAL OUTREACH

GSDMA organized the School Safety Week from 27th June to 1st July 2017, to create awareness among school children about the various hazards due to Earthquakes, Floods, Fire etc and their mitigation. ISR participated in the School Safety Week for Earthquake awareness. Three teams of ISR were deputed to provide information about Earthquake, Tsunami and what to do before, during and after an earthquake. Around 15061 students of 53 schools of Mehsana, Banaskantha, Surendranagar, Bhavnagar, Botad, Amreli, Gir Somnath and Surat districts were given the earthquake awareness tips.

Training/supervision of students

- Two B. Tech students of Geoscience Department from University of Petroleum and Energy Studies, Dehradun, completed their training on the topic “Seismic Hazard Assessment of Coastal Region of Gujarat State, Western India” under the guidance of Mr. Vasu Pancholi.
- Four students of Civil Engineering Department from BITS Pilani college completed their training on the topic “Geotechnical Investigations for Seismic Hazard Assessment, under the guidance of Mr. Vasu Pancholi”
- Vasu Pancoli was deputed to Surat city for 5 days to create awareness among school students about Earthquake hazard under the School Safety week programme organised by GSDMA.
- Mosam A. Prajapati and Sahil M. Patel, M.Sc. (Physics) students from Hemchandraacharya North Gujarat University did their MSc dissertation work on “Estimation of sediment and Trap Thickness in the south western part of Cambay region using Magnetotellurics” under the guidance of Dr. Kapil Mohan.
- Dr. Kapil Mohan guided the M.Tech. (Civil Engineering) students of Gujarat Forensic Science University, Gandhinagar for their dissertation entitled “Earthquake risk assessment in Sec.21, Gandhinagar from 15.12.2017 to 30.04.18.
- Dr. Kapil Mohan guided the M.Tech. (Civil Engineering) students of Gujarat Forensic Science University, Gandhinagar in their dissertation work entitled “Earthquake Vulnerability assessment in Rambaug, Ahmedabad done during 15 Feb-30 April 2017.
- Two MSc (Marine Geophysics) students of Cochin University of Science and Technology and one B Tech student of Pune University have completed their dissertation works under the guidance of Dr B Sairam.
- Pallabee Choudhury imparted training on “Introduction to GPS and data processing” to Mr Dhrubajyoti Bora, MSc student of Kachchh University, during the 22 May to 8 June, 2017.
- Ketan Roy guided Mr. Abhay Pandey (trainee) to estimate standard error using bootstrap analysis of HVSR curves.
- Archana Das has guided two students from KSKV Kachchh University and two more students from IIT, Kharagpur for internship.

- A student Ms. Madhuri Chauhan, 2nd semester M. Sc (Applied Geophysics) from Indian Institute of Technology (IIT), Bombay, India has been completed her dissertation in the Solid Earth Geophysics Group in June 2017 on Inversion of local S-wave velocity structure in the Gujarat region from average H/V curves and Its Implication for the Site Effects.
- A student Mr. Abhay Pandey, M. Sc (5 year - course) Earth and Space Science, University of Hyderabad, India has been completed his dissertation in the Solid Earth Geophysics Group in June 2017 on Assessment of site response using earthquake and Microtremor measurements in Arunachal Himalaya.
- Mr. Adityam Rai, a third year student of B. Tech in Geosciences Engineering, Department of Petroleum and Earth Sciences, University of Petroleum and Energy studies, Dehradun, has completed his dissertation in the Solid Earth Geophysics Group in July 2017 on Estimating the crustal thickness beneath Gujarat region using PmP phases.
- Mr. Athul P., a first year student of M.Sc in Marine Geophysics, Department of Marine Geology and Geophysics, School of Marine Sciences (under Cochin University), Cochin, Kerala, has completed his dissertation in the Solid Earth Geophysics Group in July 2017 on Variation of the amplitude and shift in the Receiver Function converted phases for various 1D single-layered Isotropic models.
- One M.Tech. (Geophysics) final year student from IIT, Khargpur came for Dissertation in May 2017 for 3 months.
- Dr Sumer Chopra guided Shreyasvi, a Ph.D student of NIT on "Probabilistic Seismic Hazard Assessment of Mangalore and its adjoining regions, a Part of Indian Peninsula: an Intraplate Region", as a part of her course work.
- Dr B Sairam guided one B Tech student of Pune University for M.Sc. dissertation work during the period January-September 2017.
- Dr B Sairam imparted training on "Seismic methods and Multichannel analysis Surface Waves (MASW)" to three B Tech students of the University of Petroleum and Energy Studies, Dehradun, during 1-30 July 2017.
- Aditya Narkhede, Abhijeet Pandey, Daksh Dangar AAkash Bajaj, B.E.(Hons.), Civil Engineering students of BITS Pilani, Seismic Risk and loss assessment (Sec.2 &23) Gandhinagar, have attended training during 22.05.2017 to 13.07.2017 (Supervisor: Dr. Kapil Mohan).
- Aniket Panchal, M.Tech. (Civil Engineering), SVNIT, Surat have attended training on Strong ground motion Liquefaction estimation in Alwar City, Rajasthan from 01.06. 2017 to 14.07.17 (Supervisor: Dr. Kapil Mohan).
- Pallabee Choudhury imparted training on "Strong motion simulation" to Mr Jaya Prakash Vemuri, a research scholar from IIT Hyderabad, during 9-11 July 2017.
- Pallabee Choudhury imparted training on "GPS data processing" to Mr M Mukundan, a research scholar from Sona College of Technology, Salem, during 16-21 July 2017.
- Dr. A. P. Singh and Mr. Arjav Shukla participated in the school-safety week - 2017 at Surendranagar, Bhavnagar, Botad, Amreli, and Gir Somnath districts of the

Saurashtra Region. About 3550 students were trained in 11 schools. The training was based on introduction to earthquake risk mitigation and safety tips.

- Mr. Avinash Chauhan helped two students (Mr. Abhishek Tiwari and Mr. Madhur) of University of Petroleum and Energy Studies, Dehradun for their winter internship.
- Dr. Chinmay Haldar supervised Mr. Bipin Kumar Maurya, a student of Department of Geophysics, Kurukshetra University from June to July 2017
- Two M.Sc. students of the Geology Department from Gujarat University, Ahmedabad are working on their MSc dissertation work on the topic “Estimation of the Index properties of Soil” under the guidance of Mr. Vasu Pancholi.
- Dr. Pavan Kumar supervised three students from Nanded University, Maharashtra for their M.Sc. (Geophysics) dissertation work.
- Falguni Bhattacharjee is supervising a student from KSKV Kachchh University for M.Sc. dissertation work.
- Two students of Geology department of Gujarat University, Ahmedabad completed their MSc dissertation on “Estimation of the index properties of soil” under the guidance of Sh. Vasu Pancholi.
- Mr. Nandamuri Dany Reginald and Mr. Mallipeddi Kethan Kumar, students from Andhra University have done their dissertation work on “Implementing the seismic refraction technique for delineation of velocities and thicknesses of subsurface layers” during 11th Dec 2017- 31st Jan 2018 under the guidance of Dr B Sairam.
- Pallabee Choudhury is guiding Mr Hardeep Panchal, a student from Kurukshetra University for his MTech dissertation work. The duration of the work is 1st Mar-31st May 2018.
- Dr. Kapil Mohan guided Mr. Jay Patel from A.D. Patel Institute of Technology, Gujarat Technical University, for his intership on "Vulnerability assessment in the Vasna area of Ahmedabad" from 11.01.2018 to 12.03.2018.
- Ms. Jyoti Sharma Supervised Ms. Deeksha, M.Sc. Earth Sciences student of Indian Institute of Technology (IIT), Bombay during 05th December 2017- 04th January 2018 on the topic “Surface Waves Dispersion Analysis”.

CAMPUS NEWS AND EVENTS

Exchanges of MoU between ISR and NGRI on 27/04/2017

Dr. R. Gopichandran, Director, Vigyan Prasar visited ISR and delived the 11th foundation day Lecture on 20/05/2017

11th Foundation Day Celebration of ISR on 20/05/2017

ISR organised Tree Plantation program on 31/08/2017 in the presence of Shri P.K. Taneja, Director General, GIDM as a part of Knowledge corridor beautification project

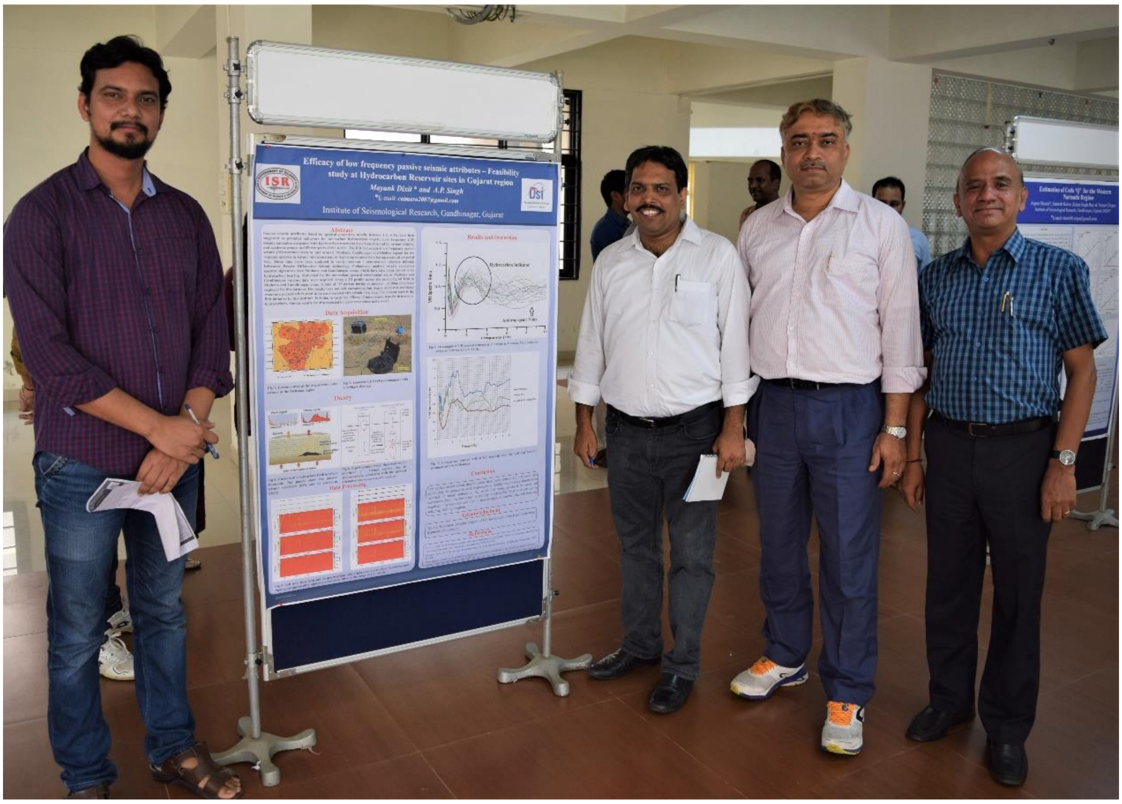

Poster presentation during 5th SAC Meeting, 11/09/2018

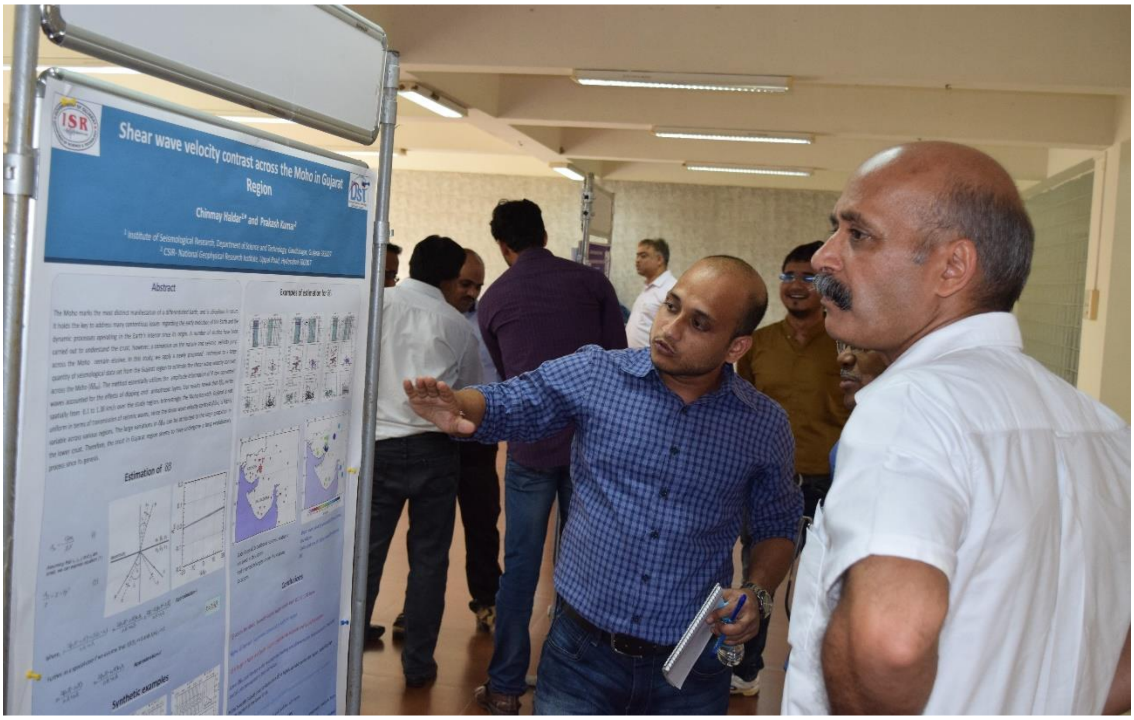

Poster presentation during 5th SAC Meeting, 11/09/2018

SERB Meeting held at ISR during 18-20 September 2017

Shri P.K. Taneja, Director General, GIDM visited ISR on 03/10/2017

A delegation of 20 officers from Nepal visited ISR on 13/10/2017

Republic Day Celebration at ISR, 26/01/2018

Exchanges of MoU between ISR and GTU on 14/02/2018

Dr. Afroz Ahmad, Member, Narmada Control Authority visited ISR on 16/02/2018

Prof. Barbara Romanowicz, renowned Seismologist from the Institut de Physique du Globe de Paris (IPGP), Paris and Professor, University of Berkeley, visited ISR and delivered the 5th CEFIPRA Annual Lecture on "Seismic Imaging of the Earth's deep interior", on 22/02/2018.

List of Existing / New Projects

Sl no	Title of the project	Name of PI	Sponsoring Agency
1.	Paleoseismology and active fault investigation in Gujarat	Girish Kothyari	DST, GoG
2.	MPGO and geochemical monitoring for earthquake precursor study in Kachchh region	K M Rao	
3.	Seismic array in Western India to decipher structure and anisotropy		
4.	Deep Seismic Sounding Profiles in Gujarat to decipher sub-surface nature of major faults and also to detect hidden faults in the region		
5.	3D MT study in Kachchh region of Gujarat	Kapil Mohan	
6.	Real time monitoring of crustal deformation in Gujarat using GPS network	Rakesh Dumka	
7.	Site amplification studies of Gujarat	A P Singh	
8.	Running and maintenance of Seismic network	Santosh Kumar	
9.	Geophysicist of ISR		
10.	Development of earthquake early warning system for Kachchh Region of Gujarat. India		
11.	Deep Seismic Sounding profile in Gujarat	P Mahesh	MoES
12.	Active fault, Paleoseismic and crustal deformation in NW and Central Himalaya, India	Rakesh Dumka	
13.	Active Fault mapping in western KMF and Gedi Fault zone	Girish Kothiyari	
14.	Seismic Microzonation of Bhuj City, Kachchh	Kapil Mohan	
15.	Reconstructing the catalogue of high energy Marine events from Gujarat coast using geological signatures during the last 6000 years	Siddharth Prizomwala	
16.	Aggradational-incisional phases in the Fluvial sequences of southern Saurashtra: Implication of Sea level/Tectonic forcing during the Late Quaternary	Siddharth Prizomwala	DST, GoI (Fast Track)
17.	Operational definition of seismic risk and intervention techniques for strategic buildings: an integrated system on HPC platform	Kapil Mohan	FVG, Italy
18.	Study of Geothermal processes in Gujarat using Remote Sensing and Geophysical techniques: A potential to Martian analogue		SAC, Ahmedabad
19.	Development of a Cal-Val site at Desalpar in Rann of Kutch for Land and Atmosphere	K M Rao	ISRO, Ahmedabad
20.	GPS & GAGAN/IRNSS data analysis for Intra-Plate Geodynamic Profiling in Active Seismic Zone	Rakesh Dumka	
21.	Documentation of aqueous and paraglacial features in and around equatorial region of Mars	Falguni Bhattacharjee	SAC, Ahmedabad
22.	Seismological studies in and around SSNNL dam	Santosh Kumar	SSNNL
23.	Earthquake data processing and interpretation of MEQ data collected during Jan. To Dec. 2014 for study of seismogenic sources around the Subansiri Lower H.E. Project Arunachal Pradesh	Santosh Kumar/ P Mahesh	NHPC

Sl no	Title of the project	Name of PI	Sponsoring Agency
24.	Micro-Earthquake (MEQ) and Local Earthquake Tomography (LET-3D) studies through a network of six seimographs around the Dam site of Bursar Hydro Electric Project within a radius of 50 km		
25.	Site Characterization for Seismic Hazard analysis using microtremor measurements in Saurashtra region of Western India	A P Singh	SERB, GoI
26.	Development of site specific spectra for IOCL Bongaigaon Refinery Assam State	Kapil Mohan	L&T-Chiyoda Ltd
27.	Probabilistic Seismic Hazard Analysis (PSHA) of Bongaigaon		Parsan Overseas Pvt. Ltd
28.	Magnetotelluric Data acquistition, processing and interpretation in the NELP Block no. CB-ONN-2005/9		Mercator Petroleum Ltd., Mumbai

DST: Department of Science and Technology

MoES: Ministry of Earth Sciences

FVG: Friuli-Venezia Giulia

ISRO: Indian Space Research Organisation

SAC: Space Application Centre

SSNNL: Sardar Sarovar Narmada Nigam Limited

NHPC: National Hydroelectric Power Corporation

SERB: Science and Engineering Research Board